SPERRY RAND

STRAPDOWN CALIBRATION AND ALIGNMENT STUDY

VOLUME I

DEVELOPMENT DOCUMENT

Prepared for

GUIDANCE LABORATORY
ELECTRONICS RESEARCH CENTER
NATIONAL AERONAUTICS AND SPACE ADMINISTRATION
CAMBRIDGE, MASSACHUSETTS

under Contract NAS 12-577

by

D.M. Garmer
E.J. Farrell
S. Kau
F.N. Bailey

UNIVAC
FEDERAL SYSTEMS DIVISION

ACKNOWLEDGEMENT

The authors would like to extend their appreciation to Mr. L. C. Smith, Mr. D. E. Jones, and Mr. D. Downing for their contributions to this document. Mr. Smith was the principal author of Section 3.3 and Appendix D, both concerning hardware descriptions. Mr. Jones was responsible for the consolidation of all appendix material. Mr. Downing, as the monitoring engineer representing NASA/ERC, significantly contributed, through his critique, to the organization and content of this and the two other volumes.

ABSTRACT

This is Volume 1 of three volumes which report the results of a strapdown calibration and alignment study performed by the Univac Federal Systems Division for the Guidance Laboratory of NASA/ERC.

This study develops techniques to accomplish laboratory calibration and alignment of a strapdown inertial sensing unit (ISU) being configured by NASA/ERC. Calibration is accomplished by measuring specific input environments and using the relationship of known kinematic input to sensor outputs, to determine the constants of the sensor models. The environments used consist of inputs from the earth angular rate, the normal reaction force of gravity, and the angular rotation imposed by a test fixture in some cases. Techniques are also developed to accomplish alignment by three methods. First, Mirror Alignment employs autocollimators to measure the earth orientation of the normals to two mirrors mounted on the ISU. Second, Level Alignment uses an autocollimator to measure the azimuth of the normal to one ISU mirror and accelerometer measurements to determine the orientation of local vertical with respect to the body axes. Third, Gyrocompass Alignment determines earth alignment of the ISU by gyro and accelerometer measurement of the earth rate and gravity normal force vectors.

The three volumes of this study are composed as follows:

- Volume 1 – Development Document. This volume contains the detailed development of the calibration and alignment techniques. The development is presented as a rigorous systems engineering task and a step by step development of specific solutions is presented.
- Volume 2 – Procedural and Parametric Trade-off Analyses Document. This volume contains the detailed trade-off studies supporting the developments given in Volume 1.
- Volume 3 – Laboratory Procedures Manual. In Volume 3 the implementation of the selected procedures is presented. The laboratory procedures are presented by use of both detailed step-by-step check sheets and schematic representations of the laboratory depicting the entire process at each major step in the procedure. The equations to be programmed in the implementation of the procedures are contained in this volume.

TABLE OF CONTENTS

TABLE OF CONTENTS (Continued)

LIST OF ILLUSTRATIONS

LIST OF CHARTS

LIST OF CHARTS (Continued)

GLOSSARY

As an aid to understanding the symbolism, we present the following rules of notation

- Wherever possible symbols will be used which suggest the name of the parameter involved.
- Lower case subscripts are used almost exclusively for indexing over several items of the same kind. Examples are the indexes used to identify the three gyros, the three accelerometers, the two pulse trains of each accelerometer, the two clock scale factors, etc.
- Lowercase superscripts are used to index over different positions.
- Uppercase superscripts and subscripts will be used to distinguish between parameters of the same kind. For example, T is used to identify a transformation matrix. Lettered superscripts such as BE in T^{BE} identify the particular transformation.
- An underline will identify a vector.
- Unit vectors are used to identify lines in space such as instrument axes and the axes of all frames of reference.
- Components of any vector along with any axis is indicated by a dot product of that vector with the unit vector along the axis of interest.
- The Greek sigma (Σ) will be used for summations. Where the limits of summation are clear from the context, they will not be indicated with the symbol.
- The Greek Δ is always used to indicate a difference.
- S ϕ and C ϕ are sometimes used to identify the sine and cosine of the angle ϕ.
- A triple line symbol ($\equiv$) will be used for definitions.
- A superior "$\sim$" denotes a prior estimate of the quantity.
- A superior "$\wedge$" denotes an estimate of the quantity from the estimation routine.

$\underline{a}$	Applied acceleration vector.
$(\underline{A}_I \cdot \underline{B}_J)$	Elements of $(Q^A)^{-1}$.
$\underline{A}_I$	Unit vector directed along the input axis of the ith accelerometer $i = 1, 2, 3$.
$\underline{b}$	A vector determined by the Alignment Parameter Evaluation Procedure and input to the Estimation Routine.
$\underline{B}_I$	Unit vector directed along the ith Body Axis $i = 1, 2, 3$.
B_I, B_O, B_S	Gyro unbalance coefficients.
$C_{II}, C_{SS}, C_{IS}, C_{IO}, C_{OS}$	Gyro Compliance Coefficients.
Counters	The six frequency counters used as data collection devices during calibration.
D_0	Accelerometer bias.
D_1	Accelerometer scale factor.
D_2	Accelerometer second order coefficient.
D_3	Accelerometer third order coefficient.
$\underline{E}$	Unit vector directed East ($\underline{E}_2$).
$\underline{E}_I$	Unit vector directed along the ith Earth Axis.
Eq	Quantization error.
f_1, f_2	Frequencies of accelerometer strings 1 and 2, in zero crossings per second.
$\underline{F}_I$	A triad of orthogonal unit vectors attached to the base of the table.
$\underline{G}_I$	Unit vector directed along the ith input axis of the gyro.
$(\underline{G}_I \cdot \underline{B}_J)$	Elements of $(Q^G)^{-1}$.
$\underline{g}$	The vector directed up that represents the normal force to counteract gravity in a static orientation. Corresponding to popular convention, this is referred to as the "gravity vector".
I/O	Input/Output.

$\underline{I}_1$	Triad of orthogonal unit vectors attached to the inner axis of test table.
IEU	Interface Electronics Unit – system interface device for the laboratory computer.
ISU	Inertial Sensing Unit.
J	Gyro angular rate coefficient.
K	Number of samples of accelerometer and gyro data taken in Alignment.
m	Position index used in calibration (superscript).
M	Matrix generated by Alignment Parameter Evaluation and used by Alignment Estimation Routine.
$\underline{M}_1$	Unit normal to ith mirror.
$\underline{N}$	Unit vector directed North ($\underline{E}_3$).
N_1, N_2	Count of output pulses from strings 1 and 2 of accelerometer.
n_A	Instrument noise in accelerometer.
n_G	Instrument noise in gyro.
Σn^{ϕ}	Count of output pulses from strings 1 and 2 of accelerometer.
Σn_1^T	Count of timing pulses from master oscillator to frequency counters.
Σn_2^T	Count of timing pulses from master oscillator to IEU.
$\underline{O}$	Unit vector directed along the output axis of gyro.
$\underline{O}_1$	Triad of orthogonal unit vectors attached to the outer axis of the table.
$\underline{P}$	Unit vector in the direction of the projection of $\underline{M}_1$ in the plane formed by $\underline{E}$ and $\underline{N}$.
P_k^A	Defined on Chart 4-12 of the Development Document.
P_k^G	Defined on Chart 4-4 of the Development Document.
Q^A	The transformation from accelerometer input axes to body axes.
Q^G	The transformation from gyro input axes to body axes.

Q_{II}, Q_{IS}	Gyro dynamic coupling coefficients.
$\underline{r}$	Position vector.
R	Gyro bias.
$\underline{R}_i$	Triad of orthogonal unit vectors attached to rotary axis of table.
Resolver	Angular resolvers on each axis of the test table.
$\underline{S}_i$	Unit vector directed along the ith gyro spin axis.
$\underline{S}^{\phi}$	Scale factor associated with pulsed output from test table rotary axis.
S_1^T	Scale factor associated with timing pulses accumulated by the frequency counters.
S_2^T	Scale factor associated with timing pulses to the IEU.
t	Time.
T	In alignment, the determined alignment matrix to transform from body to earth axes. T is equivalent to T^{BE}.
T^{BI}	Transform from ISU body axes to inner axis frame.
T^{BRm}	Transform from ISU Body Frame Axes to Rotary Axis Frame in the mth orientation.
$\underline{T}_i$	Triad of orthogonal unit vectors attached to the trunnion axis of the test table.
$\underline{U}$	Unit vector directed up (E_1).
$\underline{V}$	Velocity vector.
$\underline{W}$	Unit vector directed along $\underline{\omega}^E$.
X-Y	Dual input on frequency counter that will difference two pulse trains for comparison with a third input (Z).
Z	Input on frequency counter for pulse train.
α_i	The azimuth angle of the normal to the ith mirror.
$(\Sigma\gamma)_{ij}$	Pulsed output from the jth string of the ith accelerometer.
$(\Sigma\delta)_i$	Pulsed output of the ith gyro.
$\Delta\Phi$	Gyro scale factor.

SECTION 1

SECTION 1

SECTION 1
INTRODUCTION

This document, in conjunction with two other volumes, describes the achievements of a six month study conducted for the.

Guidance Laboratory
Electronics Research Center
National Aeronautics and Space Administration
Cambridge, Massachusetts

by the:

Aerospace Systems Analysis Department
Univac Federal Systems Division
Saint Paul, Minnesota
A Division of Sperry Rand Corporation

The purpose of the study is to develop techniques and outline procedures for the laboratory calibration and alignment of a strapdown inertial sensing unit. This document, Volume 1, presents a detailed analysis of the calibration and alignment problem and develops a specific solution. The nucleus of the study output is the contents of this document. The Procedural and Parametric Trade-off Analyses, Volume 2, is a set of addendums which serve to justify decisions made and conclusions reached in the development of specific calibration and alignment techniques. Reference is made to the contents of the trade-off document throughout Sections 4 and 5 of this document. The Laboratory Procedures Manual, Volume 3, describes specific procedures for an operational implementation of the solutions obtained in Volume 1. It is an extension of the results of Volume 1 into an operational laboratory situation. The last subsections of Sections 4 and 5 of this document (Volume 1) form the interface between the study developments and the specific procedures found in Volume 3.

At the time of this writing, the Guidance Laboratory of NASA/ERC is in the process of configuring a strapdown inertial sensing unit which they will use to evaluate many advanced concepts. By integrating this ISU with a system computer, they will attain a flexible system level research tool for testing analytical concepts, system design concepts and fabrication concepts. In parallel with the development of the Guidance and Navigation System, a laboratory facility is being designed which will contain all of the test equipment necessary for conducting the experiments on the strapdown G and N System.

Among the more important experiments to be conducted are those which determine the feasibility of easily and precisely calibrating and aligning the sensor package in an operational laboratory situation. Before such experiments can be conducted, the calibration and alignment techniques must be developed and definitively documented. The Guidance Laboratory contracted Univac's Aerospace Systems Analysis Department to develop and document those techniques. The specific tasks which Univac was contracted to accomplish are as follows:

- To specify mathematical models for the system sensors (gyros and accelerometers).
- To define the mathematical description of the sensor package.
- To develop techniques for the determination of all calibration constants.
- To develop three techniques for initializing the alignment of the ISU. The three techniques involve the use of
  - ▲ Optical measurements only
  - ▲ Accelerometer measurements for level, and an optical azimuth measurement
  - ▲ Accelerometer and gyro measurements only.
- To accomplish specified trade-off analysis on all calibration and alignment techniques.
- To specify all equations and procedures for the accomplishment of a calibration and alignment in the ERC Laboratory.
- To document, in three volumes, the calibration and alignment developments, trade-offs, and procedures.

The satisfaction of the first four items is accomplished in this Development Document. The trade-offs are described in the Procedural and Parametric Trade-off Analysis Document and the procedures are outlined in the Laboratory Procedures Manual.

The presentation of the calibration and alignment developments in this document, Volume 1, is divided into five sections. The purpose of the introduction is to briefly state the study problem (accomplished in the above listing of seven items) and to describe the developments contained in Volume 1. The purpose of Section 2 is to delineate the calibration and alignment requirements. Section 3 presents a system description of calibration and alignment with emphasis on the laboratory environment. The specific calibration and alignment techniques are then developed in Sections 4 and 5, respectively. As an introduction to the scope of this document, the following paragraphs outline the developments in these sections.

The calibration and alignment study tasks have been only generally stated in the preceding paragraphs. Before the technique developments can be described, the specific engineering

and mathematical requirements of calibration and alignment must be stated. In Section 2 we accomplish the detailed specification of those requirements. A statement of the calibration and alignment requirements will be simply presented as a list of parameters to be determined in the laboratory. As a lead-in to that listing, Section 2 shows how the requirements tie in to the larger system problem of navigation. We accomplish this by presenting the general definitions of calibration and alignment as the determination of constants required in an operational navigation loop. The mathematics of portions of the navigation loop are delineated so that calibration and alignment can be specifically defined as the determination of constants contained within the mathematics.

After specifying the calibration and alignment requirements in Section 2, Section 3 directs our attention to the laboratory environment in which the calibration and alignment is to be accomplished. As an introduction to the environment, we present in the first subsection of Section 3 functional system descriptions of both calibration and alignment. The functional description of the ERC laboratory calibration is presented in comparison with what we call an Ideal Calibration. The comparison of the ideal with the actual ERC laboratory calibration serves to illustrate those compromises necessary in the development of a test laboratory. The functional description of alignment presents those separate operations required in an operational alignment. Three functional diagrams are presented in Section 3, one for each of the three alternative alignment techniques. All functional descriptions serve to define those measurements, other than inertial instrument measurements, which are required to accomplish the calibration or alignment. The additional measurements correspond to an independent measure of the kinematic environment. The determination of those additional measurements is the subject of the second subsection of Section 3. Section 3 is concluded with a brief description of the hardware available in the laboratory, and the interfaces between those pieces of hardware.

The calibration technique developments in Section 4 are directed toward specifying the details of the calibration functions which are generally defined in Section 3. The basis of calibration is presented in Section 3 as the input of environment and inertial instrument measurements into computations which are a function of those measurements and the unknown calibration constants. The general equations from which the computations are evolved are developed in the initial subsection of Section 4. Those general equations are developed by introducing the parameters which identify the laboratory kinematic environment and the ISU geometry into the inertial instrument mathematical models. Subsequent to the development of the general equations, particular choices of test table orientation are used to define the "Positions" to be used for the determination of all calibration constants. The chosen positions are shown to produce significant reductions in the complexity of the general calibration equations. With the aid of these reductions it is possible to solve for the calibration constants by a series of relatively simple experiments.

In the third subsection of Section 4 the calibration computations are tabulated. The quantization and instrument and environment noise considerations are described in conjunction with the tabulation. The fourth subsection of Section 4 describes those laboratory activities required prior to the actual calibration. All such activities are related to either the survey of the location of the ISU relative to the test table, or the compensations for the small low frequency motion of the test table base. The last subsection of Section 4 forms the tie between this Development Document and the details of calibration implementation presented in the Laboratory Procedures Manual, Volume 3. In Volume 1 the implementation of calibration is only briefly described, the details being left as the subject of Volume 3.

The alignment techniques developed in Section 5 expand the functional descriptions of alignment as presented in Section 3 into a set of alignment techniques. Alignment is broken into three separate routines. preprocessing of sensor outputs, the application of chosen estimation procedures to the preprocessed outputs, and calculation of alignment matrices from the estimated values. Since the preprocessing and alignment matrix calculations are developed in Section 2, the major emphasis in Section 5 is centered on the estimation problem.

Before describing the development of an estimation technique, the basic functional requirements and the preprocessing computations are presented, respectively, in the first two subsections. The third subsection describes a detailed development of models for the environmental disturbance and sensor noise. The next two subsections are then devoted to the development of two approaches for estimation in Level Alignment and Gyrocompass Alignment. The first approach develops a procedure for estimating average values of the gravity and earth rate vectors, while the second approach leads to estimates of instantaneous values of these vectors. Estimation techniques are developed using three basic statistical procedures: simple average, least squares. and posterior mean. From these estimates the average and instantaneous values of the alignment matrices are then obtained. The last subsection of Section 5 describes explicit equations for the recommended alignment techniques, and ties the results of Section 5 to the procedural details of alignment described in the Laboratory Procedures Manual.

SECTION 2

SECTION 2
CALIBRATION AND ALIGNMENT REQUIREMENTS

The purpose of this study is to determine a procedure for the calibration of the NASA/ERC strapdown inertial sensing unit (ISU) and to delineate three operational laboratory techniques for the initial alignment of the same inertial sensor unit. Clearly, the initial task in this, or any study, is to carefully describe the problem as a specifically defined study task. This we propose to do in this section of our report.

The key words in the above general statement of the study purpose are the words "calibration" and "alignment". The first activity in this section will be to develop (in Section 2.1) the definitions of those key words. Our approach to the development of those definitions is to present a description of an operational navigation loop and, as a conclusion to that description, to present calibration and alignment as the determination of constants required as inputs to the navigation loop. There are alternative approaches to the definitions of these terms but we feel our approach is optimum in that it clarifies the necessary relationship between the calibration and alignment problem and the larger system problem of inertially navigating a propelled vehicle.

Subsequent to the navigation-system definition of calibration and alignment we will, in Sections 2.2 and 2.3, describe the calibration and alignment requirements as they relate to the ERC strapdown inertial sensing unit. Section 2.2 describes the calibration requirements, and Section 2.3 describes the alignment requirements.

The development of the calibration requirements in Section 2.2 will be directed toward the tabulation of the instrument constants and instrument-to-body-axes transformation matrix constants which are necessary in an operational navigation loop. The first activity in that section will be the description of the geometry of the ERC ISU. This will be followed by a description of the inertial instruments contained in that ISU. The instrument-to-body-axes transformation matrices will then be described. All of the described equipment and geometry will then be used to develop the navigation loop "Preprocessing Computations". Finally, the constants in the Preprocessing Computations will be defined as the constants to be obtained in calibration.

In Section 2.3 the alignment requirements will be described as the real-time measurement of the ISU fixed or earth-fixed coordinates of two vectors. Three alternative choices of these two vectors will be presented. The geometry of alignment will also be presented.

The final presentation will be the specific alignment matrix mathematics corresponding to the three alternative alignment techniques.

2.1 DEFINITION OF CALIBRATION AND ALIGNMENT

The necessity for a calibration and alignment of an inertial sensing unit is directly related to the use of the ISU in a vehicle guidance system. More specifically, calibration and alignment requirements are related to the necessity for a real-time transformation of the ISU instrument outputs into a best estimate of a vehicle's velocity and position. In this section we will, from a discussion of real-time inertial guidance activities, define the general calibration and alignment requirements.

The functional diagram shown in Figure 2-1 serves as a description of the initial activities in a real-time navigation loop. That diagram will be the focal point of our attention for the remainder of this subsection. Figure 2-1 shows only that portion of the navigation loop which transforms instrument outputs into estimates of velocity and position. (The remaining portions of the loop are the guidance logic, automatic control, and dynamic response which are not shown.)

The input to the ISU is the kinematic environment of the vehicle and ISU as represented by the applied acceleration $\underline{a}$ and angular velocity $\underline{\omega}$. The outputs of the ISU are (usually) sequences of pulse counts taken over small intervals of time. These outputs are the inputs to the computer. The computer's immediate task is to convert those measurements into a knowledge of velocity and position. The velocity ($\underline{v}$) and position ($\underline{r}$) must be represented as components ($\underline{v} \cdot \underline{D}_k$) and ($\underline{r} \cdot \underline{D}_k$) in the frame ($\underline{D}_k$) in which one chooses to navigate ($\underline{D}_k$ represents a triple, k = 1, 2, 3, of unit vectors directed along the orthogonal navigation axes).

The initial activity in the conversion to velocity and position is the transformation of the pulse counts into estimates of the integrals of the instrument-axes components of applied acceleration and angular velocity. The instrument axes are represented by the triads $\underline{A}_k$ and $\underline{G}_k$ of (in general) nonorthogonal unit vectors directed along the input axes of the accelerometers and gyros, respectively.

The second activity, in the conversion to velocity and position, is the transformation of the integrals of the instrument-axes components of applied acceleration and angular velocity into integrals of body-axes components. The body axes ($\underline{B}_k$) are a triad of orthogonal unit vectors which are fixed to the ISU. These body axes can be defined in various ways. They can be defined by use of any two of the instrument axes or they can,

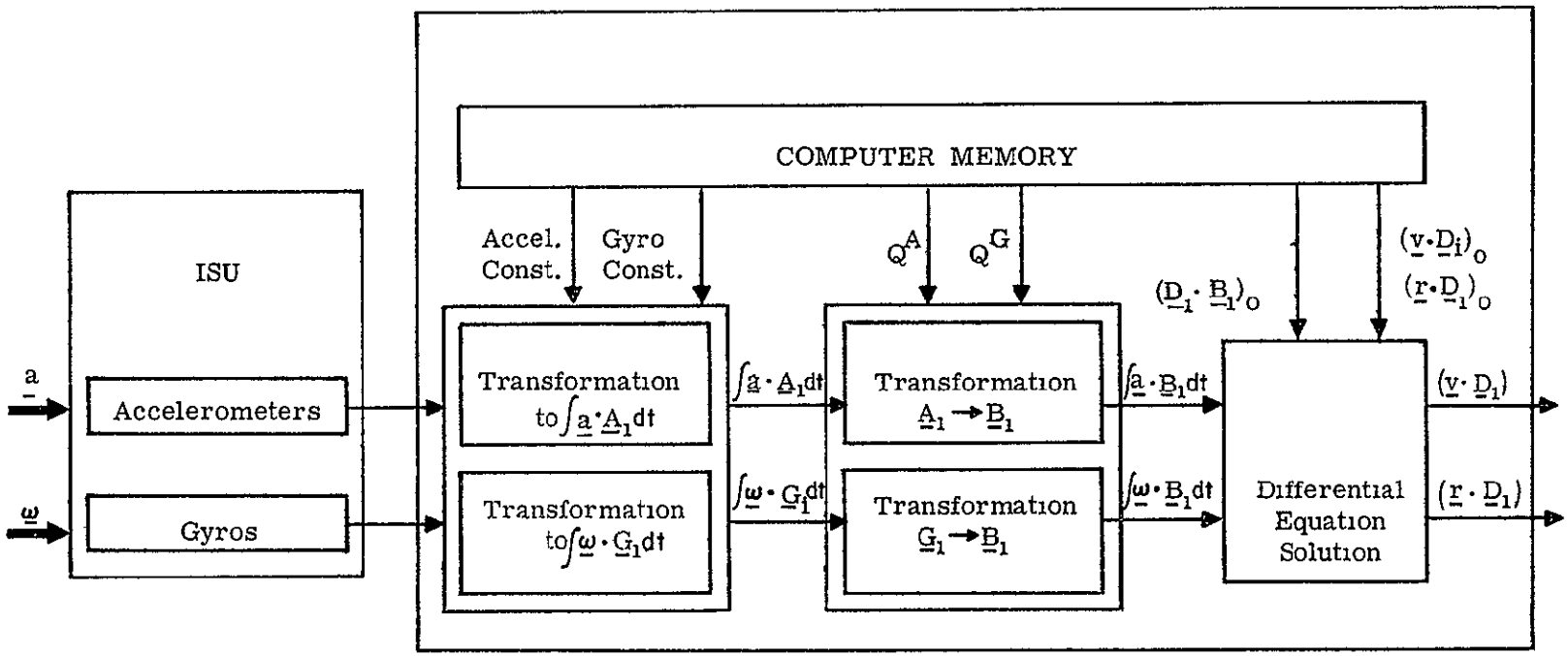

Figure 2-1. Navigation Flow Diagram

as they are in this study, be defined by use of two mirror normals. (The manner in which this definition is accomplished for the ERC system will be found in Section 2. 2.)

The final activity in the conversion of instrument outputs into navigation-axes components of velocity and position begins with the input of the body-axis integrals of applied acceleration and angular velocity to the translational and rotational differential equations of motion. The numerical solution of those differential equations yields the desired velocity and position. The solution of the rotational differential equations serves to transform the argument of the translational differential equations into navigation-axes components. The output of the translational differential equations solution is then the desired components of velocity and position.

It is noted that various constants are required from computer memory as inputs into all routines. The initial routine requires those instrument constants which scale and correct the instrument outputs. The second routine requires the nonorthogonal three-by-three matrices, Q^A and Q^G, which transform the integrals of the instrument-axes components into the integrals of the body-axes components. The third routine, being the solution of differential equations, requires initial conditions. The initial condition for the rotational differential equation solution is an initial body-to-navigation-axes transformation matrix. The initial condition of the translational differential equation solution is an initial knowledge of navigation-axes components of velocity and position. A knowledge of all of these constants is required prior to any operational use of the ISU. The development of the numerical values of these constants can be divided into three separate problems; and the statement of two of these problems can be used as a definition of calibration and alignment.

The problem of determining the instrument constants used in the first routine, and the Q^A and Q^G matrices used in the second routine, will be considered in this report as the problem of calibration. The problem of determining the initial body-to-navigation-axes transformation matrix will be referred to as the alignment problem. The remaining problem of initializing velocity and position is an operational problem, which is not within the scope of this work.

We will extend these definitions to the subject ERC strapdown ISU. Specifically, we will delineate more detailed definitions in terms of the geometry and instruments characterizing the ERC system. Section 2. 2 will treat calibration, and 2. 3 alignment.

2.2 CALIBRATION REQUIREMENTS

It was seen in the preceding subsection that calibration is defined as the determination of those instrument constants and constant matrix transformations required in the transformation of instrument outputs into integrals of body-axes components of applied acceleration and angular velocity. In this section we will describe the equations in the navigation routines which utilize the calibration constants. We will specify those equations with the assumption that the ERC strapdown ISU is the subject sensor unit. From that description, we can then specifically describe the calibration requirements as the determination of the constants contained within those navigation routines.

The desired equations are directly deducible from the geometry of the ISU and the mathematical models of the instruments. We therefore begin the presentation in this section by describing the geometry of the strapdown ISU, followed by a description of the accelerometers and gyros contained within the ISU. Following those descriptions we will define the Q^A and Q^G matrices. Next we will employ all of this information to develop the desired equations; and finally we will utilize those equations in the tabulation of the required calibration constants.

2.2.1 ISU Geometry

The ERC ISU is a strapdown sensing unit containing.

- Three vibrating-string accelerometers
- Three single degree of freedom gyros
- One mirror cube
- Associated structural and electronic devices.

The strapdown ISU has been specified such that the accelerometer input axes ($\underline{A}_k$), the gyro input axes ($\underline{G}_k$), and three mirror normals ($\underline{M}_k$) are nominally orthogonal and nominally aligned. In implementing the specification, there will naturally be deviations of small angles between the supposedly aligned instrument and mirror axes. In Figure 2-2 an exaggerated representation of those deviations from nominal is shown. It will be assumed in this study that the cosines of the angles between supposedly aligned vectors are equal to one and the cosines of the angles between supposedly orthogonal vectors are equal to small first order numbers.

Additional geometry required in subsequent developments is the nominal location of the gyro output ($\underline{O}_k$) and spin ($\underline{S}_k$) axes relative to the input axes already described. Those nominal locations are shown in Figure 2-3.

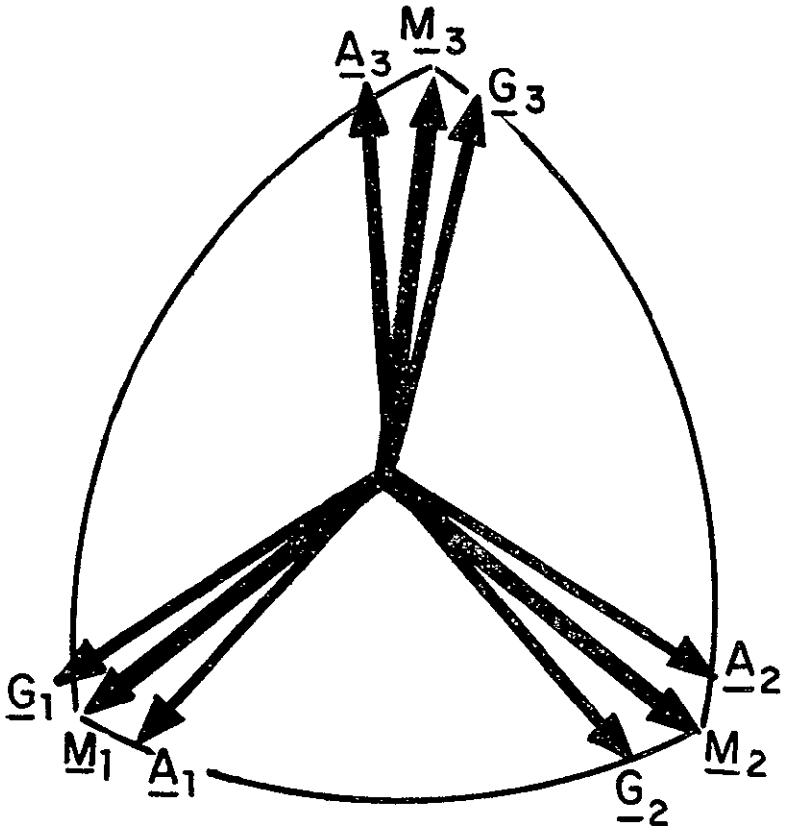

Figure 2-2. Instrument and Mirror Axes

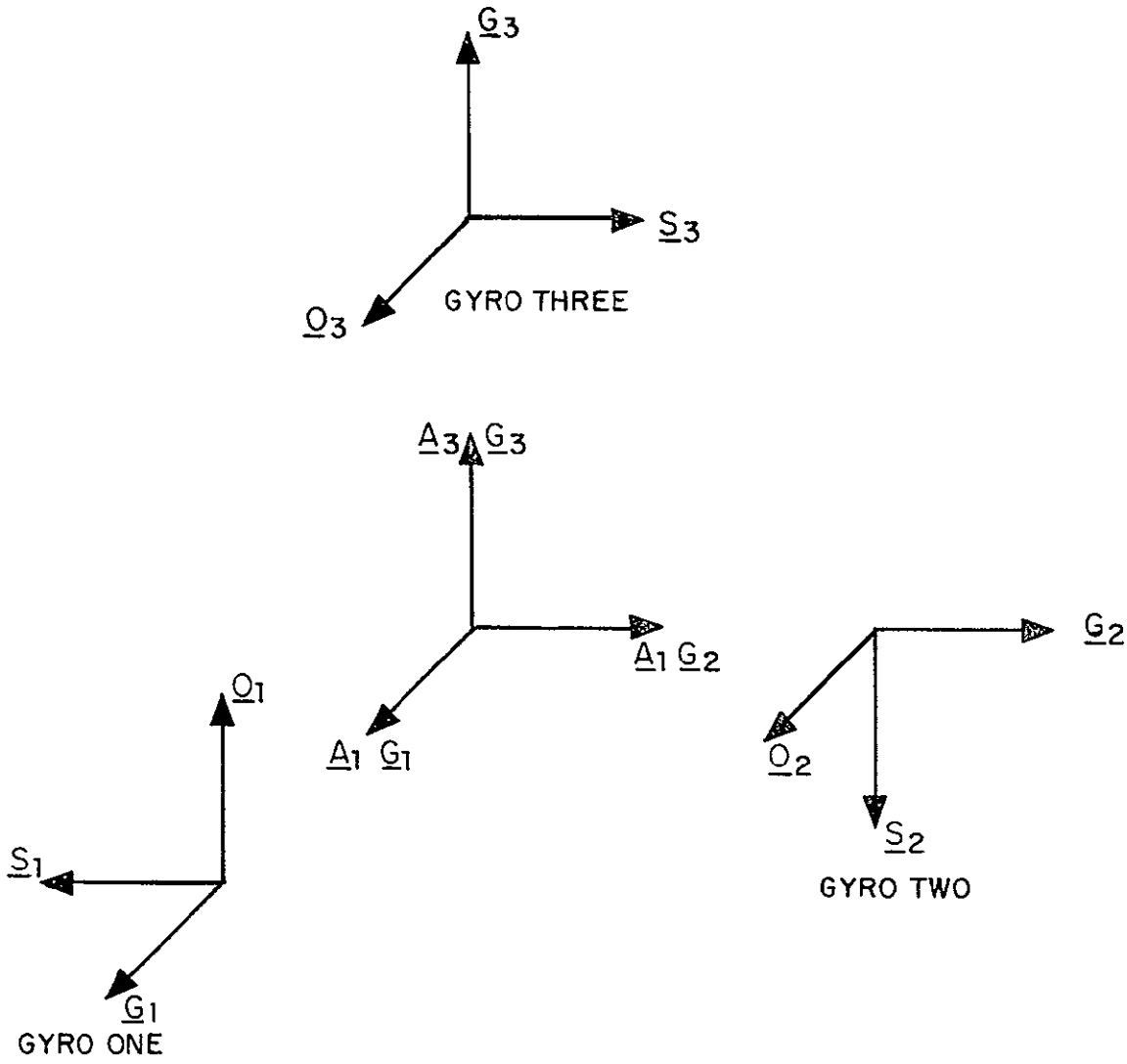

Figure 2-3. Nominal Orientation Between Gyros

It is always convenient, in inertial navigation, to define, from the geometry of the ISU, a set of orthogonal unit vectors which represent a common "body set of axes" to which all accelerometer and gyro outputs can be referred. The definition of those body axes is usually arbitrary; that is, any two ISU fixed vectors can be used. For the purpose of this study we will utilize two mirror normals. The body axes for the subject ISU are defined by

$$\underline{B}_1 = \underline{M}_1$$
$$\underline{B}_2 = (\underline{M}_1 \times \underline{M}_2) \times \underline{M}_1 / \left| \underline{M}_1 \times \underline{M}_2 \right|$$
$$\underline{B}_3 = (\underline{M}_1 \times \underline{M}_2) / \left| \underline{M}_1 \times \underline{M}_2 \right|$$

This definition is shown schematically in Figure 2-4.

2.2.2 Accelerometer Model

A schematic of the accelerometer is shown in Figure 2-5. The accelerometer consists of two masses separated by a spring and supported for centering purposes by two strings (S_1 and S_2) and ligaments normal to S_1 and S_2. When the accelerometer is at rest or moving with constant velocity, the sum of forces acting on the masses is zero. When the instrument is accelerated, the sum of forces will adjust to cause the masses to move with the same acceleration. Strings S_1 and S_2 will change in tension as a function of the component of acceleration along the strings. (This direction is the sensitive axis of the instrument.) Since the resonant frequency of a vibrating-string is a function of its tension, the frequency of strings S_1 and S_2 may be read and converted to acceleration along the sensitive axis.

The math model of the accelerometer is presented on Chart 2-1. The outputs from the accelerometer are the pulse counts, N_1 and N_2, representing the number of zero crossings from strings S_1 and S_2 in the time interval $t_a \rightarrow t_b$. Since the counting process can start and terminate at a fixed time for any sample. a quantization error (represented by Eq) of up to two counts (one per string) may occur. A fixed bias (D_0) is assumed. The entire output is multiplied by the scale factor D_1. The second and third order coefficients (D_2 and D_3) are extremely small.

In developing the model (see Appendix A) several assumptions were made. The most critical are

1. The accelerometer has negligible instrument noise.
2. The effects of terms higher than the third order are negligible.

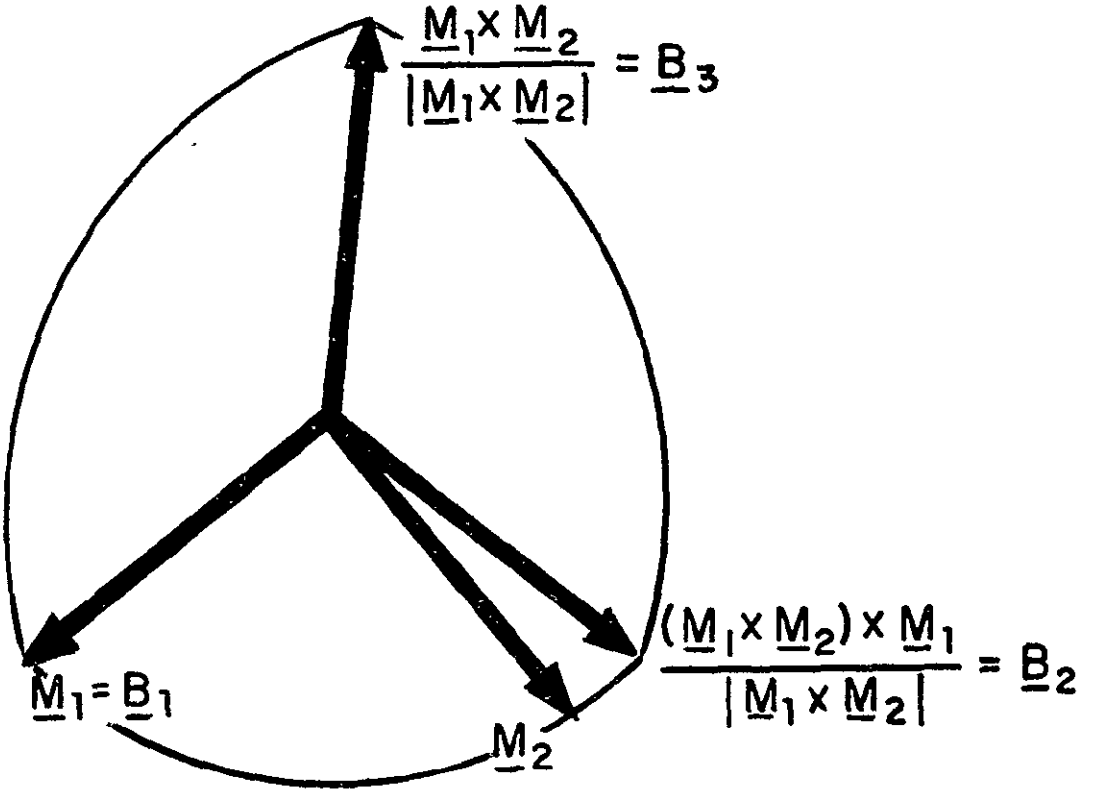

Figure 2-4. Body and Mirror Axes

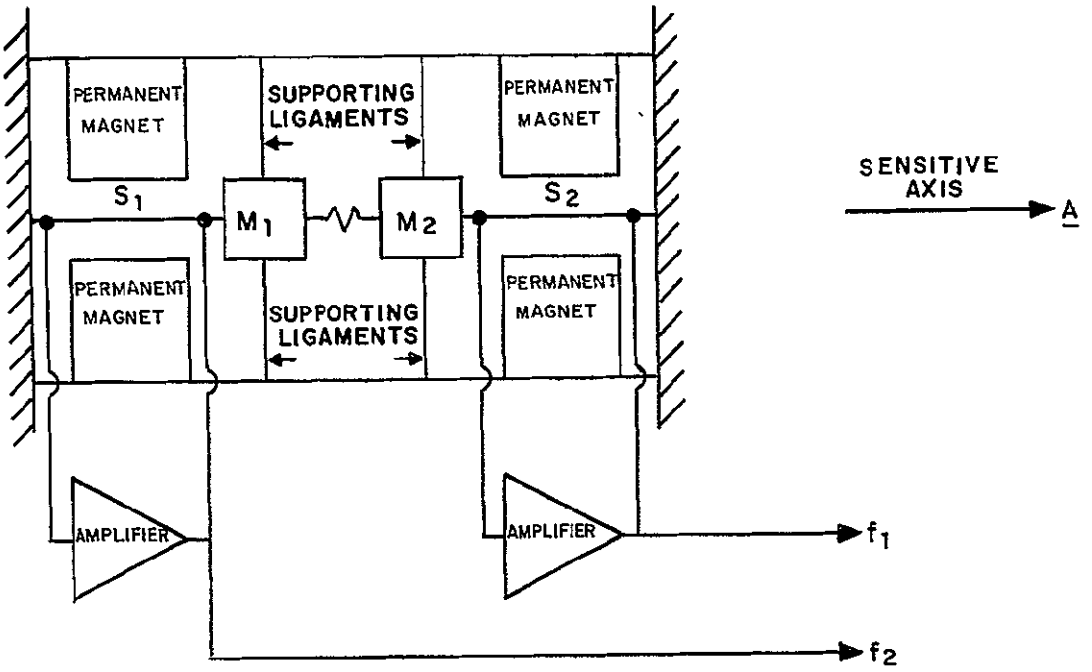

Model: ARMA D4E Vibrating String Accelerometer

Axis: $\underline{A}$ is a unit vector directed along strings S_1 and S_2 (the sensitive axis)

Figure 2-5. A Schematic Diagram of the Accelerometer

THE FUNDAMENTAL ACCELEROMETER MODEL

THE ACCELEROMETER MODEL IS:

$$\int_{t_a}^{t_b} f_2\,dt - \int_{t_a}^{t_b} f_1\,dt = (N_2 - N_1) + Eq = D_1 \int_{t_a}^{t_b} (\underline{a}\cdot\underline{A})dt + D_1 \left\{ \int_{t_a}^{t_b} [D_0 + D_2(\underline{a}\cdot\underline{A})^2 + D_3(\underline{a}\cdot\underline{A})^3]dt \right\}$$

WHERE:

- $\underline{a}$ is the acceleration applied to the accelerometer
- $t_a \leq t \leq t_b$ is the time interval over which $\underline{a}$ is measured
- $\underline{A}$ is a unit vector directed along the input axis of the accelerometer
- N_1 and N_2 are the number of zero crossings detected in $t_a \leq t \leq t_b$ from both strings of the accelerometer
- Eq is the instrument quantization error due to the fact that t_a and t_b do not correspond to zero crossings
- D_1 is the accelerometer scale factor
- D_0 is the accelerometer bias
- D_2 is the second order coefficient
- D_3 is the third order coefficient
- f_2 and f_1 are string frequencies in pulses/second

3. There are no cross coupling effects.
4. The strings are colinear.

2.2.3 Gyro Model

The gyroscopes used in the ERC strapdown ISU are Honeywell GG334A single degree of freedom, pulse rebalance gyros. The gyros contain a gimballed rotor as shown in Figure 2-6. The rotor spins at a high angular rate. The gimbal is restrained by the gimbal bearings to rotate with respect to the case about the $\underline{O}$ axis only as shown in the figure. Any angular motion of the gyro case about the input axis, $\underline{G}$, will generate a gyroscopic torque that tends to rotate the gimbal about $\underline{O}$. A signal generator measures the gimbal deflection. The deflection is compared at a 3.6 KHz rate with two equal thresholds of opposite sign and a positive, negative, or zero pulse is generated, based on the results of the comparison. This signal is sampled by the readout electronics and fed to a torque generator where a torque pulse is generated to offset the deflection.

The model of the gyro is given on the accompanying chart. (See Appendix B for a derivation.) $\sum_{k=1}^{N} \delta_K$ is the net count of positive and negative rebalance torques. $\Delta\Phi$ is the scale factor of the instrument. The term $\int_{t_0}^{t_N} (\underline{\omega} \cdot \underline{G})\, dt$ is the desired information from the instrument, and is equal to the integral of the angular velocity component along the sensitive axis. R is a fixed bias term. The three terms with coefficients, B_I, B_O and B_S are due to the fact that the center of force of the gimbal support differs from the gimbal center of mass, causing a torque proportional to acceleration (mass unbalance effect). Terms with coefficients C_{II}, C_{SS}, C_{IS}, C_{OS} and C_{IO} arise because of the deformations of the gimbal, caused by acceleration forces that produce mass unbalance effects. The term with Q_{II} coefficient is due to scale factor nonlinearities. The Q_{IS} term is due to the differences of moments of inertia about $\underline{S}$ and $\underline{O}$. The term containing J is the effect of dynamic coupling because of finite gimbal inertia.

2.2.4 Q Matrices

In Section 2.1 we defined the Q^A and Q^G matrices as those constant matrices which transform the integral of the instrument-axes components of applied acceleration and angular velocity into the integrals of the body-axes components of the same vectors. In this subsection we will specifically define those matrices.

First, the Q^A and Q^G matrices, as suggested by the superscripts, transform, respectively, the integrals of the accelerometer-axes components and the integrals of the gyro-axes components. Second, Q^A and Q^G, being constant matrices, transform all

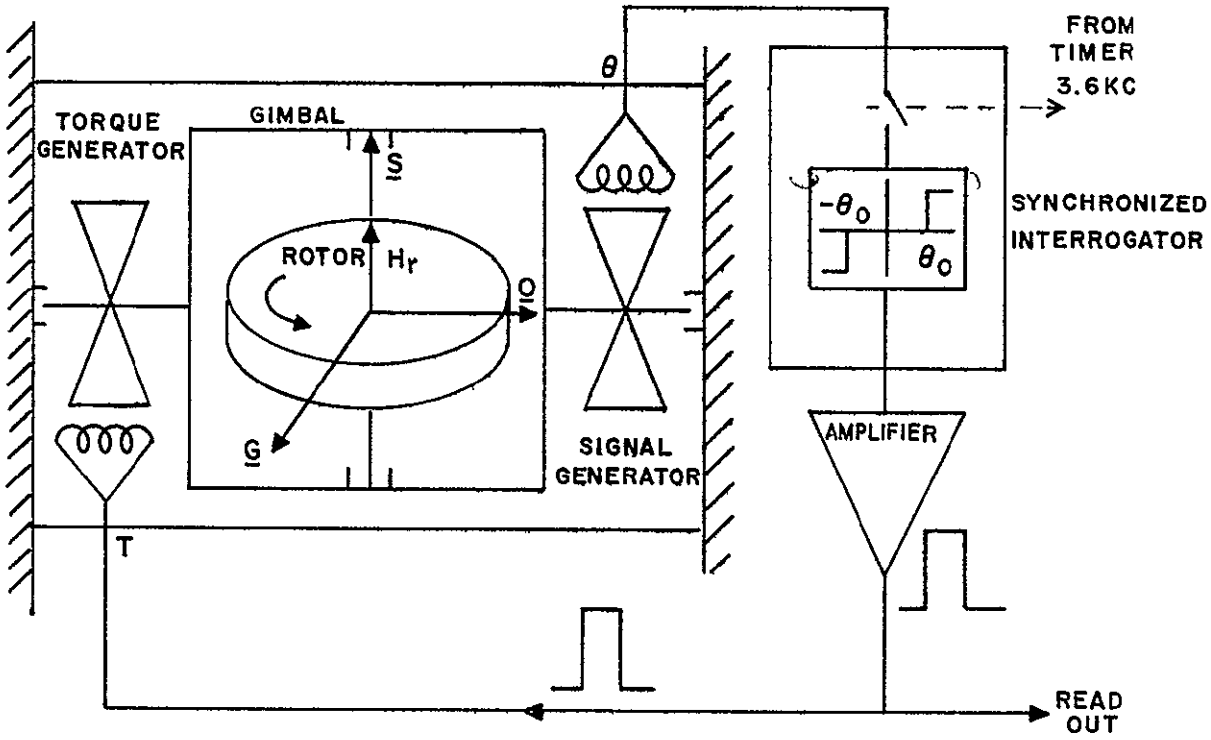

Model: Honeywell GG 334A single-degree-of-freedom, pulse rebalance gyroscope.

Axes: $\underline{S}$ is a unit vector along the spin axis of the rotor.
$\underline{O}$ is a unit vector along the output axis as defined by the gimbal.
$\underline{G} = \underline{O} \times \underline{S}$ is the sensitive axis of the gyro.

Figure 2-6. A Schematic Diagram of the Gyro

THE FUNDAMENTAL GYRO MODEL

THE GYRO MODEL IS:

$$\Delta\Phi \left[\sum_{k=1}^{N} \delta_k\right] = \int_{t_0}^{t_N} (\underline{\omega}\cdot\underline{G})\, dt + \int_{t_0}^{t_N} \Big[R + B_I(\underline{a}\cdot\underline{G}) + B_O(\underline{a}\cdot\underline{O}) + B_S(\underline{a}\cdot\underline{S}) + C_{II}(\underline{a}\cdot\underline{G})^2 + C_{SS}(\underline{a}\cdot\underline{S})^2 + C_{IS}(\underline{a}\cdot\underline{G})(\underline{a}\cdot\underline{S}) + C_{OS}(\underline{a}\cdot\underline{O})(\underline{a}\cdot\underline{S}) + C_{IO}(\underline{a}\cdot\underline{G})(\underline{a}\cdot\underline{O}) + Q_{II}(\underline{\omega}\cdot\underline{G})^2 + Q_{IS}(\underline{\omega}\cdot\underline{G})(\underline{\omega}\cdot\underline{S}) + J\frac{d}{dt}(\underline{\omega}\cdot\underline{O})\Big] dt + \Delta n + Eq$$

WHERE

- $\underline{\omega}$ is the angular velocity applied to the gyro
- $\underline{a}$ is the acceleration applied to the gyro
- $t_0 \le t \le t_N$ is the time interval over which $\underline{a}$ and $\underline{\omega}$ are measured
- $t_N - t_0 = N\tau$, where N is an integer, and τ is the gyro sampling period
- $\underline{S}$ is a unit vector along the spin axis of the rotor
- $\underline{O}$ is a unit vector directed along the output axis as defined by the gimbal
- $\underline{G}$ is a unit vector along $\underline{O} \times \underline{S}$ (that is, the sensitive axis of the gyro)
- δ_k is the kth gyro pulse, equal to +1, -1, or 0 for positive, negative, or no pulse
- $\Delta\Phi$ is the gyro scale factor
- R is the gyro bias
- B_I B_O and B_S are the gyro unbalance coefficients
- C_{II} C_{SS} C_{IS} C_{OS} and C_{IO} are the gyro compliance coefficients
- Q_{IS} and Q_{II} are dynamic coupling coefficients due to gimbal deflection and scale factor nonlinearity, respectively
- J is the angular rate coefficient
- Δn is the effect of gyro noise over the $[t_0, t_N]$ interval
- Eq is the gyro quantization error

triples of vector components between the frames, not just the integrals of those vector components. (That is, the Q matrices can be taken in and out of the integral at will.) Therefore, we can say that Q^A and Q^G are defined by:

$$\begin{bmatrix} \underline{B}_1 \\ \underline{B}_2 \\ \underline{B}_3 \end{bmatrix} = \begin{bmatrix} Q^A \end{bmatrix} \begin{bmatrix} \underline{A}_1 \\ \underline{A}_2 \\ \underline{A}_3 \end{bmatrix}$$

$$\begin{bmatrix} \underline{B}_1 \\ \underline{B}_2 \\ \underline{B}_3 \end{bmatrix} = \begin{bmatrix} Q^G \end{bmatrix} \begin{bmatrix} \underline{G}_1 \\ \underline{G}_2 \\ \underline{G}_3 \end{bmatrix}$$

It will be seen in Section 4 that calibration determines not Q^A and Q^G but $(Q^A)^{-1}$ and $(Q^G)^{-1}$. We therefore need to deduce the matrices from their inverses. From the geometry presented in Section 2.2.1 it is seen that the Q^A and Q^G matrices are approximately identity matrices. This fact makes the deduction of the matrices from their inverses quite simple. In the accompanying chart that deduction is presented. Note, in Chart 2-3, that the inverses appear, at quick glance, to be orthogonal (that is the elements are "direction cosines"). This apparent orthogonality results from $\underline{B}_k$ being orthogonal. However $\underline{G}_k$ and $\underline{A}_k$ are not, in general, orthogonal, and therefore the inverse matrices are also not orthogonal.

In Appendix C alternate forms of the Q^A and Q^G matrices are presented. Those forms are functions of the separation-angles between the unit-vectors contained within the ISU. Even though we will not specifically present techniques for finding separation-angles, the reader may be interested in those forms for the purpose of deducing separation angles from the calibration-determined $(Q^A)^{-1}$ and $(Q^G)^{-1}$ elements.

2.2.5 Preprocessing Computations

In this section we will show how the ISU geometry and mathematical models lead to the specific equations found in the initial computational routines of a navigation loop. Those equations, which we call the Preprocessing Computations, include all of the constants which must be determined during a laboratory calibration.

Referring to the flow diagram presented in Figure 2-1 we see that the initial routine in the navigation loop is the transformation of the instrument outputs into a knowledge of the integrals of the instrument-axes components of applied acceleration and angular velocity. Referring to the instrument models, we see that the models represent functional relationships between the inputs and outputs of the initial navigation routine. (This statement,

Determination of Q^A and Q^G from $(Q^A)^{-1}$ and $(Q^G)^{-1}$

- The calibration determines not Q^A and Q^G but $(Q^A)^{-1}$ and $(Q^G)^{-1}$.
- The inverse matrices have the form.

$$(Q^A)^{-1} = \begin{bmatrix} (\underline{A}_1 \cdot \underline{B}_1) & (\underline{A}_1 \cdot \underline{B}_2) & (\underline{A}_1 \cdot \underline{B}_3) \\ (\underline{A}_2 \cdot \underline{B}_1) & (\underline{A}_2 \cdot \underline{B}_2) & (\underline{A}_2 \cdot \underline{B}_3) \\ (\underline{A}_3 \cdot \underline{B}_1) & (\underline{A}_3 \cdot \underline{B}_2) & (\underline{A}_3 \cdot \underline{B}_3) \end{bmatrix}$$

$$(Q^G)^{-1} = \begin{bmatrix} (\underline{G}_1 \cdot \underline{B}_1) & (\underline{G}_1 \cdot \underline{B}_2) & (\underline{G}_1 \cdot \underline{B}_3) \\ (\underline{G}_2 \cdot \underline{B}_1) & (\underline{G}_2 \cdot \underline{B}_2) & (\underline{G}_2 \cdot \underline{B}_3) \\ (\underline{G}_3 \cdot \underline{B}_1) & (\underline{G}_3 \cdot \underline{B}_2) & (\underline{G}_3 \cdot \underline{B}_3) \end{bmatrix}$$

- Because of the excellent mechanical specifications on the strapdown ISU, each of the above matrices will have ones on the diagonals and first order small quantities on the off-diagonal. That is, each matrix can be written as.

$$I + E$$

where I is the identity matrix and E is a small off-diagonal matrix.

- The inverse of (I + E) (to first order) is (I - E).
- The Q^A and Q^G matrices can, therefore, be written as:

$$Q^A = \begin{bmatrix} 1 & -(\underline{A}_1 \cdot \underline{B}_2) & -(\underline{A}_1 \cdot \underline{B}_3) \\ -(\underline{A}_2 \cdot \underline{B}_1) & 1 & -(\underline{A}_2 \cdot \underline{B}_3) \\ -(\underline{A}_3 \cdot \underline{B}_1) & -(\underline{A}_3 \cdot \underline{B}_2) & 1 \end{bmatrix}$$

$$Q^G = \begin{bmatrix} 1 & -(\underline{G}_1 \cdot \underline{B}_2) & -(\underline{G}_1 \cdot \underline{B}_3) \\ -(\underline{G}_2 \cdot \underline{B}_1) & 1 & -(\underline{G}_2 \cdot \underline{B}_3) \\ -(\underline{G}_3 \cdot \underline{B}_1) & -(\underline{G}_3 \cdot \underline{B}_2) & 1 \end{bmatrix}$$

where all elements within the matrices are found in calibration.

of course, assumes that quantization and noise are neglected.) The mathematical model, functional relationships are not, however, explicitly in the form: routine output = f (routine input). To the contrary, the relationships are the inverse: routine input = g (routine output). The desired navigation equations must therefore result from an inversion of the instrument mathematical models.

The inversion of the models is quite a simple matter. This is due to the fact that each instrument is designed to be a linear instrument, therefore, all "nonlinear" terms are the result of design deficiencies and therefore are quite small relative to the proportional term plus bias. We conclude then that all "nonlinear" terms can be approximated by functions of the instrument outputs. The following discussion shows how this is accomplished.

The accelerometer model (neglecting quantization and noise) has the form:

$$\Delta N = D_1 \int (\underline{a} \cdot \underline{A})\, dt + D_1 D_0 \int dt + \text{higher order terms}$$

where ΔN is the difference in the number of zero crossings detected from each string in the time period over which the integrations in the equation are made. In the following discussions, this time period will always equal Δt.

As a first order approximation,

$$\int (\underline{a} \cdot \underline{A})\, dt = \frac{1}{D_1} (\Delta N - D_1 D_0 \Delta t)$$

Let us define

$$\overline{(\underline{a} \cdot \underline{A})} \Delta t \equiv \int (\underline{a} \cdot \underline{A})\, dt$$

or

$$\overline{(\underline{a} \cdot \underline{A})} = \frac{\int (\underline{a} \cdot \underline{A})\, dt}{\int dt} = \frac{1}{D_1 \Delta t} (\Delta N - D_1 D_0 \Delta t)$$

We can see that $\overline{(\underline{a} \cdot \underline{A})}$ is, from the mean value theorem of calculus, a value of $(\underline{a} \cdot \underline{A})$ somewhere in the time period of integration.

Referring to the second order term

$$\int \overline{(\underline{a} \cdot \underline{A})}^2\, dt$$

which can be written

$$\overline{(\underline{a} \cdot \underline{A})^2 \Delta t}$$

We see that, when the period of integration is chosen short enough that $(\underline{a} \cdot \underline{A})$ is essentially constant over each period, then it can be assumed that.

$$\overline{(\underline{a} \cdot \underline{A})^2} = \overline{(\underline{a} \cdot \underline{A})}^2$$

(This is a very good approximation, considering the fact that the coefficient of the square term is quite small.) From all of the above statements we can therefore infer:

$$\int (\underline{a} \cdot \underline{A})^2 \, dt = \left[\frac{1}{D_1 \Delta t} (\Delta N - D_1 D_0 \Delta t) \right]^2 \Delta t$$

Similarly, the cubic term can be written as

$$\int (\underline{a} \cdot \underline{A})^3 \, dt = \left[\frac{1}{D_1 \Delta t} (\Delta N - D_1 D_0 \Delta t) \right]^3 \Delta t$$

The expression for $\overline{(\underline{a} \cdot \underline{A})}$ can also be used to determine the gyro unbalance integrals from the approximations:

$$\int (\underline{a} \cdot \underline{G}_k) \, dt = \int (\underline{a} \cdot \underline{A}_k) \, dt$$

$$\int (\underline{a} \cdot \underline{O}_k) \, dt = \begin{bmatrix} 0 & 0 & 1 \\ 1 & 0 & 0 \\ 1 & 0 & 0 \end{bmatrix} \begin{bmatrix} \int (\underline{a} \cdot A_1) \, dt \\ \int (\underline{a} \cdot A_2) \, dt \\ \int (\underline{a} \cdot A_3) \, dt \end{bmatrix} \quad \text{(See Figure 2-3.)}$$

$$\int (\underline{a} \cdot \underline{S}_k) \, dt = \begin{bmatrix} 0 & -1 & 0 \\ 0 & 0 & -1 \\ 0 & 1 & 0 \end{bmatrix} \begin{bmatrix} \int (\underline{a} \cdot A_1) \, dt \\ \int (\underline{a} \cdot A_2) \, dt \\ \int (\underline{a} \cdot A_3) \, dt \end{bmatrix}$$

where $$\int (\underline{a} \cdot \underline{A}_k) \, dt = \frac{1}{(D_1)_k} \left[(\Delta N)_k - (D_1 D_0)_k \Delta t \right]$$

(We have refrained from using the instrument index k until it was absolutely essential. This served to keep the notation as simple as possible.)

The compliance integrals are found to be similar to the higher-order accelerometer terms. We note that all of the gyro approximations utilize the outputs of the accelerometers to compensate for the gyro acceleration-sensitive terms.

After all approximations, we will have equations of the form:

$$\int (\underline{a} \cdot \underline{A}_k)\, dt = f(\text{accelerometer outputs})$$

$$\int (\underline{\omega} \cdot \underline{G}_k)\, dt = g(\text{accelerometer and gyro outputs})$$

The Q^A and Q^G matrices can then be used to find.

$$\int (\underline{a} \cdot \underline{B}_k)\, dt = \sum_\ell Q^A_{k\ell} \int (\underline{a} \cdot \underline{A}_\ell)\, dt$$

$$\int (\underline{\omega} \cdot \underline{B}_k)\, dt = \sum_\ell Q^G_{k\ell} \int (\underline{\omega} \cdot \underline{G}_\ell)\, dt$$

The above statements lead to the complete set of computations, which are found on the following chart. We will henceforth, in this document, refer to those equations as the Preprocessing Computations. The following nomenclature is required for the understanding of the Preprocessing Computations:

- $(\Sigma\gamma)_{k1}$ and $(\Sigma\gamma)_{k2}$ are the counts from the one and two strings of the k^{th} accelerometer.
- $(\Sigma\delta)_k$ is the count from the k^{th} gyro.
- S_2^T is the clock scale factor (the subscript 2 serves to distinguish this scale factor from another used in calibration).
- (Σn_2^T) is the count from the system clock. All other terms have been previously defined.

2.2.6 Calibration Requirements

The Preprocessing Computations developed in the preceding subsection are seen to be a function of a great number of constants. Those constants were, in Section 2.1, defined as the constants to be calibrated. An explicit statement of the calibration requirements is therefore the determination of the quantitative value of the constants contained within the Preprocessing routine. In Chart 2-5 those constants are listed. As a matter of convenience, the nominal values, ranges, and precision requirements, where available, are given.

PREPROCESSING COMPUTATIONS

Inputs $(\Sigma\gamma)_{k2}, (\Sigma\gamma)_{k1}, (\Sigma\delta)_k$, and $\left(\Sigma n_2^T\right)$ for k = 1, 2, 3

The outputs $\int_t^{t+\Delta t} (\underline{\omega}\cdot\underline{B}_k)dt$ and $\int_t^{t+\Delta t} (\underline{a}\cdot\underline{B}_k)dt$ (k = 1, 2, 3) are given by the following computations

- $P_k^A \equiv [(\Sigma\gamma)_{k2} - (\Sigma\gamma)_{k1}]$
- $P_k^G \equiv (\Sigma\delta)_k$
- $\Delta t \equiv S_2^T\left(\Sigma n_2^T\right)$
- $\overline{[(\underline{\omega}\cdot\underline{G}_k)\Delta t]} \equiv P_k^G(\Delta\Phi)_k - (R)_k\Delta t$
- $\overline{[(\underline{a}\cdot\underline{A}_k)\Delta t]} \equiv P_k^A/(D_1)_k - (D_0)_k\,\Delta t$
- $\overline{(\underline{\omega}\cdot\underline{G}_k)} \equiv \overline{[(\underline{\omega}\cdot\underline{G}_k)\Delta t]}/\Delta t$
- $\overline{(\underline{a}\cdot\underline{A}_k)} \equiv \overline{[(\underline{a}\cdot\underline{A}_k)\Delta t]}/\Delta t$
- $\overline{(\underline{a}\cdot\underline{G}_k)} \equiv \overline{(\underline{a}\cdot\underline{A}_k)}$
- $$\overline{(\underline{a}\cdot\underline{O}_k)} = \begin{bmatrix} 0 & 0 & 1 \\ 1 & 0 & 0 \\ 1 & 0 & 0 \end{bmatrix} \begin{bmatrix} \overline{(\underline{a}\cdot\underline{A}_1)} \\ \overline{(\underline{a}\cdot\underline{A}_2)} \\ \overline{(\underline{a}\cdot\underline{A}_3)} \end{bmatrix}$$
- $$\overline{(\underline{a}\cdot\underline{S}_k)} = \begin{bmatrix} 0 & -1 & 0 \\ 0 & 0 & -1 \\ 0 & 1 & 0 \end{bmatrix} \begin{bmatrix} \overline{(\underline{a}\cdot\underline{A}_1)} \\ \overline{(\underline{a}\cdot\underline{A}_2)} \\ \overline{(\underline{a}\cdot\underline{A}_3)} \end{bmatrix}$$
- $$\int_t^{t+\Delta t}(\underline{\omega}\cdot\underline{G}_k)dt = \overline{[(\underline{\omega}\cdot\underline{G}_k)\Delta t]} - [(B_I)_k\overline{(\underline{a}\cdot\underline{G}_k)} + (B_O)_k\overline{(\underline{a}\cdot\underline{O}_k)} + (B_S)_k\overline{(\underline{a}\cdot\underline{S}_k)}]\Delta t$$
$$- [(C_{II})_k\overline{(\underline{a}\cdot\underline{G}_k)}^2 + (C_{SS})_k\,\overline{(\underline{a}\cdot\underline{S}_k)}^2]\,\Delta t$$
$$- [(C_{IS})_k\overline{(\underline{a}\cdot\underline{G}_k)}\,\overline{(\underline{a}\cdot\underline{S}_k)} + (C_{OS})_k\overline{(\underline{a}\cdot\underline{O}_k)}\,\overline{(\underline{a}\cdot\underline{S}_k)} + (C_{IO})_k\overline{(\underline{a}\cdot\underline{G}_k)}\,\overline{(\underline{a}\cdot\underline{O}_k)}]\Delta t$$
$$- [(Q_{II})_k\overline{(\underline{\omega}\cdot\underline{G}_k)}^2 + (Q_{IS})_k\overline{(\underline{\omega}\cdot\underline{G}_k)}\,\overline{(\underline{\omega}\cdot\underline{S}_k)}]\Delta t$$
- $$\int_t^{t-\Delta t}(\underline{a}\cdot\underline{A}_k)dt = \overline{[(\underline{a}\cdot\underline{A}_k)\Delta t]} - (D_2)_k\overline{(\underline{a}\cdot\underline{A}_k)}^2\Delta t - (D_3)_k\,\overline{(\underline{a}\cdot\underline{A}_k)}^3\Delta t$$
- $$\int_t^{t+\Delta t}(\underline{\omega}\cdot\underline{B}_k)dt = \sum_\ell Q^G_{k\ell}\int_t^{t-\Delta t}(\underline{\omega}\cdot\underline{G}_\ell)dt$$
- $$\int_t^{t+\Delta t}(\underline{a}\cdot\underline{B}_k)dt = \sum_\ell Q^A_{k\ell}\int_t^{t-\Delta t}(\underline{a}\cdot\underline{A}_\ell)dt$$

where

- $$Q^G = \begin{bmatrix} 1 & -(\underline{G}_1\cdot\underline{B}_2) & -(\underline{G}_1\cdot\underline{B}_3) \\ -(\underline{G}_2\cdot\underline{B}_1) & 1 & -(\underline{G}_2\cdot\underline{B}_3) \\ -(\underline{G}_3\cdot\underline{B}_1) & -(\underline{G}_3\cdot\underline{B}_2) & 1 \end{bmatrix}$$
- $$Q^A = \begin{bmatrix} 1 & -(\underline{A}_1\cdot\underline{B}_2) & -(\underline{A}_1\cdot\underline{B}_3) \\ -(\underline{A}_2\cdot\underline{B}_1) & 1 & -(\underline{A}_2\cdot\underline{B}_3) \\ -(\underline{A}_3\cdot\underline{B}_1) & -(\underline{A}_3\cdot\underline{B}_2) & 1 \end{bmatrix}$$

CHART 2-5

LISTING OF CALIBRATION PARAMETERS

Accelerometer Coefficients			
Name and Units	Nominal Value	Range	Precision
$D_1 \left(\frac{\text{Pulses}}{\text{sec}}/g\right)$	254	$252 \rightarrow 256$	$\Delta D_1/D_1 = 2\times10^{-6}$
D_0 (g)	10^{-1}	$0 \rightarrow 2\times10^{-1}$	$\Delta D_0 = 7\times10^{-5}$
$D_2(g/g^2)$	0	$\pm 13\times10^{-6}$	
$D_3(g/g^3)$	27×10^{-6}	$(26 \rightarrow 28)\times10^{-6}$	
$(\underline{A}_k \cdot \underline{B}_k)$	1	0	
$(\underline{A}_k \cdot \underline{B}_\ell)$	0		

Gyro Coefficients			
Name and Units	Nominal Value	Range	Precision
$\Delta\Phi$(deg/pulse)	3.3×10^{-3}		$\Delta(\Delta\Phi)/\Delta\Phi = 10^{-4}$
R(deg/hr)	0	± 2	$\Delta R = 0.005$
B_I(deg/hr/g)	0	± 1	
B_O(deg/hr/g)	0	± 1	
B_S(deg/hr/g)	0	± 1	
$C_{II}(deg/hr/g^2)$	0	± 0.04	
$C_{SS}(deg/hr/g^2)$	0	± 0.04	
$C_{IS}(deg/hr/g^2)$	0	± 0.04	
$C_{OS}(deg/hr/g^2)$	0	± 0.04	
$C_{IO}(deg/hr/g^2)$	0	negligible	
Q_{II}(hr/deg)	0		
$Q_{IS}\left(\frac{\text{deg}}{\text{hr}}\right) \Big/ \left(\frac{\text{rad}}{\text{sec}}\right)^2$	4		
J(hr)	3.7×10^{-7}		
$(\underline{G}_k \cdot \underline{B}_k)$	1	0	
$(\underline{G}_k \cdot \underline{B}_\ell)$	0		

Note that a great number of the constants have a nominal value of zero. Note also that the accelerometer bias term is the only term which has a nominal value which appreciably affects an instrument output (that is, affects the output over and above the effect of the linear term). The relatively large value of the bias term accounts for the bias being utilized in the preceding subsection as a part of the higher-order term approximations.

Only the precisions of the bias and scale factor are given. The scale factor precision is presented as a relative requirement (ratio of uncertainty to magnitude). The bias precision is presented as an absolute error. It will be shown in the trade-off document that the errors in each of the other terms act as either a scale-factor-like or bias-like error. Therefore, all precisions are inferred from either the scale factor or bias precision.

2.3 ALIGNMENT REQUIREMENTS

In Section 2.1 alignment was defined as the initialization of the matrix which transforms from an ISU-fixed frame of reference (body axes) to a navigation frame. In this section our purpose is to explicitly state the requirements for determining that matrix. Three alternative techniques will be presented. The definition of the three alignment techniques will be presented in Section 2.3.1. The alignment requirement associated with each technique will be found to be the measurement of either the body-axes or earth-axes components of two system vectors. In Section 2.3.2 the geometry associated with the alignment techniques will be presented. The explicit functional form of the alignment matrix for all three techniques will be delineated in Section 2.3.3.

2.3.1 Definition of Three Alignment Techniques

Alignment has been defined as the initialization of the body-to-navigation-axes transformation matrix. For the subject ISU, the body axes ($\underline{B}_k$) are defined by the normals to two ISU-fixed mirrors (see Section 2.2.1). For the purpose of this study, we will assume that the navigation axes are aligned with a set of local-level earth axes ($\underline{E}_k$), where

$\underline{E}_1$ is directed up (along the line of local gravity)

$\underline{E}_2$ is directed east (normal to the local meridian)

$\underline{E}_3$ is directed north (normal to $\underline{E}_1$ and $\underline{E}_2$).

(Throughout the text we will, at times, also refer to the earth axes as $\underline{U}$, $\underline{E}$, and $\underline{N}$, where

$$\underline{U} = \underline{E}_1$$
$$\underline{E} = \underline{E}_2$$
$$\underline{N} = \underline{E}_3$$

We can now more explicitly define the alignment problem as the determination (at some time, say t) of the 3x3 orthogonal matrix T, where T is defined by:

$$\begin{bmatrix} \underline{E}_1 \\ \underline{E}_2 \\ \underline{E}_3 \end{bmatrix} = \begin{bmatrix} \underline{U} \\ \underline{E} \\ \underline{N} \end{bmatrix} = \begin{bmatrix} \\ T \\ \\ \end{bmatrix} \begin{bmatrix} \underline{B}_1 \\ \underline{B}_2 \\ \underline{B}_3 \end{bmatrix}$$

There are numerous techniques for determining the elements of the matrix T. Each technique considered in this report is based upon expressing the matrix functionally in terms of the components of two vectors (which are known, in an operational situation) in both the body- and earth-fixed frames. The typical operational situation would be an earth-fixed orientation of the ISU. Assuming that the operationally available measuring devices to be used during alignment are any combination of three gyros, three accelerometers, or two two-degree-of-freedom autocollimators, then the vectors which can be used to functionally define the T matrix are:

- The unit mirror normals $\underline{M}_1$ and $\underline{M}_2$, which can be measured in the earth frame by the autocollimators and are known in the body frame because they define the body frame
- The local environment vectors $\underline{g}$ and $\underline{\omega}^E$ ("gravity"* and earth rate), which can be determined in the body frame by the accelerometers and gyros and which are known in the earth frame because they explicitly define the earth frame, that is,

$$\underline{E}_1 = \underline{U}$$
$$\underline{E}_2 = (\underline{W} \times \underline{U}) / |\underline{W} \times \underline{U}|$$
$$\underline{E}_3 = \underline{U} \times (\underline{W} \times \underline{U}) / |\underline{W} \times \underline{U}|$$

where $\underline{U} = \underline{g}/|\underline{g}|$

and $\underline{W} = \underline{\omega}^E / |\underline{\omega}^E|$

The T matrix can be expressed in terms of the components of any two of the four above-mentioned vectors ($\underline{M}_1$, $\underline{M}_2$, $\underline{g}$, and $\underline{\omega}^E$); but, as a contract requirement, only the following three combinations are of interest in this study:

*See Section 3.1.1 for a definition of "gravity".

- $\underline{M}_1$ and $\underline{M}_2$
- $\underline{M}_1$ and $\underline{g}$
- $\underline{g}$ and $\underline{\omega}^E$.

The names of the techniques which implement the use of the components of these three vector combinations are, respectively:

- Mirror Alignment
- Level Alignment
- Gyrocompass.

In the next subsection we will present the geometry of the four vectors ($\underline{M}_1$, $\underline{M}_2$, $\underline{g}$, and $\underline{\omega}^E$), and in the following subsections we will present the explicit mathematical relationships between the components of those vectors and the elements of the T matrix.

2.3.2 Alignment Geometry

In the preceding subsection we described alignment in terms of the determination of the components of two vectors in both the body- and earth-fixed frames. We chose, as alternatives, the vector combinations

- $\underline{M}_1$ and $\underline{M}_2$
- $\underline{M}_1$ and $\underline{g}$
- $\underline{g}$ and $\underline{\omega}^E$.

In this subsection we present the geometric relationship between the four vectors which are considered in our three techniques.

The required geometry is shown in Figure 2-7. The following comments explain the notation:

- $\underline{U}$ is a unit vector directed up; that is $\underline{U} = \underline{g} / |\underline{g}|$.
- $\underline{W}$ is a unit vector directed along earth-rate; that is $\underline{W} = \underline{\omega}^E / |\underline{\omega}^E|$.
- α_1 and α_2 are, respectively, "azimuths" of the one and two mirror normal, as determined by an autocollimator.
- θ_1 and θ_2 are, respectively, the "zeniths" of the one and two mirror normal, as determined by an autocollimator.

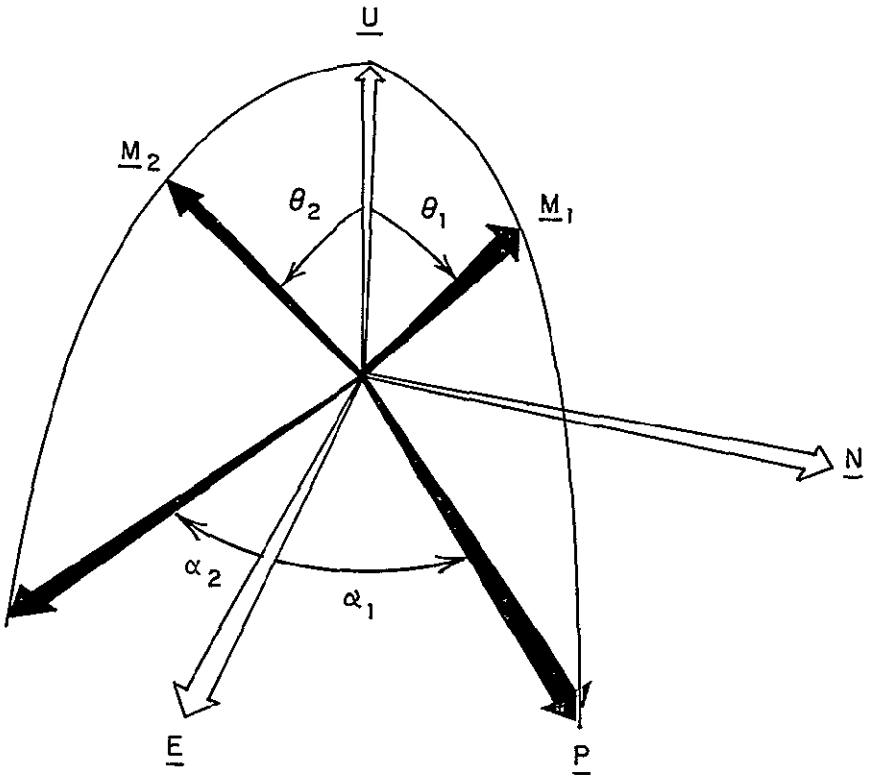

Figure 2-7. Earth and Mirror Axes

- λ is the angle between $\underline{U}$ and $\underline{W}$, which we will refer to as "local latitude".
- $\underline{P}$ is a unit vector directed along the projection of the one mirror normal into the local horizontal plane.

2.3.3 The Three Functional Forms of the Alignment Matrix

In this subsection we present the explicit mathematical relationships between the elements of the T matrix and the measurable body or earth referenced components of

- $\underline{M}_1$ and $\underline{M}_2$ for Mirror Alignment
- $\underline{M}_1$ and $\underline{g}$ for Level Alignment
- $\underline{g}$ and ω^E for Gyrocompass

These functional relationships are presented on the three accompanying charts. We will not, in this subsection, meticulously derive the relationships; but will instead present sufficient information such that the derivations are obvious. Let us consider each chart in turn.

Mirror Alignment

This derivation is quite easily explained. In Section 2.2.1 we defined the body-axes as:

$$\underline{B}_1 = \underline{M}_1$$

$$\underline{B}_2 = \frac{(\underline{M}_1 \times \underline{M}_2) \times \underline{M}_1}{|\underline{M}_1 \times \underline{M}_2|}$$

$$\underline{B}_3 = \frac{(\underline{M}_1 \times \underline{M}_2)}{|\underline{M}_1 \times \underline{M}_2|}$$

Therefore any vector, say $\underline{U}$, can be written in body coordinates as

$$\underline{U} = (\underline{U} \cdot \underline{M}_1)\underline{B}_1 + \frac{\underline{U} \cdot (\underline{M}_1 \times \underline{M}_2) \times \underline{M}_1}{|\underline{M}_1 \times \underline{M}_2|} \underline{B}_2 + \frac{\underline{U} \cdot (\underline{M}_1 \times \underline{M}_2)}{|\underline{M}_1 \times \underline{M}_2|} \underline{B}_3$$

and, after substituting the identity

$$\underline{U} = \underline{E} \times \underline{N} \text{ into the last component}$$

MIRROR ALIGNMENT MATRIX

Inputs $\theta_1, \alpha_1, \theta_2$ and α_2

From these quantities the alignment matrix is given by:

$$\begin{bmatrix} \\ T \\ \\ \end{bmatrix} = \begin{bmatrix} (\underline{U}\cdot\underline{M}_1) & \dfrac{(\underline{M}_1 \times \underline{U})\cdot(\underline{M}_1 \times \underline{M}_2)}{|\underline{M}_1 \times \underline{M}_2|} & \dfrac{(\underline{E} \times \underline{N})\cdot(\underline{M}_1 \times \underline{M}_2)}{|\underline{M}_1 \times \underline{M}_2|} \\ (\underline{E}\cdot\underline{M}_1) & \dfrac{(\underline{M}_1 \times \underline{E})\cdot(\underline{M}_1 \times \underline{M}_2)}{|\underline{M}_1 \times \underline{M}_2|} & \dfrac{(\underline{N} \times \underline{U})\cdot(\underline{M}_1 \times \underline{M}_2)}{|\underline{M}_1 \times \underline{M}_2|} \\ (\underline{N}\cdot\underline{M}_1) & \dfrac{(\underline{M}_1 \times \underline{N})\cdot(\underline{M}_1 \times \underline{M}_2)}{|\underline{M}_1 \times \underline{M}_2|} & \dfrac{(\underline{U} \times \underline{E})\cdot(\underline{M}_1 \times \underline{M}_2)}{|\underline{M}_1 \times \underline{M}_2|} \end{bmatrix}$$

where

$$|\underline{M}_1 \times \underline{M}_2| = [1 - (\underline{M}_1 \cdot \underline{M}_2)^2]^{1/2}$$

$$(\underline{M}_1 \cdot \underline{M}_2) = (\underline{M}_1 \cdot \underline{U})(\underline{M}_2 \cdot \underline{U}) + (\underline{M}_1 \cdot \underline{E})(\underline{M}_2 \cdot \underline{E}) + (\underline{M}_1 \cdot \underline{N})(\underline{M}_2 \cdot \underline{N})$$

$$\begin{bmatrix} (\underline{U}\cdot\underline{M}_1) \\ (\underline{E}\cdot\underline{M}_1) \\ (\underline{N}\cdot\underline{M}_1) \end{bmatrix} = \begin{bmatrix} \cos\theta_1 \\ \cos\alpha_1 \sin\theta_1 \\ \sin\alpha_1 \sin\theta_1 \end{bmatrix}, \quad \begin{bmatrix} (\underline{U}\cdot\underline{M}_2) \\ (\underline{E}\cdot\underline{M}_2) \\ (\underline{N}\cdot\underline{M}_2) \end{bmatrix} = \begin{bmatrix} \cos\theta_2 \\ \cos\alpha_2 \sin\theta_2 \\ \sin\alpha_2 \sin\theta_2 \end{bmatrix}$$

An optional technique might utilize the value of $|\underline{M}_1 \times \underline{M}_2|$ from a previous alignment thus eliminating the aforementioned dot product and square root operations.

and interchanging the dot and cross in the second component, we have

$$\underline{U} = [(\underline{U}\cdot\underline{M}_1)]\,\underline{B}_1 + \left[\frac{(\underline{M}_1 \times \underline{U})\cdot(\underline{M}_1 \times \underline{M}_2)}{|\underline{M}_1 \times \underline{M}_2|}\right] \underline{B}_2 + \left[\frac{\underline{E} \times \underline{N})\cdot(\underline{M}_1 \times \underline{M}_2)}{|\underline{M}_1 \times \underline{M}_2|}\right] \underline{B}_3$$

The three bracketed quantities are the elements of the first row of the T matrix. In the Mirror Alignment chart we see those elements in the first row, and similar elements for $\underline{E}$ and $\underline{N}$ in the second and third row. The relationships between those elements and the azimuth and zeniths as determined by optical equipment are listed below the matrix. The azimuth and zenith relationships are obvious from Figure 2-7.

Level Alignment

This derivation is quite simple if one separates the problem into three parts by defining matrices (T_1, T_2, and T_3 say), where the three matrices are defined by

$$\begin{bmatrix} \underline{E}_1 \\ \underline{E}_2 \\ \underline{E}_3 \end{bmatrix} = \begin{bmatrix} \\ T_1 \\ \\ \end{bmatrix} \begin{bmatrix} \underline{U} \\ \underline{P} \times \underline{U} \\ \underline{P} \end{bmatrix}$$

$$\begin{bmatrix} \underline{U} \\ \underline{P} \times \underline{U} \\ \underline{P} \end{bmatrix} = \begin{bmatrix} \\ T_2 \\ \\ \end{bmatrix} \begin{bmatrix} \underline{M}_1 \\ \underline{U} \\ \underline{M}_1 \times \underline{U} \end{bmatrix}$$

$$\begin{bmatrix} \underline{M}_1 \\ \underline{U} \\ \underline{M}_1 \times \underline{U} \end{bmatrix} = \begin{bmatrix} \\ T_3 \\ \\ \end{bmatrix} \begin{bmatrix} \underline{B}_1 \\ \underline{B}_2 \\ \underline{B}_3 \end{bmatrix}$$

Obviously $T = T_1 T_2 T_3$.

The three matrices shown in the Level Alignment chart are T_1, T_2, and T_3 respectively. The derivation of the T_1 matrix is obvious from the definition of $\underline{P}$ in Figure 2-7. The derivation of T_2 is based upon the fact that

$$\underline{P} \times \underline{U} = (\underline{M}_1 \times \underline{U}) / |\underline{M}_1 \times \underline{U}|$$

and

$$\underline{P} = \underline{U} \times (\underline{M}_1 \times \underline{U}) / |\underline{M}_1 \times \underline{U}|$$

LEVEL ALIGNMENT MATRIX

Inputs $(\underline{g}\cdot \underline{B}_1)$, $(\underline{g}\cdot \underline{B}_2)$, $(\underline{g}\cdot \underline{B}_3)$ and α_1

From these quantities the alignment matrix is given by:

$$\begin{bmatrix} \\ T \\ \\ \end{bmatrix} = \begin{bmatrix} 1 & 0 & 0 \\ 0 & \sin\alpha_1 & \cos\alpha_1 \\ 0 & -\cos\alpha_1 & \sin\alpha_1 \end{bmatrix} \begin{bmatrix} 0 & 1 & 0 \\ 0 & 0 & \dfrac{1}{|\underline{M}_1 \times \underline{U}|} \\ \dfrac{1}{|\underline{M}_1 \times \underline{U}|} & \dfrac{(\underline{M}_1\cdot \underline{U})}{|\underline{M}_1 \times \underline{U}|} & 0 \end{bmatrix} \begin{bmatrix} 1 & 0 & 0 \\ (\underline{U}\cdot\underline{B}_1) & (\underline{U}\cdot\underline{B}_2) & (\underline{U}\cdot\underline{B}_3) \\ 0 & -(\underline{U}\cdot\underline{B}_3) & (\underline{U}\cdot\underline{B}_2) \end{bmatrix}$$

where

- $(\underline{M}_1\cdot \underline{U}) = (\underline{U}\cdot \underline{B}_1)$
- $|\underline{M}_1 \times \underline{U}| = [1 - (\underline{M}_1\cdot \underline{U}^2)]^{1/2}$
- $(\underline{U}\cdot \underline{B}_k) = (\underline{g}\cdot \underline{B}_k)/g$
- $g = [(\underline{g}\cdot \underline{B}_1)^2 + (\underline{g}\cdot \underline{B}_2)^2 + (\underline{g}\cdot \underline{B}_3)^2]^{1/2}$

An optional technique might utilize any of the following additional inputs:

- The zenith angle (θ_1) of mirror one might be utilized to find $(\underline{M}_1\cdot \underline{U})$ from
$$(\underline{M}_1\cdot \underline{U}) = \cos\theta_1$$
- The magnitude of gravity (g) might be supplied from a local survey. This piece of information can be utilized to reduce the number of required accelerometers to two.

The derivation of T_3 is based upon the fact that

$$\underline{M}_1 = \underline{B}_1$$

$$\underline{U} = (\underline{U} \cdot \underline{B}_1)\,\underline{B}_1 + (\underline{U} \cdot \underline{B}_2)\,\underline{B}_2 + (\underline{U} \cdot \underline{B}_3)\,\underline{B}_3$$

$$\underline{M}_1 \times \underline{U} = (\underline{M}_1 \times \underline{U} \cdot \underline{B}_1)\,\underline{B}_1 + (\underline{M}_1 \times \underline{U} \cdot \underline{B}_2)\,B_2 + (\underline{M}_1 \times \underline{U} \cdot \underline{B}_3)\,\underline{B}_3$$

The third identity becomes, after substituting $\underline{M}_1 = \underline{B}_1$

$$\underline{M}_1 \times \underline{U} = -(\underline{U} \cdot \underline{B}_3)\,\underline{B}_2 + (\underline{U} \cdot \underline{B}_2)\,\underline{B}_3$$

Below the matrix expression we see the obvious relationships between the elements of the T_2 and T_3 matrices and the body components of $\underline{g}$(as determined by accelerometers). Below those relationships, we see alternate methods that utilize the zenith cosines and sines from an optical measurement, and g from a survey.

Gyrocompass

In this derivation we express the T matrix as a product of two matrices (T_4 and T_5 say) where T_4 and T_5 are defined by:

$$\begin{bmatrix} \underline{E}_1 \\ \underline{E}_2 \\ \underline{E}_3 \end{bmatrix} = \begin{bmatrix} T_4 \end{bmatrix} \begin{bmatrix} \underline{W} \\ \underline{U} \\ \underline{W} \times \underline{U} \end{bmatrix}$$

$$\begin{bmatrix} \underline{W} \\ \underline{U} \\ \underline{W} \times \underline{U} \end{bmatrix} = \begin{bmatrix} T_5 \end{bmatrix} \begin{bmatrix} \underline{B}_1 \\ \underline{B}_2 \\ \underline{B}_3 \end{bmatrix}$$

That separation is shown on the gyrocompass chart. The matrix T_4 is obtained from the identities

$$\underline{E}_1 = \underline{U}$$

$$\underline{E}_2 = \underline{W} \times \underline{U} \,/\, \underline{W} \times \underline{U}$$

$$\underline{E}_3 = \underline{U} \times (\underline{W} \times \underline{U}) \,/\, \underline{W} \times \underline{U}$$

GYROCOMPASS MATRIX

Inputs $(\underline{g}\cdot\underline{B}_1)$, $(\underline{g}\cdot\underline{B}_2)$, $(\underline{g}\cdot\underline{B}_3)$, $(\underline{\omega}^E\cdot\underline{B}_1)$, $(\underline{\omega}^E\cdot\underline{B}_2)$, and $(\underline{\omega}^E\cdot\underline{B}_3)$

From these quantities the alignment matrix is given by:

$$\left[\begin{array}{c} \\ T \\ \\ \end{array}\right] = \left[\begin{array}{ccc} 0 & 1 & 0 \\ 0 & 0 & \dfrac{1}{|\underline{W}\times\underline{U}|} \\ \dfrac{1}{|\underline{W}\times\underline{U}|} & -\dfrac{(\underline{W}\cdot\underline{U})}{|\underline{W}\times\underline{U}|} & 0 \end{array}\right] \left[\begin{array}{ccc} (\underline{W}\cdot\underline{B}_1) & (\underline{W}\cdot\underline{B}_2) & (\underline{W}\cdot\underline{B}_3) \\ (\underline{U}\cdot\underline{B}_1) & (\underline{U}\cdot\underline{B}_2) & (\underline{U}\cdot\underline{B}_3) \\ (\underline{W}\times\underline{U})\cdot(\underline{B}_2\times\underline{B}_3) & (\underline{W}\times\underline{U})\cdot(\underline{B}_3\times\underline{B}_1) & (\underline{W}\times\underline{U})\cdot(\underline{B}_1\times\underline{B}_2) \end{array}\right]$$

where

- $(\underline{W}\cdot\underline{U}) = (\underline{W}\cdot\underline{B}_1)(\underline{U}\cdot\underline{B}_1) + (\underline{W}\cdot\underline{B}_2)(\underline{U}\cdot\underline{B}_2) + (\underline{W}\cdot\underline{B}_3)(\underline{U}\cdot\underline{B}_3)$
- $|\underline{W}\times\underline{U}| = [1 - (\underline{W}\cdot\underline{U})^2]^{1/2}$
- $(\underline{W}\cdot\underline{B}_k) = (\underline{\omega}^E\cdot\underline{B}_k)/\omega^E$
- $(\underline{U}\cdot\underline{B}_k) = (\underline{g}\cdot\underline{B}_k)/g$
- $\omega^E = [(\underline{\omega}^E\cdot\underline{B}_1)^2 + (\underline{\omega}^E\cdot\underline{B}_2)^2 + (\underline{\omega}^E\cdot\underline{B}_3)^2]^{1/2}$
- $g = [(\underline{g}\cdot\underline{B}_1)^2 + (\underline{g}\cdot\underline{B}_2)^2 + (\underline{g}\cdot\underline{B}_3)^2]^{1/2}$

An optional technique might utilize any of the following additional inputs:

- The local latitude (λ) might be utilized to find $(\underline{W}\cdot\underline{U})$ from
$$(\underline{W}\cdot\underline{U}) = \cos\lambda$$
- The magnitude of gravity (g) might be supplied from a local survey.
- The magnitude of earth rate (ω^E) might be supplied from a local survey.

A use of all additional inputs could reduce the number of necessary instruments to three (either two accelerometers and one gyro, or one accelerometer and two gyros).

The rows of the T_5 matrix are obviously made up of the components of $\underline{W}$, $\underline{U}$, and $\underline{W}x\underline{U}$.

Below the matrix expression is found the relationships between the elements of the T_4 and T_5 matrices, and the accelerometer and gyro determined body-axes components of $\underline{g}$ and ω^E. Below those relationships is found a discussion of alternate techniques utilizing g, ω^E and λ.

SECTION 3

SECTION 3
SYSTEM DESCRIPTION

The calibration and alignment requirements for the NASA/ERC strapdown inertial sensing unit were presented in Section 2. The calibration requirements were defined as the determination of the inertial instrument model constants and the elements of the matrices which transform between the instrument and body frames of reference. Alignment was defined as the real-time initialization of the body-to-earth transformation matrix. The alignment requirements were defined as the measurement of the body and/or earth-frame components of two system vectors. Three alternative choices of sets of vectors were introduced. These alternatives characterized the three alignment techniques: Mirror Alignment, Level Alignment, and Gyrocompass. As a necessary aid to the satisfaction of the calibration and alignment requirements, various pieces of laboratory equipment are needed. It is also necessary to understand fully the nature of the kinematic environment in which the equipment and ISU are located. In this section our purpose is to describe that equipment and environment, beginning with their relationships with the problems of calibration and alignment.

3.1 FUNCTIONAL DESCRIPTIONS OF CALIBRATION AND ALIGNMENT

The following paragraphs describe the functional activities of calibration and alignment. (Section 3.1.1 discusses calibration, and 3.1.2 discusses alignment.) These functional descriptions serve as a definition of the required inputs to the calibration and alignment evaluations which come from sources other than the ISU.

3.1.1 Calibration

In the following discussion we indicate the functional requirements for determining the calibration numbers. Our discussion will be quite general, the major purpose being to introduce the reason why the equipment described in subsequent subsections is required.

As an aid to our presentation, we find it useful to compare the ERC laboratory calibration with an "Ideal Calibration". This comparison serves to indicate the compromises which are necessary in defining an operational calibration laboratory.

On the following chart (entitled Calibration) we present two calibration functional diagrams. We refer to the two techniques represented by those diagrams as Ideal Calibration and ERC

CHART 3-1

CALIBRATION

IDEAL CALIBRATION (OR STANDARDIZATION)

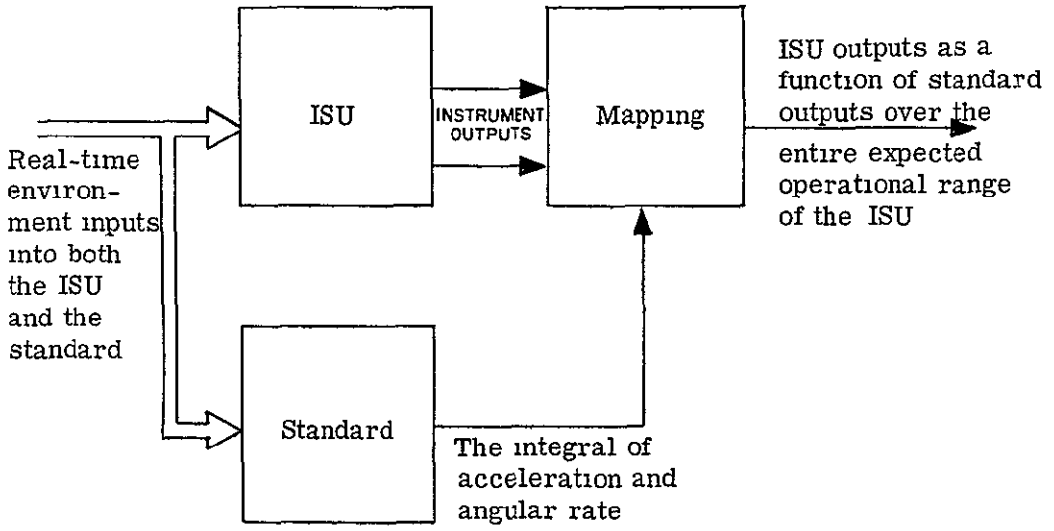

ERC LABORATORY CALIBRATION

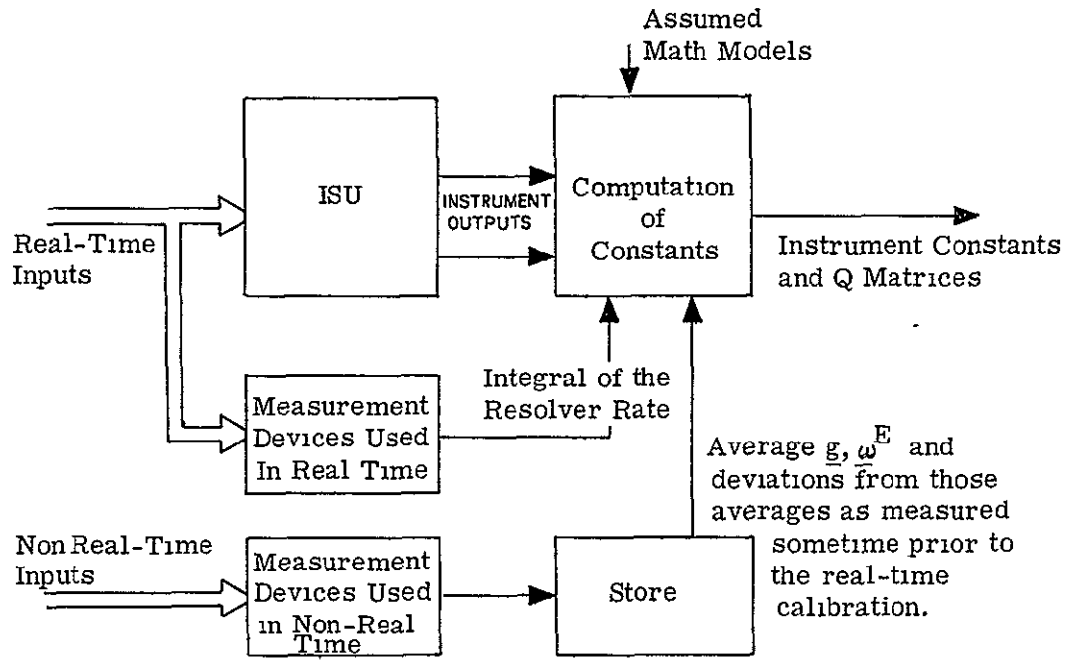

Laboratory Calibration. The Ideal Calibration diagram represents the manner in which calibration would be accomplished if an unlimited amount of time and money were available. The ERC Laboratory Calibration diagram represents the manner in which the calibration will be accomplished under more realistic constraints.

If one wished to calibrate a "black-box" (ISU) ideally, he would operate in the manner indicated in the Ideal Calibration functional diagram. Subsequent to the development of an ISU, whose outputs are designed to vary over a range of kinematic environment inputs ($\underline{a}$ and $\underline{\omega}$), one would wish to determine the quantitative relationship between the ISU outputs and that environment. However, that environment exists only conceptually, and not quantitatively, until a device is available which is defined as the measurer of these kinematic quantities. That device is referred to as the "Standard" measuring device. With the Standard available, it is then possible to calibrate the ISU by placing both the ISU and the Standard in the same environment and mapping the output of both over the range of the kinematic quantities which are considered to be significant. This mapping would take the form of a table of ISU and Standard outputs over the required operational range of the ISU. The mapping would necessarily be accomplished in a frame which characterizes the ISU and is known relative to the Standard. In our case, this frame will be the body axes as defined by the ISU mirror normals.

We see from the aforementioned statements that calibration is nothing more than the implementing of the requirement that the ISU behave as the Standard would under the same kinematic conditions. Thus, after calibration the ISU will have been "standardized". Subsequent to the standardization, it is assumed that the ISU can measure the kinematic environment, as the Standard would under the same conditions. This is accomplished by a transformation of the ISU outputs into a measure of the environment by use of the mapping information.

This is all rather interesting but not, operationally, very feasible. First, such a Standard is not available in the laboratory, and even if it were, time would not allow for a mapping over the entire operational range of the kinematic inputs. Secondly, in the case of applied acceleration, the typical operational range of the kinematic inputs cannot be easily generated in the laboratory. (A centrifuge would be required for accelerations higher than one g.) Thirdly, it is not always feasible to have even a substitute for the Standard operating at the same time as the ISU. All of these problems explain the deviations of the ERC Laboratory Calibration from the Ideal Calibration. Before elaborating those differences, a description of the ERC environment is necessary.

The kinematic inputs found in the ERC laboratory include:

1) The applied accelerations and angular velocities characteristic of any point on the earth's surface

2) The local deviations from those accelerations and angular velocities due to such things as earthquakes and cultural noise

3) The generated environments, caused by the ERC test table.

The first category includes earth-rate and the applied acceleration (normal-specific force) which negates the acceleration due to gravity in a "static" orientation relative to the earth. (This acceleration is often confused with gravity. It is, on the average, equal in magnitude and opposite in sign to gravity. The very common convention is to refer to this applied acceleration as $\underline{g}$. We will, in the remainder of this document, also refer to it as $\underline{g}$. Note, however, that we always direct $\underline{g}$ away from the surface of the earth.) The second category will be referred to as "noise". The laboratory test table (see Figure 3-1), mentioned in the third category, has a motor-driven capability of rotating at speeds up to several thousand earth rates. Such rotations will develop angular velocity and angular-velocity-related acceleration inputs to the ISU (the ISU being always attached, during calibration, to the table).

As suggested in the discussion of the Ideal Calibration, it is necessary that an independent measure (Standard Output) of the laboratory environment be available in order that calibration can be accomplished. This independent measure, even when a substitute for the Standard is used, should be accomplished at the same time that the ISU is yielding outputs. In the case of the angular velocity of the test table, an independent, real-time measure will be accomplished through the use of the output of the test table resolver.

The measurements of the $\underline{g}$ and $\underline{\omega}^E$ vectors are, however, accomplished at some time prior to calibration and "stored" for use during calibration. The storage of the direction of those two vectors is evidenced in the location of such things as optical lines, resolver zeros, etc., and the magnitudes by storage of numbers in a computer memory. Information about the noise is stored in the form of graphs showing characteristics such as power spectral densities. Because $\underline{g}$, $\underline{\omega}^E$, and noise are not measured in real time, it is assumed that their behavior is the same at the time of calibration as it was at the time of measurement, therefore, they can be considered a good approximation of a real-time measurement.

To this point we have described the manner in which the Standard output is evidenced in the ERC laboratory. We require only one more statement, in this presentation of the calibration functional activity, about the substitution of ERC Laboratory Calibration for

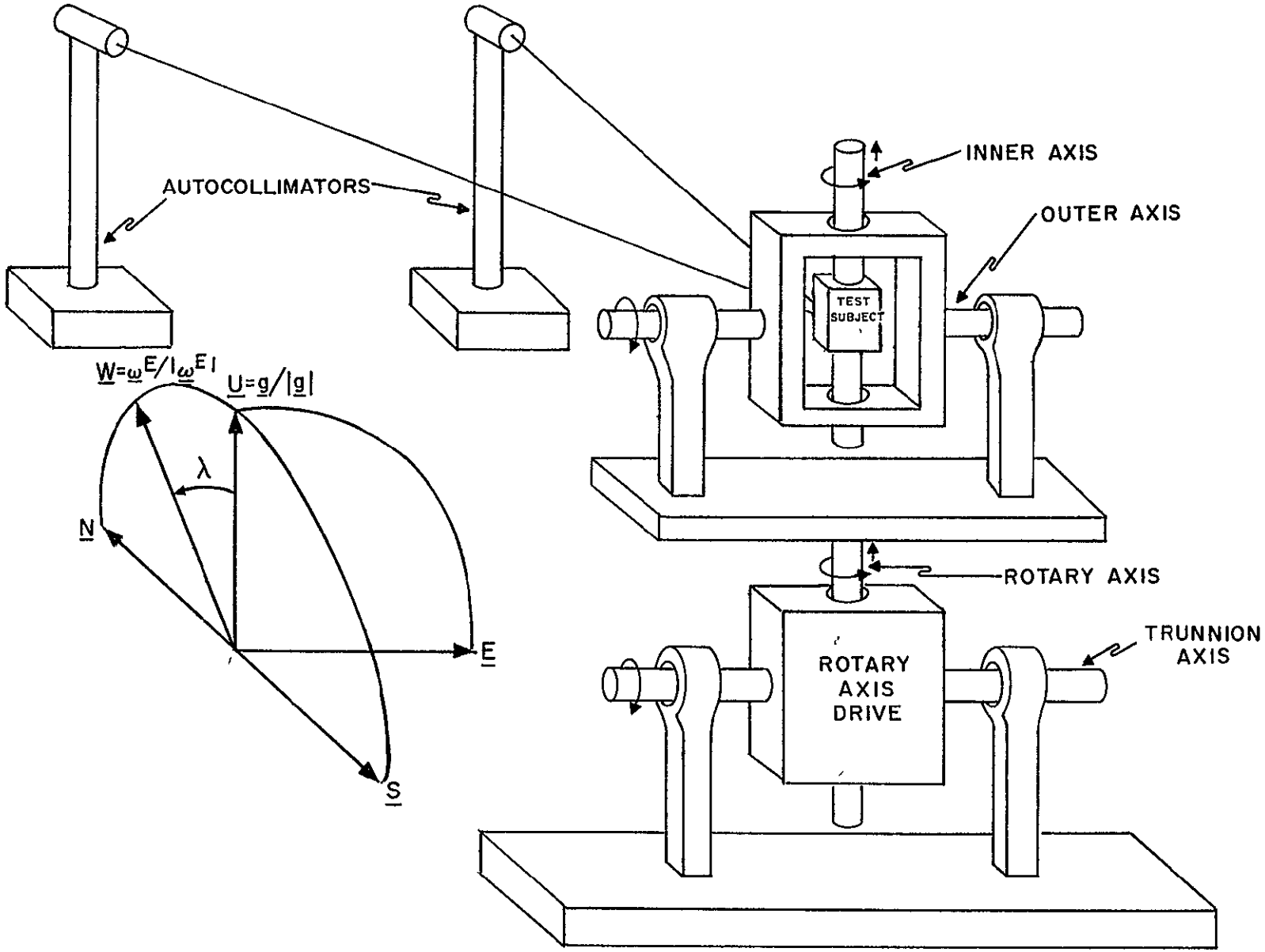

Figure 3-1. Laboratory Schematic Diagram

Ideal Calibration. The Ideal Calibration was described as a standardization over the entire range of inputs. Fortunately, in the case of Laboratory Calibration, some of the standardization has been accomplished by instrument designers prior to the placement of the accelerometers and gyros in the ISU. A great deal of time and effort has already been devoted to the development of a functional relationship between the output of the instruments and their environment inputs. Those functional relationships are referred to as mathematical models. As seen earlier, the instrument models contain many constants. Because of the availability of the models, it is only necessary in calibration to map a number of environments equal to the number of calibration constants for the determination of those constants. It is assumed that a knowledge of the models, and the model constants, serves to interpolate the mapping between the chosen environments.

In this subsection we discussed the independent measurements required as an aid to calibration. In Section 3.2 we will discuss how those measurements are specifically developed as inputs into the determination of the calibration constants.

3.1.2 Alignment

In Section 2.1 alignment was defined as the initialization of the matrix which transforms from an ISU-fixed set of axes to a navigation set of axes. In Section 2.2 the ISU-fixed axes were defined by two ISU-fixed mirror normals, and in Section 2.3 the navigation axes were defined as an earth-fixed, local-level frame of reference. Further, in Section 2.3, three alternate mathematical forms of the alignment matrix (T) were derived. Each form showed a requirement for a different set of optical or inertial-instrument measurements as an input into the quantitative determination of the alignment matrix. In this section we will discuss the techniques for determining each set of inputs.

As an aid to this disucssion we present in the accompanying chart, entitled "Alignment Functional Diagrams", a schematic of each of the three alignment techniques. In the remaining paragraphs of this section we discuss, in turn, the contents of each functional diagram.

Mirror Alignment

The routine labeled Alignment Matrix Computations represents the computations described in the Mirror Alignment Chart found in Section 2.3.3. As shown in Section 2.3.3 those computations require, as inputs, the optically determined azimuth and zenith of both the one and two mirror normals. (In practice, the actual optical measurements might be angles other than the azimuth and/or zenith angle. It is always an easy matter, however, to convert the actual measurements into the required azimuth and zenith.) The optical

CHART 3-2

ALIGNMENT FUNCTIONAL DIAGRAMS

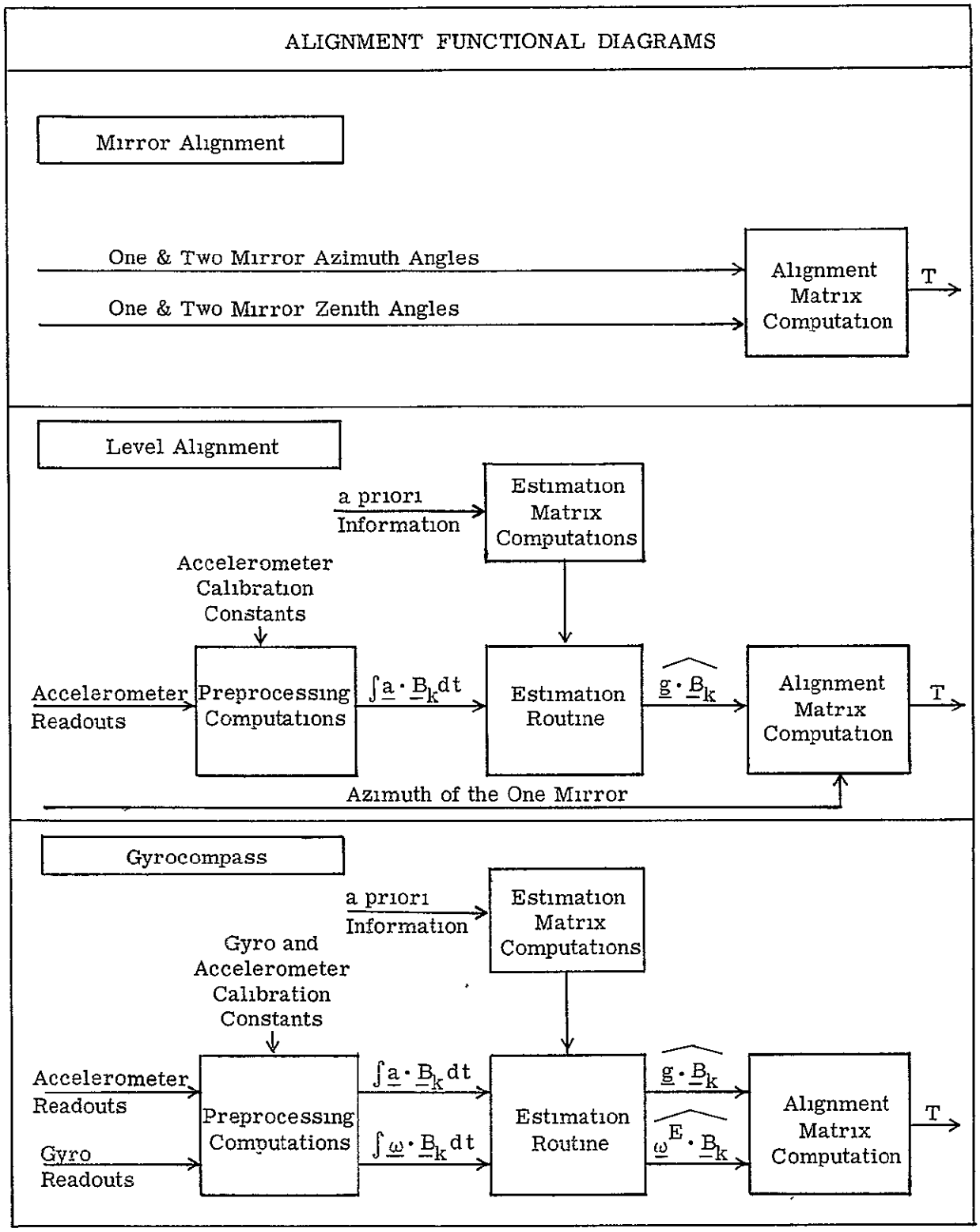

measurements will be manually transferred to the matrix computation routine, which will be part of a digital computer program in the ERC facility. Because optical measurements are extremely accurate by design, we do not include in the functional diagram any data-filtering function.

Level Alignment

The second functional diagram represents the Level Alignment procedure. The Alignment Matrix Computations indicated in the last block in the diagram represent the computations found in the Level Alignment chart described in Section 2.3.3. That routine requires, as inputs, the body-axes components of $\underline{g}$ and the azimuth of the one mirror. In Section 2.3 it was mentioned that the body-axes components of $\underline{g}$ will be available as the result of accelerometer measurements and the azimuth of the one mirror as an optical measurement. At the left side of the diagram we see the input of these measurements. The optically obtained azimuth goes directly to the matrix routine (as it did in Mirror Alignment). The accelerometer inputs, however, will require further processing, since they will be in the form of three digital pulse counts.

We saw, in Section 2.2.5, that the Preprocessing Computations convert such counts into integrals of body-axes components of the applied acceleration inputs to the accelerometers. However, those computations assumed no quantization and instrument noise. Therefore, the transformation of the outputs of the Preprocessing Computations into the desired body-axes components of $\underline{g}$ would require four additional operations in order to accomplish a good estimation of $\underline{g} \cdot \underline{B}_k$. These are:

- A differentiation of the integral outputs of the Preprocessing Computations
- A compensation for instrument quantization
- A compensation for instrument noise
- Separation of $\underline{g}$ from random environmental accelerations.

If the ISU were to be in a stationary orientation relative to $\underline{g}$ during alignment (that is, if the accelerometer input were a constant $\underline{g}$ acceleration), the first operation would be simply a division of the Preprocessing output by the total time of integration (say Δt). Additionally, the compensation for instrument quantization could then be accomplished by simply waiting sufficiently long such that the quantization residual would be arbitrarily small. However, the ISU at the ERC facility will not be in a constant $\underline{g}$ environment. Due to such things as local vehicle motion, personnel movement, etc., the ISU will be, in fact, in the presence of the nominal local $\underline{g}$ plus "noisy" vibrations. If some a priori knowledge of that noisy environment is available, it is possible to accomplish some of the aforementioned compensations by the development of mathematical filtering operations on the "Preprocessing" outputs. Those mathematical operations are presented in Chart 3-2 as the Estimation Matrix Computations and Estimation Routine. The former involves the computation of constants prior to the actual alignment. The input to those computations is the a priori noise information.

The Estimation Routine represents the on-line operations on the Preprocessing outputs. The outputs of the Estimation Routine are the required estimates of the body-axes components of $\underline{g}$.

The Preprocessing routine has been completely defined in Section 2.2.5, and the Alignment Matrix Computations have been defined in Section 2.3.3; hence, the development of the alignment techniques presented in Section 5 of this report will be preoccupied with the Estimation Matrix Computations and the Estimation Routine. In Section 3.2.2 we will present a discussion of the a priori noise information which is required as inputs to the estimation routines described in Section 5.

Gyrocompass

The third functional diagram in Chart 3-2 represents the operational gyrocompass procedures. The Alignment Matrix Computations shown in the diagram were presented in Section 2.3.3. Required inputs are the body-axes components of $\underline{g}$ and $\underline{\omega}^E$. At the left-hand side of the diagram we see the inputs of accelerometer and gyro readouts required for the determination of the body-axes components of $\underline{g}$ and $\underline{\omega}^E$. In the preceding section there is a discussion relating to the transformation of the accelerometer outputs into an estimate of the body-axes components of $\underline{g}$. This discussion also applies to Gyrocompass with the following modifications

- In Gyrocompass the Preprocessing computations as presented in Section 2.2.5 will be used entirely, whereas the Level Alignment uses only the accelerometer-related computations.
- The estimation routines will operate on both gyro and accelerometer data.

3.2 ENVIRONMENT MODEL

In the preceding discussions we showed that independent environment measurements are required for calibration, and a priori noise information is required for alignment. We indicated the manner in which that information is available at the ERC facility. In this section we will show specifically how the required measurement information is made quantitatively available to the calibration and alignment computational routines.

The reference environment information takes on different forms, and therefore can be discussed independently. First, there are the stored $\underline{g}$ and $\underline{\omega}^E$ vectors which must be expressed in terms of body-axes components for calibration purposes. There is the $\underline{\omega}^T$ vector (angular velocity of the test table), which must also be expressed in body-axes components. We will refer to these three vectors as the deterministic environment. We will show in Section 3.2.1 how the body-axes components of the deterministic environment are obtained as a function of test table gimbal angles. The remaining environment inputs have been referred to as random noise. They will be described in Section 3.2.2.

3.2.1 Deterministic Environment

The deterministic environment is made up of the three vectors $\underline{g}$, $\underline{\omega}^E$, and $\underline{\omega}^T$, which are assumed known in frames well surveyed in the laboratory. Our purpose in this section is to show how those vectors are transformed from the laboratory frames into ISU body-axes components. The transformation will be accomplished through the use of quantitative measurements taken from both the laboratory test table and the system autocollimators. We begin our discussion (in 3.2.1.1) by describing the geometry of those pieces of equipment. We then define the transformations between the many rigid bodies making up the equipment. Finally, (in Section 3.2.1.3) we will develop the operational transformation of the deterministic environment into body-axes components.

3.2.1.1 Laboratory Geometry

The geometry of the test table and autocollimators is the geometry which enables us to transform $\underline{g}$, $\underline{\omega}^E$, and $\underline{\omega}^T$ into body-axes components in the ERC laboratory. In Figure 3-2 we present a schematic of this geometry. This figure is a repeat of Figure 3-1, with the addition of the defined laboratory frames. Chart 3-3 presents the definitions of the frames indicated in Figure 3-2. A few comments are necessary as an aid to the understanding of Figure 3-2 and the chart containing the definitions of the frames.

- All frames are defined by orthogonal unit vectors directed along the frame axes.
- The $\underline{S}_k$ frame is not explicitly defined in Figure 3-2. The explicit definition will depend upon the (at this time) unknown geometry of the autocollimators. (The lack of an explicit definition has, however, proved to be no burden in the work that follows.)
- The body axes are not shown in Figure 3-2, because their relative orientation depends upon the manner in which the ISU is attached to the inner-axis rigid body.
- The $\underline{F}_k$ frame will be required to line up with the $\underline{E}_k$ frame. This alignment will naturally be with the laboratory frame, which, in turn, is thought to be coincident with the earth axes defined by $\underline{g}$ and $\underline{\omega}^E$. We will see in Section 4.4.4 that this alignment will have to be corrected periodically by the use of bubble levels.
- Each adjacent pair of test table frames is assumed to have a common axis.
- The four test table rotation angles are defined as ϕ_1, ϕ_2, ϕ_3, and ϕ_4, as shown in Figure 3-2.
- The test table orientation shown in Figure 3-2 is the zero orientation – that is, the orientation when all resolvers yield a zero output.
- The ISU will be attached to the section labeled "test subject" throughout the entire calibration.

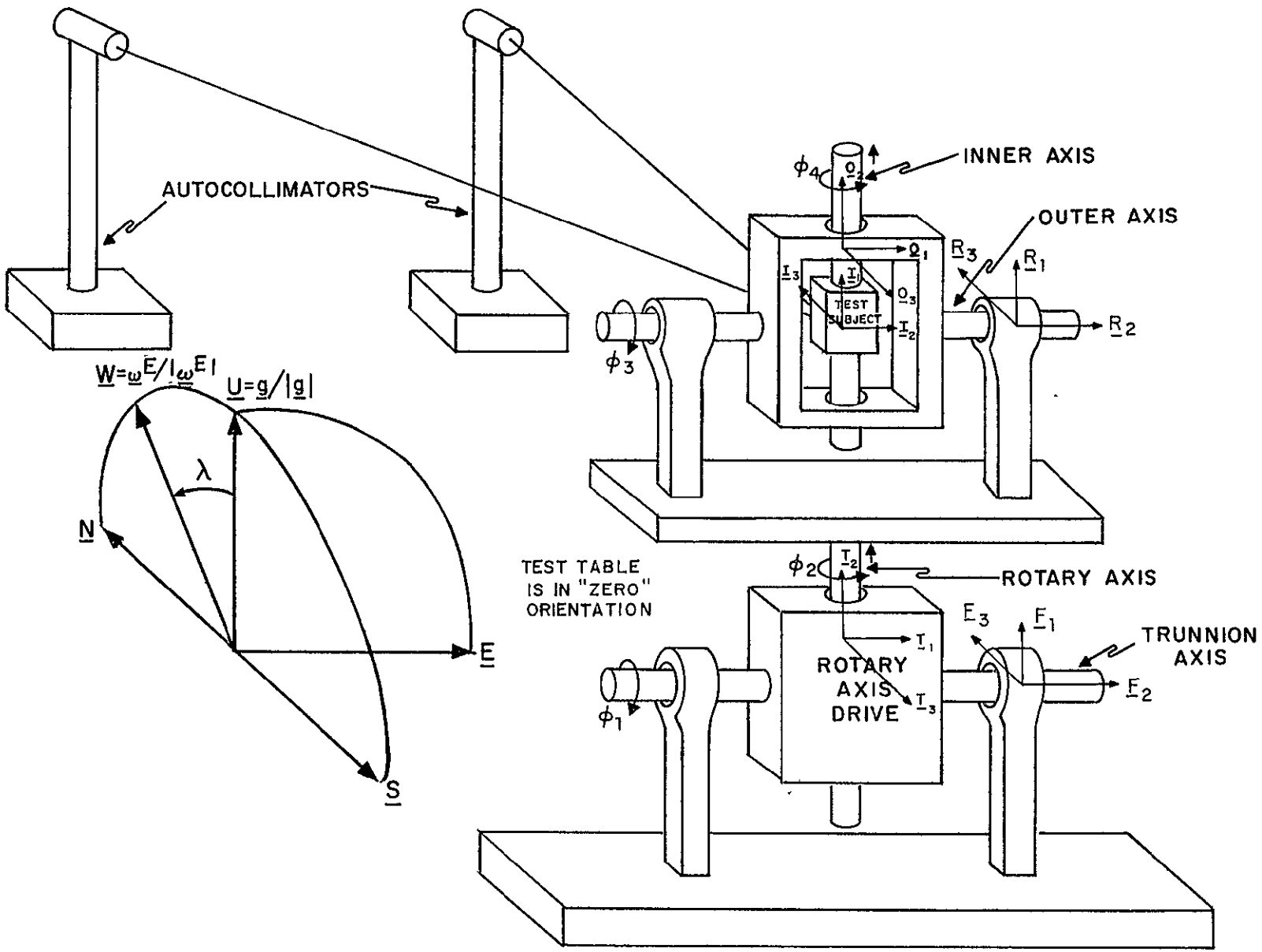

Figure 3-2. Laboratory Frames

DEFINITION OF FRAMES

LABORATORY FIXED FRAMES

• $\underline{E}_1\ \underline{E}_2\ \underline{E}_3$	A triad of unit vectors directed up, east, and north, respectively
• $\underline{S}_1\ \underline{S}_2\ \underline{S}_3$	A triad of unit vectors defined by the two optical lines of the autocollimators
• $\underline{F}_1\ \underline{F}_2\ \underline{F}_3$	A triad of unit vectors fixed to the base of the test table

TEST TABLE FRAMES

• $\underline{F}_1\ \underline{F}_2\ \underline{F}_3$	A triad of unit vectors fixed to the base of the test table
• $\underline{T}_1\ \underline{T}_2\ \underline{T}_3$	A triad of unit vectors fixed to the body containing the trunnion axis
• $\underline{R}_1\ \underline{R}_2\ \underline{R}_3$	A triad of unit vectors fixed to the body containing the rotary axis
• $\underline{O}_1\ \underline{O}_2\ \underline{O}_3$	A triad of unit vectors fixed to the body containing the outer axis
• $\underline{I}_1\ \underline{I}_2\ \underline{I}_3$	A triad of unit vectors fixed to the body containing the inner axis

ISU FIXED FRAMES

• $\underline{I}_1\ \underline{I}_2\ \underline{I}_3$	A triad of unit vectors fixed to the body containing the inner axis
• $\underline{B}_1\ \underline{B}_2\ \underline{B}_3$	A triad of unit vectors defining the body axes as defined by the mirror normals (see Section 2.2.1)

3.2.1.2 Definition of Transformations

Let us choose the $\underline{T}_k$ and $\underline{R}_k$ frames for our example. The relationship between the unit vectors of the two frames is given by:

$$\begin{bmatrix} \underline{R}_1 \\ \underline{R}_2 \\ \underline{R}_3 \end{bmatrix} = \begin{bmatrix} T^{RT} \end{bmatrix} \begin{bmatrix} \underline{T}_1 \\ \underline{T}_2 \\ \underline{T}_3 \end{bmatrix}$$

where a multiplication of the k^{th} row of the 3x3 matrix T^{RT} with the $\underline{T}_\ell$ column represents $\underline{R}_k$ expressed in the $\underline{T}_\ell$ frame. If $\underline{x}$ is any vector known in the $\underline{T}_\ell$ frame and one wishes to express that vector in the $\underline{R}_k$ frame, we dot the above definition with $\underline{x}$, yielding:

$$\begin{bmatrix} (\underline{x} \cdot \underline{R}_1) \\ (\underline{x} \cdot \underline{R}_2) \\ (\underline{x} \cdot \underline{R}_3) \end{bmatrix} = \begin{bmatrix} T^{RT} \end{bmatrix} \begin{bmatrix} (\underline{x} \cdot \underline{T}_1) \\ (\underline{x} \cdot \underline{T}_2) \\ (\underline{x} \cdot \underline{T}_3) \end{bmatrix}$$

If, further, we wish to transform to the $\underline{F}_k$ frame, we have:

$$\begin{bmatrix} (\underline{x} \cdot \underline{F}_1) \\ (\underline{x} \cdot \underline{F}_2) \\ (\underline{x} \cdot \underline{F}_3) \end{bmatrix} = \begin{bmatrix} T^{FR} \end{bmatrix} \begin{bmatrix} T^{RT} \end{bmatrix} \begin{bmatrix} (\underline{x} \cdot \underline{T}_1) \\ (\underline{x} \cdot \underline{T}_2) \\ (\underline{x} \cdot \underline{T}_3) \end{bmatrix} = \begin{bmatrix} T^{FT} \end{bmatrix} \begin{bmatrix} (\underline{x} \cdot \underline{T}_1) \\ (\underline{x} \cdot \underline{T}_2) \\ (\underline{x} \cdot \underline{T}_3) \end{bmatrix}$$

and so forth.

3.2.1.3 Operational Transformations

With the geometry information now completely described, it is possible to show how $\underline{g}$, $\underline{\omega}^E$, and $\underline{\omega}^T$ are transformed into body-axes components. The accompanying chart shows how that transformation is accomplished. Note that the chart specifies that the test table gimbal angles will always be used in determining the transformation, instead of autocollimator surveys. This is purely a matter of convenience. It certainly would be cumbersome to survey via the autocollimators over the 4π steradians in which the mirror normals can be located. Besides, the test table was designed to accomplish the necessary transformations. Note that the autocollimators are absolutely essential for one very important operation, namely the determination of the matrix T^{BI}.

Transformations of $\underline{\omega}^E$, $\underline{g}$ and $\underline{\omega}^T$ into Body Axes Components

During calibration there is a requirement for the transformation of $\underline{\omega}^E$, $\underline{g}$ and $\underline{\omega}^T$ into body axes components. Gravity and earth rate are vectors explicitly known in the $\underline{E}_k$ frame and $\underline{\omega}^T$ is a vector explicitly measured in the $\underline{R}_k$ frame. The body axes components of these vectors can, therefore, be written:

$$(\underline{\omega}^E \cdot \underline{B}_k) = \sum_{\ell} T^{BE}_{k\ell}\ \underline{\omega}^E \cdot \underline{E}_\ell$$

$$(\underline{g} \cdot \underline{B}_k) = \sum_{\ell} T^{BE}_{k\ell}\ \underline{g} \cdot \underline{E}_\ell$$

$$(\underline{\omega}^T \cdot \underline{B}_k) = \sum_{\ell} T^{BR}_{k\ell}\ \underline{\omega}^T \cdot \underline{R}_\ell$$

The matrices T^{BE} and T^{BR} are, therefore, required. These matrices, as a matter of convenience, will always be found as a function of test table gimbal angles. Therefore

$$T^{BR} = T^{BI}\ T^{IO}\ T^{OR}$$

$$\text{and } T^{BE} = T^{BI}\ T^{IO}\ T^{OR}\ T^{RT}\ T^{TF}\ T^{FE}$$

The matrix T^{BI} is a constant which must be found from an initial survey (see Section 4.4.1). The remaining matrices can be seen from the previous definitions to be:

$$[T^{IO}] = \begin{bmatrix} 0 & 1 & 0 \\ C\phi_4 & 0 & -S\phi_4 \\ -S\phi_4 & 0 & -C\phi_4 \end{bmatrix} \qquad [T^{OR}] = \begin{bmatrix} 0 & 1 & 0 \\ C\phi_3 & 0 & -S\phi_3 \\ -S\phi_3 & 0 & -C\phi_3 \end{bmatrix}$$

$$[T^{RT}] = \begin{bmatrix} 0 & 1 & 0 \\ C\phi_2 & 0 & -S\phi_2 \\ -S\phi_2 & 0 & -C\phi_2 \end{bmatrix} \qquad [T^{TF}] = \begin{bmatrix} 0 & 1 & 0 \\ C\phi_1 & 0 & -S\phi_1 \\ -S\phi_1 & 0 & -C\phi_1 \end{bmatrix}$$

$$[T^{FE}] = \begin{bmatrix} 1 & 0 & 0 \\ 0 & 1 & 0 \\ 0 & 0 & 1 \end{bmatrix}$$

(Note, the frames are defined so that each matrix has the same form.)

3.2.2 Random Environment

The laboratory test environment introduces a random translational and rotational "noise" input. In describing the noise inputs, we will utilize the worst-case model. Namely, the translational input and angular input are assumed to be independent, and the components of the random input vectors are assumed to be independent.

The random translational inputs about the up-down, east-west, and north-south axes have been assumed to be statistically independent and identically distributed. Each input has a power spectrum illustrated in Figure 3-3.* It follows that the translational motions along any three perpendicular axes are uncorrelated and have the spectrum given in Figure 3-3. The nominal input (local gravity) is assumed to be the long-term average input. Assuming ergodicity of the expectation, the translational inputs have zero expectations. The random translational inputs do not produce a significant output from the gyros.

The random rotational input produces a rotation about an axis in the horizontal plane. The rotation about the vertical axis can be neglected. The random angular inputs about the east-west axis and the north-south axis are statistically independent, and each has the power spectrum illustrated in Figure 3-4. These inputs are assumed to have zero expectations.

The spectra given in Figures 3-3 and 3-4 are the basis of numerical computations involving environment noise. The selection of the "Recommended Alignment Techniques" in Section 5.7 assumed an environment as indicated in Figures 3-3 and 3-4. The alignment processing techniques derived in Sections 5.4 and 5.5 use the power spectra of the translational and rotational noise inputs but do not depend on the specific numbers given in Figures 3-3 and 3-4.

3.3 HARDWARE DESCRIPTION AND INTERFACE

The material presented to this point has been introductory in nature. That is, all discussions were either related to the detailed statement of the calibration and alignment problem, the definition of terms, the description of necessary equipment, or the description of the laboratory environment. In this section we will complete the presentation of introductory material by covering two descriptive tasks which aid in the understanding of the calibration and alignment development in Sections 4 and 5 and the operational

---

*Spectra data is given by H. Weinstock in "Limitations on Inertial Sensor Testing Produced by Test Platform Vibration", NASA Electronics Research Center, Cambridge, NASA TN D-3683, 1966.

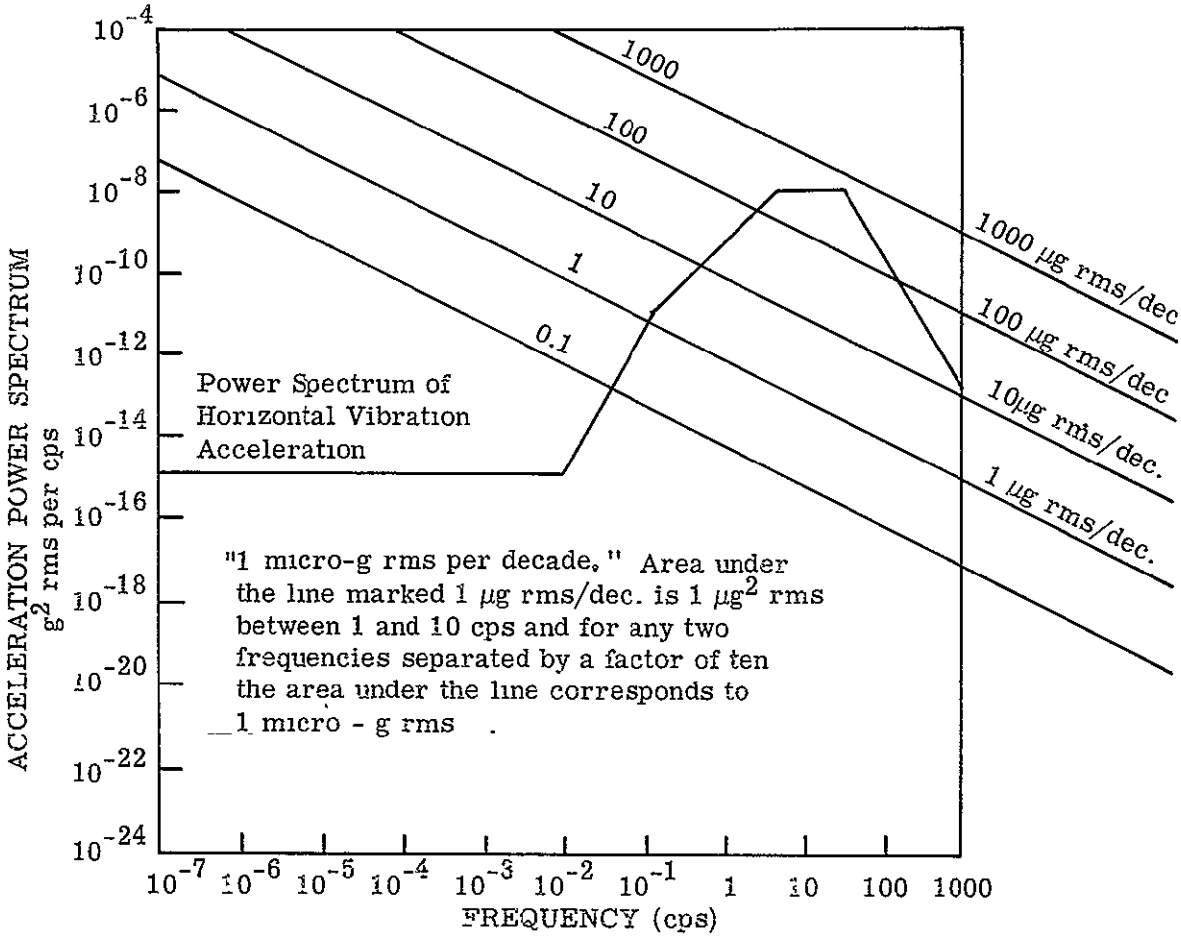

Figure 3-3. Representative Linear Vibration Environment of an Urban Test Laboratory

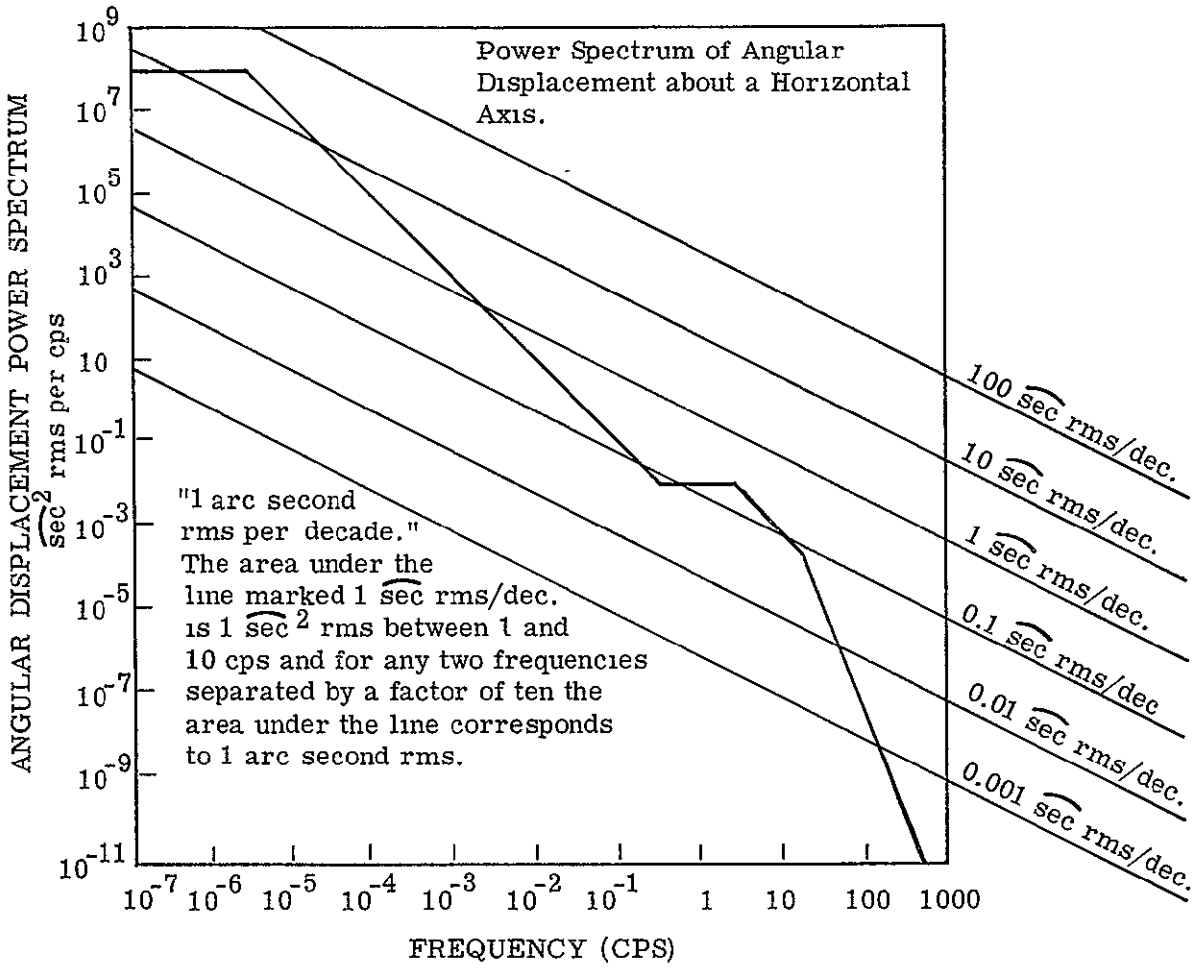

Figure 3-4. Representative Angular Vibration Environment of an Urban Test Laboratory

procedures presented in the Laboratory Procedures Manual. First, there is laboratory equipment which is necessary for the implementation of calibration and alignment procedures and which has not yet been described. Second, the laboratory equipment has not been presented as a system as a whole, with all of its interconnections. In this section the description of that equipment and interface will be accomplished through the use of a system diagram. In Section 3.3.1 that diagram is introduced but without the lines denoting the equipment interface. In conjunction with the introduction of that diagram, we will present brief descriptions of the equipment which each block in the diagram represents. In Section 3.3.2 the useful interfaces between all equipment will be presented in tabular form.

3.3.1 System Diagram and Equipment Description

The master system flow diagram is shown in Figure 3-5. This diagram will be used as an aid in the Laboratory Procedures Manual to describe the system activities during various phases of calibration and alignment. In those applications of the diagram, interface lines will be added to indicate specific modes of operation. Data flows are indicated by narrow lines; dynamic or monitor interfaces are indicated by wide lines. A brief description of each of the boxes represented on the master system diagram, in Figure 3-5, follows:

Input/Output Console – The input/output console consists of the equipment that provides a manual computer interface. Included in the input/output console are· computer control panel, keyboard and typewriter, paper tape reader and punch, and the display panel.

Operator – The operator in this system must perform many of the tasks of control and data transfer. The box "operator" includes not only the person(s) directing the laboratory, but also his worksheets, instructions, and notes.

Systems Control and Monitor – This box represents the equipment, capability, and activity used to monitor and control the system during calibration and alignment.

Frequency Counters – Six frequency counters are available for use in calibration to measure instrument output. These counters measure the number of counts on one pulse train for a fixed number of counts on another. One of the two trains may be a difference train formed from two inputs. The frequency counters are used in calibration, because they can read the leading edge of one pulse train and thus substantially reduce the quantization error relative to the use of the computer registers.

Auxliary Data Sources – These include data sources available to the operator but not sufficiently well defined as equipment or measuring devices to be represented individually

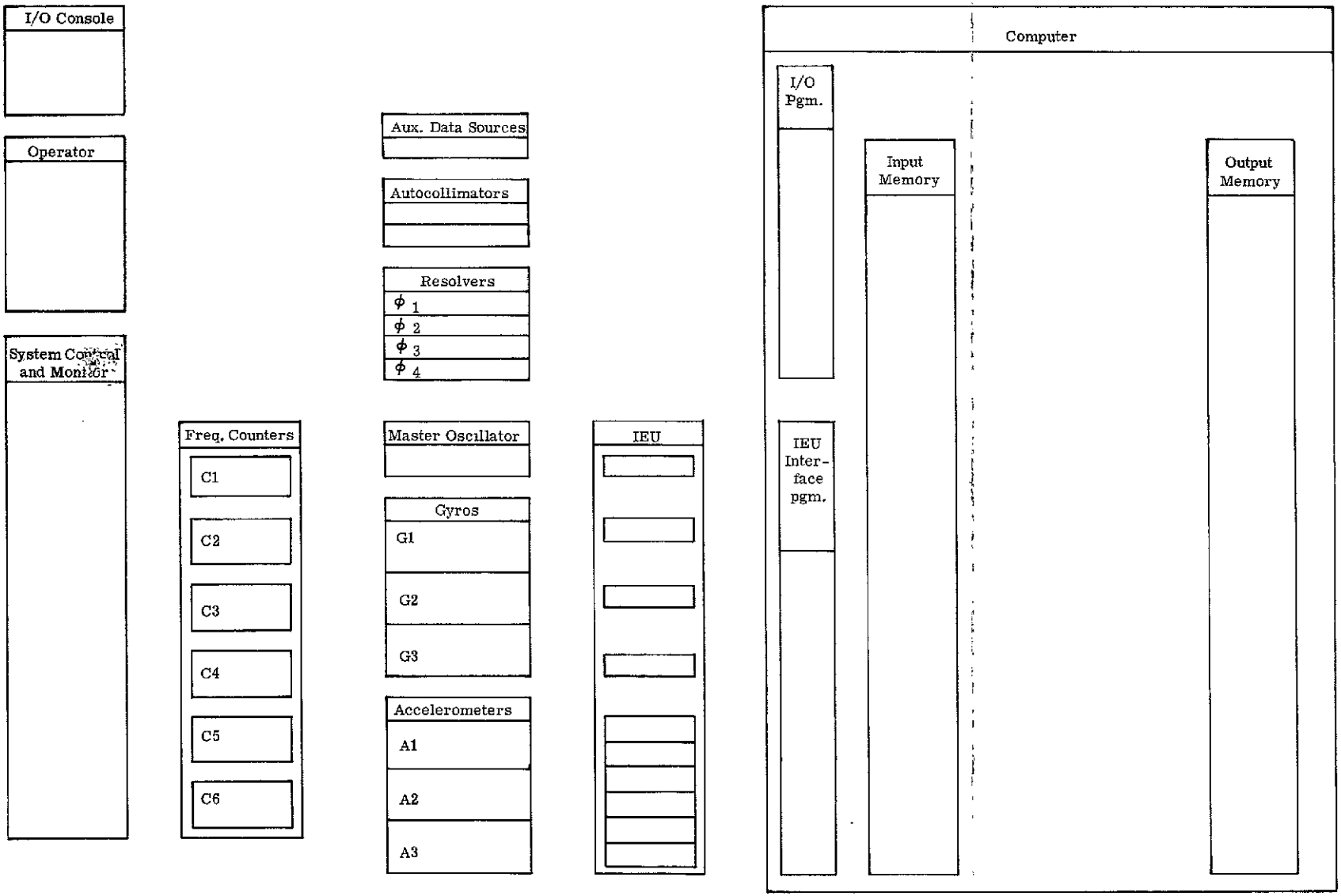

Figure 3-5. Laboratory Flow Diagram

FOLDOUT FRAME 1

FOLDOUT FRAME 2

on the system flow diagram. Examples of these sources are bubble levels and survey information on the magnitude of $\underline{g}$ and $\underline{\omega}^E$.

Autocollimators – The two-degree-of-freedom autocollimators are available to measure the earth-fixed coordinates of the ISU mirror normals.

Resolvers – These resolvers measure the orientation of the test table. The angles ϕ_1, ϕ_3, and ϕ_4 are static resolver readouts on the trunnion, outer and inner axes of the test table. The angle ϕ_2 is a rotary axis readout which can be used in either a static or dynamic mode.

Master Oscillator – This is the central timing source of the system. The master oscillator includes countdown circuitry.

Gyros, Accelerometers – These are the instruments contained within the strapdown ISU (see Section 2.2).

Interface Electronics Unit (IEU)* – The IEU allows the computer to sample outputs of the inertial instruments and timer. The IEU contains accumulating registers for each of the inputs shown in the diagram and the capability to periodically interrupt the computer to allow for sampling and resetting (without loss of data) of each of the registers.

Computer* – The computer schematically indicated in the system diagram is the laboratory computer Honeywell DDP-124. Other portions of the data processing shown may, however, be performed on other computers at the discretion of the programmers and operators. Blocks shown within the computer represent functions used in both calibration and alignment. Shown are programs to input and output data from and to the console, a program to input data from the IEU, and memory buffers for input data and output data (the results of computations). Space has been left within the computer block to allow representation of the various data processing tasks.

3.3.2 Equipment Interface

Figure 3-6 illustrates the principle data paths that might be of interest during calibration and alignment. Each of the paths is numbered and described by number in Chart 3-5. These paths represent the calibration or alignment data flow.

---

*More detailed descriptions are presented in Appendix C.

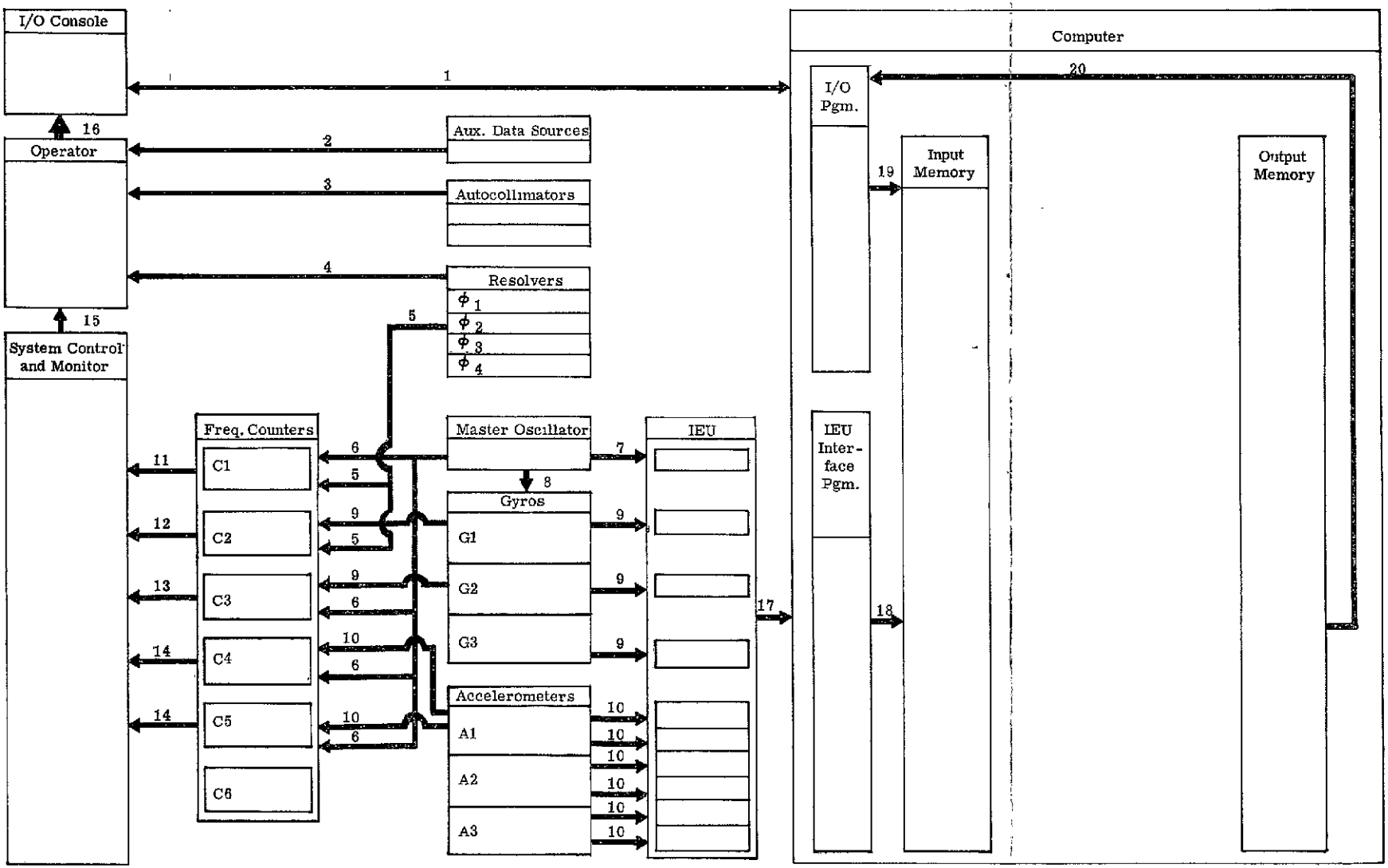

Figure 3-6. Laboratory Flow Diagram System Data Interfaces

FOLDOUT FRAME 1

FOLDOUT FRAME 2

Description of Equipment Data Paths

Data Interface #	Type	Data Description
1	Coded	Input – Includes magnetic and paper tape, keyboard, and display and computer control panel inputs. Data represents information and control from or through the computer plus data or program filed on magnetic or paper tape. Output – Display, typewriter, or paper tape panel output to the operator.
2	Visual or tape	Various types of data
3	Visual	Two angles/autocollimator
4	Visual	Four angles test table position
5	Pulsed	Rotary axis motion probably one pulse
6	Timing	Frequency less than 1 MHz
7	Timing	2.034 MHz
8	Timing	3.6 KHz
9	0, +1 or -1 pulses at 3.6 KHz	Gyro output to frequency counters and IEU
10	Pulsed	Zero crossing pulses from each of two vibrating strings per accelerometer to frequency counters and IEU
11	Count	For inputs shown – count would be number of time pulses per n turns
12	Count	For input shown – count would be number of gyro pulses (signed) for n turns of table
13	Count	For inputs shown – count would be number of time pulses per |n| gyro pulses
14	Count	For inputs shown – count would be numbers of time pulses per N accelerometer pulses
15	Visual	Status and monitor information plus output from the counters Low visual display and printed
16	Manual	Manual input of data to computer (includes key punching, mounting of tapes and punching of buttons)

Description of Equipment Data Paths (Continued)

Data Interface #	Type	Data Description
17	Binary Data	Counts from IEU registers. Input in succession with data valid for same period of time.
18	Binary Data	Counts from IEU registers. May be summations of data from several successive transfer across interface #17
19	Binary Data	Input data shown in buffer
20	Binary Data	Output data shown in buffer

Manual and monitor interfaces are shown in Figure 3-7. The manual interfaces correspond to operator activities during various portions of the calibration and alignment procedure. Monitor is performed during the many procedures to verify the operation of equipment being used at that time. Explanations for each interface on Figure 3-7 are presented on the figure.

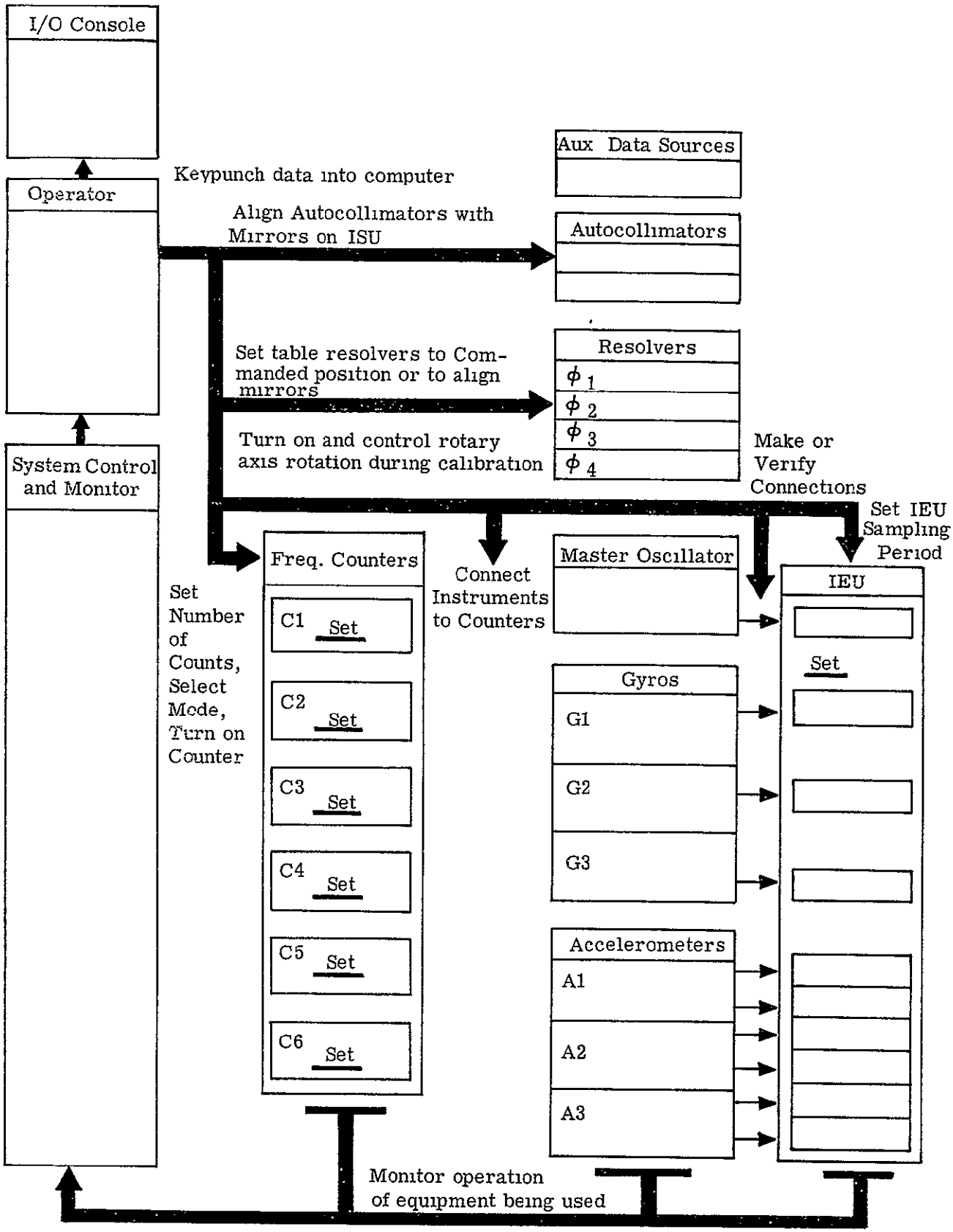

Figure 3-7. Laboratory Flow Diagram Manual and Monitor Interfaces

SECTION 4
DEVELOPMENT OF CALIBRATION TECHNIQUES

The functional description of calibration in Chart 3-1 in Section 3.1.1 indicated inputs of instrument data and environment measurements to a computation routine, which in turn outputs the calibration constants. The obvious sources of the relationships contained within that routine are the instrument mathematical models. In Section 4.1 we will use the instrument models to develop general equations from which the relations found in the computation routine are evolved The general equations will be seen to contain certain controllable parameters which describe the input environment in terms of the test table controllable orientation and angular speed. In Section 4.2 a number of sets of particular values for the control parameters will be chosen such that the general equations reduce considerably in form. Each set of particular values corresponds to a different calibration "Position". It will be shown that the determination of any constant can be accomplished by the simultaneous solution of at most two of the reduced equations. In Section 4.3 the complete set of calibration computations will be delineated The relations employed in the computation routine correspond to the solution of the calibration constants from the data gathered in Positions 1 through 15.

In Section 4.4 we will describe the operations and computations required prior to the collection of calibration data. An example of a precalibration operation is the determination of the orientation of the ISU body axes relative to the test table inner-gimbal frame (i.e., T^{BI}). In Section 4.5 a brief discussion of the implementation of the proposed techniques will be presented. The discussion of the implementation of the calibration techniques is directed towards clarifying the relation between the developments in this document and the operational procedures described in the Laboratory Procedures Manual.

Before proceeding to the development of the calibration techniques, it is appropriate to describe those incentives which motivated our specific choices of calibration techniques:

- The determination of any calibration constant should be made as insensitive as possible to the imprecision of any other constant(s).
- It is advisable to use as few different test table orientations as possible; and where the orientations are different, to try to make the orientations differ from one another by as little adjustment of the table as possible. The satisfaction of this requirement serves two purposes. First, it will allow for the simultaneous calibration of many instruments. Secondly, by limiting the number of table orientations, the amount of manual activity will be limited, thus minimizing calibration time, and also the chances of human error.

- The imprecisions of the test table orientations should have a limited influence on the values of the calibration constants.
- The calibration should be made as flexible as possible. We wish to present the calibration in such a way that additional experiments can be accomplished with a minimum number of changes to existing calibration procedures
- We wish to accomplish our calibration with little or no data filtering. We would like to minimize the effects of noise by judicious choices of approaches other than involved software processing.
- The computation program should be as simple as possible.
- Data collection time should be limited to about 10 minutes, and the total calibration time to less than eight hours.
- The precision of calibration, as a function of time, should be apparent from error analyses accomplished on the resultant techniques.

In the discussions which follow, it will be found that it is possible to satisfy a majority of the above requirements.

4.1 DEVELOPMENT OF GENERAL CALIBRATION EQUATIONS

The routine that accomplishes the evaluation of the calibration constants we indicated in Chart 3-1 as a routine entitled "Computation of Constants". In this section we will develop the general equations from which the computational routine is developed Those general equations will be seen to contain the control parameters which describe the environment inputs. The chosen control parameters are the angular speed of the test table, the first two gimbal angles (φ_1 and φ_2) of the test table, and the T^{BR} matrix (which is a function of the ϕ_3 and ϕ_4 gimbal angles). In Section 4.2 we will show how particular choices of these control parameters result in relations from which the calibration constants can be extracted.

The presentation in this section is divided into two parts. In Section 4.1.1 we develop the general equations for the three system gyros, and in Section 4 1.2 we develop the general equations for the three accelerometers.

4.1.1 Gyro Equations

The development of the general equations begins with a presentation of the Fundamental Gyro Model. After introducing the ERC environment and geometry into that model we will have developed equations which are a function of, among other things, the angular speed of the test table and test table orientation parameters. In subsequent subsections we will show how the control of those test table parameters is employed in the determination of the required instrument calibration constants

The presentation in this subsection contains a great deal of mathematics. So as not to interfere with the prose, we will present the mathematical development as a series of eight charts. In each chart, after the first, the equations found on the preceding chart will be modified to indicate certain assumptions about the environment. In the discussions which follow we describe, in turn, the assumptions and the related mathematics presented on each chart.

The Fundamental Gyro Model (Chart 4-1)

The development of the generalized gyro calibration equations begins with the gyro mathematical model. That model was described in Section 2.2.3 and presented as Chart 2-2. Chart 2-2 is repeated here as Chart 4-1. The gyro mathematical model describes the relationship between the output ($\Sigma\delta$) of the gyro and the input kinematic environment ($\underline{a}$ and $\underline{\omega}$) over a time period $t_0 \rightarrow t_N$.

Introduction of Laboratory Environment (Chart 4-2)

We first introduce into the gyro mathematical model the vector representation of the ERC laboratory kinematic environment. At the top of the chart the kinematic inputs are listed. Note that every possible input has been listed. This is done so that, at one point in the development, there exists an expression which assumes nothing about the negative effect of any possible input. Note also that the environment description assumes that the gyro is subjected to an input angular velocity $\underline{\omega}^T$ as generated by the test table rotary axis motor.

Approximations (Chart 4-3)

The next step is to neglect those kinematic inputs to the gyro which can reasonably be expected to have a negligible effect on the gyro output. A gyro is designed to be nominally a linear angular velocity measuring device; therefore all acceleration-sensitive terms are small. The noise acceleration and the test table-induced accelerations are also small relative to the nominal $\underline{g}$ input. Therefore the effects of these small accelerations are second order in all unbalance and compliance terms and are assumed negligible. Similarly, it is assumed that the small angular velocity noise terms can be neglected in all angular velocity-sensitive terms other than the linear term. Note that in Chart 4-3 we have arranged the equations such that only the deterministic $\underline{g}$, $\underline{\omega}^E$, and $\underline{\omega}^T$ inputs exist to the right of the equality. Note also that the equation has been divided by the gyro scale factor.

Introduction of Body Axes and Instrument Indexing (Chart 4-4)

The equations presented thus far have referred to a single gyro. At this point we introduce the index i defining three gyros (i = 1, 2, 3).

We mentioned in Section 3.2 that for calibration purposes, the vectors $\underline{g}$, $\underline{\omega}^E$, and $\underline{\omega}^T$ must be known in body-axis components. In Chart 4-4 we introduce the body axes, and express the integrals of these vectors in terms of body-axis components. Because the nominally known instrument-to-body-axis transformations differ from the actual transformations by small numbers, it is assumed that the nominal values can be used in other than the proportional angular velocity term. Note that the first three elements in the equation represent the i^{th} row of the $(Q^G)^{-1}$ matrix, scaled by the gyro scale factor Note also that these elements are assumed constants whereas, on a microscopic scale, they are time-varying within the limit cycle amplitude of the instruments.

The function found to the left of the equality has, at this point in the development, been defined as the triple $P_i^G (i = 1, 2, 3)$. This vector, which we will refer to as the gyro processing vector, contains the instrument readout term plus the quantization and noise terms. The P_i^G vector, and the approximations made in its evaluation during calibration, will be discussed in Section 4.3.1.

Choice of Body Axes (Chart 4-5)

The next step in the development is to introduce the ERC ISU nominal geometry. Those transformations which describe that geometry were defined in Section 2.2.1. Because the orientations of the output and spin axes are not cyclic, a general index equation cannot be developed. Therefore a separate equation for each gyro is presented in Chart 4-5.

At this point the general equations relate the gyro processing vector (which includes measurable gyro readout, noise, and quantization error) to the measurable body-axis components of the environment (described by $\underline{g}$, $\underline{\omega}^E$, and $\underline{\omega}^T$). In the remaining charts we will relate the body-axis components of the environment to the controllable test table parameters.

Integral Evaluations (Charts 4-6, 4-7, and 4-8)

The preceding chart listed the required equations as three expressions which are linear in the unknown calibration constants. The coefficients of those unknown constants are presented as integrals of body-axis components of $\underline{g}$, $\underline{\omega}^E$, and $\underline{\omega}^T$. In the discussions of

calibration techniques which follow this subsection we will show how calibration is accomplished by a control of the values of these integrals. Before we can show this we must functionally relate the integrals to the controllable test table geometry. The following three charts develop those functions.

In the first chart (4-6) the integrals of the body-axis components of $\underline{g}$, $\underline{\omega}^E$, and $\underline{\omega}^T$ are expressed as transformations from the frames in which they are well known. The definitions of the transformation geometry and notation were explained in Section 3.2.1.

In Chart 4-7 the earth-axes components of $\underline{g}$ and $\underline{\omega}^E$ and the rotary axes components of $\underline{\omega}^T$ are introduced. Additionally, the T^{TE} and T^{RT} matrices are expressed as functions of the ϕ_1 and ϕ_2 gimbal angles. (See Section 3.2.1 for definitions of this geometry.) With these equalities introduced, we can now extract all but the time-varying parameter (ϕ_2) from the integrands of the equations

In the final chart (4-8) the integrals are combined as the calibration constant coefficients. The equalities listed at the top of the chart allow the integrals to be separated into sums of monotonically increasing terms, harmonic terms, and terms which are functions of terminal conditions only. The only harmonic terms are those which contain integrals of sines and cosines. The monotonic increasing terms are those containing Δt, and the terminal condition terms are those which contain Δ's other than Δt.

Charts 4-5 and 4-8 constitute the required general gyro calibration equations. Note that our result is a set of three functional relationships among: the "processing vector" P_k^G, the unknown calibration constants; the magnitudes of gravity (g), earth rate (ω^E), and latitude (λ); the total time of integration (Δt), and the controllable test table parameters, which are

ϕ_1 – The trunnion axis angle

ϕ_2 – The total angle of revolution about the rotary axis

$\omega^T = \frac{d\phi_2}{dt}$ – The speed of the test table

and T^{BRm} – The matrix which transforms from the rotary axis frame to the body axes for the m^{th} calibration position.

(See Section 3 for definitions of all test table geometry.)

In Section 4.2 we will show how gyro calibration is accomplished by a control of the test table parameters contained within the functional relationships.

THE FUNDAMENTAL GYRO MODEL

THE GYRO MODEL IS

$$\Delta\Phi \left[\sum_{k=1}^{N} \delta_k \right] = \int_{t_0}^{t_N} (\underline{\omega}\cdot\underline{G})\, dt + \int_{t_0}^{t_N} \Big[R + B_I(\underline{a}\cdot\underline{G}) + B_O(\underline{a}\cdot\underline{O}) + B_S(\underline{a}\cdot\underline{S}) + C_{II}(\underline{a}\cdot\underline{G})^2 + C_{SS}(\underline{a}\cdot\underline{S})^2 + C_{IS}(\underline{a}\cdot\underline{G})(\underline{a}\cdot\underline{S}) + C_{OS}(\underline{a}\cdot\underline{O})(\underline{a}\cdot\underline{S}) + C_{IO}(\underline{a}\cdot\underline{G})(\underline{a}\cdot\underline{O}) + Q_{II}(\underline{\omega}\cdot\underline{G})^2 + Q_{IS}(\underline{\omega}\cdot\underline{G})(\underline{\omega}\cdot\underline{S}) + J\frac{d}{dt}(\underline{\omega}\cdot\underline{O}) \Big] dt + \Delta n + Eq$$

WHERE

- $\underline{\omega}$ is the angular velocity applied to the gyro
- $\underline{a}$ is the acceleration applied to the gyro
- $t_0 \le t \le t_N$ is the time interval over which $\underline{a}$ and $\underline{\omega}$ are measured
- $t_N - t_0 = N\tau$, where N is an integer, and τ is the gyro sampling period
- $\underline{S}$ is a unit vector along the spin axis of the rotor
- $\underline{O}$ is a unit vector directed along the output axis as defined by the gimbal
- $\underline{G}$ is a unit vector along $\underline{O} \times \underline{S}$ (that is, the sensitive axis of the gyro)
- δ_k is the kth gyro pulse, equal to +1, -1, or 0 for positive, negative, or no pulse
- $\Delta\Phi$ is the gyro scale factor
- R is the gyro bias
- B_I B_O and B_S are the gyro unbalance coefficients
- C_{II} C_{SS} C_{IS} C_{OS} and C_{IO} are the gyro compliance coefficients
- Q_{IS} and Q_{II} are dynamic coupling coefficients due to gimbal deflection and scale factor nonlinearity, respectively
- J is the angular rate coefficient
- Δn is the effect of gyro noise over the $[t_0, t_N]$ interval
- Eq is the gyro quantization error

INTRODUCTION OF LABORATORY ENVIRONMENT

ASSUME

- $\underline{\omega}^{L} = \underline{\omega}^{TT} + \underline{\omega}^{EE} = (\underline{\omega}^{T} + \Delta\underline{\omega}^{T}) + (\underline{\omega}^{E} + \Delta\underline{\omega}^{E})$ is the total applied angular velocity

  where: $\underline{\omega}^{TT}$ is the total test table angular velocity

  $\underline{\omega}^{T}$ is the measured test table angular velocity

  $\underline{\omega}^{EE}$ is the total laboratory angular velocity

  $\underline{\omega}^{E}$ is the assumed (surveyed) laboratory angular velocity

- $\underline{a}^{L} = \underline{g} + \underline{\omega}^{TT} \times (\underline{\omega}^{TT} \times \underline{r}) + \dot{\underline{\omega}}^{TT} \times \underline{r} + \Delta\underline{a}$ is the total applied specific force

  where: $\underline{g}$ is the assumed (surveyed) laboratory specific force

  $\underline{\omega}^{TT} \times (\underline{\omega}^{TT} \times \underline{r})$ is the centripetal specific force due to the table motion

  $\dot{\underline{\omega}}^{TT} \times \underline{r}$ is the angular rate specific force due to the table motion

  $\Delta\underline{a}$ is the deviation of the assumed laboratory specific force from the true

- $\underline{\omega}^{TT} \times (\underline{\omega}^{TT} \times \underline{r})$ and $\dot{\underline{\omega}}^{TT} \times \underline{r}$ are formal expressions, as $\underline{r}$ is not explicitly defined.

INTRODUCING THESE ASSUMPTIONS INTO THE EQUATION IN CHART 4-1, WE HAVE

$$
\begin{aligned}
\Delta\Phi\left[\sum_{k=1}^{N}\delta_k\right] = {} & \int_{t_0}^{t_N}\left[(\underline{\omega}^{E} + \underline{\omega}^{T} + \Delta\underline{\omega}^{E} + \Delta\underline{\omega}^{T})\,\underline{G}\right]dt \\
& + \int_{t_0}^{t_N}\Big\{\Big[R + B_I\left[(\underline{g} + \underline{\omega}^{TT} \times (\underline{\omega}^{TT} \times \underline{r}) + \underline{\omega}^{TT} \times \underline{r} + \Delta\underline{a})\,\underline{G}\right] + B_O\left[(\underline{g} + \underline{\omega}^{TT} \times (\underline{\omega}^{TT} \times \underline{r}) + \underline{\omega}^{TT} \times \underline{r} + \Delta\underline{a})\,\underline{O}\right] \\
& + B_S\left[(\underline{g} + \underline{\omega}^{TT} \times (\underline{\omega}^{TT} \times \underline{r}) + \underline{\omega}^{TT} \times \underline{r} + \Delta\underline{a})\,\underline{S}\right] + C_{II}\left[(\underline{g} + \underline{\omega}^{TT} \times (\underline{\omega}^{TT} \times \underline{r}) + \underline{\omega}^{TT} \times \underline{r} + \Delta\underline{a})\,\underline{G}\right]^2 \\
& + C_{SS}\left[(\underline{g} + \underline{\omega}^{TT} \times (\underline{\omega}^{TT} \times \underline{r}) + \underline{\omega}^{TT} \times \underline{r} + \Delta\underline{a})\,\underline{S}\right]^2 \\
& + C_{IS}\left[(\underline{g} + \underline{\omega}^{TT} \times (\underline{\omega}^{TT} \times \underline{r}) + \underline{\omega}^{TT} \times \underline{r} + \Delta\underline{a})\,\underline{G}\right]\left[(\underline{g} + \underline{\omega}^{TT} \times (\underline{\omega}^{TT} \times \underline{r}) + (\underline{\omega}^{TT} \times \underline{r} + \Delta\underline{a})\,\underline{S}\right] \\
& + C_{OS}\left[(\underline{g} + \underline{\omega}^{TT} \times (\underline{\omega}^{TT} \times \underline{r}) + \underline{\omega}^{TT} \times \underline{r} + \Delta\underline{a})\,\underline{O}\right]\left[(\underline{g} + \underline{\omega}^{TT} \times (\underline{\omega}^{TT} \times \underline{r}) + \underline{\omega}^{TT} \times \underline{r} + \Delta\underline{a})\,\underline{S}\right] \\
& + C_{IO}\left[(\underline{g} + \underline{\omega}^{TT} \times (\underline{\omega}^{TT} \times \underline{r}) + \underline{\omega}^{TT} \times \underline{r} + \Delta\underline{a})\,\underline{G}\right]\left[(\underline{g} + \underline{\omega}^{TT} \times (\underline{\omega}^{TT} \times \underline{r}) + \underline{\omega}^{TT} \times \underline{r} + \Delta\underline{a})\,\underline{O}\right] \\
& + Q_{II}\left[(\underline{\omega}^{E} + \underline{\omega}^{T} + \Delta\underline{\omega}^{E} + \Delta\underline{\omega}^{T})\,\underline{G}\right]^2 \\
& + Q_{IS}\left[(\underline{\omega}^{E} + \underline{\omega}^{T} + \Delta\underline{\omega}^{E} + \Delta\underline{\omega}^{T})\,\underline{G}\right]\left[(\underline{\omega}^{E} + \underline{\omega}^{T} + \Delta\underline{\omega}^{E} + \Delta\underline{\omega}^{T})\,\underline{S}\right] + J\,d/dt\left[(\underline{\omega}^{E} + \underline{\omega}^{T} + \Delta\underline{\omega}^{E} + \Delta\underline{\omega}^{T})\,\underline{O}\right]\Big\}dt \\
& + \Delta n + Eq
\end{aligned}
$$

APPROXIMATIONS

ASSUME

- Terms containing the integral of components of $\Delta \underline{a}$ always have negligible effect on the gyro readout.
- Terms containing the integral of components of $\underline{\omega}^{TT} \times (\underline{\omega}^{TT} \times \underline{r})$ and $\dot{\underline{\omega}}^{TT} \times \underline{r}$ have a negligible effect on the gyro readout.

  $| \underline{\omega}^{TT} \times (\underline{\omega}^{TT} \times \underline{r}) | < (0.22)^2 \times 0.5 = 0.024 \text{ ft./sec.}^2 = 0.008 \text{ g.}$
- Terms containing Q_{IS} or Q_{II} and the integrals of components of $\Delta \underline{\omega}^{E}$ or $\Delta \underline{\omega}^{T}$ have a negligible effect on the gyro readout.
- Terms containing J and the integrals of the rate of change of $\Delta \underline{\omega}^{E}$ and $\Delta \underline{\omega}^{T}$ have a negligible effect on the gyro readout.

INTRODUCING THESE ASSUMPTIONS INTO THE EQUATION IN CHART 4-2 WE HAVE (AFTER SOME ARRANGEMENTS):

$$\left(\sum_{k=1}^{N} \delta_k\right) - (1/\Delta\Phi)\,\Delta n - (1/\Delta\Phi)\,Eq - (1/\Delta\Phi) \int_{t_0}^{t_N} \left[(\Delta\underline{\omega}^{E} + \Delta\underline{\omega}^{T}) \cdot \underline{G}\right] dt$$

$$= (1/\Delta\Phi) \int_{t_0}^{t_N} [(\underline{\omega}^{E} + \underline{\omega}^{T}) \cdot \underline{G}]\, dt + (R/\Delta\Phi) \int_{t_0}^{t_N} dt + (B_I/\Delta\Phi) \int_{t_0}^{t_N} (\underline{g} \cdot \underline{G})\, dt$$

$$+ (B_O/\Delta\Phi) \int_{t_0}^{t_N} (\underline{g} \cdot \underline{O})\, dt + B_S/\Delta\Phi) \int_{t_0}^{t_N} (\underline{g} \cdot \underline{S})\, dt + (C_{II}/\Delta\Phi) \int_{t_0}^{t_N} (\underline{g} \cdot \underline{G})^2 dt$$

$$+ C_{SS}/\Delta\Phi) \int_{t_0}^{t_N} (\underline{g} \cdot \underline{S})^2\, dt + (C_{IS}/\Delta\Phi) \int_{t_0}^{t_N} (\underline{g} \cdot \underline{G})\,(\underline{g} \cdot \underline{S})\, dt + (C_{OS}/\Delta\Phi) \int_{t_0}^{t_N} (\underline{g} \cdot \underline{O})(\underline{g} \cdot \underline{S})\, dt$$

$$+ (C_{IO}/\Delta\Phi) \int_{t_0}^{t_N} (\underline{g} \cdot \underline{G})(\underline{g} \cdot \underline{O})\, dt + (Q_{II}/\Delta\Phi) \int_{t_0}^{t_N} [(\underline{\omega}^{E} + \underline{\omega}^{T}) \cdot \underline{G}]^2\, dt$$

$$+ (Q_{IS}/\Delta\Phi) \int_{t_0}^{t_N} [(\underline{\omega}^{E} + \underline{\omega}^{T}) \cdot \underline{G}]\,[(\underline{\omega}^{E} + \underline{\omega}^{T}) \cdot \underline{S}]\, dt + (J/\Delta\Phi) \int_{t_0}^{t_N} d/dt\, [(\underline{\omega}^{E} + \underline{\omega}^{T}) \cdot \underline{O}]\, dt$$

INTRODUCTION OF BODY AXES AND INSTRUMENT INDEXING

ASSUME

- $\underline{B}_1\ \underline{B}_2\ \underline{B}_3$ are a triad of orthogonal unit vectors which have a fixed orientation relative to $\underline{G}_1 \cdot \underline{O}_1$ and $\underline{S}_1$ where i is the instrument index equal to 1, 2, or 3.

  Therefore, $\underline{G}_1 = \sum_k (\underline{G}_1 \cdot \underline{B}_k)\underline{B}_k$, $\underline{O}_1 = \sum_k (\underline{O}_1 \cdot \underline{B}_k)\underline{B}_k$, $\underline{S}_1 = \sum_k (\underline{S}_1 \cdot \underline{B}_k)\underline{B}_k$

- $(\underline{G}_1 \cdot \underline{B}_k)$, $(\underline{O}_1 \cdot \underline{B}_k)$ and $(\underline{S}_1\ \underline{B}_k)$ differ from their nominal values $(\underline{G}_1 \cdot \underline{B}_k)^n$, $(\underline{O}_1 \cdot \underline{B}_k)^n$ and $(\underline{S}_1 \cdot \underline{B}_k)^n$ by small numbers. Those differences are sufficiently small as to only affect the gyro readout via the proportional angular velocity term.

WITH THESE ASSUMPTIONS THE GYRO EQUATION BECOMES

$$
\begin{aligned}
P_i^G = {} & \left\{(\underline{G}_1\ \underline{B}_1)/\Delta\Phi\right\}_i \left\{\int_{t_0}^{t_N} (\underline{\omega}^E\ \underline{B}_1)dt + \int_{t_0}^{t_N} (\underline{\omega}^T\ \underline{B}_1)dt\right\} \\
& + \left\{(\underline{G}_1\ \underline{B}_2)/\Delta\Phi\right\}_i \left\{\int_{t_0}^{t_N} (\underline{\omega}^E\ \underline{B}_2)dt + \int_{t_0}^{t_N} (\underline{\omega}^T\ \underline{B}_2)dt\right\} \\
& + \left\{(\underline{G}_1\ \underline{B}_3)/\Delta\Phi\right\}_i \left\{\int_{t_0}^{t_N} (\underline{\omega}^E\ \underline{B}_3)dt + \int_{t_0}^{t_N} (\underline{\omega}^T\ \underline{B}_3)dt\right\} \\
& + \left\{R/\Delta\Phi\right\}_i \left\{\int_{t_0}^{t_N} dt\right\} \\
& + \left\{B_I/\Delta\Phi\right\}_i \left\{\sum_k (\underline{G}_1\ \underline{B}_k)^n \int_{t_0}^{t_N} (g\ \underline{B}_k)dt\right\} \\
& + \left\{B_O/\Delta\Phi\right\}_i \left\{\sum_k (\underline{O}_1\ \underline{B}_k)^n \int_{t_0}^{t_N} (g\ \underline{B}_k)dt\right\} \\
& + \left\{B_S/\Delta\Phi\right\}_i \left\{\sum_k (\underline{S}_1\ \underline{B}_k)^n \int_{t_0}^{t_N} (g\ \underline{B}_k)dt\right\} \\
& + \left\{C_{II}/\Delta\Phi\right\}_i \left\{\sum_k \sum_r (\underline{G}_1\ \underline{B}_k)^n (\underline{G}_1\ \underline{B}_r)^n \int_{t_0}^{t_N} (g\ \underline{B}_k)(g\ \underline{B}_r)dt\right\} \\
& + \left\{C_{SS}/\Delta\Phi\right\}_i \left\{\sum_k \sum_r (\underline{S}_1\ \underline{B}_k)^n (\underline{S}_1\ \underline{B}_r)^n \int_{t_0}^{t_N} (g\ \underline{B}_k)(g\ \underline{B}_r)dt\right\} \\
& + \left\{C_{IO}/\Delta\Phi\right\}_i \left\{\sum_k \sum_r (\underline{G}_1\ \underline{B}_k)^n (\underline{O}_1\ \underline{B}_r)^n \int_{t_0}^{t_N} (g\ \underline{B}_k)(g\ \underline{B}_r)dt\right\} \\
& + \left\{C_{IS}/\Delta\Phi\right\}_i \left\{\sum_k \sum_r (\underline{G}_1\ \underline{B}_k)^n (\underline{S}_1\ \underline{B}_r)^n \int_{t_0}^{t_N} (g\ \underline{B}_k)(g\ \underline{B}_r)dt\right\} \\
& + \left\{C_{OS}/\Delta\Phi\right\}_i \left\{\sum_k \sum_r (\underline{O}_1\ \underline{B}_k)^n (\underline{S}_1\ \underline{B}_r)^n \int_{t_0}^{t_N} (g\ \underline{B}_k)(g\ \underline{B}r)dt\right\} \\
& + \left\{Q_{II}/\Delta\Phi\right\}_i \left\{\sum_k \sum_r (\underline{G}_1\ \underline{B}_k)^n (\underline{G}_1\ \underline{B}_r)^n \int_{t_0}^{t_N} (\underline{\omega}^E\ \underline{B}_k)(\underline{\omega}^E\ \underline{B}_r)dt + \int_{t_0}^{t_N} (\underline{\omega}^E\ \underline{B}_k)(\underline{\omega}^T\ \underline{B}_r)dt + \int_{t_0}^{t_N} (\underline{\omega}^T\ \underline{B}_k)(\underline{\omega}^E\ \underline{B}_r)dt + \int_{t_0}^{t_N} (\underline{\omega}^T\ \underline{B}_k)(\underline{\omega}^T\ \underline{B}_r)dt\right\} \\
& + \left\{Q_{IS}/\Delta\Phi\right\}_i \left\{\sum_k \sum_r (\underline{G}_1\ \underline{B}_k)^n (\underline{S}_1\ \underline{B}_r)^n \int_{t_0}^{t_N} (\underline{\omega}^E\ \underline{B}_k)(\underline{\omega}^E\ \underline{B}_r)dt + \int_{t_0}^{t_N} (\underline{\omega}^E\ \underline{B}_k)(\underline{\omega}^T\ \underline{B}_r)dt + \int_{t_0}^{t_N} (\underline{\omega}^T\ \underline{B}_k)(\underline{\omega}^E\ \underline{B}_r)dt + \int_{t_0}^{t_N} (\underline{\omega}^T\ \underline{B}_k)(\underline{\omega}^T\ \underline{B}_r)dt\right\} \\
& + \left\{J/\Delta\Phi\right\}_i \left\{\sum_k (\underline{O}_1\ \underline{B}_k)^n \int_{t_0}^{t_N} \frac{d}{dt}\ (\underline{\omega}^E\ \underline{B}_k) + (\underline{\omega}^T\ \underline{B}_k)\ dt\right\}
\end{aligned}
$$

WHERE

$$
P_i^G = \left\{\left[\sum_{k=1}^{N} \delta_k\right]_i - (1/\Delta\Phi)_i(\Delta n)_i - (1/\Delta\Phi)_i(Eq)_i - (1/\Delta\Phi)_i \int_{t_0}^{t_N} (\Delta\underline{\omega}^E + \Delta\underline{\omega}^T)\underline{G}_i\ dt\right\}
$$

A CHOICE OF NOMINAL INSTRUMENT AXES

ASSUME

$$[\underline{G}_i \cdot \underline{B}_k]^n = \begin{bmatrix} 1 & 0 & 0 \\ 0 & 1 & 0 \\ 0 & 0 & 1 \end{bmatrix} \quad [\underline{O}_i \cdot \underline{B}_k]^n = \begin{bmatrix} 0 & 0 & 1 \\ 1 & 0 & 0 \\ 0 & 1 & 0 \end{bmatrix} \quad [\underline{S}_i \cdot \underline{B}_k]^n = \begin{bmatrix} 0 & -1 & 0 \\ 0 & 0 & -1 \\ 0 & 0 & 0 \end{bmatrix}$$

THEN

$$\begin{aligned}
P_1^G = {} & \left\{(\underline{G}_1 \cdot \underline{B}_1)/\Delta\Phi\right\}_1 \left\{\int_{t_0}^{t_N} (\underline{\omega}^E \cdot \underline{B}_1)dt + \int_{t_0}^{t_N} (\underline{\omega}^T \cdot \underline{B}_1)dt\right\} \\
& + \left\{(\underline{G}_1 \cdot \underline{B}_2)/\Delta\Phi\right\}_1 \left\{\int_{t_0}^{t_N} (\underline{\omega}^E \cdot \underline{B}_2)dt + \int_{t_0}^{t_N} (\underline{\omega}^T \cdot \underline{B}_2)dt\right\} \\
& + \left\{(\underline{G}_1 \cdot \underline{B}_3)/\Delta\Phi\right\}_1 \left\{\int_{t_0}^{t_N} (\underline{\omega}^E \cdot \underline{B}_3)dt + \int_{t_0}^{t_N} (\underline{\omega}^T \cdot \underline{B}_3)dt\right\} \\
& + \left\{R/\Delta\Phi\right\}_1 \left\{\int_{t_0}^{t_N} dt\right\} \\
& + \left\{B_I/\Delta\Phi\right\}_1 \left\{\int_{t_0}^{t_N} (\underline{g} \cdot \underline{B}_1)dt\right\} \\
& + \left\{B_O/\Delta\Phi\right\}_1 \left\{\int_{t_0}^{t_N} (\underline{g} \cdot \underline{B}_3)dt\right\} \\
& + \left\{B_S/\Delta\Phi\right\}_1 \left\{-\int_{t_0}^{t_N} (\underline{g} \cdot \underline{B}_2)dt\right\} \\
& + \left\{C_{II}/\Delta\Phi\right\}_1 \left\{\int_{t_0}^{t_N} (\underline{g} \cdot \underline{B}_1)^2 dt\right\} \\
& + \left\{C_{SS}/\Delta\Phi\right\}_1 \left\{\int_{t_0}^{t_N} (\underline{g} \cdot \underline{B}_2)^2 dt\right\} \\
& + \left\{C_{IO}/\Delta\Phi\right\}_1 \left\{\int_{t_0}^{t_N} (\underline{g} \cdot \underline{B}_1)(\underline{g} \cdot \underline{B}_3)dt\right\} \\
& + \left\{C_{IS}/\Delta\Phi\right\}_1 \left\{-\int_{t_0}^{t_N} (\underline{g} \cdot \underline{B}_1)(\underline{g} \cdot \underline{B}_2)dt\right\} \\
& + \left\{C_{OS}/\Delta\Phi\right\}_1 \left\{-\int_{t_0}^{t_N} (\underline{g} \cdot \underline{B}_2)(\underline{g} \cdot \underline{B}_3)dt\right\} \\
& + \left\{Q_{II}/\Delta\Phi\right\}_1 \left\{\int_{t_0}^{t_N} (\underline{\omega}^E \cdot \underline{B}_1)^2 dt + \int_{t_0}^{t_N} (\underline{\omega}^T \cdot \underline{B}_1)^2 dt\right. \\
& \qquad \left. + 2\int_{t_0}^{t_N} (\underline{\omega}^E \cdot \underline{B}_1)(\underline{\omega}^T \cdot \underline{B}_1)dt\right\} \\
& + \left\{Q_{IS}/\Delta\Phi\right\}_1 \left\{-\int_{t_0}^{t_N} (\underline{\omega}^E \cdot \underline{B}_1)(\underline{\omega}^E \cdot \underline{B}_2)dt\right. \\
& \qquad -\int_{t_0}^{t_N} (\underline{\omega}^E \cdot \underline{B}_1)(\underline{\omega}^T \cdot \underline{B}_2)dt \\
& \qquad -\int_{t_0}^{t_N} (\underline{\omega}^T \cdot \underline{B}_1)(\underline{\omega}^E \cdot \underline{B}_2)dt \\
& \qquad \left. -\int_{t_0}^{t_N} (\underline{\omega}^T \cdot \underline{B}_1)(\underline{\omega}^T \cdot \underline{B}_2)dt\right\} \\
& + \left\{J/\Delta\Phi\right\}_1 \left\{\int_{t_0}^{t_N} \frac{d}{dt}[(\underline{\omega}^E \cdot \underline{B}_3) + (\underline{\omega}^T \cdot \underline{B}_3)]dt\right\}
\end{aligned}$$

$$\begin{aligned}
P_2^G = {} & \left\{(\underline{G}_2 \cdot \underline{B}_1)/\Delta\Phi\right\}_2 \left\{\int_{t_0}^{t_N} (\underline{\omega}^E \cdot \underline{B}_1)dt + \int_{t_0}^{t_N} (\underline{\omega}^T \cdot \underline{B}_1)dt\right\} \\
& + \left\{(\underline{G}_2 \cdot \underline{B}_2)/\Delta\Phi\right\}_2 \left\{\int_{t_0}^{t_N} (\underline{\omega}^E \cdot \underline{B}_2)dt + \int_{t_0}^{t_N} (\underline{\omega}^T \cdot \underline{B}_2)dt\right\} \\
& + \left\{(\underline{G}_2 \cdot \underline{B}_3)/\Delta\Phi\right\}_2 \left\{\int_{t_0}^{t_N} (\underline{\omega}^E \cdot \underline{B}_3)dt + \int_{t_0}^{t_N} (\underline{\omega}^T \cdot \underline{B}_3)dt\right\} \\
& + \left\{R/\Delta\Phi\right\}_2 \left\{\int_{t_0}^{t_N} dt\right\} \\
& + \left\{B_I/\Delta\Phi\right\}_2 \left\{\int_{t_0}^{t_N} (\underline{g} \cdot \underline{B}_2)dt\right\} \\
& + \left\{B_O/\Delta\Phi\right\}_2 \left\{\int_{t_0}^{t_N} (\underline{g} \cdot \underline{B}_1)dt\right\} \\
& + \left\{B_S/\Delta\Phi\right\}_2 \left\{-\int_{t_0}^{t_N} (\underline{g} \cdot \underline{B}_3)dt\right\} \\
& + \left\{C_{II}/\Delta\Phi\right\}_2 \left\{\int_{t_0}^{t_N} (\underline{g} \cdot \underline{B}_2)^2 dt\right\} \\
& + \left\{C_{SS}/\Delta\Phi\right\}_2 \left\{\int_{t_0}^{t_N} (\underline{g} \cdot \underline{B}_3)^2 dt\right\} \\
& + \left\{C_{IO}/\Delta\Phi\right\}_2 \left\{\int_{t_0}^{t_N} (\underline{g} \cdot \underline{B}_1)(\underline{g} \cdot \underline{B}_2)dt\right\} \\
& + \left\{C_{IS}/\Delta\Phi\right\}_2 \left\{-\int_{t_0}^{t_N} (\underline{g} \cdot \underline{B}_2)(\underline{g} \cdot \underline{B}_3)dt\right\} \\
& + \left\{C_{OS}/\Delta\Phi\right\}_2 \left\{-\int_{t_0}^{t_N} (\underline{g} \cdot \underline{B}_1)(\underline{g} \cdot \underline{B}_3)dt\right\} \\
& + \left\{Q_{II}/\Delta\Phi\right\}_2 \left\{\int_{t_0}^{t_N} (\underline{\omega}^E \cdot \underline{B}_2)^2 dt + \int_{t_0}^{t_N} (\underline{\omega}^T \cdot \underline{B}_2)^2 dt\right. \\
& \qquad \left. + 2\int_{t_0}^{t_N} (\underline{\omega}^E \cdot \underline{B}_2)(\underline{\omega}^T \cdot \underline{B}_2)dt\right\} \\
& + \left\{Q_{IS}/\Delta\Phi\right\}_2 \left\{-\int_{t_0}^{t_N} (\underline{\omega}^E \cdot \underline{B}_2)(\underline{\omega}^E \cdot \underline{B}_3)dt\right. \\
& \qquad -\int_{t_0}^{t_N} (\underline{\omega}^E \cdot \underline{B}_2)(\underline{\omega}^T \cdot \underline{B}_3)dt \\
& \qquad -\int_{t_0}^{t_N} (\underline{\omega}^T \cdot \underline{B}_2)(\underline{\omega}^E \cdot \underline{B}_3)dt \\
& \qquad \left. -\int_{t_0}^{t_N} (\underline{\omega}^T \cdot \underline{B}_2)(\underline{\omega}^T \cdot \underline{B}_3)dt\right\} \\
& + \left\{J/\Delta\Phi\right\}_2 \left\{\int_{t_0}^{t_N} \frac{d}{dt}[(\underline{\omega}^E \cdot \underline{B}_1) + (\underline{\omega}^T \cdot \underline{B}_1)]dt\right\}
\end{aligned}$$

$$\begin{aligned}
P_3^G = {} & \left\{(\underline{G}_3 \cdot \underline{B}_1)/\Delta\Phi\right\}_3 \left\{\int_{t_0}^{t_N} (\underline{\omega}^E \cdot \underline{B}_1)dt + \int_{t_0}^{t_N} (\underline{\omega}^T \cdot \underline{B}_1)dt\right\} \\
& + \left\{(\underline{G}_3 \cdot \underline{B}_2/\Delta\Phi\right\}_3 \left\{\int_{t_0}^{t_N} (\underline{\omega}^E \cdot \underline{B}_2)dt + \int_{t_0}^{t_N} (\underline{\omega}^T \cdot \underline{B}_2)dt\right\} \\
& + \left\{(\underline{G}_3 \cdot \underline{B}_3)/\Delta\Phi\right\}_3 \left\{\int_{t_0}^{t_N} (\underline{\omega}^E \cdot \underline{B}_3)dt + \int_{t_0}^{t_N} (\underline{\omega}^T \cdot \underline{B}_3)dt\right\} \\
& + \left\{R/\Delta\Phi\right\}_3 \left\{\int_{t_0}^{t_N} dt\right\} \\
& + \left\{B_I/\Delta\Phi\right\}_3 \left\{\int_{t_0}^{t_N} (\underline{g} \cdot \underline{B}_3)dt\right\} \\
& + \left\{B_O/\Delta\Phi\right\}_3 \left\{\int_{t_0}^{t_N} (\underline{g} \cdot \underline{B}_1)dt\right\} \\
& + \left\{B_S/\Delta\Phi\right\}_3 \left\{\int_{t_0}^{t_N} (\underline{g} \cdot \underline{B}_2)dt\right\} \\
& + \left\{C_{II}/\Delta\Phi\right\}_3 \left\{\int_{t_0}^{t_N} (\underline{g} \cdot \underline{B}_3)^2 dt\right\} \\
& + \left\{C_{SS}/\Delta\Phi\right\}_3 \left\{\int_{t_0}^{t_N} (\underline{g} \cdot \underline{B}_2)^2 dt\right\} \\
& + \left\{C_{IO}/\Delta\Phi\right\}_3 \left\{\int_{t_0}^{t_N} (\underline{g} \cdot \underline{B}_1)(\underline{g} \cdot \underline{B}_3)dt\right\} \\
& + \left\{C_{IS}/\Delta\Phi\right\}_3 \left\{\int_{t_0}^{t_N} (\underline{g} \cdot \underline{B}_2)(\underline{g} \cdot \underline{B}_3)dt\right\} \\
& + \left\{C_{OS}/\Delta\Phi\right\}_3 \left\{\int_{t_0}^{t_N} (\underline{g} \cdot \underline{B}_1)(\underline{g} \cdot \underline{B}_2)dt\right\} \\
& + \left\{Q_{II}/\Delta\Phi\right\}_3 \left\{\int_{t_0}^{t_N} (\underline{\omega}^E \cdot \underline{B}_3)^2 dt + \int_{t_0}^{t_N} (\underline{\omega}^T \cdot \underline{B}_3)^2 dt\right. \\
& \qquad \left. + 2\int_{t_0}^{t_N} (\underline{\omega}^E \cdot \underline{B}_3)(\underline{\omega}^T \cdot \underline{B}_3)dt\right\} \\
& + \left\{Q_{IS}/\Delta\Phi\right\}_3 \left\{\int_{t_0}^{t_N} (\underline{\omega}^E \cdot \underline{B}_2)(\underline{\omega}^E \cdot \underline{B}_3)dt\right. \\
& \qquad +\int_{t_0}^{t_N} (\underline{\omega}^E \cdot \underline{B}_2)(\underline{\omega}^T \cdot \underline{B}_3)dt \\
& \qquad +\int_{t_0}^{t_N} (\underline{\omega}^T \cdot \underline{B}_2)(\underline{\omega}^E \cdot \underline{B}_3)dt \\
& \qquad \left. +\int_{t_0}^{t_N} (\underline{\omega}^T \cdot \underline{B}_2)(\underline{\omega}^T \cdot \underline{B}_3)dt\right\} \\
& + \left\{J/\Delta\Phi\right\}_3 \left\{\int_{t_0}^{t_N} \frac{d}{dt}[(\underline{\omega}^E \cdot \underline{B}_1) + (\underline{\omega}^T \cdot \underline{B}_1)]dt\right\}
\end{aligned}$$

FOLDOUT FRAME 1

FOLDOUT FRAME 2

INTEGRAL EVALUATIONS

ASSUME

- $\underline{\omega}^E$, $\underline{g}$ and $\underline{\omega}^T$ are located as shown in Figure 3-2
- All transformations between frames follow the convention given by the following example:

$$\underline{B}_i = \sum_m T^{BR}_{im} \underline{R}_m$$

- $\int_{t_0}^{t_N} dt = t_N - t_0 + \epsilon_C = \Delta t + \epsilon_C$ where ϵ_C is the clock quantization error
- The effect of ϵ_C is negligible

THE NINE INTEGRALS CAN NOW BE WRITTEN AS:

$$\int_{t_0}^{t_N} (\underline{\omega}^E \cdot \underline{B}_i)\, dt = \int_{t_0}^{t_N} \sum_m \sum_n \sum_p T^{BR}_{im} T^{RT}_{mn} T^{TE}_{np} (\underline{\omega}^E \cdot \underline{E}_p)\, dt$$

$$\int_{t_0}^{t_N} (\underline{\omega}^T \cdot \underline{B}_i)\, dt = \int_{t_0}^{t_N} \sum_m T^{BR}_{im} (\underline{\omega}^T \cdot \underline{R}_m)\, dt$$

$$\int_{t_0}^{t_N} (\underline{g} \cdot \underline{B}_i)\, dt = \int_{t_0}^{t_N} \sum_m \sum_n \sum_p T^{BR}_{im} T^{RT}_{mn} T^{TE}_{np} (\underline{g} \cdot \underline{E}_p)\, dt$$

$$\int_{t_0}^{t_N} (\underline{g} \cdot \underline{B}_k)(\underline{g} \cdot \underline{B}_r)\, dt = \int_{t_0}^{t_N} \left[\sum_m \sum_n \sum_p T^{BR}_{km} T^{RT}_{mn} T^{TE}_{np} (\underline{g} \cdot \underline{E}_p)\right]\left[\sum_q \sum_u \sum_s T^{BR}_{rq} T^{RT}_{qu} T^{TE}_{us} (\underline{g} \cdot \underline{E}_s)\right] dt$$

$$\int_{t_0}^{t_N} (\underline{\omega}^E \cdot \underline{B}_k)(\underline{\omega}^E \cdot \underline{B}_r)\, dt = \int_{t_0}^{t_N} \left[\sum_m \sum_n \sum_p T^{BR}_{km} T^{RT}_{mn} T^{TE}_{np} (\underline{\omega}^E \cdot \underline{E}_p)\right]\left[\sum_q \sum_u \sum_s T^{BR}_{rq} T^{RT}_{qu} T^{TE}_{us} (\underline{\omega}^E \cdot \underline{E}_s)\right] dt$$

$$\int_{t_0}^{t_N} (\underline{\omega}^E \cdot \underline{B}_k)(\underline{\omega}^T \cdot \underline{B}_r)\, dt = \int_{t_0}^{t_N} \left[\sum_m \sum_n \sum_p T^{BR}_{km} T^{RT}_{mn} T^{TE}_{np} (\underline{\omega}^E \cdot \underline{E}_p)\right]\left[\sum_q T^{BR}_{rq} (\underline{\omega}^T \cdot \underline{R}_q)\right] dt$$

$$\int_{t_0}^{t_N} (\underline{\omega}^T \cdot \underline{B}_k)(\underline{\omega}^T \cdot \underline{B}_r)\, dt = \int_{t_0}^{t_N} \left[\sum_m T^{BR}_{km} (\underline{\omega}^T \cdot \underline{R}_m)\right]\left[\sum_q T^{BR}_{rq} (\underline{\omega}^T \cdot \underline{R}_q)\right] dt$$

$$\int_{t_0}^{t_N} dt = t_N - t_0 \equiv \Delta t$$

$$\int_{t_0}^{t_N} \frac{d}{dt}\left[(\underline{\omega}^E \cdot \underline{B}_k) + (\underline{\omega}^T \cdot \underline{B}_k)\right] dt = \left[\sum_m \sum_n \sum_p T^{BR}_{km} T^{RT}_{mn} T^{TE}_{np} (\underline{\omega}^E \cdot \underline{E}_p) + \sum_q T^{BR}_{kq} (\underline{\omega}^T \cdot \underline{R}_q)\right]_{t_0}^{t_N}$$

INTEGRAL EVALUATIONS (Continued)

ASSUME

$$[\underline{\omega}^E \cdot \underline{E}_1] = \begin{bmatrix} \omega^E \cos\lambda \\ 0 \\ \omega^E \sin\lambda \end{bmatrix} \quad [\underline{g} \cdot \underline{E}_1] = \begin{bmatrix} g \\ 0 \\ 0 \end{bmatrix} \quad [\underline{\omega}^T \cdot \underline{R}_1] = \begin{bmatrix} \omega^T \\ 0 \\ 0 \end{bmatrix}$$

$$[T_{1j}^{TE}] = \begin{bmatrix} 0 & 1 & 0 \\ \cos\phi_1 & 0 & -\sin\phi_1 \\ -\sin\phi_1 & 0 & -\cos\phi_1 \end{bmatrix} \quad [T_{1j}^{RT}] = \begin{bmatrix} 0 & 1 & 0 \\ \cos\phi_2 & 0 & -\sin\phi_2 \\ -\sin\phi_2 & 0 & -\cos\phi_2 \end{bmatrix}$$

THEN

$$\int_{t_0}^{t_N} (\underline{\omega}^E \cdot \underline{B}_1) dt = \omega^E \cos(\phi_1 + \lambda)\, T_{11}^{BR} \int_{t_0}^{t_N} dt + \omega^E \sin(\phi_1 + \lambda) \left[T_{12}^{BR} \int_{t_0}^{t_N} \sin\phi_2 dt + T_{13}^{BR} \int_{t_0}^{t_N} \cos\phi_3 dt \right]$$

$$\int_{t_0}^{t_N} (\underline{\omega}^T \cdot \underline{B}_1) dt = T_{11}^{BR} \int_{t_0}^{t_N} \omega^T dt$$

$$\int_{t_0}^{t_N} (\underline{g} \cdot \underline{B}_1) dt = g \cos\phi_1\, T_{11}^{BR} \int_{t_0}^{t_N} dt + g \sin\phi_1 \left[T_{12}^{BR} \int_{t_0}^{t_N} \sin\phi_2 dt + T_{13}^{BR} \int_{t_0}^{t_N} \cos\phi_2\, dt \right]$$

$$\int_{t_0}^{t_N} (\underline{g} \cdot \underline{B}_k)(\underline{g} \cdot \underline{B}_r) dt = g^2 \cos^2\phi_1\, T_{k1}^{BR}\, T_{r1}^{BR} \int_{t_0}^{t_N} dt$$

$$+ g^2 \sin^2\phi_1 \left[T_{k2}^{BR} T_{r2}^{BR} \int_{t_0}^{t_N} \sin^2\phi_2 dt + T_{k3}^{BR} T_{r3}^{BR} \int_{t_0}^{t_N} \cos^2\phi_2 dt + (T_{k2}^{BR} T_{r3}^{BR} + T_{k3}^{BR} T_{r2}^{BR}) \int_{t_0}^{t_N} \sin\phi_2 \cos\phi_2 dt \right]$$

$$+ g^2 \sin\phi_1 \cos\phi_1 \left[(T_{k1}^{BR} T_{r2}^{BR} + T_{k2}^{BR} T_{r1}^{BR}) \int_{t_0}^{t_N} \sin\phi_2 dt + (T_{k1}^{BR} T_{r3}^{BR} + T_{k3}^{BR} T_{r1}^{BR}) \int_{t_0}^{t_N} \cos\phi_2 dt \right]$$

$$\int_{t_0}^{t_N} (\underline{\omega}^E \cdot \underline{B}_k)(\underline{\omega}^E \cdot \underline{B}_r) dt = (\omega^E)^2 \cos^2(\phi_1 + \lambda)\, T_{k1}^{BR} T_{r1}^{BR} \int_{t_0}^{t_N} dt$$

$$+ (\omega^E)^2 \sin^2(\phi_1 + \lambda) \left[T_{k2}^{BR} T_{r2}^{BR} \int_{t_0}^{t_N} \sin^2\phi_2 dt + T_{k3}^{BR} T_{r3}^{BR} \int_{t_0}^{t_N} \cos^2\phi_2 dt + (T_{k2}^{BR} T_{r3}^{BR} + T_{k3}^{BR} T_{r2}^{BR}) \int_{t_0}^{t_N} \sin\phi_2 \cos\phi_2 dt \right]$$

$$+ (\omega^E)^2 \sin(\phi_1 + \lambda) \cos(\phi_1 + \lambda) \left[(T_{k1}^{BR} T_{r2}^{BR} + T_{k2}^{BR} T_{r1}^{BR}) \int_{t_0}^{t_N} \sin\phi_2 dt + (T_{k1}^{BR} T_{r3}^{BR} + T_{k3}^{BR} T_{r1}^{BR}) \int_{t_0}^{t_N} \cos\phi_2 dt \right]$$

$$\int_{t_0}^{t_N} (\underline{\omega}^E \cdot \underline{B}_k)(\underline{\omega}^T \cdot \underline{B}_r) dt = \omega^E\, T_{r1}^{BR} T_{k1}^{BR} \cos(\phi_1 + \lambda) \int_{t_0}^{t_N} \omega^T dt + \omega^E\, T_{r1}^{BR} T_{k2}^{BR} \sin(\phi_1 + \lambda) \int_{t_0}^{t_N} \omega^T \sin\phi_2 dt$$

$$+ \omega^E\, T_{r1}^{BR} T_{k3}^{BR} \sin(\phi_1 + \lambda) \int_{t_0}^{t_N} \omega^T \cos\phi_2\, dt$$

$$\int_{t_0}^{t_N} (\underline{\omega}^T \cdot \underline{B}_k)(\underline{\omega}^T \cdot \underline{B}_r) dt = T_{k1}^{BR}\, T_{r1}^{BR} \int_{t_0}^{t_N} (\omega^T)^2\, dt$$

$$\int_{t_0}^{t_N} dt = \Delta t$$

$$\int_{t_0}^{t_N} \frac{d}{dt} \left[(\underline{\omega}^E \cdot \underline{B}_k)(\underline{\omega}^T \cdot \underline{B}_k) \right] dt = \left\{ \omega^E \cos(\phi_1 + \lambda)\, T_{k1}^{BR} + \omega^E \sin(\phi_1 + \lambda) \left[T_{k2}^{BR} \sin\phi_2 + T_{k3}^{BR} \cos\phi_2 \right] + T_{k1}^{BR}\, \omega^T \right\} \Big|_{t_0}^{t_N}$$

FOLDOUT FRAME 1

FOLDOUT FRAME 2

INTEGRAL EVALUATIONS (Continued)

LET

$$\sin^2 \phi_2 = 1/2 - (\cos 2\phi_2) / 2$$

$$\cos^2 \phi_2 = 1/2 + (\cos 2\phi_2) / 2$$

$$\sin \phi_2 \cos \phi_2 = \left(\sin 2\phi_2\right) / 2$$

$$\omega^T = \frac{d\phi_2}{dt}$$

THEN

$$\left[\int_{t_0}^{t_N} (\underline{\omega}^T \cdot \underline{B}_i)dt + \int_{t_0}^{t_N} (\underline{\omega}^E \cdot \underline{B}_i)dt\right] = \left[\Delta\phi_2 + \omega^E \Delta t \cos(\phi_1 + \lambda)\right] T_{i1}^{BR} + \omega^E \sin(\phi_1 + \lambda) \left[T_{i2}^{BR} \int_{t_0}^{t_N} \sin\phi_2 \, dt + T_{i3}^{BR} \int_{t_0}^{t_N} \cos\phi_2 \, dt\right]$$

$$\left[\int_{t_0}^{t_N} (\underline{g} \cdot \underline{B}_i)dt\right] = g\Delta t \cos\phi_1 \left[T_{i1}^{BR}\right] + g \sin\phi_1 \left[T_{i2}^{BR} \int_{t_0}^{t_N} \sin\phi_2 \, dt + T_{i3}^{BR} \int_{t_0}^{t_N} \cos\phi_2 \, dt\right]$$

$$\left[\int_{t_0}^{t_N} (\underline{g} \cdot \underline{B}_k)(\underline{g} \cdot \underline{B}_r)dt\right] = g^2 \Delta t \left[\frac{T_{k1}^{BR} T_{r1}^{BR}}{2} (3\cos^2\phi_1 - 1) + \frac{\delta_{kr}}{2} (\sin^2\phi_1)\right]$$

$$+ g^2 \sin^2\phi_1 \left[\frac{T_{k3}^{BR} T_{r3}^{BR} - T_{k2}^{BR} T_{r2}^{BR}}{2} \int_{t_0}^{t_N} \cos 2\phi_2 \, dt + \frac{T_{k2}^{BR} T_{r3}^{BR} + T_{k3}^{BR} T_{r2}^{BR}}{2} \int_{t_0}^{t_N} \sin 2\phi_2 \, dt\right]$$

$$+ g^2 \sin\phi_1 \cos\phi_1 \left[(T_{k1}^{BR} T_{r2}^{BR} + T_{k2}^{BR} T_{r1}^{BR}) \int_{t_0}^{t_N} \sin\phi_2 \, dt + (T_{k1}^{BR} T_{r3}^{BR} + T_{k3}^{BR} T_{r1}^{BR}) \int_{t_0}^{t_N} \cos\phi_2 \, dt\right]$$

$$\left[\int_{t_0}^{t_N} (\underline{\omega}^E \cdot \underline{B}_k)(\underline{\omega}^E \cdot \underline{B}_r)dt + \int_{t_0}^{t_N} (\omega^E \cdot \underline{B}_k)(\omega^T \cdot \underline{B}_r)dt + \int_{t_0}^{t_N} (\omega^T \cdot \underline{B}_k)(\omega^E \cdot \underline{B}_r)dt + \int_{t_0}^{t_N} (\omega^T \cdot \underline{B}_k)(\omega^T \cdot \underline{B}_r)dt\right]$$

$$= (\omega^E)^2 \Delta t \left[\frac{T_{k1}^{BR} T_{r1}^{BR}}{2} \left(3\cos^2(\phi_1 + \lambda) - 1\right) + \frac{\delta_{kr}}{2} \left(\sin^2(\phi_1 + \lambda)\right)\right] + 2\omega^E \Delta\phi_2 \, T_{k1}^{BR} T_{r1}^{BR} \cos(\phi_1 + \lambda)$$

$$+ T_{k1}^{BR} T_{r1}^{BR} \int_{t_0}^{t_N} (\omega^T)^2 \, dt + (\omega^E)^2 \sin^2(\phi_1 + \lambda) \left[\frac{(T_{k3}^{BR} T_{r3}^{BR} - T_{k2}^{BR} T_{r2}^{BR})}{2} \int_{t_0}^{t_N} \cos 2\phi_2 \, dt\right.$$

$$\left. + \frac{T_{k2}^{BR} T_{r3}^{BR} + T_{k3}^{BR} T_{r2}^{BR}}{2} \int_{t_0}^{t_N} \sin 2\phi_2 \, dt\right]$$

$$+ (\omega^E)^2 \sin(\phi_1 + \lambda) \cos(\phi_1 + \lambda) \left[(T_{k1}^{BR} T_{r2}^{BR} + T_{k2}^{BR} T_{r1}^{BR}) \int_{t_0}^{t_N} \sin\phi_2 \, dt + (T_{k1}^{BR} T_{r3}^{BR} + T_{k3}^{BR} T_{r1}^{BR}) \int_{t_0}^{t_N} \cos\phi_2 dt\right]$$

$$+ (\omega^E) \sin(\phi_1 + \lambda) \left[(T_{r1}^{BR} T_{k3}^{BR} + T_{k1}^{BR} T_{r3}^{BR}) \Delta \sin\phi_2 - (T_{r1}^{BR} T_{k2}^{BR} + T_{k1}^{BR} T_{r2}^{BR}) \Delta \cos\phi_2\right.$$

$$\left[\int_{t_0}^{t_N} dt\right] = \Delta t$$

$$\left[\int_{t_0}^{t_N} \frac{d}{dt} \left[(\underline{\omega}^E \cdot \underline{B}_k) + (\underline{\omega}^T \cdot \underline{B}_k)\right] dt\right] = \omega^E \sin(\phi_1 + \lambda) \left[T_{k2}^{BR} \Delta \sin\phi_2 + T_{k3}^{BR} \Delta \cos\phi_2\right] + T_{k1}^{BR} \Delta \omega^T$$

where $\delta_{kr} = 1$ if $k = r$
$= 0$ if $k \neq r$

FOLDOUT FRAME 1

FOLDOUT FRAME 2

4.1.2 Accelerometer Equations

As with the preceding gyro equation development, we develop the general accelerometer calibration equations by introducing the laboratory geometry and environment into the instrument model. A great number of the comments relative to the development of the general gyro equations apply equally well to the development of the general accelerometer equations.

As in Section 4.1.1, we discuss each of the charts in turn.

Fundamental Accelerometer Model (Chart 4-9)

The accelerometer mathematical model was introduced in Section 2.2.2. Chart 4-9 is a repeat of Chart 2-1, showing the input/output relationships for a vibrating-string accelerometer. The notation presented is self-explanatory.

Introduction of Laboratory Environment (Chart 4-10)

In Chart 4-9 the accelerometer output is seen to be influenced by only applied acceleration inputs. Note that the accelerometers are assumed to be in a stationary attitude relative to the earth. The stationary attitude assumption dictates that all accelerometer calibrations will be accomplished without a use of the dynamic rotational ability of the test table. The main reason for this constraint is the fact that a motion of the test table introduces undesirable angular velocity-related accelerations. (See Section 2.1 of the trade-off document.)

Approximations (Chart 4-11)

The environment approximations are self-explanatory. All neglected terms are assumed to have a second order effect on the accelerometer readout

Introduction of Body Axes and Instrument Indexing (Chart 4-12)

The comments presented in the gyro equation development apply equally well here.

A Choice of Body Axes (Chart 4-13)

These equations are the desired general form. In Section 4.2 the determination of the calibration constants will be shown to be dictated by a control of the parameters found in the Environment Evaluation part of Chart 4-13.

THE FUNDAMENTAL ACCELEROMETER MODEL

THE ACCELEROMETER MODEL IS:

$$\int_{t_a}^{t_b} f_2\,dt - \int_{t_a}^{t_b} f_1\,dt = (N_2 - N_1) + Eq = D_1 \int_{t_a}^{t_b} (\underline{a}\cdot\underline{A})dt + D_1 \left\{ \int_{t_a}^{t_b} [D_0 + D_2(\underline{a}\cdot\underline{A})^2 + D_3(\underline{a}\cdot\underline{A})^3]dt \right\}$$

WHERE:

- $\underline{a}$ is the acceleration applied to the accelerometer
- $t_a \leq t \leq t_b$ is the time interval over which $\underline{a}$ is measured
- $\underline{A}$ is a unit vector directed along the input axis of the accelerometer
- N_1 and N_2 are the number of zero crossings detected in $t_a \leq t \leq t_b$ from both strings of the accelerometer
- Eq is the instrument quantization error due to the fact that t_a and t_b do not correspond to zero crossings
- D_1 is the accelerometer scale factor
- D_0 is the accelerometer bias
- D_2 is the second order coefficient
- D_3 is the third order coefficient
- f_2 and f_1 are string frequencies in pulses/second

INTRODUCTION OF LABORATORY ENVIRONMENT

ASSUME

- $\underline{a}^{L} = \underline{g} + \Delta\underline{a}$ is the total applied specific force

  Where:

  $\underline{g}$ is the assumed (surveyed) laboratory specific force

  $\Delta\underline{a}$ is the deviation of the assumed laboratory specific force from the true

INTRODUCING THESE ASSUMPTIONS INTO THE EQUATION IN CHART 4-9 WE HAVE:

$$(N_2 - N_1) + Eq = D_1 \int_{t_a}^{t_b} [(\underline{g} + \Delta\underline{a}) \cdot \underline{A}]\,dt + D_1 \left\{ \int_{t_a}^{t_b} [D_0 + D_2 (\underline{g} \cdot \underline{A} + \Delta\underline{a} \cdot \underline{A})^2 + D_3 (\underline{g} \cdot \underline{A} + \Delta\underline{a} \cdot \underline{A})^3]\,dt \right\}$$

NOTE THAT THE TEST STAND IS ASSUMED STATIONARY

(THAT IS $\underline{\omega}^{TT} \times (\underline{\omega}^{TT} \times \underline{r})$ and $\dot{\underline{\omega}}^{TT} \times \underline{r}$ WILL NEVER BE SENSED)

APPROXIMATIONS

ASSUME

- Terms containing the product of the integrals of components of $\Delta\underline{a}$ with D_2 or D_3 have a negligible effect on the accelerometer readout.
- $(\underline{g}\cdot\underline{A})$ is a constant over the time interval $t_a \leq t \leq t_b$
- $\int_{t_0}^{t_b} dt = \Delta t + \epsilon$

  where:

  $\Delta t = N\tau$, N is an integer and τ is the clock period

  ϵ_C is the clock quantization error
- Terms containing the product of ϵ_C with D_0, D_2, or D_3 have a negligible effect on the accelerometer readout.

WITH THESE ASSUMPTIONS, THE ACCELEROMETER EQUATION BECOMES:

$$\left[(N_2 - N_1) + Eq - D_1 \int_{t_a}^{t_b} (\Delta\underline{a}\cdot\underline{A})\, dt - D_1 (\underline{g}\cdot\underline{A})\,\epsilon\right]$$

$$= \left\{ D_1 (\underline{g}\cdot\underline{A}) + D_1\left[D_0 + D_2 (\underline{g}\cdot\underline{A})^2 + D_3(\underline{g}\cdot\underline{A})^3\right] \right\} \Delta t$$

INTRODUCTION OF BODY AXES AND INSTRUMENT INDEXING

ASSUME

- $\underline{B}_1$, $\underline{B}_2$, and $\underline{B}_3$ are a triad of orthogonal unit vectors which have a constant orientation relative to $\underline{A}_i$, where i is the instrument index equal to 1, 2, or 3.

  Therefore,
  $$\underline{A}_i = \sum_{k=1}^{3} (\underline{A}_i \cdot \underline{B}_k)\, B_k$$

- $(\underline{A}_i \cdot \underline{B}_k)$ differ from their nominal values $(\underline{A}_i \cdot \underline{B}_k)^n$ by small numbers. Those differences are sufficiently small as to only affect the accelerometer readout via the proportional acceleration term.

- The effect of ϵ_C is negligible.

THEN

$$\begin{aligned}
P_i^A = {} & \left\{ D_1(\underline{A}_i \cdot \underline{B}_1) \right\}_i \left\{ (\underline{g} \cdot \underline{B}_1)\Delta t \right\} \\
& + \left\{ D_1(\underline{A}_i \cdot \underline{B}_2) \right\}_i \left\{ (\underline{g} \cdot \underline{B}_2)\Delta t \right\} \\
& + \left\{ D_1(\underline{A}_i \cdot \underline{B}_3) \right\}_i \left\{ (\underline{g} \cdot \underline{B}_3)\Delta t \right\} \\
& + \left\{ D_1 D_0 \right\}_i \left\{ \Delta t \right\} \\
& + \left\{ D_1 D_2 \right\}_i \left\{ \left[\sum_k \sum_r (\underline{A}_i \cdot \underline{B}_k)^n (\underline{A}_i \cdot \underline{B}_r)^n (\underline{g} \cdot \underline{B}_k)(\underline{g} \cdot \underline{B}_r) \right] \Delta t \right\} \\
& + \left\{ D_1 D_3 \right\}_i \left\{ \left[\sum_k \sum_r \sum_m (\underline{A}_i \cdot \underline{B}_k)^n (\underline{A}_i \cdot \underline{B}_r)^n (\underline{A}_i \cdot \underline{B}_m)^n (\underline{g} \cdot \underline{B}_k)(\underline{g} \cdot \underline{B}_r)(\underline{g} \cdot \underline{B}_m) \right] \Delta t \right\}
\end{aligned}$$

WHERE

- $$P_i^A = (N_2 - N_1) - [D_1]_i \int_{t_a}^{t_b} (\Delta \underline{a} \cdot \underline{A}_i)\, dt + Eq$$

- The first three terms in the right hand side of the equation include the effect of the misalignment.

- The second order cross couplings due to the misalignment have been neglected by the second assumption.

A CHOICE OF NOMINAL INSTRUMENT AXES

ASSUME

$$[\underline{A}_i \cdot \underline{B}_k]^n = \begin{bmatrix} 1 & 0 & 0 \\ 0 & 1 & 0 \\ 0 & 0 & 1 \end{bmatrix}$$

THEN

$$P_1^A = \left\{D_1(\underline{A}_1\cdot\underline{B}_1)\right\}_1\left\{(\underline{g}\cdot\underline{B}_1)\Delta t\right\} + \left\{D_1(\underline{A}_1\cdot\underline{B}_2)\right\}_1\left\{(\underline{g}\cdot\underline{B}_2)\Delta t\right\} + \left\{D_1(\underline{A}_1\cdot\underline{B}_3)\right\}_1\left\{(\underline{g}\cdot\underline{B}_3)\Delta t\right\} + \left\{D_1D_0\right\}_1\left\{\Delta t\right\} + \left\{D_1D_2\right\}_1\left\{(\underline{g}\cdot\underline{B}_1)^2\Delta t\right\} + \left\{D_1D_3\right\}_1\left\{(\underline{g}\cdot\underline{B}_1)^3\Delta t\right\}$$

$$P_2^A = \left\{D_1(\underline{A}_2\cdot\underline{B}_1)\right\}_2\left\{(\underline{g}\cdot\underline{B}_1)\Delta t\right\} + \left\{D_1(\underline{A}_2\cdot\underline{B}_2)\right\}_2\left\{(\underline{g}\cdot\underline{B}_2)\Delta t\right\} + \left\{D_1(\underline{A}_2\cdot\underline{B}_3)\right\}_2\left\{(\underline{g}\cdot\underline{B}_3)\Delta t\right\} + \left\{D_1D_0\right\}_2\left\{\Delta t\right\} + \left\{D_1D_2\right\}_2\left\{(\underline{g}\cdot\underline{B}_2)^2\Delta t\right\} + \left\{D_1D_3\right\}_2\left\{(\underline{g}\cdot\underline{B}_2)^3\Delta t\right\}$$

$$P_3^A = \left\{D_1(\underline{A}_3\cdot\underline{B}_1)\right\}_3\left\{(\underline{g}\cdot\underline{B}_1)\Delta t\right\} + \left\{D_1(\underline{A}_3\cdot\underline{B}_2)\right\}_3\left\{(\underline{g}\cdot\underline{B}_2)\Delta t\right\} + \left\{D_1(\underline{A}_3\cdot\underline{B}_3)\right\}_3\left\{(\underline{g}\cdot\underline{B}_3)\Delta t\right\} + \left\{D_1D_0\right\}_3\left\{\Delta t\right\} + \left\{D_1D_2\right\}_3\left\{(\underline{g}\cdot\underline{B}_3)^2\Delta t\right\} + \left\{D_1D_3\right\}_3\left\{(\underline{g}\cdot\underline{B}_3)^3\Delta t\right\}$$

ENVIRONMENT EVALUATION

ASSUME

- $\underline{g}$ is located as shown in Figure 3-2.
- All transformations between frames follow the convention given by the following example:

$$\underline{B}_i = \sum_m T_{im}^{BR}\ \underline{R}_m$$

THE i^{th} BODY AXIS COMPONENT OF $\underline{g}$ IS.

$$(\underline{g}\cdot\underline{B}_i) = \sum_m \sum_n \sum_p T_{im}^{BR}\ T_{mn}^{RT}\ T_{np}^{TE}\ (\underline{g}\cdot\underline{E}_p) \qquad \text{(Test Table readout)}$$

$$= \sum_m \sum_n T_{im}^{BS}\ T_{mn}^{SE}\ (\underline{g}\cdot\underline{E}_n) \qquad \text{(Autocolimator alignment)}$$

4.2 CHOICES OF CALIBRATION ENVIRONMENTS

The general gyro equations are presented in Charts 4-5 and 4-8 and the general accelerometer equations are presented in Chart 4-13. These equations represent the functional relationships among the instrument outputs, the input environment measurements, and the calibration constants.

Each instrument equation is linear in n unknown calibration constants. Therefore, it is possible to determine the numerical value of all calibration constants contained within any equation from the simultaneous solution of n equations corresponding to n different measurements of instrument outputs and input environments. Such a technique of constant determination would involve the inversion of an n x n matrix When n is large, as it is in these instrument equations, matrix inversion is very cumbersome.

There is, fortunately, an easier technique for determining the calibration constants That technique involves the control of the environment inputs (by a control of the test table parameters) such that the instrument outputs would be insensitive to a large number of terms. This corresponds to the adjustment of the environment-sensitive coefficients of a large number of constants in the general calibration equations to zero. If it were possible to null all but one, the determination of the remaining constant would naturally be trivial. In this system, however, it is not possible to null all but one but we can in many cases null all but a few coefficients. In the subsections that follow we will apply this "nulling technique" to the calibration of the ERC ISU. The result will be a set of equations from which any calibration constant can be determined by the simultaneous solution of at most two equations. Each equation corresponds to the input/output relationship for an instrument subjected to a particular environment, by control of the test table parameters.

We begin our presentation, in Section 4.2.1, by dictating the environments and developing the equations from which the gyro scale factor and $(Q^G)^{-1}$ matrix can be determined. In Section 4.2.2 which follows we will show how to calibrate the gyro unbalance, bias, and square compliance terms. In Section 4.2.3 we will show how to determine the compliance-product coefficients, and in Section 4.2.4 we will complete the discussion of gyro calibration by describing the experiments for investigating the gyro scale factor nonlinearity and J term. The discussion of the calibration of gyro constants in any subsection will assume that the constants discussed in previous subsections are well known from previous calibrations.

The description of accelerometer calibration begins in Section 4.2.5 with a description of the calibration of all but the cubic term. In Section 4 2.6 we complete the calibration

developments by describing the determination of the remaining accelerometer cubic terms.

4.2.1 Determination of Gyro Scale Factor and Misalignment

In this subsection we show how particular choices of input environments reduce the general gyro equations to forms which enable a relatively simple calibration of the gyro scale factors and elements of the $(Q^G)^{-1}$ matrix. (The matrix elements are sometimes referred to as "misalignments" from the nominal ISU design) Our attention is directed to the general gyro equations found on Charts 4-5 and 4-8. We will dictate choices of the test table parameters found in the integrals shown in Chart 4-8 such that the desired angular velocity-sensitive terms predominate.

We see that many of the integrals found in Chart 4-8 are functions of harmonic terms as well as terms which increase monotonically with time The harmonic terms are terms involving integrals of trigonometric functions of ϕ_2. Such integrals are bounded in value; as a matter of fact, if $\omega^T = \frac{d\phi_2}{dt}$ can be made constant, the harmonic terms would equate to zero for any multiple of whole turns ($\phi_2 = 2n\pi$) of the table. Under such conditions a large number of the terms in Chart 4-8 would disappear. In Chart 4-14 we see the substitution of the integrals into Chart 4-5 under the condition of whole turns of the table, while rotating at a constant speed. (See Section 2.1 of the trade-off document for further comment about whole-turn equations.) The assumptions made in the equations in Chart 4-14 are shown at the top of the chart. The condition on the transient terms requires additional comment.

The ERC table will have a precision limitation on its ability to rotate at a constant speed. That limitation is two parts in ten thousand, that is $\Delta\omega^T/\omega^T \leq 2 \times 10^{-4}$, where $\Delta\omega^T$ is the error in the speed of the table, and ω^T is the speed of the table. Assuming that a maximum error of plus ϵ is evidenced in a first half turn, and a maximum error of minus ϵ is evidenced in a second half turn, then

$$\int_0^{2\pi} \sin\phi_2 \, dt = \int_0^{\pi} \sin(\omega^T + \Delta\omega^T)t\,dt + \int_{\pi}^{2\pi} \sin(\omega^T - \Delta\omega^T)t\,dt$$

$$= 4\left(\frac{\Delta\omega^T}{\omega^T}\right)\left(\frac{1}{\omega^T}\right) \equiv A$$

During all scale factor and misalignment determination experiments the maximum possible speed will be used. That speed will be just below the saturation level of the gyros, which is 15 degrees per second. (See Section 2.1 of the Trade-Off Document for further comments.) Under such conditions:

- The proportional transient terms go as

  $\omega^{E} \equiv A = 120 \times 10^{-7}$ deg = 0.04 $\widehat{sec}$ (per revolution)

- The unbalance transient terms go as

  $BgA = 8 \times 10^{-7}$ deg

- The compliance transient terms go as

  $Cg^2A = 0.32 \times 10^{-7}$ deg

which are all obviously very small and can be neglected (under the assumption, of course, that the above analysis typifies the worst-case deviation from a constant speed).

Referring again to Chart 4-14, we see that a horizontal position of the test table rotary axes (i.e., $\phi_1 = 90^{\circ}$) would null all unbalance terms. Chart 4-15 introduces that condition The remaining test table control parameters in Chart 4-15 are the first column of the T^{BR} matrix. (The first column of the T^{BR} matrix dictates the orientation of the table rotary axes ($\underline{R}_1$) relative to the ISU body axes.) The orientation of $\underline{R}_1$ is a function of the inner and outer gimbal angles (ϕ_3 and ϕ_4). Having two gimbal angle degrees of freedom dictates that any values of the first column of T^{BR} can be requested. (Equating the T^{BR} choices to ϕ_3 and ϕ_4 settings is the subject of Section 4.4 2.) In Charts 4-16, 4-17, and 4-18 we show the calibration equations for six choices of the first column of T^{BR}. All choices are shown at the top of the charts. We see that

- Chart 4-16 corresponds to the alignment of the first body axis with the rotary axis in both the plus and minus sense.
- Chart 4-17 corresponds to the alignment of the second body axis with the rotary axis in both the plus and minus sense.
- Chart 4-18 corresponds to the alignment of the third body axis with the rotary axis in both the plus and minus sense

In Charts 4-16, 4-17, and 4-18 the test table parameters have been completely specified The first table gimbal angle ϕ_1 is equated to 90°. The second gimbal is rotating over whole turns at a constant speed. And the third and fourth gimbals are <u>implicitly</u> specified by choices of the first column of T^{BR}. We will refer to these six orientations as Positions 1 through 6, respectively.

We note in Chart 4-16 that only the first terms in the three gyro equations have opposite signs in Positions 1 and 2. Therefore, those terms can be isolated as a function of P_k^G (k = 1, 2, 3) by simply subtracting the equation for Position 1 from the equation for Position 2. From known environment inputs and known P_k^G values the first gyro constants can therefore be determined. (The manner in which P_k^G is known is the subject of Section 4. 3. 1.) The second and third constants can be found by similar uses of Charts 4-17 and 4-18, respectively. The final equations for the gyro scale factors and $(Q^G)^{-1}$ elements are found in Section 4. 3. 2. As a matter of convenience the computational equations from this and subsequent subsections are tabulated at a single point in this document, which is Section 4. 3. 2.

4. 2. 2 Determination of R, B_I, B_O, B_S, C_{II} and C_{SS}

Subsequent to the calibration of the principal angular velocity sensitive terms (scale factors and $(Q^G)^{-1}$ elements), the gyro equations predominantly contain, as unknowns, acceleration-sensitive terms (i. e., unbalance and compliance coefficients). This predominance is even more evidenced when the angular velocity input is controlled to a small constant value. Under that condition the remaining angular velocity terms (Q_{II} and Q_{IS}) become relatively unimportant as influences on the gyro outputs. These points suggest that the calibration of the unknown unbalance and compliance coefficients should be accomplished under the conditions of extremely small angular velocity inputs. Not only will the Q_{II} and Q_{IS} be negligible, but also the imprecision in the already calibrated scale factor and $(Q^G)^{-1}$ elements will have a minimum influence on the precision of the unbalance and compliance coefficients to be determined

In Chart 4-19 we present the general gyro calibration equations under the influence of the minimum practical angular velocity environment. That angular velocity input is earth rate, that is, the table is stationary relative to the laboratory. We say minimum "practical" environment because it would be possible to rotate the table at near minus earth rate, thus reducing the total angular velocity input below earth rate, but earth rate alone is so small that there appears to be no reason to try to regulate the speed of the table to a small number

At the top of Chart 4-19 we present our gimbal angle choices of $\phi_1 = 0$ and $\phi_2 = 90^o$. There are several reasons for these choices. First, it must be pointed out that we are interested, for the purpose of calibrating acceleration-sensitive coefficients, in controlling the orientation of only the input g vector relative to the body axes. To completely control one vector relative to the body axes requires only two orientation degrees of freedom. Two of the four test table degrees of freedom can therefore be chosen for matters of convenience. We choose the particular values of ϕ_1 and ϕ_2, as shown in Chart 4-19, for the following reasons of convenience:

GYRO CALIBRATION WHOLE-TURN EQUATIONS

ASSUME

For whole turns of ϕ_2.

1) All transient terms are negligible
2) Terms of $0(\omega^E)^2$ are negligible
3) Terms of $0(\omega^E \Delta\phi_2)$ are negligible
4) ϕ_2 is constant

For whole turns of ϕ_2 the gyro equations are given on this page.

$$
\begin{aligned}
P_1^G = {} & \left\{(\underline{G}_1 \cdot \underline{B}_1)/\Delta\Phi\right\}_1 [\Delta\phi_2 + \omega^E \Delta t \cos(\phi_1 + \lambda)]\, T_{11}^{BR} \\
& + \left\{(\underline{G}_1 \cdot \underline{B}_2)/\Delta\Phi\right\}_1 [\Delta\phi_2 + \omega^E \Delta t \cos(\phi_1 + \lambda)]\, T_{21}^{BR} \\
& + \left\{(\underline{G}_1 \cdot \underline{B}_3)/\Delta\Phi\right\}_1 [\Delta\phi_2 + \omega^E \Delta t \cos(\phi_1 + \lambda)]\, T_{31}^{BR} \\
& + \left\{R/\Delta\Phi\right\}_1 [\Delta t] \\
& + \left\{B_I/\Delta\Phi\right\}_1 [g \Delta t \cos\phi_1]\, T_{11}^{BR} \\
& + \left\{B_O/\Delta\Phi\right\}_1 [g \Delta t \cos\phi_1]\, T_{31}^{BR} \\
& + \left\{B_S/\Delta\Phi\right\}_1 \left\{[g \Delta t \cos\phi_1]\, T_{21}^{BR}\right\} \\
& + \left\{C_{II}/\Delta\Phi\right\}_1 \left[\frac{g^2\Delta t}{2}\right] [(T_{11}^{BR})^2 (3\cos^2\phi_1 - 1) + \sin^2\phi_1] \\
& + \left\{C_{SS}/\Delta\Phi\right\}_1 \left[\frac{g^2\Delta t}{2}\right] [(T_{21}^{BR})^2 (3\cos^2\phi_1 - 1) + \sin^2\phi_1] \\
& + \left\{C_{IO}/\Delta\Phi\right\}_1 \left[\frac{g^2\Delta t}{2}\right] [T_{11}^{BR} T_{31}^{BR} (3\cos^2\phi_1 - 1)] \\
& + \left\{C_{IS}/\Delta\Phi\right\}_1 -\left[\frac{g^2\Delta t}{2}\right] [T_{11}^{BR} T_{21}^{BR} (3\cos^2\phi_1 - 1)] \\
& + \left\{C_{OS}/\Delta\Phi\right\}_1 -\left[\frac{g^2\Delta t}{2}\right] [T_{21}^{BR} T_{31}^{BR} (3\cos^2\phi_1 - 1)] \\
& + \left\{Q_{II}/\Delta\Phi\right\}_1 [(\omega^T)^2 \Delta t](T_{11}^{BR})^2 \\
& + \left\{Q_{IS}/\Delta\Phi\right\}_1 \left\{-[(\omega^T)^2 \Delta t]\, T_{11}^{BR} T_{21}^{BR}\right\} \\
& + \left\{J/\Delta\Phi\right\}_1 0
\end{aligned}
$$

$$
\begin{aligned}
P_2^G = {} & \left\{(\underline{G}_2 \cdot \underline{B}_1)/\Delta\Phi\right\}_2 [\Delta\phi_2 + \omega^E \Delta t \cos(\phi_1 + \lambda)]\, T_{11}^{BR} \\
& + \left\{(\underline{G}_2 \cdot \underline{B}_2)/\Delta\Phi\right\}_2 [\Delta\phi_2 + \omega^E \Delta t \cos(\phi_1 + \lambda)]\, T_{21}^{BR} \\
& + \left\{(\underline{G}_2 \cdot \underline{B}_3)/\Delta\Phi\right\}_2 [\Delta\phi_2 + \omega^E \Delta t \cos(\phi_1 + \lambda)]\, T_{31}^{BR} \\
& + \left\{R/\Delta\Phi\right\}_2 [\Delta t] \\
& + \left\{B_I/\Delta\Phi\right\}_2 [g \Delta t \cos\phi_1]\, T_{21}^{BR} \\
& + \left\{B_O/\Delta\Phi\right\}_2 [g \Delta t \cos\phi_1]\, T_{11}^{BR} \\
& + \left\{B_S/\Delta\Phi\right\}_2 \left\{[g \Delta t \cos\phi_1]\, T_{31}^{BR}\right\} \\
& + \left\{C_{II}/\Delta\Phi\right\}_2 \left[\frac{g^2\Delta t}{2}\right] [(T_{21}^{BR})^2 (3\cos^2\phi_1 - 1) + \sin^2\phi_1] \\
& + \left\{C_{SS}/\Delta\Phi\right\}_2 \left[\frac{g^2\Delta t}{2}\right] [(T_{31}^{BR})^2 (3\cos^2\phi_1 - 1) + \sin^2\phi_1] \\
& + \left\{C_{IO}/\Delta\Phi\right\}_2 \left[\frac{g^2\Delta t}{2}\right] [T_{11}^{BR} T_{21}^{BR} (3\cos^2\phi_1 - 1)] \\
& + \left\{C_{IS}/\Delta\Phi\right\}_2 \left\{-\left[\frac{g^2\Delta t}{2}\right] [T_{21}^{BR} T_{31}^{BR} (3\cos^2\phi_1 - 1)]\right\} \\
& + \left\{C_{OS}/\Delta\Phi\right\}_2 \left\{-\left[\frac{g^2\Delta t}{2}\right] [T_{11}^{BR} T_{31}^{BR} (3\cos^2\phi_1 - 1)]\right\} \\
& + \left\{Q_{II}/\Delta\Phi\right\}_2 [(\omega^T)^2 \Delta t](T_{21}^{BR})^2 \\
& + \left\{Q_{IS}/\Delta\Phi\right\}_2 \left\{[(\omega^T)^2 \Delta t]\, T_{21}^{BR} T_{31}^{BR}\right\} \\
& + \left\{J/\Delta\Phi\right\}_2 0
\end{aligned}
$$

$$
\begin{aligned}
P_3^G = {} & \left\{(\underline{G}_3 \cdot \underline{B}_1)/\Delta\Phi\right\}_3 [\Delta\phi_2 + \omega^E \Delta t \cos(\phi_1 + \lambda)]\, T_{11}^{BR} \\
& + \left\{(\underline{G}_3 \cdot \underline{B}_2)/\Delta\Phi\right\}_3 [\Delta\phi_2 + \omega^E \Delta t \cos(\phi_1 + \lambda)]\, T_{21}^{BR} \\
& + \left\{(\underline{G}_3 \cdot \underline{B}_3)/\Delta\Phi\right\}_3 [\Delta\phi_2 + \omega^E \Delta t \cos(\phi_1 + \lambda)]\, T_{31}^{BR} \\
& + \left\{R/\Delta\Phi\right\}_3 [\Delta t] \\
& + \left\{B_I/\Delta\Phi\right\}_3 [g \Delta t \cos\phi_1]\, T_{31}^{BR} \\
& + \left\{B_O/\Delta\Phi\right\}_3 [g \Delta t \cos\phi_1]\, T_{11}^{BR} \\
& + \left\{B_S/\Delta\Phi\right\}_3 [g \Delta t \cos\phi_1]\, T_{21}^{BR} \\
& + \left\{C_{II}/\Delta\Phi\right\}_3 \left[\frac{g^2\Delta t}{2}\right] [(T_{31}^{BR})^2 (3\cos^2\phi_1 - 1) + \sin^2\phi_1] \\
& + \left\{C_{SS}/\Delta\Phi\right\}_3 \left[\frac{g^2\Delta t}{2}\right] [(T_{21}^{BR})^2 (3\cos^2\phi_1 - 1) + \sin^2\phi_1] \\
& + \left\{C_{IO}/\Delta\Phi\right\}_3 \left[\frac{g^2\Delta t}{2}\right] [T_{11}^{BR} T_{31}^{BR} (3\cos^2\phi_1 - 1)] \\
& + \left\{C_{IS}/\Delta\Phi\right\}_3 \left[\frac{g^2\Delta t}{2}\right] [T_{21}^{BR} T_{31}^{BR} (3\cos^2\phi_1 - 1)] \\
& + \left\{C_{OS}/\Delta\Phi\right\}_3 \left[\frac{g^2\Delta t}{2}\right] [T_{11}^{BR} T_{21}^{BR} (3\cos^2\phi_1 - 1)] \\
& + \left\{Q_{II}/\Delta\Phi\right\}_3 [(\omega^T)^2 \Delta t](T_{31}^{BR})^2 \\
& + \left\{Q_{IS}/\Delta\Phi\right\}_3 [(\omega^T)^2 \Delta t]\, T_{21}^{BR} T_{31}^{BR} \\
& + \left\{J/\Delta\Phi\right\}_3 0
\end{aligned}
$$

FOLDOUT FRAME 1

FOLDOUT FRAME 2

GYRO CALIBRATION WHOLE-TURN EQUATIONS

$\phi_1 = 90°$

ϕ_2 is moving (whole turns)

$$P_1^G = \left\{(\underline{G}_1 \cdot \underline{B}_1)/\Delta\Phi\right\}_1 [\Delta\phi_2 - \omega^E \Delta t \sin\lambda]\, T_{11}^{BR}$$
$$+ \left\{(\underline{G}_1 \cdot \underline{B}_2)/\Delta\Phi\right\}_1 [\Delta\phi_2 - \omega^E \Delta t \sin\lambda]\, T_{21}^{BR}$$
$$+ \left\{(\underline{G}_1 \cdot \underline{B}_3)/\Delta\Phi\right\}_1 [\Delta\phi_2 - \omega^E \Delta t \sin\lambda]\, T_{31}^{BR}$$
$$+ \left\{R/\Delta\Phi\right\}_1 [\Delta t]$$
$$+ \left\{B_I/\Delta\Phi\right\}_1 0$$
$$+ \left\{B_O/\Delta\Phi\right\}_1 0$$
$$+ \left\{B_S/\Delta\Phi\right\}_1 0$$
$$+ \left\{C_{II}/\Delta\Phi\right\}_1 \left[\frac{g^2\Delta t}{2}\right][1 - (T_{11}^{BR})^2]$$
$$+ \left\{C_{SS}/\Delta\Phi\right\}_1 \left[\frac{g^2\Delta t}{2}\right][1 - (T_{21}^{BR})^2]$$
$$+ \left\{C_{IO}/\Delta\Phi\right\}_1 \left\{\left[\frac{g^2\Delta t}{2}\right][T_{11}^{BR} T_{31}^{BR}]\right\}$$
$$+ \left\{C_{IS}/\Delta\Psi\right\}_1 \left[\frac{g^2\Delta t}{2}\right][T_{21}^{BR} T_{31}^{BR}]$$
$$+ \left\{C_{OS}/\Delta\Phi\right\}_1 \left[\frac{g^2\Delta t}{2}\right][T_{21}^{BR} T_{31}^{BR}]$$
$$+ \left\{Q_{II}/\Delta\Phi\right\}_1 [(\omega^T)^2\Delta t][(T_{11}^{BR})^2]$$
$$+ \left\{Q_{IS}/\Delta\Phi\right\}_1 \left\{-[(\omega^T)^2\Delta t][T_{11}^{BR} T_{21}^{BR}]\right\}$$
$$+ \left\{J/\Delta\Phi\right\}_1 0$$

$$P_2^G = \left\{(\underline{G}_2 \cdot \underline{B}_1)/\Delta\Phi\right\}_2 [\Delta\phi_2 - \omega^E \Delta t \sin\lambda]\, T_{11}^{BR}$$
$$+ \left\{(\underline{G}_2 \cdot \underline{B}_2)/\Delta\Phi\right\}_2 [\Delta\phi_2 - \omega^E \Delta t \sin\lambda]\, T_{21}^{BR}$$
$$+ \left\{(\underline{G}_2 \cdot \underline{B}_3)/\Delta\Phi\right\}_2 [\Delta\phi_2 - \omega^E \Delta t \sin\lambda]\, T_{31}^{BR}$$
$$+ \left\{R/\Delta\Phi\right\}_2 [\Delta t]$$
$$+ \left\{B_I/\Delta\Phi\right\}_2 0$$
$$+ \left\{B_O/\Delta\Phi\right\}_2 0$$
$$+ \left\{B_S/\Delta\Phi\right\}_2 0$$
$$+ \left\{C_{II}/\Delta\Phi\right\}_2 \left[\frac{g^2\Delta t}{2}\right][1 - (T_{21}^{BR})^2]$$
$$+ \left\{C_{SS}/\Delta\Phi\right\}_2 \left[\frac{g^2\Delta t}{2}\right][1 - (T_{31}^{BR})^2]$$
$$+ \left\{C_{IO}/\Delta\Phi\right\}_2 \left\{\left[\frac{g^2\Delta t}{2}\right][T_{11}^{BR} T_{21}^{BR}]\right\}$$
$$+ \left\{C_{IS}/\Delta\Phi\right\}_2 \left[\frac{g^2\Delta t}{2}\right][T_{21}^{BR} T_{31}^{BR}]$$
$$+ \left\{C_{OS}/\Delta\Phi\right\}_2 \left[\frac{g^2\Delta t}{2}\right][T_{11}^{BR} T_{31}^{BR}]$$
$$+ \left\{Q_{II}/\Delta\Phi\right\}_2 [(\omega^T)^2\Delta t][(T_{21}^{BR})^2]$$
$$+ \left\{Q_{IS}/\Delta\Phi\right\}_2 \left\{-[(\omega^T)^2\Delta t][T_{21}^{BR} T_{31}^{BR}]\right\}$$
$$+ \left\{J/\Delta\Phi\right\}_2 0$$

$$P_3^G = \left\{(\underline{G}_3 \cdot \underline{B}_1)/\Delta\Phi\right\}_3 [\Delta\phi_2 - \omega^E \Delta t \sin\lambda]\, T_{11}^{BR}$$
$$+ \left\{(\underline{G}_3 \cdot \underline{B}_2)/\Delta\Phi\right\}_3 [\Delta\phi_2 - \omega^E \Delta t \sin\lambda]\, T_{21}^{BR}$$
$$+ \left\{(\underline{G}_3 \cdot \underline{B}_3)/\Delta\Phi\right\}_3 [\Delta\phi_2 - \omega^E \Delta t \sin\lambda]\, T_{31}^{BR}$$
$$+ \left\{R/\Delta\Phi\right\}_3 [\Delta t]$$
$$+ \left\{B_I/\Delta\Phi\right\}_3 0$$
$$+ \left\{B_O/\Delta\Phi\right\}_3 0$$
$$+ \left\{B_S/\Delta\Phi\right\}_3 0$$
$$+ \left\{C_{II}/\Delta\Phi\right\}_3 \left[\frac{g^2\Delta t}{2}\right][1 - (T_{31}^{BR})^2]$$
$$+ \left\{C_{SS}/\Delta\Phi\right\}_3 \left[\frac{g^2\Delta t}{2}\right][1 - (T_{21}^{BR})^2]$$
$$+ \left\{C_{IO}/\Delta\Phi\right\}_3 \left\{\left[\frac{g^2\Delta t}{2}\right][T_{11}^{BR} T_{31}^{BR}]\right\}$$
$$+ \left\{C_{IS}/\Delta\Phi\right\}_3 \left\{\left[\frac{g^2\Delta t}{2}\right][T_{21}^{BR} T_{31}^{BR}]\right\}$$
$$+ \left\{C_{OS}/\Delta\Phi\right\}_3 \left\{\left[\frac{g^2\Delta t}{2}\right][T_{11}^{BR} T_{21}^{BR}]\right\}$$
$$+ \left\{Q_{II}/\Delta\Phi\right\}_3 [(\omega^T)^2\Delta t][(T_{31}^{BR})^2]$$
$$+ \left\{Q_{IS}/\Delta\Phi\right\}_3 [(\omega^T)^2\Delta t][T_{21}^{BR} T_{31}^{BR}]$$
$$+ \left\{J/\Delta\Phi\right\}_3 0$$

FOLDOUT FRAME 1

FOLDOUT FRAME 2

GYRO CALIBRATION WHOLE-TURN EQUATIONS POSITIONS 1 AND 2

$\phi_1 = 90°$

ϕ_2 is moving

$T_{11}^{BR} = \pm 1$

$T_{21}^{BR} = 0$

$T_{31}^{BR} = 0$

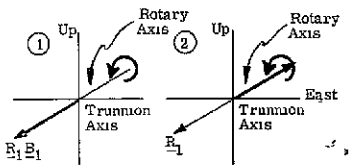

$$P_1^G = \left\{(\underline{G}_1 \cdot \underline{B}_1)/\Delta\Phi\right\}_1 \left\{\pm[\Delta\phi_2 - \omega^E \Delta t \sin\lambda]\right\}$$
$$+ \left\{(\underline{G}_1 \cdot \underline{B}_2)/\Delta\Phi\right\}_1 0$$
$$+ \left\{(\underline{G}_1 \cdot \underline{B}_3)/\Delta\Phi\right\}_1 0$$
$$+ \left\{R/\Delta\Phi\right\}_1 [\Delta t]$$
$$+ \left\{B_I/\Delta\Phi\right\}_1 0$$
$$+ \left\{B_O/\Delta\Phi\right\}_1 0$$
$$+ \left\{B_S/\Delta\Phi\right\}_1 0$$
$$+ \left\{C_{II}/\Delta\Phi\right\}_1 0$$
$$+ \left\{C_{SS}/\Delta\Phi\right\}_1 [g^2\Delta t/2]$$
$$+ \left\{C_{IO}/\Delta\Phi\right\}_1 0$$
$$+ \left\{C_{IS}/\Delta\Phi\right\}_1 0$$
$$+ \left\{C_{OS}/\Delta\Phi\right\}_1 0$$
$$+ \left\{Q_{II}/\Delta\Phi\right\}_1 [(\omega^T)^2\Delta t]$$
$$+ \left\{Q_{IS}/\Delta\Phi\right\}_1 0$$
$$+ \left\{J/\Delta\Phi\right\}_1 0$$

$$P_2^G = \left\{(\underline{G}_2 \cdot \underline{B}_1)/\Delta\Phi\right\}_2 \left\{\pm[\Delta\phi_2 - \omega^E \Delta t \sin\lambda]\right\}$$
$$+ \left\{(\underline{G}_2 \cdot \underline{B}_2)/\Delta\Phi\right\}_2 0$$
$$+ \left\{(\underline{G}_2 \cdot \underline{B}_3)/\Delta\Phi\right\}_2 0$$
$$+ \left\{R/\Delta\Phi\right\}_2 [\Delta t]$$
$$+ \left\{B_I/\Delta\Phi\right\}_2 0$$
$$+ \left\{B_O/\Delta\Phi\right\}_2 0$$
$$+ \left\{B_S/\Delta\Phi\right\}_2 0$$
$$+ \left\{C_{II}/\Delta\Phi\right\}_2 [g^2\Delta t/2]$$
$$+ \left\{C_{SS}/\Delta\Phi\right\}_2 [g^2\Delta t/2]$$
$$+ \left\{C_{IO}/\Delta\Phi\right\}_2 0$$
$$+ \left\{C_{IS}/\Delta\Phi\right\}_2 0$$
$$+ \left\{C_{OS}/\Delta\Phi\right\}_2 0$$
$$+ \left\{Q_{II}/\Delta\Phi\right\}_2 0$$
$$+ \left\{Q_{IS}/\Delta\Phi\right\}_2 0$$
$$+ \left\{J/\Delta\Phi\right\}_2 0$$

$$P_3^G = \left\{(\underline{G}_3 \cdot \underline{B}_1)/\Delta\Phi\right\}_3 \left\{\pm[\Delta\phi_2 - \omega^E \Delta t \sin\lambda]\right\}$$
$$+ \left\{(\underline{G}_3 \cdot \underline{B}_2)/\Delta\Phi\right\}_3 0$$
$$+ \left\{(\underline{G}_3 \cdot \underline{B}_3)/\Delta\Phi\right\}_3 0$$
$$+ \left\{R/\Delta\Phi\right\}_3 [\Delta t]$$
$$+ \left\{B_I/\Delta\Phi\right\}_3 0$$
$$+ \left\{B_O/\Delta\Phi\right\}_3 0$$
$$+ \left\{B_S/\Delta\Phi\right\}_3 0$$
$$+ \left\{C_{II}/\Delta\Phi\right\}_3 [g^2\Delta t/2]$$
$$+ \left\{C_{SS}/\Delta\Phi\right\}_3 [g^2\Delta t/2]$$
$$+ \left\{C_{IO}/\Delta\Phi\right\}_3 0$$
$$+ \left\{C_{IS}/\Delta\Phi\right\}_3 0$$
$$+ \left\{C_{OS}/\Delta\Phi\right\}_3 0$$
$$+ \left\{Q_{II}/\Delta\Phi\right\}_3 0$$
$$+ \left\{Q_{IS}/\Delta\Phi\right\}_3 0$$
$$+ \left\{J/\Delta\Phi\right\}_3 0$$

FOLDOUT FRAME 1

FOLDOUT FRAME 2

GYRO CALIBRATION WHOLE-TURN EQUATIONS POSITIONS 3 AND 4

$\phi_1 = 90°$

ϕ_2 is moving

$T_{11}^{BR} = 0$

$T_{21}^{BR} = \pm 1$

$T_{31}^{BR} = 0$

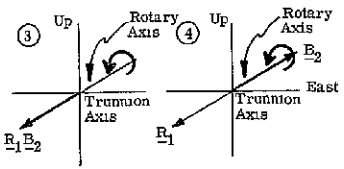

$$P_1^G = \left|(\underline{G}_1 \cdot \underline{B}_1)/\Delta\Phi\right|_1 0$$
$$+ \left|(\underline{G}_1 \cdot \underline{B}_2)/\Delta\Phi\right|_1 \{\pm[\Delta\phi_2 - \omega^E \Delta t \sin\lambda]\}$$
$$+ \left|(\underline{G}_1 \cdot \underline{B}_3)/\Delta\Phi\right|_1 0$$
$$+ \left|R/\Delta\Phi\right|_1 [\Delta t]$$
$$+ \left|B_I/\Delta\Phi\right|_1 0$$
$$+ \left|B_O/\Delta\Phi\right|_1 0$$
$$+ \left|B_S/\Delta\Phi\right|_1 0$$
$$+ \left|C_{II}/\Delta\Phi\right|_1 [g^2\Delta t/2]$$
$$+ \left|C_{SS}/\Delta\Phi\right|_1 0$$
$$+ \left|C_{IO}/\Delta\Phi\right|_1 0$$
$$+ \left|C_{IS}/\Delta\Phi\right|_1 0$$
$$+ \left|C_{OS}/\Delta\Phi\right|_1 0$$
$$+ \left|Q_{II}/\Delta\Phi\right|_1 0$$
$$+ \left|Q_{IS}/\Delta\Phi\right|_1 0$$
$$+ \left|J/\Delta\Phi\right|_1 0$$

$$P_2^G = \left|(\underline{G}_2 \cdot \underline{B}_1)/\Delta\Phi\right|_2 0$$
$$+ \left|(\underline{G}_2 \cdot \underline{B}_2)/\Delta\Phi\right|_2 \{\pm[\Delta\phi_2 - \omega^E \Delta t \sin\lambda]\}$$
$$+ \left|(\underline{G}_2 \cdot \underline{B}_3)/\Delta\Phi\right|_2 0$$
$$+ \left|R/\Delta\Phi\right|_2 [\Delta t]$$
$$+ \left|B_I/\Delta\Phi\right|_2 0$$
$$+ \left|B_O/\Delta\Phi\right|_2 0$$
$$+ \left|B_S/\Delta\Phi\right|_2 0$$
$$+ \left|C_{II}/\Delta\Phi\right|_2 0$$
$$+ \left|C_{SS}/\Delta\Phi\right|_2 [g^2\Delta t/2]$$
$$+ \left|C_{IO}/\Delta\Phi\right|_2 0$$
$$+ \left|C_{IS}/\Delta\Phi\right|_2 0$$
$$+ \left|C_{OS}/\Delta\Phi\right|_2 0$$
$$+ \left|Q_{II}/\Delta\Phi\right|_2 [(\omega^T)^2\Delta t]$$
$$+ \left|Q_{IS}/\Delta\Phi\right|_2 0$$
$$+ \left|J/\Delta\Phi\right|_2 0$$

$$P_3^G = \left|(\underline{G}_3 \cdot \underline{B}_1)/\Delta\Phi\right|_3 0$$
$$+ \left|(\underline{G}_3 \cdot \underline{B}_2)/\Delta\Phi\right|_3 \{\pm[\Delta\phi_2 - \omega^E \Delta t \sin\lambda]\}$$
$$+ \left|(\underline{G}_3 \cdot \underline{B}_3)/\Delta\Phi\right|_3 0$$
$$+ \left|R/\Delta\Phi\right|_3 [\Delta t]$$
$$+ \left|B_I/\Delta\Phi\right|_3 0$$
$$+ \left|B_O/\Delta\Phi\right|_3 0$$
$$+ \left|B_S/\Delta\Phi\right|_3 0$$
$$+ \left|C_{II}/\Delta\Phi\right|_3 [g^2\Delta t/2]$$
$$+ \left|C_{SS}/\Delta\Phi\right|_3 0$$
$$+ \left|C_{IO}/\Delta\Phi\right|_3 0$$
$$+ \left|C_{IS}/\Delta\Phi\right|_3 0$$
$$+ \left|C_{OS}/\Delta\Phi\right|_3 0$$
$$+ \left|Q_{II}/\Delta\Phi\right|_3 0$$
$$+ \left|Q_{IS}/\Delta\Phi\right|_3 0$$
$$+ \left|J/\Delta\Phi\right|_3 0$$

FOLDOUT FRAME 1

FOLDOUT FRAME 2

GYRO CALIBRATION WHOLE-TURN EQUATIONS POSITIONS 5 AND 6

$\phi_1 = 90°$

ϕ_2 is moving

$T_{11}^{BR} = 0$

$T_{21}^{BR} = 0$

$T_{31}^{BR} = \pm 1$

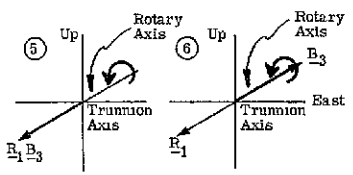

$$P_1^G = \left\{(\underline{G}_1 \cdot \underline{B}_1)/\Delta\Phi\right\}_1 0$$
$$+ \left\{(\underline{G}_1 \cdot \underline{B}_2)/\Delta\Phi\right\}_1 0$$
$$+ \left\{(\underline{G}_1 \cdot \underline{B}_3)/\Delta\Phi\right\}_1 \left\{\pm[\Delta\phi_2 - \omega^E \Delta t \sin\lambda]\right\}$$
$$+ \left\{R/\Delta\Phi\right\}_1 [\Delta t]$$
$$+ \left\{B_I/\Delta\Phi\right\}_1 0$$
$$+ \left\{B_O/\Delta\Phi\right\}_1 0$$
$$+ \left\{B_S/\Delta\Phi\right\}_1 0$$
$$+ \left\{C_{II}/\Delta\Phi\right\}_1 [g^2\Delta t/2]$$
$$+ \left\{C_{SS}/\Delta\Phi\right\}_1 [g^2\Delta t/2]$$
$$+ \left\{C_{IO}/\Delta\Phi\right\}_1 0$$
$$+ \left\{C_{IS}/\Delta\Phi\right\}_1 0$$
$$+ \left\{C_{OS}/\Delta\Phi\right\}_1 0$$
$$+ \left\{Q_{II}/\Delta\Phi\right\}_1 0$$
$$+ \left\{Q_{IS}/\Delta\Phi\right\}_1 0$$
$$+ \left\{J/\Delta\Phi\right\}_1 0$$

$$P_2^G = \left\{(\underline{G}_2 \cdot \underline{B}_1)/\Delta\Phi\right\}_2 0$$
$$+ \left\{(\underline{G}_2 \cdot \underline{B}_2)/\Delta\Phi\right\}_2 0$$
$$+ \left\{(\underline{G}_2 \cdot \underline{B}_3)/\Delta\Phi\right\}_2 \left\{\pm[\Delta\phi_2 - \omega^E \Delta t \sin\lambda]\right\}$$
$$+ \left\{R/\Delta\Phi\right\}_2 [\Delta t]$$
$$+ \left\{B_I/\Delta\Phi\right\}_2 0$$
$$+ \left\{B_O/\Delta\Phi\right\}_2 0$$
$$+ \left\{B_S/\Delta\Phi\right\}_2 0$$
$$+ \left\{C_{II}/\Delta\Phi\right\}_2 [g^2\Delta t/2]$$
$$+ \left\{C_{SS}/\Delta\Phi\right\}_2 0$$
$$+ \left\{C_{IO}/\Delta\Phi\right\}_2 0$$
$$+ \left\{C_{IS}/\Delta\Phi\right\}_2 0$$
$$+ \left\{C_{OS}/\Delta\Phi\right\}_2 0$$
$$+ \left\{Q_{II}/\Delta\Phi\right\}_2 0$$
$$+ \left\{Q_{IS}/\Delta\Phi\right\}_2 0$$
$$+ \left\{J/\Delta\Phi\right\}_2 0$$

$$P_3^G = \left\{(\underline{G}_3 \cdot \underline{B}_1)/\Delta\Phi\right\}_3 0$$
$$+ \left\{(\underline{G}_3 \cdot \underline{B}_2)/\Delta\Phi\right\}_3 0$$
$$+ \left\{(\underline{G}_3 \cdot \underline{B}_3)/\Delta\Phi\right\}_3 \left\{\pm[\Delta\phi_2 - \omega^E \Delta t \sin\lambda]\right\}$$
$$+ \left\{R/\Delta\Phi\right\}_3 [\Delta t]$$
$$+ \left\{B_I/\Delta\Phi\right\}_3 0$$
$$+ \left\{B_O/\Delta\Phi\right\}_3 0$$
$$+ \left\{B_S/\Delta\Phi\right\}_3 0$$
$$+ \left\{C_{II}/\Delta\Phi\right\}_3 0$$
$$+ \left\{C_{SS}/\Delta\Phi\right\}_3 [g^2\Delta t/2]$$
$$+ \left\{C_{IO}/\Delta\Phi\right\}_3 0$$
$$+ \left\{C_{IS}/\Delta\Phi\right\}_3 0$$
$$+ \left\{C_{OS}/\Delta\Phi\right\}_3 0$$
$$+ \left\{Q_{II}/\Delta\Phi\right\}_3 [(\omega^T)^2\Delta t]$$
$$+ \left\{Q_{IS}/\Delta\Phi\right\}_3 0$$
$$+ \left\{J/\Delta\Phi\right\}_3 0$$

FOLDOUT FRAME 1

FOLDOUT FRAME 2

- The value $\phi_1 = 0^o$ is chosen because it results in the same ϕ_3 and ϕ_4 settings for the six positions required for the subject calibration as required for the first six positions.

- The value $\phi_2 = 90^o$ was chosen for two reasons. the first reason is that it places the ϕ_3 gimbal in the north-south direction, and that gimbal, in conjunction with the east-west ϕ_1 gimbal, can be used for small angle corrections of the table base motions as measured by bubble levels (see Section 4.4.4). The second reason for the choice of $\phi_2 = 90^o$ is that it results in only the second column of T^{BR} being required in calibration computations. This results in a minimum amount of data handling during precalibration survey activities.

The equations in Chart 4-19 contain, as control parameters, only the first and second column of the T^{BR} matrix. The acceleration-sensitive terms are, however, a function of the first column only. The table orientation control will therefore be preoccupied with that column. In Charts 4-20, 4-21 and 4-22 we introduce the choices for the first column of T^{BR} corresponding to Positions 7 through 12. These choices for the first column of T^{BR} are the same, respectively, as they were for Positions 1 through 6. With the assumption that the first three gyro coefficients are known from the calibration described in the preceding subsection, we see that Charts 4-20, 4-21 and 4-22 present six equations in the six unknowns:

$$R,\ B_I,\ B_O,\ B_S,\ C_{II},\ C_{SS}$$

We note that at most two equations are required for the solution of any required unknown. In Section 4.3 the solution of the equations for the six unknowns is presented.

4.2.3 Determination of C_{IO}, C_{IS} and C_{OS}

The three product-compliance coefficients (C_{IO}, C_{IS} and C_{OS}) were not evidenced in any equation for Positions 1 through 12. None of those positions senses the minimum of two body-axes components of acceleration required for the detection of product-compliance coefficients. In this subsection we choose three additional laboratory-fixed orientations (Positions 13, 14 and 15), each position detecting two (and only two) body-axes components of $\underline{g}$. On Charts 4-23, 4-24 and 4-25 we present the instrument equations for those three positions. In each equation on those three charts there exists only one unknown product-compliance coefficient. The solution for that coefficient, in terms of the known input environment vector $\underline{P}^G$, and the previously determined calibration constants, is found in Section 4.3. The determination of the second column of the T^{BR} matrix is considered a precalibration activity. In Section 4.4.3 that activity is described.

4.2.4 Gyro Nonlinearity and J Term Experiments

There are three remaining constants to be described, namely: Q_{II}, Q_{IS} and J. The Q_{II} constant is intended to represent the scale factor nonlinearity. In the following

GYRO CALIBRATION FIXED ORIENTATION

$\phi_1 = 0°$

$\phi_2 = 90°$

Let:

$\cos\lambda\, T_{11}^{BR} + \sin\lambda\, T_{12}^{BR} = x_1$

$\cos\lambda\, T_{21}^{BR} + \sin\lambda\, T_{22}^{BR} = x_2$

$\cos\lambda\, T_{31}^{BR} + \sin\lambda\, T_{32}^{BR} = x_3$

Assuming $0(\omega^E)^2$ is negligible

$$P_1^G = \left\{(\underline{G}_1 \cdot \underline{B}_1)/\Delta\Phi\right\}_1 [\omega^E \Delta t] x_1$$
$$+ \left\{(\underline{G}_1 \cdot \underline{B}_2)/\Delta\Phi\right\}_1 [\omega^E \Delta t] x_2$$
$$+ \left\{(\underline{G}_1 \cdot \underline{B}_3)/\Delta\Phi\right\}_1 [\omega^E \Delta t] x_3$$
$$+ \left\{R/\Delta\Phi\right\}_1 [\Delta t]$$
$$+ \left\{B_F/\Delta\Phi\right\}_1 [g\Delta t] T_{11}^{BR}$$
$$+ \left\{B_O/\Delta\Phi\right\}_1 [g\Delta t] T_{31}^{BR}$$
$$+ \left\{B_S/\Delta\Phi\right\}_1 [g\Delta t] T_{21}^{BR}$$
$$+ \left\{C_{II}/\Delta\Phi\right\}_1 [g^2\Delta t] (T_{11}^{BR})^2$$
$$+ \left\{C_{SS}/\Delta\Phi\right\}_1 [g^2\Delta t] (T_{21}^{BR})^2$$
$$+ \left\{C_{IO}/\Delta\Phi\right\}_1 [g^2\Delta t] T_{11}^{BR} T_{31}^{BR}$$
$$+ \left\{C_{IS}/\Delta\Phi\right\}_1 \left\{-[g^2\Delta t] T_{11}^{BR} T_{21}^{BR}\right\}$$
$$+ \left\{C_{OS}/\Delta\Phi\right\}_1 \left\{-[g^2\Delta t] T_{21}^{BR} T_{31}^{BR}\right\}$$
$$+ \left\{Q_{II}/\Delta\Phi\right\}_1 0$$
$$+ \left\{Q_{IS}/\Delta\Phi\right\}_1 0$$
$$+ \left\{J/\Delta\Phi\right\}_1 0$$

$$P_2^G = \left\{(\underline{G}_2 \cdot \underline{B}_1)/\Delta\Phi\right\}_2 [\omega^E \Delta t] x_1$$
$$+ \left\{(\underline{G}_2 \cdot \underline{B}_2)/\Delta\Phi\right\}_2 [\omega^E \Delta t] x_2$$
$$+ \left\{(\underline{G}_2 \cdot \underline{B}_3)/\Delta\Phi\right\}_2 [\omega^E \Delta t] x_3$$
$$+ \left\{R/\Delta\Phi\right\}_2 [\Delta t]$$
$$+ \left\{B_F/\Delta\Phi\right\}_2 [g\Delta t] T_{21}^{BR}$$
$$+ \left\{B_O/\Delta\Phi\right\}_2 [g\Delta t] T_{11}^{BR}$$
$$+ \left\{B_S/\Delta\Phi\right\}_2 \left\{-[g\Delta t] T_{31}^{BR}\right\}$$
$$+ \left\{C_{II}/\Delta\Phi\right\}_2 [g^2\Delta t] (T_{21}^{BR})^2$$
$$+ \left\{C_{SS}/\Delta\Phi\right\}_2 [g^2\Delta t] (T_{31}^{BR})^2$$
$$+ \left\{C_{IO}/\Delta\Phi\right\}_2 [g^2\Delta t] T_{11}^{BR} T_{21}^{BR}$$
$$+ \left\{C_{IS}/\Delta\Phi\right\}_2 \left\{-[g^2\Delta t] T_{21}^{BR} T_{31}^{BR}\right\}$$
$$+ \left\{C_{OS}/\Delta\Phi\right\}_2 \left\{-[g^2\Delta t] T_{11}^{BR} T_{31}^{BR}\right\}$$
$$+ \left\{Q_{II}/\Delta\Phi\right\}_2 0$$
$$+ \left\{Q_{IS}/\Delta\Phi\right\}_2 0$$
$$+ \left\{J/\Delta\Phi\right\}_2 0$$

$$P_3^G = \left\{(\underline{G}_3 \cdot \underline{B}_1)/\Delta\Phi\right\}_3 [\omega^E \Delta t] x_1$$
$$+ \left\{(\underline{G}_3 \cdot \underline{B}_2)/\Delta\Phi\right\}_3 [\omega^E \Delta t] x_2$$
$$+ \left\{(\underline{G}_3 \cdot \underline{B}_3)/\Delta\Phi\right\}_3 [\omega^E \Delta t] x_3$$
$$+ \left\{R/\Delta\Phi\right\}_3 [\Delta t]$$
$$+ \left\{B_F/\Delta\Phi\right\}_3 [g\Delta t] T_{31}^{BR}$$
$$+ \left\{B_O/\Delta\Phi\right\}_3 [g\Delta t] T_{11}^{BR}$$
$$+ \left\{B_S/\Delta\Phi\right\}_3 [g\Delta t] T_{21}^{BR}$$
$$+ \left\{C_{II}/\Delta\Phi\right\}_3 [g^2\Delta t] (T_{31}^{BR})^2$$
$$+ \left\{C_{SS}/\Delta\Phi\right\}_3 [g^2\Delta t] (T_{21}^{BR})^2$$
$$+ \left\{C_{IO}/\Delta\Phi\right\}_3 [g^2\Delta t] T_{11}^{BR} T_{31}^{BR}$$
$$+ \left\{C_{IS}/\Delta\Phi\right\}_3 [g^2\Delta t] T_{21}^{BR} T_{31}^{BR}$$
$$+ \left\{C_{OS}/\Delta\Phi\right\}_3 [g^2\Delta t] T_{11}^{BR} T_{21}^{BR}$$
$$+ \left\{Q_{II}/\Delta\Phi\right\}_3 0$$
$$+ \left\{Q_{IS}/\Delta\Phi\right\}_3 0$$
$$+ \left\{J/\Delta\Phi\right\}_3 0$$

FOLDOUT FRAME 1

FOLDOUT FRAME 2

GYRO CALIBRATION FIXED ORIENTATION POSITIONS 7 AND 8

$\phi_1 = 0°$

$\phi_2 = 90°$

$T_{11}^{BR} = \pm 1$

$T_{21}^{BR} = 0$

$T_{31}^{BR} = 0$

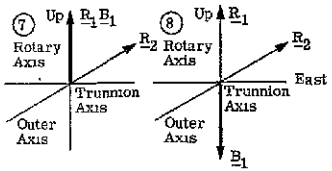

$$P_1^G = \{(\underline{G}_1 \cdot \underline{B}_1)/\Delta\Phi\}_1 \quad [\pm \omega^E \Delta t] \cos\lambda$$
$$+ \{(\underline{G}_1 \cdot \underline{B}_2)/\Delta\Phi\}_1 \quad [\omega^E \Delta t] \sin\lambda \, T_{22}^{BR1}$$
$$+ \{(\underline{G}_1 \cdot \underline{B}_3)/\Delta\Phi\}_1 \quad [\omega^E \Delta t] \sin\lambda \, T_{32}^{BR1}$$
$$+ \{R/\Delta\Phi\}_1 \quad [\Delta t]$$
$$+ \{B_I/\Delta\Phi\}_1 \quad [\pm g \Delta t]$$
$$+ \{B_O/\Delta\Phi\}_1 \quad 0$$
$$+ \{B_S/\Delta\Phi\}_1 \quad 0$$
$$+ \{C_{II}/\Delta\Phi\}_1 \quad [g^2 \Delta t]$$
$$+ \{C_{SS}/\Delta\Phi\}_1 \quad 0$$
$$+ \{C_{IO}/\Delta\Phi\}_1 \quad 0$$
$$+ \{C_{IS}/\Delta\Psi\}_1 \quad 0$$
$$+ \{C_{OS}/\Delta\Phi\}_1 \quad 0$$
$$+ \{Q_{II}/\Delta\Phi\}_1 \quad 0$$
$$+ \{Q_{IS}/\Delta\Phi\}_1 \quad 0$$
$$+ \{J/\Delta\Phi\}_1 \quad 0$$

$$P_2^G = \{(\underline{G}_2 \cdot \underline{B}_1)/\Delta\Phi\}_2 \quad [\pm \omega^E \Delta t] \cos\lambda$$
$$+ \{(\underline{G}_2 \cdot \underline{B}_2)/\Delta\Phi\}_2 \quad [\omega^E \Delta t] \sin\lambda \, T_{22}^{BR1}$$
$$+ \{(\underline{G}_2 \cdot \underline{B}_3)/\Delta\Phi\}_2 \quad [\omega^E \Delta t] \sin\lambda \, T_{32}^{BR1}$$
$$+ \{R/\Delta\Phi\}_2 \quad [\Delta t]$$
$$+ \{B_I/\Delta\Phi\}_2 \quad 0$$
$$+ \{B_O/\Delta\Phi\}_2 \quad [\pm g \Delta t]$$
$$+ \{B_S/\Delta\Phi\}_2 \quad 0$$
$$+ \{C_{II}/\Delta\Phi\}_2 \quad 0$$
$$+ \{C_{SS}/\Delta\Phi\}_2 \quad 0$$
$$+ \{C_{IO}/\Delta\Phi\}_2 \quad 0$$
$$+ \{C_{IS}/\Delta\Phi\}_2 \quad 0$$
$$+ \{C_{OS}/\Delta\Phi\}_2 \quad 0$$
$$+ \{Q_{II}/\Delta\Phi\}_2 \quad 0$$
$$+ \{Q_{IS}/\Delta\Phi\}_2 \quad 0$$
$$+ \{J/\Delta\Phi\}_2 \quad 0$$

$$P_3^G = \{(\underline{G}_3 \cdot \underline{B}_1)/\Delta\Phi\}_3 \quad [\pm \omega^E \Delta t] \cos\lambda$$
$$+ \{(\underline{G}_3 \cdot \underline{B}_2/\Delta\Phi\}_3 \quad [\omega^E \Delta t] \sin\lambda \, T_{22}^{BR1}$$
$$+ \{(\underline{G}_3 \cdot \underline{B}_3)/\Delta\Phi\}_3 \quad [\omega^E \Delta t] \sin\lambda \, T_{32}^{BR1}$$
$$+ \{R/\Delta\Phi\}_3 \quad [\Delta t]$$
$$+ \{B_I/\Delta\Phi\}_3 \quad 0$$
$$+ \{B_O/\Delta\Phi\}_3 \quad [\pm g \Delta t]$$
$$+ \{B_S/\Delta\Phi\}_3 \quad 0$$
$$+ \{C_{II}/\Delta\Phi\}_3 \quad 0$$
$$+ \{C_{SS}/\Delta\Phi\}_3 \quad 0$$
$$+ \{C_{IO}/\Delta\Phi\}_3 \quad 0$$
$$+ \{C_{IS}/\Delta\Phi\}_3 \quad 0$$
$$+ \{C_{OS}/\Delta\Phi\}_3 \quad 0$$
$$+ \{Q_{II}/\Delta\Phi\}_3 \quad 0$$
$$+ \{Q_{IS}/\Delta\Phi\}_3 \quad 0$$
$$+ \{J/\Delta\Phi\}_3 \quad 0$$

GYRO CALIBRATION FIXED ORIENTATION POSITIONS 9 AND 10

$\phi_1 = 0°$

$\phi_2 = 90°$

$T_{11}^{BR} = 0$

$T_{21}^{BR} = \pm 1$

$T_{31}^{BR} = 0$

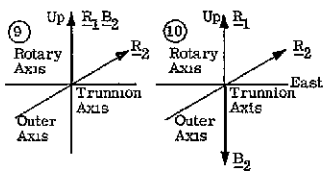

$$P_1^G = \left\{(\underline{G}_1 \cdot \underline{B}_1)/\Delta\Phi\right\}_1 [\omega^E \Delta t] \sin\lambda \; T_{12}^{BR3}$$
$$+ \left\{(\underline{G}_1 \cdot \underline{B}_2)/\Delta\Phi\right\}_1 [\pm\omega^E \Delta t] \cos\lambda$$
$$+ \left\{(\underline{G}_1 \cdot \underline{B}_3)/\Delta\Phi\right\}_1 [\omega^E \Delta t] \sin\lambda \; T_{32}^{BR3}$$
$$+ \left\{R/\Delta\Phi\right\}_1 [\Delta t]$$
$$+ \left\{B_I/\Delta\Phi\right\}_1 0$$
$$+ \left\{B_O/\Delta\Phi\right\}_1 0$$
$$+ \left\{B_S/\Delta\Phi\right\}_1 [\pm g\Delta t]$$
$$+ \left\{C_{II}/\Delta\Phi\right\}_1 0$$
$$+ \left\{C_{SS}/\Delta\Phi\right\}_1 [g^2\Delta t]$$
$$+ \left\{C_{IO}/\Delta\Phi\right\}_1 0$$
$$+ \left\{C_{IS}/\Delta\Phi\right\}_1 0$$
$$+ \left\{C_{OS}/\Delta\Phi\right\}_1 0$$
$$+ \left\{Q_{II}/\Delta\Phi\right\}_1 0$$
$$+ \left\{Q_{IS}/\Delta\Phi\right\}_1 0$$
$$+ \left\{J/\Delta\Phi\right\}_1 0$$

$$P_2^G = \left\{(\underline{G}_2 \cdot \underline{B}_1)/\Delta\Phi\right\}_2 [\omega^E \Delta t] \sin\lambda \; T_{12}^{BR3}$$
$$+ \left\{(\underline{G}_2 \cdot \underline{B}_2)/\Delta\Phi\right\}_2 [\pm\omega^E \Delta t] \cos\lambda$$
$$+ \left\{(\underline{G}_2 \cdot \underline{B}_3)/\Delta\Phi\right\}_2 [\omega^E \Delta t] \sin\lambda \; T_{32}^{BR3}$$
$$+ \left\{R/\Delta\Phi\right\}_2 [\Delta t]$$
$$+ \left\{B_I/\Delta\Phi\right\}_2 [\pm g\Delta t]$$
$$+ \left\{B_O/\Delta\Phi\right\}_2 0$$
$$+ \left\{B_S/\Delta\Phi\right\}_2 0$$
$$+ \left\{C_{II}/\Delta\Phi\right\}_2 [g^2\Delta t]$$
$$+ \left\{C_{SS}/\Delta\Phi\right\}_2 0$$
$$+ \left\{C_{IO}/\Delta\Phi\right\}_2 0$$
$$+ \left\{C_{IS}/\Delta\Phi\right\}_2 0$$
$$+ \left\{C_{OS}/\Delta\Phi\right\}_2 0$$
$$+ \left\{Q_{II}/\Delta\Phi\right\}_2 0$$
$$+ \left\{Q_{IS}/\Delta\Phi\right\}_2 0$$
$$+ \left\{J/\Delta\Phi\right\}_2 0$$

$$P_3^G = \left\{(\underline{G}_3 \cdot \underline{B}_1)/\Delta\Phi\right\}_3 [\omega^E \Delta t] \sin\lambda \; T_{12}^{BR3}$$
$$+ \left\{(\underline{G}_3 \cdot \underline{B}_2/\Delta\Phi\right\}_3 [\pm\omega^E \Delta t] \cos\lambda$$
$$+ \left\{(\underline{G}_3 \cdot \underline{B}_3)/\Delta\Phi\right\}_3 [\omega^E \Delta t] \sin\lambda \; T_{32}^{BR3}$$
$$+ \left\{R/\Delta\Phi\right\}_3 [\Delta t]$$
$$+ \left\{B_I/\Delta\Phi\right\}_3 0$$
$$+ \left\{B_O/\Delta\Phi\right\}_3 0$$
$$+ \left\{B_S/\Delta\Phi\right\}_3 [\pm g\Delta t]$$
$$+ \left\{C_{II}/\Delta\Phi\right\}_3 0$$
$$+ \left\{C_{SS}/\Delta\Phi\right\}_3 [g^2\Delta t]$$
$$+ \left\{C_{IO}/\Delta\Phi\right\}_3 0$$
$$+ \left\{C_{IS}/\Delta\Phi\right\}_3 0$$
$$+ \left\{C_{OS}/\Delta\Phi\right\}_3 0$$
$$+ \left\{Q_{II}/\Delta\Phi\right\}_3 0$$
$$+ \left\{Q_{IS}/\Delta\Psi\right\}_3 0$$
$$+ \left\{J/\Delta\Phi\right\}_3 0$$

FOLDOUT FRAME 1

FOLDOUT FRAME 2

GYRO CALIBRATION FIXED ORIENTATION POSITIONS 11 AND 12

$\phi_1 = 0°$

$\phi_2 = 90°$

$T_{11}^{BR} = 0$

$T_{21}^{BR} = 0$

$T_{31}^{BR} = \pm 1$

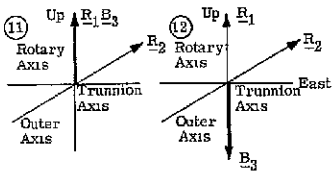

$$P_1^G = \left\{(\underline{G}_1 \cdot \underline{B}_1)/\Delta\Phi\right\}_1 [\omega^E \Delta t] \sin\lambda \; T_{12}^{BR5}$$
$$+ \left\{(\underline{G}_1 \cdot \underline{B}_2)/\Delta\Phi\right\}_1 [\omega^E \Delta t] \sin\lambda \; T_{22}^{BR5}$$
$$+ \left\{(\underline{G}_1 \cdot \underline{B}_3)/\Delta\Phi\right\}_1 [\pm\omega^E \Delta t] \cos\lambda$$
$$+ \left\{R/\Delta\Phi\right\}_1 [\Delta t]$$
$$+ \left\{B_I/\Delta\Phi\right\}_1 0$$
$$+ \left\{B_O/\Delta\Phi\right\}_1 [\pm g\Delta t]$$
$$+ \left\{B_S/\Delta\Phi\right\}_1 0$$
$$+ \left\{C_{II}/\Delta\Phi\right\}_1 0$$
$$+ \left\{C_{SS}/\Delta\Phi\right\}_1 0$$
$$+ \left\{C_{IO}/\Delta\Phi\right\}_1 0$$
$$+ \left\{C_{IS}/\Delta\Phi\right\}_1 0$$
$$+ \left\{C_{OS}/\Delta\Phi\right\}_1 0$$
$$+ \left\{Q_{II}/\Delta\Phi\right\}_1 0$$
$$+ \left\{Q_{IS}/\Delta\Phi\right\}_1 0$$
$$+ \left\{J/\Delta\Phi\right\}_1 0$$

$$P_2^G = \left\{(\underline{G}_2 \cdot \underline{B}_1)/\Delta\Phi\right\}_2 [\omega^E \Delta t] \sin\lambda \; T_{12}^{BR5}$$
$$+ \left\{(\underline{G}_2 \cdot \underline{B}_2)/\Delta\Phi\right\}_2 [\omega^E \Delta t] \sin\lambda \; T_{22}^{BR5}$$
$$+ \left\{(\underline{G}_2 \cdot \underline{B}_3)/\Delta\Phi\right\}_2 [\pm\omega^E \Delta t] \cos\lambda$$
$$+ \left\{R/\Delta\Phi\right\}_2 [\Delta t]$$
$$+ \left\{B_I/\Delta\Phi\right\}_2 0$$
$$+ \left\{B_O/\Delta\Phi\right\}_2 0$$
$$+ \left\{B_S/\Delta\Phi\right\}_2 [\pm g\Delta t]$$
$$+ \left\{C_{II}/\Delta\Phi\right\}_2 0$$
$$+ \left\{C_{SS}/\Delta\Phi\right\}_2 [g^2\Delta t]$$
$$+ \left\{C_{IO}/\Delta\Phi\right\}_2 0$$
$$+ \left\{C_{IS}/\Delta\Phi\right\}_2 0$$
$$+ \left\{C_{OS}/\Delta\Phi\right\}_2 0$$
$$+ \left\{Q_{II}/\Delta\Phi\right\}_2 0$$
$$+ \left\{Q_{IS}/\Delta\Phi\right\}_2 0$$
$$+ \left\{J/\Delta\Phi\right\}_2 0$$

$$P_3^G = \left\{(\underline{G}_3 \cdot \underline{B}_1)/\Delta\Phi\right\}_3 [\omega^E \Delta t] \sin\lambda \; T_{12}^{BR5}$$
$$+ \left\{(\underline{G}_3 \cdot \underline{B}_2/\Delta\Phi\right\}_3 [\omega^E \Delta t] \sin\lambda \; T_{22}^{BR5}$$
$$+ \left\{(\underline{G}_3 \cdot \underline{B}_3)/\Delta\Phi\right\}_3 [\pm\omega^E \Delta t] \cos\lambda$$
$$+ \left\{R/\Delta\Phi\right\}_3 [\Delta t]$$
$$+ \left\{B_I/\Delta\Phi\right\}_3 [\pm g\Delta t]$$
$$+ \left\{B_O/\Delta\Phi\right\}_3 0$$
$$+ \left\{B_S/\Delta\Phi\right\}_3 0$$
$$+ \left\{C_{II}/\Delta\Phi\right\}_3 [g^2\Delta t]$$
$$+ \left\{C_{SS}/\Delta\Phi\right\}_3 0$$
$$+ \left\{C_{IO}/\Delta\Phi\right\}_3 0$$
$$+ \left\{C_{IS}/\Delta\Phi\right\}_3 0$$
$$+ \left\{C_{OS}/\Delta\Phi\right\}_3 0$$
$$+ \left\{Q_{II}/\Delta\Phi\right\}_3 0$$
$$+ \left\{Q_{IS}/\Delta\Phi\right\}_3 0$$
$$+ \left\{J/\Delta\Phi\right\}_3 0$$

GYRO CALIBRATION FIXED ORIENTATION POSITION 13

$\varphi_1 = 0°$

$\varphi_2 = 90°$

$T_{11}^{BR} = \sqrt{1/2}$ $\quad x_1 = \sqrt{1/2}\cos\lambda + T_{12}^{BR13}\sin\lambda$

$T_{21}^{BR} = \sqrt{1/2}$ $\quad x_2 = \sqrt{1/2}\cos\lambda + T_{22}^{BR13}\sin\lambda$

$T_{31}^{BR} = 0$ $\quad x_3 = T_{32}^{BR13}\sin\lambda$

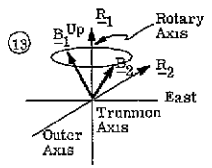

$$P_1^G = \left\{(\underline{G}_1\cdot\underline{B}_1)/\Delta\Phi\right\}_1 [\omega^E\Delta t]x_1 + \left\{(\underline{G}_1\cdot\underline{B}_2)/\Delta\Phi\right\}_1 [\omega^E\Delta t]x_2 + \left\{(\underline{G}_1\cdot\underline{B}_3)/\Delta\Phi\right\}_1 [\omega^E\Delta t]x_3 + \left\{R/\Delta\Phi\right\}_1 [\Delta t] + \left\{B_I/\Delta\Phi\right\}_1 [\sqrt{1/2}\,g\Delta t] + \left\{B_O/\Delta\Phi\right\}_1 0 + \left\{B_S/\Delta\Phi\right\}_1 [-\sqrt{1/2}\,g\Delta t] + \left\{C_{II}/\Delta\Phi\right\}_1 [\sqrt{1/2}\,g^2\Delta t] + \left\{C_{SS}/\Delta\Phi\right\}_1 [\sqrt{1/2}\,g^2\Delta t] + \left\{C_{IO}/\Delta\Phi\right\}_1 0 + \left\{C_{IS}/\Delta\Phi\right\}_1 [-1/2\,g^2\Delta t] + \left\{C_{OS}/\Delta\Phi\right\}_1 0 + \left\{Q_{II}/\Delta\Phi\right\}_1 0 + \left\{Q_{IS}/\Delta\Phi\right\}_1 0 + \left\{J/\Delta\Phi\right\}_1 0$$

$$P_2^G = \left\{(\underline{G}_2\cdot\underline{B}_1)/\Delta\Phi\right\}_2 [\omega^E\Delta t]x_1 + \left\{(\underline{G}_2\cdot\underline{B}_2)/\Delta\Phi\right\}_2 [\omega^E\Delta t]x_2 + \left\{(\underline{G}_2\cdot\underline{B}_3)/\Delta\Phi\right\}_2 [\omega^E\Delta t]x_3 + \left\{R/\Delta\Phi\right\}_2 [\Delta t] + \left\{B_I/\Delta\Phi\right\}_2 [\sqrt{1/2}\,g\Delta t] + \left\{B_O/\Delta\Phi\right\}_2 [\sqrt{1/2}\,g\Delta t] + \left\{B_S/\Delta\Phi\right\}_2 0 + \left\{C_{II}/\Delta\Phi\right\}_2 [1/2\,g^2\Delta t] + \left\{C_{SS}/\Delta\Phi\right\}_2 0 + \left\{C_{IO}/\Delta\Phi\right\}_2 [1/2\,g^2\Delta t] + \left\{C_{IS}/\Delta\Phi\right\}_2 0 + \left\{C_{OS}/\Delta\Phi\right\}_2 0 + \left\{Q_{II}/\Delta\Phi\right\}_2 0 + \left\{Q_{IS}/\Delta\Phi\right\}_2 0 + \left\{J/\Delta\Phi\right\}_2 0$$

$$P_3^G = \left\{(\underline{G}_3\cdot\underline{B}_1)/\Delta\Phi\right\}_3 [\omega^E\Delta t]x_1 + \left\{(\underline{G}_3\cdot\underline{B}_2/\Delta\Phi\right\}_3 [\omega^E\Delta t]x_2 + \left\{(\underline{G}_3\cdot\underline{B}_3)/\Delta\Phi\right\}_3 [\omega^E\Delta t]x_3 + \left\{R/\Delta\Phi\right\}_3 [\Delta t] + \left\{B_I/\Delta\Phi\right\}_3 0 + \left\{B_O/\Delta\Phi\right\}_3 [\sqrt{1/2}\,g\Delta t] + \left\{B_S/\Delta\Phi\right\}_3 [\sqrt{1/2}\,g\Delta t] + \left\{C_{II}/\Delta\Phi\right\}_3 0 + \left\{C_{SS}/\Delta\Phi\right\}_3 [1/2\,g^2\Delta t] + \left\{C_{IO}/\Delta\Phi\right\}_3 0 + \left\{C_{IS}/\Delta\Phi\right\}_3 0 + \left\{C_{OS}/\Delta\Phi\right\}_3 [1/2\,g^2\Delta t] + \left\{Q_{II}/\Delta\Phi\right\}_3 0 + \left\{Q_{IS}/\Delta\Phi\right\}_3 0 + \left\{J/\Delta\Phi\right\}_3 0$$

FOLDOUT FRAME 1

FOLDOUT FRAME 2

GYRO CALIBRATION FIXED ORIENTATION POSITION 14

$\phi_1 = 0°$

$\phi_2 = 90°$

$T_{11}^{BR} = \sqrt{1/2}$ $\quad x_1 = \sqrt{1/2}\cos\lambda + T_{12}^{BR14}\sin\lambda$

$T_{21}^{BR} = 0$ $\quad x_2 = T_{22}^{BR14}\sin\lambda$

$T_{31}^{BR} = \sqrt{1/2}$ $\quad x_3 = \sqrt{1/2}\cos\lambda + T_{32}^{BR14}\sin\lambda$

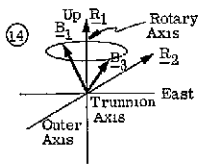

$$P_1^G = \left\{(\underline{G}_1\cdot\underline{B}_1)/\Delta\Phi\right\}_1 [\omega^E\Delta t]x_1 + \left\{(\underline{G}_1\cdot\underline{B}_2)/\Delta\Phi\right\}_1 [\omega^E\Delta t]x_2 + \left\{(\underline{G}_1\cdot\underline{B}_3)/\Delta\Phi\right\}_1 [\omega^E\Delta t]x_3 + \left\{R/\Delta\Phi\right\}_1 [\Delta t] + \left\{B_I/\Delta\Phi\right\}_1 [\sqrt{1/2}\, g\Delta t] + \left\{B_O/\Delta\Phi\right\}_1 [\sqrt{1/2}\, g\Delta t] + \left\{B_S/\Delta\Phi\right\}_1 0 + \left\{C_{II}/\Delta\Phi\right\}_1 [1/2\, g^2\Delta t] + \left\{C_{SS}/\Delta\Phi\right\}_1 0 + \left\{C_{IO}/\Delta\Phi\right\}_1 [1/2\, g^2\Delta t] + \left\{C_{IS}/\Delta\Phi\right\}_1 0 + \left\{C_{OS}/\Delta\Phi\right\}_1 0 + \left\{Q_{II}/\Delta\Phi\right\}_1 0 + \left\{Q_{IS}/\Delta\Phi\right\}_1 0 + \left\{J/\Delta\Phi\right\}_1 0$$

$$P_2^G = \left\{(\underline{G}_2\cdot\underline{B}_1)/\Delta\Phi\right\}_2 [\omega^E\Delta t]x_1 + \left\{(\underline{G}_2\cdot\underline{B}_2)/\Delta\Phi\right\}_2 [\omega^E\Delta t]x_2 + \left\{(\underline{G}_2\cdot\underline{B}_3)/\Delta\Phi\right\}_2 [\omega^E\Delta t]x_3 + \left\{R/\Delta\Phi\right\}_2 [\Delta t] + \left\{B_I/\Delta\Phi\right\}_2 0 + \left\{B_O/\Delta\Phi\right\}_2 [\sqrt{1/2}\, g\Delta t] + \left\{B_S/\Delta\Phi\right\}_2 [-\sqrt{1/2}\, g\Delta t] + \left\{C_{II}/\Delta\Phi\right\}_2 0 + \left\{C_{SS}/\Delta\Phi\right\}_2 [1/2\, g^2\Delta t] + \left\{C_{IO}/\Delta\Phi\right\}_2 0 + \left\{C_{IS}/\Delta\Phi\right\}_2 0 + \left\{C_{OS}/\Delta\Phi\right\}_2 [-1/2\, g^2\Delta t] + \left\{Q_{II}/\Delta\Phi\right\}_2 0 + \left\{Q_{IS}/\Delta\Phi\right\}_2 0 + \left\{J/\Delta\Phi\right\}_2 0$$

$$P_3^G = \left\{(\underline{G}_3\cdot\underline{B}_1)/\Delta\Phi\right\}_3 [\omega^E\Delta t]x_1 + \left\{(\underline{G}_3\cdot\underline{B}_2/\Delta\Phi\right\}_3 [\omega^E\Delta t]x_2 + \left\{(\underline{G}_3\cdot\underline{B}_3)/\Delta\Phi\right\}_3 [\omega^E\Delta t]x_3 + \left\{R/\Delta\Phi\right\}_3 [\Delta t] + \left\{B_I/\Delta\Phi\right\}_3 [\sqrt{1/2}\, g\Delta t] + \left\{B_O/\Delta\Phi\right\}_3 [\sqrt{1/2}\, g\Delta t] + \left\{B_S/\Delta\Phi\right\}_3 0 + \left\{C_{II}/\Delta\Phi\right\}_3 [1/2\, g^2\Delta t] + \left\{C_{SS}/\Delta\Phi\right\}_3 0 + \left\{C_{IO}/\Delta\Phi\right\}_3 [1/2\, g^2\Delta t] + \left\{C_{IS}/\Delta\Phi\right\}_3 0 + \left\{C_{OS}/\Delta\Phi\right\}_3 0 + \left\{Q_{II}/\Delta\Phi\right\}_3 0 + \left\{Q_{IS}/\Delta\Phi\right\}_3 0 + \left\{J/\Delta\Phi\right\}_3 0$$

FOLDOUT FRAME 1

FOLDOUT FRAME 2

GYRO CALIBRATION FIXED ORIENTATION POSITION 15

$\phi_1 = 0°$

$\phi_2 = 90°$

$T_{11}^{BR} = 0$ $\quad x_1 = T_{12}^{BR15} \sin\lambda$

$T_{21}^{BR} = \sqrt{1/2}$ $\quad x_2 = \sqrt{1/2}\cos\lambda + T_{22}^{BR15}\sin\lambda$

$T_{31}^{BR} = \sqrt{1/2}$ $\quad x_3 = \sqrt{1/2}\cos\lambda + T_{32}^{BR15}\sin\lambda$

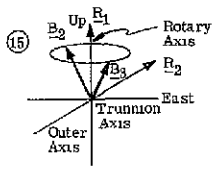

$$P_1^G = \{(\underline{G}_1\cdot\underline{B}_1)/\Delta\Phi\}_1 [\omega^E\Delta t]x_1$$
$$+ \{(\underline{G}_1\cdot\underline{B}_2)/\Delta\Phi\}_1 [\omega^E\Delta t]x_2$$
$$+ \{(\underline{G}_1\cdot\underline{B}_3)/\Delta\Phi\}_1 [\omega^E\Delta t]x_3$$
$$+ \{R/\Delta\Phi\}_1 [\Delta t]$$
$$+ \{B_I/\Delta\Phi\}_1 0$$
$$+ \{B_O/\Delta\Phi\}_1 [\sqrt{1/2}\, g\Delta t]$$
$$+ \{B_S/\Delta\Phi\}_1 [-\sqrt{1/2}\, g\Delta t]$$
$$+ \{C_{II}/\Delta\Phi\}_1 0$$
$$+ \{C_{SS}/\Delta\Phi\}_1 [1/2\, g^2\Delta t]$$
$$+ \{C_{IO}/\Delta\Phi\}_1 0$$
$$+ \{C_{IS}/\Delta\Phi\}_1 0$$
$$+ \{C_{OS}/\Delta\Phi\}_1 [-1/2\, g^2\Delta t]$$
$$+ \{Q_{II}/\Delta\Phi\}_1 0$$
$$+ \{Q_{IS}/\Delta\Phi\}_1 0$$
$$+ \{J/\Delta\Phi\}_1 0$$

$$P_2^G = \{(\underline{G}_2\cdot\underline{B}_1)/\Delta\Phi\}_2 [\omega^E\Delta t]x_1$$
$$+ \{(\underline{G}_2\cdot\underline{B}_2)/\Delta\Phi\}_2 [\omega^E\Delta t]x_2$$
$$+ \{(\underline{G}_2\cdot\underline{B}_3)/\Delta\Phi\}_2 [\omega^E\Delta t]x_3$$
$$+ \{R/\Delta\Phi\}_2 [\Delta t]$$
$$+ \{B_I/\Delta\Phi\}_2 [\sqrt{1/2}\, g\Delta t]$$
$$+ \{B_O/\Delta\Phi\}_2 0$$
$$+ \{B_S/\Delta\Phi\}_2 [-\sqrt{1/2}\, g\Delta t]$$
$$+ \{C_{II}/\Delta\Phi\}_2 [1/2\, g^2\Delta t]$$
$$+ \{C_{SS}/\Delta\Phi\}_2 [1/2\, g^2\Delta t]$$
$$+ \{C_{IO}/\Delta\Phi\}_2 0$$
$$+ \{C_{IS}/\Delta\Phi\}_2 [-1/2\, g^2\Delta t]$$
$$+ \{C_{OS}/\Delta\Phi\}_2 0$$
$$+ \{Q_{II}/\Delta\Phi\}_2 0$$
$$+ \{Q_{IS}/\Delta\Phi\}_2 0$$
$$+ \{J/\Delta\Phi\}_2 0$$

$$P_3^G = \{(\underline{G}_3\cdot\underline{B}_1)/\Delta\Phi\}_3 [\omega^E\Delta t]x_1$$
$$+ \{(\underline{G}_3\cdot\underline{B}_2/\Delta\Phi\}_3 [\omega^E\Delta t]x_2$$
$$+ \{(\underline{G}_3\cdot\underline{B}_3)/\Delta\Phi\}_3 [\omega^E\Delta t]x_3$$
$$+ \{R/\Delta\Phi\}_3 [\Delta t]$$
$$+ \{B_I/\Delta\Phi\}_3 [\sqrt{1/2}\, g\Delta t]$$
$$+ \{B_O/\Delta\Phi\}_3 0$$
$$+ \{B_S/\Delta\Phi\}_3 [\sqrt{1/2}\, g\Delta t]$$
$$+ \{C_{II}/\Delta\Phi\}_3 [1/2\, g^2\Delta t]$$
$$+ \{C_{SS}/\Delta\Phi\}_3 [1/2\, g^2\Delta t]$$
$$+ \{C_{IO}/\Delta\Phi\}_3 0$$
$$+ \{C_{IS}/\Delta\Phi\}_3 [1/2\, g^2\Delta t]$$
$$+ \{C_{OS}/\Delta\Phi\}_3 0$$
$$+ \{Q_{II}/\Delta\Phi\}_3 0$$
$$+ \{Q_{IS}/\Delta\Phi\}_3 0$$
$$+ \{J/\Delta\Phi\}_3 0$$

FOLDOUT FRAME 1

FOLDOUT FRAME 2

discussions we will describe not only how that constant is found, but also any other higher order $\underline{\omega}$ sensitive coefficients that are evidenced in the gyro readout. The Q_{IS} calibration is not presented. It is assumed that this term is too small to be detected. The last paragraphs in this subsection discuss the calibration of the J term. It will be seen that this calibration requires test table speed controls not found in any other calibration.

Gyro Nonlinearity

The Q_{II} term in the gyro equation was described in Section 2 as the nonlinearity term. This term is intended to describe, in conjunction with the scale factor term, the output rate (say $\dot{P}$) as a function of the input (say ω) as:

$$\dot{P} = A + B\omega + C\omega^2$$

rather than the more familiar

$$\dot{P} = A + B\omega$$

The interpretation by many is that this term introduces a nonconstant scale factor assumption, that is

$$\dot{P} = A + (B + C\omega)\omega$$

Regardless of the interpretation, it seems appropriate to assume nothing about the highest power of ω and in fact to try to conduct experiments to find all coefficients (say A_k) where

$$\dot{P} = A_0 + A_1\omega + A_2\omega^2 = \cdots A_n\omega^n$$

Such experiments are very simply described but would probably be somewhat time consuming to implement.

Let us direct our attention to the equations for the one gyro in Position 1, the two gyro in Position 3, and the three gyro in Position 5. We see that each equation can be written:

$$\frac{P}{\Delta t} = A_0 + A_1\omega + A_2\omega^2$$

where $A_0 = R/\Delta\Phi + f(\text{acceleration})$

$A_1 = \underline{G}_k \cdot \underline{B}_k / \Delta\Phi \approx 1/\Delta\Phi$

$A_2 = Q_{II}/\Delta\Phi$

If experiments are conducted where only ω is changed (and not acceleration), A_0 would always be a constant. We see that a variation of the table speed only, in the positions mentioned, accomplishes this need. Also the equations can be generalized to contain higher order ω terms. That is:

$$P/\Delta t = A_0 + A_1\omega + A_2\omega^2 + \cdots A_n\omega^n$$

The experiments can now be delineated:

- Collect gyro data $\Sigma\delta$ from Position 1, 3, or 5 for n different speeds of the test table.
- Collect the table speed data by measuring $\Delta\phi_2$ and Δt.

  $\omega^T = \dfrac{\Delta\phi 2}{\Delta t}$ for constant ω^T and whole turns of $\Delta\phi_2$.
- Let the total speed imposed on the gyro be described by

$$\omega = \frac{\Delta\phi_2}{\Delta t} + \omega^E \sin\lambda$$

- Let $\dot{P}$ be given by

$$\dot{P} = \frac{(\Sigma\delta)}{\Delta t}$$

  that is, data is collected sufficiently long such that quantization and noise are negligible (see Section 2.2 of the Trade-Off Document).
- Plot $\dot{P}$ against ω

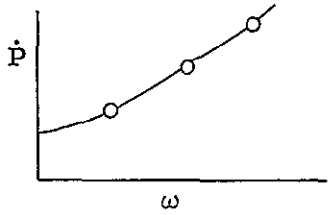

- Analyze the plot to find f, where $\dot{P} = f(\omega)$.

J Term

The environments chosen for the determination of the J terms are shown in Chart 4-26. Note that the positions chosen correspond to Positions 7 and 11 (which were used in Section 4.2.2) with the modification of a rotating table. The gyro data will be collected over a period during which the angular speed has changed. This calibration is the only one which requires the determination of the time-varying integrals:

GYRO CALIBRATION ROTATING TABLE POSITIONS 7 AND 11

ASSUME

Terms containing $(\omega^E)^2$ are negligible

Terms containing the product of ω^E and $\underline{G}_i \cdot \underline{B}_j$ for $i \neq j$ are negligible

Position 7 (P_1^G)

$\phi_1 = 0$

$T_{11}^{BR} = 0$

$T_{21}^{BR} = 0$

$T_{31}^{BR} = 1$

Position 11 (P_2^G and P_3^G)

$\phi_1 = 0$

$T_{11}^{BR} = 1$

$T_{21}^{BR} = 0$

$T_{31}^{BR} = 0$

$$P_1^G = \left\{(\underline{G}_1 \cdot \underline{B}_1)/\Delta\Phi\right\}_1 [\,y_1\,] + \left\{(\underline{G}_1 \cdot \underline{B}_2)/\Delta\Phi\right\}_1 0 + \left\{(\underline{G}_1 \cdot \underline{B}_3)/\Delta\Phi\right\}_1 [\Delta\phi_2] + \left\{R/\Delta\Phi\right\}_1 [\Delta t] + \left\{B_I/\Delta\Phi\right\}_1 0 + \left\{B_O/\Delta\Phi\right\}_1 [g\Delta t] + \left\{B_S/\Delta\Phi\right\}_1 0 + \left\{C_{II}/\Delta\Phi\right\}_1 0 + \left\{C_{SS}/\Delta\Phi\right\}_1 0 + \left\{C_{IO}/\Delta\Phi\right\}_1 0 + \left\{C_{IS}/\Delta\Phi\right\}_1 0 + \left\{C_{OS}/\Delta\Phi\right\}_1 0 + \left\{Q_{II}/\Delta\Phi\right\}_1 0 + \left\{Q_{IS}/\Delta\Phi\right\}_1 0 + \left\{J/\Delta\Phi\right\}_1 [\Delta\omega^T]$$

$$P_2^G = \left\{(\underline{G}_2 \cdot \underline{B}_1)/\Delta\Phi\right\}_2 [\Delta\phi_2] + \left\{(\underline{G}_2 \cdot \underline{B}_2)/\Delta\Phi\right\}_2 [\,y_2\,] + \left\{(\underline{G}_2 \cdot \underline{B}_3)/\Delta\Phi\right\}_2 0 + \left\{R/\Delta\Phi\right\}_2 [\Delta t] + \left\{B_I/\Delta\Phi\right\}_2 0 + \left\{B_O/\Delta\Phi\right\}_2 [g\Delta t] + \left\{B_S/\Delta\Phi\right\}_2 0 + \left\{C_{II}/\Delta\Phi\right\}_2 0 + \left\{C_{SS}/\Delta\Phi\right\}_2 0 + \left\{C_{IO}/\Delta\Phi\right\}_2 0 + \left\{C_{IS}/\Delta\Phi\right\}_2 0 + \left\{C_{OS}/\Delta\Phi\right\}_2 0 + \left\{Q_{II}/\Delta\Phi\right\}_2 0 + \left\{Q_{IS}/\Delta\Phi\right\}_2 0 + \left\{J/\Delta\Phi\right\}_2 [\Delta\omega^T]$$

$$P_3^G = \left\{(\underline{G}_3 \cdot \underline{B}_1)/\Delta\Phi\right\}_3 [\Delta\phi_2] + \left\{(\underline{G}_3 \cdot \underline{B}_2/\Delta\Phi\right\}_3 0 + \left\{(\underline{G}_3 \cdot \underline{B}_3)/\Delta\Phi\right\}_3 [\,y_3\,] + \left\{R/\Delta\Phi\right\}_3 [\Delta t] + \left\{B_I/\Delta\Phi\right\}_3 0 + \left\{B_O/\Delta\Phi\right\}_3 [g\Delta t] + \left\{B_S/\Delta\Phi\right\}_3 0 + \left\{C_{II}/\Delta\Phi\right\}_3 0 + \left\{C_{SS}/\Delta\Phi\right\}_3 0 + \left\{C_{IO}/\Delta\Phi\right\}_3 0 + \left\{C_{IS}/\Delta\Phi\right\}_3 0 + \left\{C_{OS}/\Delta\Phi\right\}_3 0 + \left\{Q_{II}/\Delta\Phi\right\}_3 0 + \left\{Q_{IS}/\Delta\Phi\right\}_3 0 + \left\{J/\Delta\Phi\right\}_3 [\Delta\omega^T]$$

where $y_k = \omega^E \sin\lambda \left[T_{k2}^{BR} \int_{t_o}^{t_N} \sin\phi_2 dt + T_{k3}^{BR} \int_{t_o}^{t_N} \cos\phi_2 dt\right]$ k = 1, 2 or 3

FOLDOUT FRAME 1

FOLDOUT FRAME 2

- $\int \sin \phi_2 \, dt$
- $\int \cos \phi_2 \, dt$

The manner in which these integrals are determined will depend completely upon the manner in which the test table angular acceleration is commanded during the experiment. The calibration procedures will therefore be dictated by the commanded angular acceleration profile. There appear to be only three interesting alternatives:

- The first alternative, which appears to be the best, is when the angular acceleration can be controlled to a desired function of time In that event the aforementioned integrals could be evaluated prior to the data collection A good example of a commanded profile might be a constant angular acceleration over a short data collection time.
- Another alternative, almost as good as the above, would be an angular acceleration profile which is an analytic function, but not known until the time of the experiment. An example would be the ability to command a constant angular acceleration, but not any given constant. In this event the integrals would be evaluated after data collection.
- The least attractive alternative would be when the profile cannot be commanded as a clean analytic function. The J term experiment could be conducted under such circumstances, but there would be a requirement for the ϕ_2 resolver to be collected in real time for the purpose of evaluating the integrals.

There is no reason to specify which of the above alternatives is to be used until the test table is evaluated to discern its ability to control angular accelerations. As a consequence, the J term equations in Section 4.3.2 are not specified as the equations to be programmed, as are the other calibration constant equations. Instead they are presented as functions of terms which will be described as functions of the angular acceleration profile at that time when the control characteristics of the table are better known. As a matter of convenience to the reader the form of the equation is presented for the case when a constant angular acceleration profile is commanded.

4.2.5 Determination of Accelerometer Coefficients

The general accelerometer calibration equations were developed in Section 4 1.2, and the results presented on Chart 4-13. We recall that it was assumed in the development of those equations that the test table would always be stationary (relative to the laboratory) during the entire accelerometer calibration. We recall also that nine of the gyro positions were also stationary. Analysis shows that the nine stationary gyro positions are very good choices for the entire accelerometer calibration.

We mentioned in Section 4.2.2 that, subsequent to the calibration of the principal angular velocity-sensitive coefficients, the gyro acceleration-sensitive terms predominate as unknowns. Thus, when concerned with calibration only, we can treat the gyro as an accelerometer. We note that the three unbalance terms in the gyro equation play the same role, functionally, as the three scale factor and $(Q^A)^{-1}$ terms in the accelerometer equation. We also note that the square term in the accelerometer equation appears functionally the same as the square compliance terms in the gyro equation. These facts, and the fact that the gyro and accelerometer input axes are nominally aligned, results in the use of the same positions for the determination of acceleration-sensitive coefficients in both the gyro and accelerometer equations.

In Chart 4-27 we see the accelerometer equations when $\phi_1 = 0^o$ and $\phi_2 = 90^o$. As with the gyro calibration discussed in Section 4.2.2, the accelerometer calibration requires only two table angle degrees of freedom. Therefore, two of the four table degrees of freedom can be arbitrarily chosen. The particular values of ϕ_1 and ϕ_2 shown in Chart 4-27 are chosen for the same reasons mentioned in Section 4.2.2 (where the gyro bias, unbalance, and square compliance calibration is described). In Charts 4-28 and 4-29 we present the accelerometer equations for Positions 7 through 12. We note that all but the cubic term can be explicitly extracted from these equations. (The cubic term always appears in any equation with the scale factor term and therefore cannot be separated from the scale factor term.) In Section 4.3.2 the explicit solution for the accelerometer bias, square coefficient and off-diagonal $(Q^A)^{-1}$ matrix elements are presented. Three additional sets of equations are presented which relate the scale factor and cubic term combination to the instrument and environment measurements.

4.2.6 Determination of Accelerometer Cubic Term

It was noted in Section 4.2.5 that the six positions (7-12) did not allow for the explicit evaluation of the cubic or scale factor terms. We therefore require additional positions for the extraction of the cubic terms Positions 13, 14, and 15 (described in the calibration of the gyro product compliance coefficients) are appropriate as the additional positions. In Charts 4-30 and 4-31 we present the accelerometer equations for those positions. The equations for the solution of the cubic terms are presented in Section 4-3.

For each accelerometer, either of the two positions in which the corresponding body axis is nominally oriented 45^o off the vertical may be used. Therefore any two of the three positions may be chosen to complete the calibration. The equations presented in Section 4.3 utilize Positions 13 and 14.

ACCELEROMETER CALIBRATION

$\phi_1 = 0^o$

$\phi_2 = 90^o$ (trivial)

$$P_1^A = \left\{D_1(\underline{A}_1\cdot\underline{B}_1)\right\}_1[g\Delta t]T_{11}^{BR} + \left\{D_1(\underline{A}_1\cdot\underline{B}_2)\right\}_1[g\Delta t]T_{21}^{BR} + \left\{D_1(\underline{A}_1\cdot\underline{B}_3)\right\}_1[g\Delta t]T_{31}^{BR} + \left\{D_1D_0\right\}_1[\Delta t] + \left\{D_1D_2\right\}_1[g^2\Delta t]\left[T_{11}^{BR}\right]^2 + \left\{D_1D_3\right\}_1[g^3\Delta t]\left[T_{11}^{BR}\right]^3$$

$$P_2^A = \left\{D_1(\underline{A}_2\cdot\underline{B}_1)\right\}_2[g\Delta t]T_{11}^{BR} + \left\{D_1(\underline{A}_2\cdot\underline{B}_2)\right\}_2[g\Delta t]T_{21}^{BR} + \left\{D_1(\underline{A}_2\cdot\underline{B}_3)\right\}_2[g\Delta t]T_{31}^{BR} + \left\{D_1D_0\right\}_2[\Delta t] + \left\{D_1D_2\right\}_2[g^2\Delta t]\left[T_{21}^{BR}\right]^2 + \left\{D_1D_3\right\}_2[g^3\Delta t]\left[T_{21}^{BR}\right]^3$$

$$P_3^A = \left\{D_1(\underline{A}_3\cdot\underline{B}_1)\right\}_3[g\Delta t]T_{11}^{BR} + \left\{D_1(\underline{A}_3\cdot\underline{B}_2)\right\}_3[g\Delta t]T_{21}^{BR} + \left\{D_1(\underline{A}_3\cdot\underline{B}_3)\right\}_3[g\Delta t]T_{31}^{BR} + \left\{D_1D_0\right\}_3[\Delta t] + \left\{D_1D_2\right\}_3[g^2\Delta t]\left[T_{31}^{BR}\right]^2 + \left\{D_1D_3\right\}_3[g^3\Delta t]\left[T_{31}^{BR}\right]^3$$

ACCELEROMETER CALIBRATION POSITIONS 7 AND 8

$\phi_1 = 0^o$
$\phi_2 = 90^o$
$T_{11}^{BR} = \pm 1$
$T_{21}^{BR} = 0$
$T_{31}^{BR} = 0$

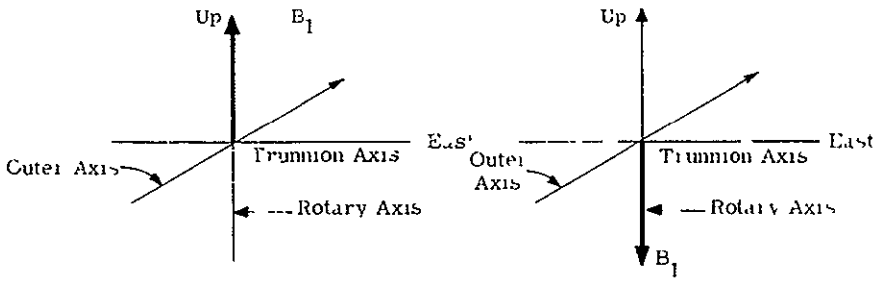

$P_1^A =$	$P_2^A =$	$P_3^A =$
$\{D_1(\underline{A}_1\cdot\underline{B}_1)\}_1\{\pm[g\Delta t]\}$	$\{D_1(\underline{A}_2\cdot\underline{B}_1)\}_2\{\pm[g\Delta t]\}$	$\{D_1(\underline{A}_3\cdot\underline{B}_1)\}_3\{\pm[g\Delta t]\}$
$+\{D_1(\underline{A}_1\cdot\underline{B}_2)\}_1$ 0	$+\{D_1(\underline{A}_2\cdot\underline{B}_2)\}_2$ 0	$+\{D_1(\underline{A}_3\cdot\underline{B}_2)\}_3$ 0
$+\{D_1(\underline{A}_1\cdot\underline{B}_3)\}_1$ 0	$+\{D_1(\underline{A}_2\cdot\underline{B}_3)\}_2$ 0	$+\{D_1(\underline{A}_3\cdot\underline{B}_3)\}_3$ 0
$+\{D_1D_0\}_1$ $[\Delta t]$	$+\{D_1D_0\}_2$ $[\Delta t]$	$+\{D_1D_0\}_3$ $[\Delta t]$
$+\{D_1D_2\}_1$ $[g^2\Delta t]$	$+\{D_1D_2\}_2$ 0	$+\{D_1D_2\}_3$ 0
$+\{D_1D_3\}_1$ $\{\pm[g^3\Delta t]\}$	$+\{D_1D_3\}_2$ 0	$+\{D_1D_3\}_3$ 0

POSITIONS 9 AND 10

$\phi_1 = 0^o$
$\phi_2 = 90^o$
$T_{11}^{BR} = 0$
$T_{21}^{BR} = \pm 1$
$T_{31}^{BR} = 0$

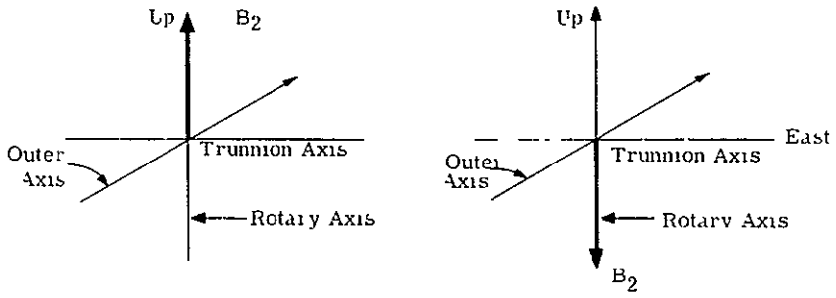

$P_1^A =$	$P_2^A =$	$P_3^A =$
$\{D_1(\underline{A}_1\cdot\underline{B}_1)\}_1$ 0	$\{D_1(\underline{A}_2\cdot\underline{B}_1)\}_2$ 0	$\{D_1(\underline{A}_3\cdot\underline{B}_1)\}_3$ 0
$+\{D_1(\underline{A}_1\underline{B}_2)\}_1\{\pm[g\Delta t]\}$	$+\{D_1(\underline{A}_2\cdot\underline{B}_2)\}_2\{\pm[g\Delta t]\}$	$+\{D_1(\underline{A}_3\cdot\underline{B}_2)\}_3\{\pm[g\Delta t]\}$
$+\{D_1(\underline{A}_1\cdot\underline{B}_3)\}_1$ 0	$+\{D_1(\underline{A}_2\cdot\underline{B}_3)\}_2$ 0	$+\{D_1(\underline{A}_3\cdot\underline{B}_3)\}_3$ 0
$+\{D_1D_0\}_1$ $[\Delta t]$	$+\{D_1D_0\}_2$ $[\Delta t]$	$+\{D_1D_0\}_3$ $[\Delta t]$
$+\{D_1D_2\}_1$ 0	$+\{D_1D_2\}_2$ $[g^2\Delta t]$	$+\{D_1D_2\}_3$ 0
$+\{D_1D_3\}_1$ 0	$+\{D_1D_3\}_2$ $\{\pm[g^3\Delta t]\}$	$+\{D_1D_3\}_3$ 0

ACCELEROMETER CALIBRATION POSITIONS 11 AND 12

$\phi_1 = 0^o$

$\phi_2 = 90^o$

$T_{11}^{BR} = 0$

$T_{21}^{BR} = 0$

$T_{31}^{BR} = \pm 1$

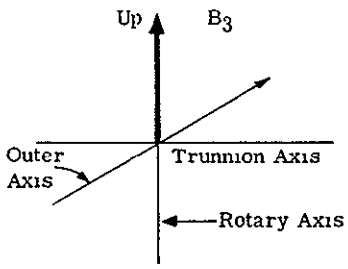

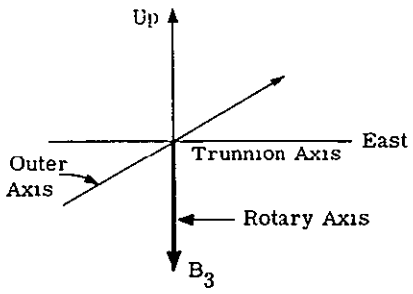

$P_1^A = \{D_1(\underline{A}_1 \underline{B}_1)\}_1$	0	
$+ \{D_1(\underline{A}_1 \cdot \underline{B}_2)\}_1$	0	
$+ \{D_1(\underline{A}_1 \cdot \underline{B}_3)\}_1$	$\{\pm[g\Delta t]\}$	
$+ \{D_1 D_0\}_1$	$[\Delta t]$	
$+ \{D_1 D_2\}_1$	0	
$+ \{D_1 D_3\}_1$	0	

$P_2^A = \{D_1(\underline{A}_2 \cdot \underline{B}_1)\}_2$	0	
$+ \{D_1(\underline{A}_2 \cdot \underline{B}_2)\}_2$	0	
$+ \{D_1(\underline{A}_2 \cdot \underline{B}_3)\}_2$	$\{\pm[g\Delta t]\}$	
$+ \{D_1 D_0\}_2$	$[\Delta t]$	
$+ \{D_1 D_2\}_2$	0	
$+ \{D_1 D_3\}_2$	0	

$P_3^A = \{D_1(\underline{A}_3 \cdot \underline{B}_1)\}_3$	0	
$+ \{D_1(\underline{A}_3 \cdot \underline{B}_2)\}_3$	0	
$+ \{D_1(\underline{A}_3 \cdot \underline{B}_3)\}_3$	$\{\pm[g\Delta t]\}$	
$+ \{D_1 D_0\}_3$	$[\Delta t]$	
$+ \{D_1 D_2\}_3$	$[g^2 \Delta t]$	
$+ \{D_1 D_3\}_3$	$\{\pm[g^3 \Delta t]\}$	

ACCELEROMETER CALIBRATION POSITION 13

$\phi_1 = 0^o$
$\phi_2 = 90^o$
$T_{11}^{BR} = \sqrt{1/2}$
$T_{21}^{BR} = \sqrt{1/2}$
$T_{31}^{BR} = 0$

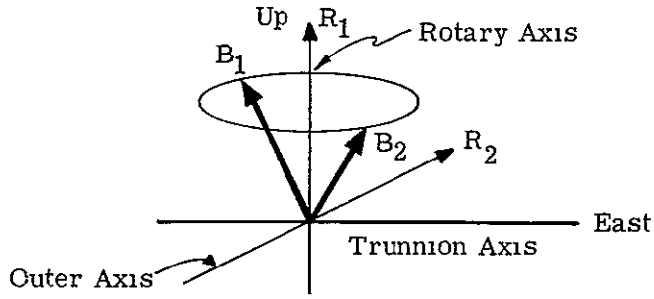

$P_1^A =$	$P_2^A =$	$P_3^A =$
$\{D_1(\underline{A}_1\cdot\underline{B}_1)\}_1[\sqrt{1/2}\ g\Delta t]$	$\{D_1(\underline{A}_2\cdot\underline{B}_1)\}_2[\sqrt{1/2}\ g\Delta t]$	$\{D_1(\underline{A}_3\cdot\underline{B}_1)\}_3[\sqrt{1/2}\ g\Delta t]$
$+\{D_1(\underline{A}_1\cdot\underline{B}_2)\}_1[\sqrt{1/2}\ g\Delta t]$	$+\{D_1(\underline{A}_2\cdot\underline{B}_2)\}_2[\sqrt{1/2}\ g\Delta t]$	$+\{D_1(\underline{A}_3\cdot\underline{B}_2)\}_3[\sqrt{1/2}\ g\Delta t]$
$+\{D_1(\underline{A}_1\cdot\underline{B}_3)\}_1\ 0$	$+\{D_1(\underline{A}_2\cdot\underline{B}_3)\}_2\ 0$	$+\{D_1(\underline{A}_3\cdot\underline{B}_3)\}_3\ 0$
$+\{D_1D_0\}_1\ [\Delta t]$	$+\{D_1D_0\}_2\ [\Delta t]$	$+\{D_1D_0\}_3\ [\Delta t]$
$+\{D_1D_2\}_1\ [1/2\ g^2\Delta t]$	$+\{D_1D_2\}_2\ [1/2\ g^2\Delta t]$	$+\{D_1D_2\}_3\ 0$
$+\{D_1D_3\}_1\ [1/2\sqrt{1/2}g^3\Delta t]$	$+\{D_1D_3\}_2\ [1/2\sqrt{1/2}g^3\Delta t]$	$+\{D_1D_3\}_3\ 0$

POSITION 14

$\phi_1 = 0^o$
$\phi_2 = 90^o$
$T_{11}^{BR} = \sqrt{1/2}$
$T_{21}^{BR} = 0$
$T_{31}^{BR} = \sqrt{1/2}$

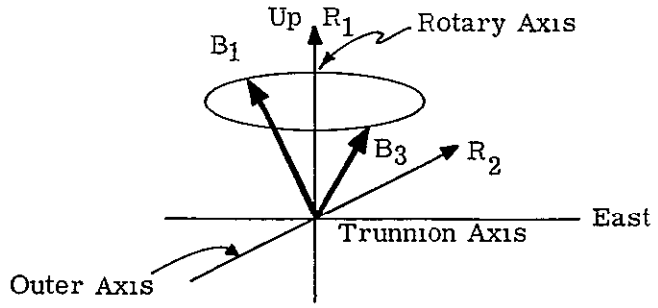

$P_1^A =$	$P_2^A =$	$P_3^A =$
$\{D_1(\underline{A}_1\cdot\underline{B}_1)\}_1[\sqrt{1/2}g\Delta t]$	$\{D_1(\underline{A}_2\cdot\underline{B}_1)\}_2[\sqrt{1/2}g\Delta t]$	$\{D_1(\underline{A}_3\cdot\underline{B}_1)\}_3[\sqrt{1/2}g\Delta t]$
$+\{D_1(\underline{A}_1\cdot\underline{B}_2)\}_1\ 0$	$+\{D_1(\underline{A}_2\cdot\underline{B}_2)\}_2\ 0$	$+\{D_1(\underline{A}_3\cdot\underline{B}_2)\}_3\ 0$
$+\{D_1(\underline{A}_1\cdot\underline{B}_3)\}_1[\sqrt{1/2}g\Delta t]$	$+\{D_1(\underline{A}_2\cdot\underline{B}_3)\}_2[\sqrt{1/2}g\Delta t]$	$+\{D_1(\underline{A}_3\cdot\underline{B}_3)\}_3[\sqrt{1/2}g\Delta t]$
$+\{D_1D_0\}_1\ [\Delta t]$	$+\{D_1D_0\}_2\ [\Delta t]$	$+\{D_1D_0\}_3\ [\Delta t]$
$+\{D_1D_2\}_1\ [1/2g^2\Delta t]$	$+\{D_1D_2\}_2\ 0$	$+\{D_1D_2\}_3\ [1/2g^2\Delta t]$
$+\{D_1D_3\}_1[1/2\sqrt{1/2}g^3\Delta t]$	$+\{D_1D_3\}_2\ 0$	$+\{D_1D_3\}_3[1/2\sqrt{1/2}g^3\Delta t]$

ACCELEROMETER CALIBRATION POSITION 15

$\phi_1 = 0^\circ$

$\phi_2 = 90^\circ$

$T_{11}^{BR} = 0$

$T_{21}^{BR} = \sqrt{1/2}$

$T_{31}^{BR} = \sqrt{1/2}$

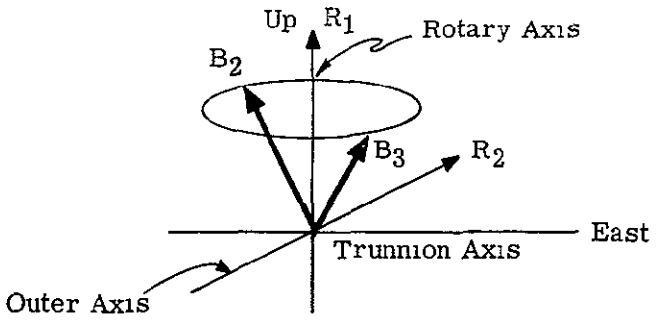

$P_1^A = \{D_1(\underline{A}_1 \cdot \underline{B}_1)\}_1$ 0	$P_2^A = \{D_1(\underline{A}_2 \cdot \underline{B}_1)\}_2$ 0	$P_3^A = \{D_1(\underline{A}_3 \cdot \underline{B}_1)\}_3$ 0
$+ \{D_1(\underline{A}_1 \cdot \underline{B}_2)\}_1 [\sqrt{1/2} g \Delta t]$	$+ \{D_1(\underline{A}_2 \cdot \underline{B}_2)\}_2 [\sqrt{1/2} g \Delta t]$	$+ \{D_1(\underline{A}_3 \cdot \underline{B}_2)\}_3 [\sqrt{1/2} g \Delta t]$
$+ \{D_1(\underline{A}_1 \cdot \underline{B}_3)\}_1 [\sqrt{1/2} g \Delta t]$	$+ \{D_1(\underline{A}_2 \cdot \underline{B}_3)\}_2 [\sqrt{1/2} g \Delta t]$	$+ \{D_1(\underline{A}_3 \cdot \underline{B}_3)\}_3 [\sqrt{1/2} g \Delta t]$
$+ \{D_1 D_0\}_1$ $[\Delta t]$	$+ \{D_1 D_0\}_2$ $[\Delta t]$	$+ \{D_1 D_0\}_3$ $[\Delta t]$
$+ \{D_1 D_2\}_1$ 0	$+ \{D_1 D_2\}_2$ $[1/2 g^2 \Delta t]$	$+ \{D_1 D_2\}_3$ $[1/2 g^2 \Delta t]$
$+ \{D_1 D_3\}_1$ 0	$+ \{D_1 D_3\}_2 [1/2 \sqrt{1/2} g^3 \Delta t]$	$+ \{D_1 D_3\}_3 [1/2 \sqrt{1/2} g^3 \Delta t]$

4.3 CALIBRATION EQUATIONS

We noted in Section 4.2 that the simultaneous solution of at most two equations would yield the value of a required calibration constant as a function of the input environment and the defined P_k^G or P_k^A vectors. The P_k^G and P_k^A vectors were seen in Section 4.1 to be a function of the instrument outputs, noise, and quantization error. In the first subsection which follows we will approximate the P_k^G and P_k^A vectors by the instrument outputs only. Those approximations will be incorporated into the determination of the calibration computations, which are tabulated in Section 4.3.2.

4.3.1 Processing

We showed in Section 4.2 that each calibration constant can be solved for as a function of at most two input environments, two P_k^A or two P_k^G components, and previously determined constants. That is, the solution for any constant (say y) can be written as:

$$y = Ax + B$$

where

$$x = \frac{1}{2}\left(\frac{P}{\Delta t} \pm \frac{P}{\Delta t}\right) \text{ or } \frac{P}{\Delta t}$$

$$A = \frac{1}{\text{environment coefficient of y}}$$

$P = P_k^A$ or P_k^G for k = 1, 2, or 3

B = function of other calibration constants and environment inputs.

In Section 4.1 we defined the P vectors as a function of instrument readout, quantization error, and noise. We suggested in the introduction to Section 4 that we wish to approximate the P vectors as functions of instrument readouts only. We would like therefore to collect the instrument data in such a way that the effects of quantization and noise fall below some required threshold. Fortunately the noise can be represented by random processes with bounded means and variances. The quantization error is by its very nature also bounded. On the other hand, for a nominally constant input environment, the instrument output is a monotone increasing function of the observation time. Thus by choosing sufficiently long observation intervals, the percent error in the assumption that the instrument output equals P can be made arbitrarily small.

In Section 2 of the trade-off document the analysis which leads to the above conclusions is presented. The results of that analysis are presented in form of graphs in which the precisions of the calibration constants (with the assumption of neglected noise and quantization in P_k^G or P_k^A) are plotted against time. Those graphs will be used in the Laboratory Procedures Manual to determine the calibration time required to obtain a desired precision in any constant.

4.3.2 Computation of Constants

With the approximations described in the previous section, it is now possible to solve explicitly for the calibration constants in terms of well-known instrument and environment measurements. The equations are presented in tabular form on the Calibration Equations Charts. These equations are those which are to be programmed. An exception is the J term equations which will not be in program form until the time when the test table is evaluated (see Section 4.2.4).

It has been noted in Section 4.2.5 that the accelerometer third order term cannot be separated from the scale factor by a choice of positions. In the following set of equations there are two equations given for each accelerometer that relate the scale factor term $[D_1(A_i \cdot B_1)]_1$ to the third order term $(D_1 D_3)_i$. If a simultaneous solution of the two equations is used to determine the scale factor and the third order term, then the scale factor will be sensitive to errors in the bias and the second order term. These terms appear on the equation listed second in each of the three sets of two equations. This may be avoided by determining $(D_1 D_3)_1$ (by simultaneous solution or other methods) and using this value to solve the first equation for $[D_1(A_i \cdot B_i)]_1$. This value is subject to the accuracy of other terms only through the extremely small term containing D_3. (D_1) is then given by the square root of the sum of the squares of $[D_1(A_1 \cdot B_j)]_1$ for $j = 1, 2, 3$.

In developing these equations several equalities are used which introduce previously unmentioned parameters. The following comments describe those parameters and their nomenclature:

- Because we are dealing with the measurement of quantities in many different positions, a position index must be introduced. The numerical superscripts in all equations refer to the positions

- The vector P_k^G $(k = 1, 2, 3)$ is approximated by the gyro readouts, therefore

$$P_k^G \Rightarrow (\Sigma \delta)_k$$

GYRO CALIBRATION EQUATIONS

Scale Factor and Misalignments

$$[\Delta\Phi]_k = \left\{ \left[\frac{\underline{G}_k \cdot \underline{B}_1}{\Delta\Phi}\right]_k^2 + \left[\frac{\underline{G}_k \cdot \underline{B}_2}{\Delta\Phi}\right]_k^2 + \left[\frac{\underline{G}_k \cdot \underline{B}_3}{\Delta\Phi}\right]_k^2 \right\}^{-1/2}$$

Gyro One

$$[(\underline{G}_1 \cdot \underline{B}_1)/\Delta\Phi]_1 = \frac{\left[\dfrac{(\Sigma\delta)_1^1}{(\Sigma n_1^T)^1} - \dfrac{(\Sigma\delta)_1^2}{(\Sigma n_1^T)^2}\right]}{\left[S^\phi\left(\dfrac{(\Sigma n^\phi)^1}{(\Sigma n_1^T)^1} + \dfrac{(\Sigma n^\phi)^2}{(\Sigma n_1^T)^2}\right) - 2S_1^T \omega^E \sin\lambda\right]}$$

$$[\underline{G}_1 \cdot \underline{B}_2)/\Delta\Phi]_1 = \frac{\left[\dfrac{(\Sigma\delta)_1^3}{(\Sigma n_1^T)^3} - \dfrac{(\Sigma\delta)_1^4}{(\Sigma n_1^T)^4}\right]}{\left[S^\phi\left(\dfrac{(\Sigma n^\phi)^3}{(\Sigma n_1^T)^3} + \dfrac{(\Sigma n^\phi)^4}{(\Sigma n_1^T)^4}\right) - 2S_1^T \omega^E \sin\lambda\right]}$$

$$[(\underline{G}_1 \cdot \underline{B}_3)/\Delta\Phi]_1 = \frac{\left[\dfrac{(\Sigma\delta)_1^5}{(\Sigma n_1^T)^5} - \dfrac{(\Sigma\delta)_1^6}{(\Sigma n_1^T)^6}\right]}{\left[S^\phi\left(\dfrac{(\Sigma n^\phi)^5}{(\Sigma n_1^T)^5} + \dfrac{(\Sigma n^\phi)^6}{(\Sigma n_1^T)^6}\right) - 2S_1^T \omega^E \sin\lambda\right]}$$

Gyro Two

$$[(\underline{G}_2 \cdot \underline{B}_1)/\Delta\Phi]_2 = \frac{\left[\dfrac{(\Sigma\delta)_2^1}{(\Sigma n_1^T)^1} - \dfrac{(\Sigma\delta)_2^2}{(\Sigma n_1^T)^2}\right]}{\left[S^\phi\left(\dfrac{(\Sigma n^\phi)^1}{(\Sigma n_1^T)^1} + \dfrac{(\Sigma n^\phi)^2}{(\Sigma n_1^T)^2}\right) - 2S_1^T \omega^E \sin\lambda\right]}$$

Gyro Two (Continued)

$$\left[(\underline{G}_2 \cdot \underline{B}_2)/\Delta\Phi\right]_2 = \frac{\left[\dfrac{(\Sigma\delta)_2^3}{(\Sigma n_1^T)^3} - \dfrac{(\Sigma\delta)_2^4}{(\Sigma n_1^T)^4}\right]}{\left[S^{\phi}\left(\dfrac{(\Sigma n^{\phi})^3}{(\Sigma n_1^T)^3} + \dfrac{(\Sigma n^{\phi})^4}{(\Sigma n_1^T)^4}\right) - 2S_1^T\,\omega^E \sin\lambda\right]}$$

$$\left[(\underline{G}_2 \cdot \underline{B}_3)/\Delta\Phi\right]_2 = \frac{\left[\dfrac{(\Sigma\delta)_2^5}{(\Sigma n_1^T)^5} - \dfrac{(\Sigma\delta)_2^6}{(\Sigma n_1^T)^6}\right]}{\left[S^{\phi}\left(\dfrac{(\Sigma n^{\phi})^5}{(\Sigma n_1^T)^5} + \dfrac{(\Sigma n^{\phi})^6}{(\Sigma n_1^T)^6}\right) - 2S_1^T\,\omega^E \sin\lambda\right]}$$

Gyro Three

$$\left[(\underline{G}_3 \cdot \underline{B}_1)/\Delta\Phi\right]_3 = \frac{\left[\dfrac{(\Sigma\delta)_3^1}{(\Sigma n_1^T)^1} - \dfrac{(\Sigma\delta)_3^2}{(\Sigma n_1^T)^2}\right]}{\left[S^{\phi}\left(\dfrac{(\Sigma n^{\phi})^1}{(\Sigma n_1^T)^1} + \dfrac{(\Sigma n^{\phi})^2}{(\Sigma n_1^T)^2}\right) - 2S_1^T\,\omega^E \sin\lambda\right]}$$

$$\left[(\underline{G}_3 \cdot \underline{B}_2)/\Delta\Phi\right]_3 = \frac{\left[\dfrac{(\Sigma\delta)_3^3}{(\Sigma n_1^T)^3} - \dfrac{(\Sigma\delta)_3^4}{(\Sigma n_1^T)^4}\right]}{\left[S^{\phi}\left(\dfrac{(\Sigma n^{\phi})^3}{(\Sigma n_1^T)^3} + \dfrac{(\Sigma n^{\phi})^4}{(\Sigma n_1^T)^4}\right) - 2S_1^T\,\omega^E \sin\lambda\right]}$$

GYRO CALIBRATION EQUATIONS (Continued)

Gyro Three (Continued)

$$\left[(\underline{G}_3 \cdot \underline{B}_3)/\Delta\Phi\right]_3 = \frac{\left[\dfrac{(\Sigma\delta)_3^5}{(\Sigma n_1^T)^5} - \dfrac{(\Sigma\delta)_3^6}{(\Sigma n_1^T)^6}\right]}{\left[S^{\phi}\left(\dfrac{(\Sigma n^{\phi})^5}{(\Sigma n_1^T)^5} + \dfrac{(\Sigma n^{\phi})^6}{(\Sigma n_1^T)^6}\right) - 2S_1^T\,\omega^E \sin\lambda\right]}$$

Bias

$$\left[R\right]_k = \left[R/\Delta\Phi\right]_k \left[\Delta\Phi\right]_k$$

Gyro One

$$\left[R/\Delta\Phi\right]_1 = \frac{1}{2S_1^T}\left[\frac{(\Sigma\delta)_1^{11}}{(\Sigma n_1^T)_1^{G11}} + \frac{(\Sigma\delta)_1^{12}}{(\Sigma n_1^T)_1^{G12}}\right] - \omega^E \sin\lambda\left[T_{12}^{BR5}\left[(\underline{G}_1 \cdot \underline{B}_1)/\Delta\Phi\right]_1 + T_{22}^{BR5}\left[(\underline{G}_1 \cdot \underline{B}_2)/\Delta\Phi\right]_1\right]$$

Gyro Two

$$\left[R/\Delta\Phi\right]_2 = \frac{1}{2S_1^T}\left[\frac{(\Sigma\delta)_2^7}{(\Sigma n_1^T)_2^{G7}} + \frac{(\Sigma\delta)_2^8}{(\Sigma n_1^T)_2^{G8}}\right] - \omega^E \sin\lambda\left[T_{22}^{BR1}\left[(\underline{G}_2 \cdot \underline{B}_2)/\Delta\Phi\right]_2 + T_{32}^{BR1}\left[(\underline{G}_2 \cdot \underline{B}_3)/\Delta\Phi\right]_2\right]$$

Gyro Three

$$\left[R/\Delta\Phi\right]_3 = \frac{1}{2S_1^T}\left[\frac{(\Sigma\delta)_3^7}{(\Sigma n_1^T)_3^{G7}} + \frac{(\Sigma\delta)_3^8}{(\Sigma n_1^T)_3^{G8}}\right] - \omega^E \sin\lambda\left[T_{32}^{BR1}\left[(\underline{G}_3 \cdot \underline{B}_3)/\Delta\Phi\right]_3 + T_{22}^{BR1}\left[(\underline{G}_3 \cdot \underline{B}_2)/\Delta\Phi\right]_3\right]$$

Unbalance

$$[B]_k = [B/\Delta\Phi]_k \, [\Delta\Phi]_k$$

Gyro One

$$[B_I/\Delta\Phi]_1 = \frac{1}{2gS_1^T}\left[\frac{(\Sigma\delta)_1^7}{(\Sigma n_1^T)_1^{G7}} - \frac{(\Sigma\delta)_1^8}{(\Sigma n_1^T)_1^{G8}}\right] - \frac{\omega^E \cos\lambda}{g}\,[(\underline{G}_1 \cdot \underline{B}_1)/\Delta\Phi]_1$$

$$[B_O/\Delta\Phi]_1 = \frac{1}{2gS_1^T}\left[\frac{(\Sigma\delta)_1^{11}}{(\Sigma n_1^T)_1^{G11}} - \frac{(\Sigma\delta)_1^{12}}{(\Sigma n_1^T)_1^{G12}}\right] - \frac{\omega^E \cos\lambda}{g}\,[(\underline{G}_1 \cdot \underline{B}_3)/\Delta\Phi]_1$$

$$[B_S/\Delta\Phi]_1 = \frac{-1}{2gS_1^T}\left[\frac{(\Sigma\delta)_1^9}{(\Sigma n_1^T)_1^{G9}} - \frac{(\Sigma\delta)_1^{10}}{(\Sigma n_1^T)_1^{G10}}\right] - \frac{\omega^E \cos\lambda}{g}\,[(\underline{G}_1 \cdot \underline{B}_2)/\Delta\Phi]_1$$

Gyro Two

$$[B_I/\Delta\Phi]_2 = \frac{1}{2gS_1^T}\left[\frac{(\Sigma\delta)_2^9}{(\Sigma n_1^T)_2^{G9}} - \frac{(\Sigma\delta)_2^{10}}{(\Sigma n_1^T)_2^{G10}}\right] - \frac{\omega^E \cos\lambda}{g}\,[(\underline{G}_2 \cdot \underline{B}_2)/\Delta\Phi]_2$$

$$[B_O/\Delta\Phi]_2 = \frac{1}{2gS_1^T}\left[\frac{(\Sigma\delta)_2^7}{(\Sigma n_1^T)_2^{G7}} - \frac{(\Sigma\delta)_2^8}{(\Sigma n_1^T)_2^{G8}}\right] - \frac{\omega^E \cos\lambda}{g}\,[(\underline{G}_2 \cdot \underline{B}_1)/\Delta\Phi]_2$$

$$[B_S/\Delta\Phi]_2 = \frac{-1}{2gS_1^T}\left[\frac{(\Sigma\delta)_2^{11}}{(\Sigma n_1^T)_2^{G11}} - \frac{(\Sigma\delta)_2^{12}}{(\Sigma n_1^T)_2^{G12}}\right] - \frac{\omega^E \cos\lambda}{g}\,[(\underline{G}_2 \cdot \underline{B}_3)/\Delta\Phi]_2$$

GYRO CALIBRATION EQUATIONS (Continued)

Gyro Three

$$\left[B_I/\Delta\Phi\right]_1 = \frac{1}{2gS_1^T}\left[\frac{(\Sigma\delta)_3^{11}}{(\Sigma n_1^T)_3^{G11}} - \frac{(\Sigma\delta)_3^{12}}{(\Sigma n_1^T)_3^{G12}}\right] - \frac{\omega^E \cos\lambda}{g}\left[(\underline{G}_3 \cdot \underline{B}_3)/\Delta\Phi\right]_3$$

$$\left[B_O/\Delta\Phi\right]_3 = \frac{1}{2gS_1^T}\left[\frac{(\Sigma\delta)_3^{7}}{(\Sigma n_1^T)_3^{G7}} - \frac{(\Sigma\delta)_3^{8}}{(\Sigma n_1^T)_3^{G8}}\right] - \frac{\omega^E \cos\lambda}{g}\left[(\underline{G}_3 \cdot \underline{B}_1)/\Delta\Phi\right]_3$$

$$\left[B_S/\Delta\Phi\right]_3 = \frac{1}{2gS_1^T}\left[\frac{(\Sigma\delta)_3^{9}}{(\Sigma n_1^T)_3^{G9}} - \frac{(\Sigma\delta)_3^{10}}{(\Sigma n_1^T)_3^{G10}}\right] - \frac{\omega^E \cos\lambda}{g}\left[(\underline{G}_3 \cdot \underline{B}_2)/\Delta\Phi\right]_3$$

Square Compliance

$$\left[C\right]_k = \left[C/\Delta\Phi\right]_k \left[\Delta\Phi\right]_k$$

Gyro One

$$\left[C_{II}/\Delta\Phi\right]_1 = \frac{1}{2g^2S_1^T}\left[\frac{(\Sigma\delta)_1^{7}}{(\Sigma n_1^T)_1^{G7}} + \frac{(\Sigma\delta)_1^{8}}{(\Sigma n_1^T)_1^{G8}}\right] - \frac{1}{g^2}\left[R/\Delta\Phi\right]_1$$
$$- \frac{\omega^E \sin\lambda}{g^2}\left[T_{22}^{BR1}\left[(\underline{G}_1 \cdot \underline{B}_2)/\Delta\Phi\right]_1 + T_{32}^{BR1}\left[(\underline{G}_1 \cdot \underline{B}_3)/\Delta\Phi\right]_1\right]$$

$$\left[C_{SS}/\Delta\Phi\right]_1 = \frac{1}{2g^2S_1^T}\left[\frac{(\Sigma\delta)_1^{9}}{(\Sigma n_1^T)_1^{G9}} + \frac{(\Sigma\delta)_1^{10}}{(\Sigma n_1^T)_1^{G10}}\right] - \frac{1}{g^2}\left[R/\Delta\Phi\right]_1$$
$$- \frac{\omega^E \sin\lambda}{g^2}\left[T_{12}^{BR3}\left[(\underline{G}_1 \cdot \underline{B}_1)/\Delta\Phi\right]_1 + T_{32}^{BR3}\left[(\underline{G}_1 \cdot \underline{B}_3)/\Delta\Phi\right]_1\right]$$

GYRO CALIBRATION EQUATIONS (Continued)

Gyro Two

$$\left[C_{II}/\Delta\Phi\right]_2 = \frac{1}{2g^2 S_1^T}\left[\frac{(\Sigma\delta)_2^9}{(\Sigma n_1^T)_2^{G9}} + \frac{(\Sigma\delta)_2^{10}}{(\Sigma n_1^T)_2^{G10}}\right] - \frac{1}{g^2}\left[R/\Delta\Phi\right]_2$$

$$- \frac{\omega^E \sin\lambda}{g^2}\left[T_{12}^{BR3}\left[(\underline{G}_2 \cdot \underline{B}_1)\Delta\Phi\right]_2 + T_{32}^{BR3}\left[(\underline{G}_2 \cdot \underline{B}_3)/\Delta\Phi\right]_2\right]$$

$$\left[C_{SS}/\Delta\Phi\right]_2 = \frac{1}{2g^2 S_1^T}\left[\frac{(\Sigma\delta)_2^{11}}{(\Sigma n_1^T)_2^{G11}} + \frac{(\Sigma\delta)_2^{12}}{(\Sigma n_1^T)_2^{G12}}\right] - \frac{1}{g^2}\left[R/\Delta\Phi\right]_2$$

$$- \frac{\omega^E \sin\lambda}{g^2}\left[T_{12}^{BR5}\left[(\underline{G}_2 \cdot \underline{B}_1)/\Delta\Phi\right]_2 + T_{22}^{BR5}\left[(\underline{G}_2 \circ \underline{B}_2)/\Delta\Phi\right]_2\right]$$

Gyro Three

$$\left[C_{II}/\Delta\Phi\right]_3 = \frac{1}{2g^2 S_I^T}\left[\frac{(\Sigma\delta)_3^{11}}{(\Sigma n_1^T)_3^{G11}} + \frac{(\Sigma\delta)_3^{12}}{(\Sigma n_1^T)_3^{G12}}\right] - \frac{1}{g^2}\left[R/\Delta\Phi\right]_3$$

$$- \frac{\omega^E \sin\lambda}{g^2}\left[T_{12}^{BR5}\left[(\underline{G}_3 \cdot \underline{B}_1)/\Delta\Phi\right]_3 + T_{22}^{BR5}\left[(\underline{G}_3 \circ \underline{B}_2)\Delta\Phi\right]_3\right]$$

$$\left[C_{SS}/\Delta\Phi\right]_3 = \frac{1}{2g^2 S_1^T}\left[\frac{(\Sigma\delta)_3^9}{(\Sigma n_1^T)_3^{G9}} + \frac{(\Sigma\delta)_3^{10}}{(\Sigma n_1^T)_3^{G10}}\right] - \frac{1}{g^2}\left[R/\Delta\Phi\right]_3$$

$$- \frac{\omega^E \sin\lambda}{g^2}\left[T_{12}^{BR3}\left[(\underline{G}_3 \cdot \underline{B}_1)/\Delta\Phi\right]_3 + T_{32}^{BR3}\left[(\underline{G}_3 \cdot \underline{B}_3)/\Delta\Phi\right]_3\right]$$

Product Compliance

Gyro One

$$\left[C_{IS}/\Delta\Phi\right]_1 = -\frac{2}{g^2 S_1^T}\left[\frac{(\Sigma\delta)_1^{13}}{(\Sigma n_1^T)_1^{G13}}\right] + \frac{2}{g^2}\left[R/\Delta\Phi\right]_1 + \frac{\sqrt{2}}{g}\left[\left[B_I/\Delta\Phi\right]_1 - \left[B_S/\Delta\Phi\right]_1\right]$$

$$- \frac{2\omega^E}{g^2}\left[\left[\underline{G}_1 \cdot \underline{B}_1/\Delta\Phi\right]_1 \left[\sqrt{1/2}\cos\lambda + T_{12}^{BR13}\sin\lambda\right] + \left[(\underline{G}_1 \cdot \underline{B}_2)/\Delta\Phi\right]_1\right.$$

$$\left.\left[\sqrt{1/2}\cos\lambda + T_{22}^{BR13}\sin\lambda\right] + \left[\underline{G}_1 \cdot \underline{B}_3/\Delta\Phi\right]_1 \left[T_{32}^{BR13}\sin\lambda\right]\right]$$

$$+ \left[C_{II}/\Delta\Phi\right]_1 + \left[C_{SS}/\Delta\Phi\right]_1$$

$$\left[C_{IO}/\Delta\Phi\right]_1 = + \frac{2}{g^2 S_1^T}\left[\frac{(\Sigma\delta)_1^{14}}{(\Sigma n_1^T)_1^{G14}}\right] - \frac{2}{g^2}\left[R/\Delta\Phi\right]_1 - \frac{\sqrt{2}}{g}\left[\left[B_I/\Delta\Phi\right]_1 + \left[B_O/\Delta\Phi\right]_1\right]$$

$$- \frac{2\omega^E}{g^2}\left[\left[\underline{G}_1 \cdot \underline{B}_1/\Delta\Phi\right]_1 \left[\sqrt{1/2}\cos\lambda + T_{12}^{BR14}\sin\lambda\right] + \left[\underline{G}_1 \cdot \underline{B}_2/\Delta\Phi\right]_1\right.$$

$$\left.\left[T_{22}^{BR14}\sin\lambda\right] + \left[\underline{G}_1 \cdot \underline{B}_3/\Delta\Phi\right]_1 \left[\sqrt{1/2}\cos\lambda + T_{32}^{BR14}\sin\lambda\right]\right] - \left[C_{II}/\Delta\Phi\right]_1$$

$$\left[C_{OS}/\Delta\Phi\right]_1 = -\frac{2}{g^2 S_1^T}\left[\frac{(\Sigma\delta)_1^{15}}{(\Sigma n_1^T)_1^{G15}}\right] + \frac{2}{g^2}\left[R/\Delta\Phi\right]_1 + \frac{\sqrt{2}}{g}\left[-\left[B_S/\Delta\Phi\right]_1 + \left[B_O/\Delta\Phi\right]_1\right]$$

$$+ \frac{2\omega^E}{g^2}\left[\left[\underline{G}_1 \cdot \underline{B}_1/\Delta\Phi\right]_1 \left(T_{12}^{BR15}\sin\lambda\right) + \left[\underline{G}_1 \cdot \underline{B}_2/\Delta\Phi\right]_1\right.$$

$$\left.\left(\sqrt{1/2}\cos\lambda + T_{22}^{BR15}\sin\lambda\right) + \left[\underline{G}_1 \cdot \underline{B}_3/\Delta\Phi\right]_1 \left[\sqrt{1/2}\cos\lambda + T_{32}^{BR15}\sin\lambda\right]\right]$$

$$+ \left[C_{SS}/\Delta\Phi\right]_1$$

Gyro Two

$$[C_{IS}/\Delta\Phi]_2 = -\frac{2}{g^2 S_1^T}\left[\frac{(\Sigma\delta)_2^{15}}{(\Sigma n_1^T)_2^{G15}}\right] + \frac{2}{g^2}[R/\Delta\Phi]_2 + \frac{\sqrt{2}}{g}\left[[B_I/\Delta\Phi]_2 - [B_S/\Delta\Phi]_2\right]$$
$$+\frac{2\omega^E}{g^2}\left[[\underline{G}_2\cdot\underline{B}_1/\Delta\Phi]_2\left[T_{12}^{BR15}\sin\lambda\right] + [\underline{G}_2\cdot\underline{B}_2/\Delta\Phi]_2\right.$$
$$\left.\left[\sqrt{1/2}\cos\lambda + T_{22}^{BR15}\sin\lambda\right] + [\underline{G}_2\cdot\underline{B}_3/\Delta\Phi]_2\left[\sqrt{1/2}\cos\lambda + T_{32}^{BR15}\sin\lambda\right]\right]$$
$$+ [C_{II}/\Delta\Phi]_2 + [C_{SS}/\Delta\Phi]_2$$

$$[C_{IO}/\Delta\Phi]_2 = \frac{2}{g^2 S_1^T}\left[\frac{(\Sigma\delta)_2^{13}}{(\Sigma n_1^T)_2^{G13}}\right] - \frac{2}{g^2}[R/\Delta\Phi]_2 - \frac{\sqrt{2}}{g}\left[[B_I/\Delta\Phi]_2 + [B_O/\Delta\Phi]_2\right]$$
$$-\frac{2\omega^E}{g^2}\left[[\underline{G}_2\cdot\underline{B}_1/\Delta\Phi]_2\left[\sqrt{1/2}\cos\lambda + T_{12}^{BR13}\sin\lambda\right]\right.$$
$$+ [\underline{G}_2\cdot\underline{B}_2/\Delta\Phi]_2\left[\sqrt{1/2}\cos\lambda + T_{22}^{BR13}\sin\lambda\right] + [\underline{G}_2\cdot\underline{B}_3/\Delta\Phi]_2$$
$$\left.\left[T_{32}^{BR13}\sin\lambda\right]\right] - [C_{II}/\Delta\Phi]_2$$

$$[C_{OS}/\Delta\Phi]_2 = -\frac{2}{g^2 S_1^T}\left[\frac{(\Sigma\delta)_2^{14}}{(\Sigma n_1^T)_2^{G14}}\right] + \frac{2}{g^2}[R/\Delta\Phi]_2 + \frac{\sqrt{2}}{g}\left[-[B_S/\Delta\Phi]_2 + [B_O/\Delta\Phi]_2\right]$$
$$+\frac{2\omega^E}{g^2}\left[[\underline{G}_2\cdot\underline{B}_1/\Delta\Phi]_2\left[\sqrt{1/2}\cos\lambda + T_{12}^{BR14}\sin\lambda\right] + [\underline{G}_2\cdot\underline{B}_2/\Delta\Phi]_2\right.$$
$$\left.\left[T_{22}^{BR14}\sin\lambda\right] + [\underline{G}_2\cdot\underline{B}_3/\Delta\Phi]_2\left[\sqrt{1/2}\cos\lambda + T_{32}^{BR14}\sin\lambda\right]\right]$$
$$+ [C_{SS}/\Delta\Phi]_2$$

GYRO CALIBRATION EQUATIONS (Continued)

Gyro Three

$$[C_{IS}/\Delta\Phi]_3 = \frac{2}{g^2 S_1^T}\left[\frac{(\Sigma\delta)_3^{15}}{(\Sigma n_1^T)_3^{G15}}\right] - \frac{2}{g^2}[R/\Delta\Phi]_3 - \frac{\sqrt{2}}{g}\left[[B_I/\Delta\Phi]_3 + [B_S/\Delta\Phi]_3\right]$$

$$- \frac{2\omega^E}{g^2}\left[[\underline{G}_3 \cdot \underline{B}_1/\Delta\Phi]_3\left[T_{12}^{BR15}\sin\lambda\right] + [\underline{G}_3 \cdot \underline{B}_2/\Delta\Phi]_3\right.$$

$$\left.\left[\sqrt{1/2}\cos\lambda + T_{22}^{BR15}\sin\lambda\right] + [\underline{G}_3 \cdot \underline{B}_3/\Delta\Phi]_3\left[\sqrt{1/2}\cos\lambda + T_{32}^{BR15}\sin\lambda\right]\right]$$

$$- [C_{II}/\Delta\Phi]_3 - [C_{SS}/\Delta\Phi]_3$$

$$[C_{IO}/\Delta\Phi]_3 = \frac{2}{g^2 S_1^T}\left[\frac{(\Sigma\delta)_3^{14}}{(\Sigma n_1^T)_3^{G14}}\right] - \frac{2}{g^2}[R/\Delta\Phi]_3 - \frac{\sqrt{2}}{g}\left[[B_I/\Delta\Phi]_3 + [B_O/\Delta\Phi]_3\right]$$

$$- \frac{2\omega^E}{g^2}\left[[\underline{G}_3 \cdot \underline{B}_1/\Delta\Phi]_3\left[\sqrt{1/2}\cos\lambda + T_{12}^{BR14}\sin\lambda\right] + [\underline{G}_3 \cdot \underline{B}_2/\Delta\Phi]_3\right.$$

$$\left.\left[T_{22}^{BR14}\sin\lambda\right] + [\underline{G}_3 \cdot \underline{B}_3/\Delta\Phi]_3\left[\sqrt{1/2}\cos\lambda + T_{32}^{BR14}\sin\lambda\right]\right] - [C_{II}/\Delta\Phi]_3$$

$$[C_{OS}/\Delta\Phi]_3 = \frac{2}{g^2 S_1^T}\left[\frac{(\Sigma\delta)_3^{13}}{(\Sigma n_1^T)_3^{G13}}\right] - \frac{2}{g^2}[R/\Delta\Phi]_3 - \frac{\sqrt{2}}{g}\left[[B_S/\Delta\Phi]_3 + [B_O/\Delta\Phi]_3\right]$$

$$- \frac{2\omega^E}{g^2}\left[[\underline{G}_3 \cdot \underline{B}_1/\Delta\Phi]_3\left[\sqrt{1/2}\cos\lambda + T_{12}^{BR13}\sin\lambda\right] + [\underline{G}_3 \cdot \underline{B}_2/\Delta\Phi]_3\right.$$

$$\left.\left[\sqrt{1/2}\cos\lambda + T_{22}^{BR13}\sin\lambda\right] + [\underline{G}_3 \cdot \underline{B}_3/\Delta\Phi]_3\left[T_{32}^{BR13}\sin\lambda\right]\right] - [C_{SS}/\Delta\Phi]_3$$

J Term

$$[J]_k = [J/\Delta\Phi]_k [\Delta\Phi]_k$$

Gyro One

$$[J/\Delta\Phi]_1 = \frac{(P_1^G)}{\Delta\omega^T} - [R/\Delta\Phi]_1 \frac{\Delta t}{\Delta\omega^T} - [B_0/\Delta\Phi]_1 \frac{\Delta tg}{\Delta\omega^T}$$

$$- [\underline{G}_1 \cdot \underline{B}_3/\Delta\Phi]_1 \frac{\Delta\phi_2}{\Delta\omega^T}$$

$$- [\underline{G}_1 \cdot \underline{B}_1/\Delta\Phi]_1 \left[\frac{\omega^E \sin\lambda}{\Delta\omega^T}\right] [T_{12}^{BR5} \int \sin\phi_2 dt + T_{13}^{BR5} \int \cos\phi_2 dt]$$

Gyro Two

$$[J/\Delta\Phi]_2 = \frac{P_2^G}{\Delta\omega^T} - [R/\Delta\Phi]_2 \frac{\Delta t}{\Delta\omega^T} - [B_0/\Delta\Phi]_2 \frac{\Delta tg}{\Delta\omega^T}$$

$$- [\underline{G}_2 \cdot \underline{B}_1/\Delta\Phi]_2 \frac{\Delta\phi_2}{\Delta\omega^T}$$

$$- [\underline{G}_2 \cdot \underline{B}_2/\Delta\Phi]_2 \left[\frac{\omega^E \sin\lambda}{\Delta\omega^T}\right] [T_{22}^{BR1} \int \sin\phi_2 dt + T_{23}^{BR1} \int \cos\phi_2 dt]$$

Gyro Three

$$[J/\Delta\Phi]_3 = \frac{P_3^G}{\Delta\omega^T} - [R/\Delta\Phi]_3 \frac{\Delta t}{\Delta\omega^T} - [B_o/\Delta\Phi]_3 \frac{\Delta tg}{\Delta\omega^T}$$

$$- [\underline{G}_3 \cdot \underline{B}_1/\Delta\Phi]_3 \frac{\Delta\phi_2}{\Delta\omega^T}$$

$$- [\underline{G}_3 \cdot \underline{B}_3/\Delta\Phi]_3 \left[\frac{\omega^E \sin\lambda}{\Delta\omega^T}\right] [T_{32}^{BR1} \int \sin\phi_2 dt + T_{33}^{BR1} \int \cos\phi_2 dt]$$

if $\dot{\omega}^T = \text{const} = K$

$\omega_o^T = 0 \quad \left(\phi_2\right)_o = 0$

Then

$$J = \left(\frac{\Delta\Phi}{K}\right)\left(\frac{G}{\Delta t}\right) - \left[\frac{R}{K} + \frac{B_0 g}{K} + \frac{G_k \cdot B_e}{2} \Delta t\right]$$

$$- \frac{\omega^E \sin\lambda}{K\Delta t} \int_0^{\Delta t} \cos\left[\frac{Kt^2}{2} - \tan^{-1}\left(\frac{T_{k2}^{BR}}{T_{k3}^{BR}}\right)\right] dt$$

ACCELEROMETER CALIBRATION EQUATIONS

Scale Factor and Cubic Term

Accelerometer One

$$[D_1(\underline{A}_1 \cdot \underline{B}_1)]_1 + g^2[D_1D_3]_1 = \frac{1}{2gS_1^T}\left[\frac{(\Sigma\gamma)^7_{12}}{(\Sigma n_1^T)^{A7}_{12}} - \frac{(\Sigma\gamma)^7_{11}}{(\Sigma n_1^T)^{A7}_{11}} - \frac{(\Sigma\gamma)^8_{12}}{(\Sigma n_1^T)^{A8}_{12}} + \frac{(\Sigma\gamma)^8_{11}}{(\Sigma n_1^T)^{A8}_{11}}\right]$$

$$[D_1(\underline{A}_1 \cdot \underline{B}_1)]_1 + \frac{g^2}{2}[D_1D_3]_1 = \frac{\sqrt{2}}{gS_1^T}\left[\frac{(\Sigma\gamma)^{13}_{12}}{(\Sigma n_1^T)^{A13}_{12}} - \frac{(\Sigma\gamma)^{13}_{11}}{(\Sigma n_1^T)^{A13}_{11}}\right] - [D_1(\underline{A}_1 \cdot \underline{B}_2)]_1 - \frac{\sqrt{2}}{g}[D_1D_0]_1 - \frac{\sqrt{2}g}{2}[D_1D_2]_1$$

Accelerometer Two

$$[D_1(\underline{A}_2 \cdot \underline{B}_2)]_2 + g^2[D_1D_3]_2 = \frac{1}{2gS_1^T}\left[\frac{(\Sigma\gamma)^9_{22}}{(\Sigma n_1^T)^{A9}_{22}} - \frac{(\Sigma\gamma)^9_{21}}{(\Sigma n_1^T)^{A9}_{21}} - \frac{(\Sigma\gamma)^{10}_{22}}{(\Sigma n_1^T)^{A10}_{22}} + \frac{(\Sigma\gamma)^{10}_{21}}{(\Sigma n_1^T)^{A10}_{21}}\right]$$

$$[D_1(\underline{A}_2 \cdot \underline{B}_2)]_2 + \frac{g^2}{2}[D_1D_3]_2 = \frac{\sqrt{2}}{gS_1^T}\left[\frac{(\Sigma\gamma)^{13}_{22}}{(\Sigma n_1^T)^{A13}_{22}} - \frac{(\Sigma\gamma)^{13}_{21}}{(\Sigma n_1^T)^{A13}_{21}}\right] - [D_1(\underline{A}_2 \cdot \underline{B}_1)]_2 - \frac{\sqrt{2}}{g}[D_1D_0]_2 - \frac{\sqrt{2}g}{2}[D_1D_2]_2$$

Accelerometer Three

$$[D_1(\underline{A}_3 \cdot \underline{B}_3)]_3 + g^2[D_1D_3]_3 = \frac{1}{2gS_1^T}\left[\frac{(\Sigma\gamma)^{11}_{32}}{(\Sigma n_1^T)^{A11}_{32}} - \frac{(\Sigma\gamma)^{11}_{31}}{(\Sigma n_1^T)^{A11}_{31}} - \frac{(\Sigma\gamma)^{12}_{32}}{(\Sigma n_1^T)^{A12}_{32}} + \frac{(\Sigma\gamma)^{12}_{31}}{(\Sigma n_1^T)^{A12}_{31}}\right]$$

$$[D_1(\underline{A}_3 \cdot \underline{B}_3)]_3 + \frac{g^2}{2}[D_1D_3]_3 = \frac{\sqrt{2}}{gS_1^T}\left[\frac{(\Sigma\gamma)^{14}_{32}}{(\Sigma n_1^T)^{A14}_{32}} - \frac{(\Sigma\gamma)^{14}_{31}}{(\Sigma n_1^T)^{A14}_{31}}\right] - [D_1(\underline{A}_3 \cdot \underline{B}_1)]_3 - \frac{\sqrt{2}}{g}[D_1D_0]_3 - \frac{\sqrt{2}g}{2}[D_1D_2]_3$$

Bias and Second Order Term

Accelerometer One

$$[D_1D_0]_1 = \frac{1}{2S_1^T}\left[\frac{(\Sigma\gamma)_{12}^{9}}{(\Sigma n_1^T)_{12}^{A9}} - \frac{(\Sigma\gamma)_{11}^{9}}{(\Sigma n_1^T)_{11}^{A9}} + \frac{(\Sigma\gamma)_{12}^{10}}{(\Sigma n_1^T)_{12}^{A10}} - \frac{(\Sigma\gamma)_{11}^{10}}{(\Sigma n_1^T)_{11}^{A10}}\right]$$

$$= \frac{1}{2S_1^T}\left[\frac{(\Sigma\gamma)_{12}^{11}}{(\Sigma n_1^T)_{12}^{A11}} - \frac{(\Sigma\gamma)_{11}^{11}}{(\Sigma n_1^T)_{11}^{A11}} + \frac{(\Sigma\gamma)_{12}^{12}}{(\Sigma n_1^T)_{12}^{A12}} - \frac{(\Sigma\gamma)_{11}^{12}}{(\Sigma n_1^T)_{11}^{A12}}\right]$$

$$[D_1D_2]_1 + \frac{1}{g^2}[D_1D_0]_1 = \frac{1}{2g^2S_1^T}\left[\frac{(\Sigma\gamma)_{12}^{7}}{(\Sigma n_1^T)_{12}^{A7}} - \frac{(\Sigma\gamma)_{11}^{7}}{(\Sigma n_1^T)_{11}^{A7}} + \frac{(\Sigma\gamma)_{12}^{8}}{(\Sigma n_1^T)_{12}^{A8}} - \frac{(\Sigma\gamma)_{11}^{8}}{(\Sigma n_1^T)_{11}^{A8}}\right]$$

Accelerometer Two

$$[D_1D_0]_2 = \frac{1}{2S_1^T}\left[\frac{(\Sigma\gamma)_{22}^{7}}{(\Sigma n_1^T)_{22}^{A7}} - \frac{(\Sigma\gamma)_{21}^{7}}{(\Sigma n_1^T)_{21}^{A7}} + \frac{(\Sigma\gamma)_{22}^{8}}{(\Sigma n_1^T)_{22}^{A8}} - \frac{(\Sigma\gamma)_{21}^{8}}{(\Sigma n_1^T)_{21}^{A8}}\right]$$

$$= \frac{1}{2S_1^T}\left[\frac{(\Sigma\gamma)_{22}^{11}}{(\Sigma n_1^T)_{22}^{A11}} - \frac{(\Sigma\gamma)_{21}^{11}}{(\Sigma n_1^T)_{21}^{A11}} + \frac{(\Sigma\gamma)_{22}^{12}}{(\Sigma n_1^T)_{22}^{A12}} - \frac{(\Sigma\gamma)_{21}^{12}}{(\Sigma n_1^T)_{21}^{A12}}\right]$$

$$[D_1D_2]_2 + \frac{1}{g^2}[D_1D_0]_2 = \frac{1}{2g^2S_1^T}\left[\frac{(\Sigma\gamma)_{22}^{9}}{(\Sigma n_1^T)_{22}^{A9}} - \frac{(\Sigma\gamma)_{21}^{9}}{(\Sigma n_1^T)_{21}^{A9}} + \frac{(\Sigma\gamma)_{22}^{10}}{(\Sigma n_1^T)_{22}^{A10}} - \frac{(\Sigma\gamma)_{21}^{10}}{(\Sigma n_1^T)_{21}^{A10}}\right]$$

ACCELEROMETER CALIBRATION EQUATIONS (Continued)

Accelerometer Three

$$[D_1D_0]_3 = \frac{1}{2S_1^T}\left[\frac{(\Sigma\gamma)_{32}^{7}}{(\Sigma n_1^T)_{32}^{A7}} - \frac{(\Sigma\gamma)_{31}^{7}}{(\Sigma n_1^T)_{31}^{A7}} + \frac{(\Sigma\gamma)_{32}^{8}}{(\Sigma n_1^T)_{32}^{A8}} - \frac{(\Sigma\gamma)_{31}^{8}}{(\Sigma n_1^T)_{31}^{A8}}\right]$$

$$= \frac{1}{2S_1^T}\left[\frac{(\Sigma\gamma)_{32}^{9}}{(\Sigma n_1^T)_{32}^{A9}} - \frac{(\Sigma\gamma)_{31}^{9}}{(\Sigma n_1^T)_{31}^{A9}} + \frac{(\Sigma\gamma)_{32}^{10}}{(\Sigma n_1^T)_{32}^{A10}} - \frac{(\Sigma\gamma)_{31}^{10}}{(\Sigma n_1^T)_{31}^{A10}}\right]$$

$$[D_1D_2]_3 + \frac{1}{g^2}[D_1D_0]_3 = \frac{1}{2g^2S_1^T}\left[\frac{(\Sigma\gamma)_{32}^{11}}{(\Sigma n_1^T)_{32}^{A11}} - \frac{(\Sigma\gamma)_{31}^{11}}{(\Sigma n_1^T)_{31}^{A11}} + \frac{(\Sigma\gamma)_{32}^{12}}{(\Sigma n_1^T)_{32}^{A12}} - \frac{(\Sigma\gamma)_{31}^{12}}{(\Sigma n_1^T)_{31}^{A12}}\right]$$

Misalignments

Accelerometer One

$$[D_1(\underline{A}_1\cdot\underline{B}_2)]_1 = \frac{1}{2gS_1^T}\left[\frac{(\Sigma\gamma)_{12}^{9}}{(\Sigma n_1^T)_{12}^{A9}} - \frac{(\Sigma\gamma)_{11}^{9}}{(\Sigma n_1^T)_{11}^{A9}} - \frac{(\Sigma\gamma)_{12}^{10}}{(\Sigma n_1^T)_{12}^{A10}} + \frac{(\Sigma\gamma)_{11}^{10}}{(\Sigma n_1^T)_{11}^{A10}}\right]$$

$$[D_1(\underline{A}_1\cdot\underline{B}_3)]_1 = \frac{1}{2gS_1^T}\left[\frac{(\Sigma\gamma)_{12}^{11}}{(\Sigma n_1^T)_{12}^{A11}} - \frac{(\Sigma\gamma)_{11}^{11}}{(\Sigma n_1^T)_{11}^{A11}} - \frac{(\Sigma\gamma)_{12}^{12}}{(\Sigma n_1^T)_{12}^{A12}} + \frac{(\Sigma\gamma)_{11}^{12}}{(\Sigma n_1^T)_{11}^{A12}}\right]$$

Accelerometer Two

$$[D_1(\underline{A}_2\cdot\underline{B}_1)]_2 = \frac{1}{2gS_1^T}\left[\frac{(\Sigma\gamma)_{22}^{7}}{(\Sigma n_1^T)_{22}^{A7}} - \frac{(\Sigma\gamma)_{21}^{7}}{(\Sigma n_1^T)_{21}^{A7}} - \frac{(\Sigma\gamma)_{22}^{8}}{(\Sigma n_1^T)_{22}^{A8}} + \frac{(\Sigma\gamma)_{21}^{8}}{(\Sigma n_1^T)_{21}^{A8}}\right]$$

$$[D_1(\underline{A}_2\cdot\underline{B}_3)]_2 = \frac{1}{2gS_1^T}\left[\frac{(\Sigma\gamma)_{22}^{11}}{(\Sigma n_1^T)_{22}^{A11}} - \frac{(\Sigma\gamma)_{21}^{11}}{(\Sigma n_1^T)_{21}^{A11}} - \frac{(\Sigma\gamma)_{22}^{12}}{(\Sigma n_1^T)_{22}^{A12}} + \frac{(\Sigma\gamma)_{21}^{12}}{(\Sigma n_1^T)_{21}^{A12}}\right]$$

ACCELEROMETER CALIBRATION EQUATIONS (Continued)

Accelerometer Three

$$[D_1(\underline{A}_3 \cdot \underline{B}_1)]_3 = \frac{1}{2gS_1^T}\left[\frac{(\Sigma\gamma)_{32}^{7}}{(\Sigma n_1^T)_{32}^{A7}} - \frac{(\Sigma\gamma)_{31}^{7}}{(\Sigma n_1^T)_{31}^{A7}} - \frac{(\Sigma\gamma)_{32}^{8}}{(\Sigma n_1^T)_{32}^{A8}} + \frac{(\Sigma\gamma)_{31}^{8}}{(\Sigma n_1^T)_{31}^{A8}}\right]$$

$$[D_1(\underline{A}_3 \cdot \underline{B}_2)]_3 = \frac{1}{2gS_1^T}\left[\frac{(\Sigma\gamma)_{32}^{9}}{(\Sigma n_1^T)_{32}^{A9}} - \frac{(\Sigma\gamma)_{31}^{9}}{(\Sigma n_1^T)_{31}^{A9}} - \frac{(\Sigma\gamma)_{32}^{10}}{(\Sigma n_1^T)_{32}^{A10}} + \frac{(\Sigma\gamma)_{31}^{10}}{(\Sigma n_1^T)_{31}^{A10}}\right]$$

where $(\Sigma\delta)_K$ corresponds to the pulse count from the kth gyro over the total time of data collection.

- The vector P_k^A (k = 1, 2, 3) is approximated by the accelerometer readouts, therefore

$$P_k^A \Rightarrow (\Sigma\gamma)_{k2} - (\Sigma\gamma)_{k1}$$

where $(\Sigma\gamma)_{k2}$ and $(\Sigma\gamma)_{k1}$ correspond to the pulse counts from the second and first string of the kth accelerometer, respectively.

- The total time of data collecting will be recorded as a count (Σn_1^T) from the system clock, therefore

$$\Delta t \Rightarrow S_1^T(\Sigma n_1^T)$$

where S_1^T is the scale factor of the system clock. The subscript 1 serves to distinguish the clock pulse train used in calibration from the pulse train used in the Preprocessing computations.

- The total test table angle $(\Delta\phi_2)$ will be recorded as a number of whole turns (or a number of fractions of whole turns), therefore

$$\Delta\phi_2 \Rightarrow S^\phi(\Sigma n^\phi)$$

where (Σn^ϕ) is the number of increments of angular displacement, and S^ϕ is the scale factor which converts the number of increments to a finite angle.

In Section 3.3 we presented a description of the laboratory facility with all of its measurement and computational devices. In Figure 3-6 we showed the possible equipment interfaces. For the purpose of calibration all instrument data collections will be accomplished with the frequency counters shown in Figure 3-6. (See Section 2.1 of the trade-off document for the reason why the counters are used.) The specific employment of the counters for all positions is described in the Laboratory Procedures Manual in the sections entitled Fundamental Modes. Also found in the Fundamental Modes sections are all events in the collections, transfers, and computations during calibration in the form of flow diagrams accompanied by descriptions of the activities

4.4 PRECALIBRATION REQUIREMENTS

The required constants contained within the equations tabulated in Section 4.3 were presented as functions of instrument outputs and parameters describing the environment inputs. Before the data can be collected which is necessary as inputs into the equations, several initial survey tasks must be accomplished.

- The environment selections were presented in Section 4.2 as choices of the ϕ_1 and ϕ_2 gimbal angles and the first column of the T^{BR} matrix. The test table orientation is, however, controlled by choices of four gimbal angles; therefore, the choices of the first column of T^{BR} must be expressed in terms of the gimbal angles, which we know from Section 3 to be ϕ_3 and ϕ_4.
- The T^{BR} matrix is a function of the T^{BI} matrix as well as the ϕ_3 and ϕ_4 gimbal angles. We must, therefore, determine T^{BI} before we can equate the first column of T^{BR} to ϕ_3 and ϕ_4.
- The gyro bias and compliance constants are seen (see Section 4.3.2) to be a function of (among other things) the second column of the T^{BR} matrix. That column can be determined (once T^{BI}, ϕ_3, and ϕ_4 are known) by a use of equalities presented in Section 3.
- In all previous developments it was assumed that T^{FE} (the transformation between the test table base frame and the earth frame) was equal to the identity matrix. In the operational laboratory this matrix will deviate (by small numbers) from the identity matrix. It is, however, possible to correct for the deviation by the use of bubble levels.

In the following subsections we present the manner in which all of the above tasks are accomplished. The order of presentation is the chronological order in which these tasks should be accomplished in the laboratory.

4.4.1 T^{BI} Survey

The initial activity subsequent to the attachment of the ISU to the test table is the determination of the orientation of the ISU body axes relative to the test table frames. This corresponds to the evaluation of the T^{BI} matrix (see Section 3.2.1). In Chart 4-32 we see how this is accomplished.

In Chart 4-32 we refer to the test table orientation used in the determination of T^{BI} as Position Zero. Position Zero can be any orientation, but the zero orientation shown in Figure 3-2 might be the most convenient for it results in

$$(T^{IO}\, T^{OR}\, T^{RT}\, T^{TF}\, T^{FE})^{-1} = I \text{ (the identity matrix)}$$

(The matrix product $T^{BS}\, T^{SE} = T^{BE}$ is functionally equal to the Mirror Alignment Matrix shown in Chart 2-6. As mentioned in the discussion of the Mirror Alignment Matrix is Section 3.1.2 the particular evaluation of this matrix depends upon the particular geometric angles which are outputted from the autocollimators. At the time that the form of those outputs are known, the exact form of $T^{BS}\, T^{SE}$ can easily be determined.)

The T^{BI} Survey activity is formalized as a "Precalibration" activity in the Laboratory Procedures Manual. It will most probably be accomplished very near the time that the ISU is placed on the test table. It will probably not be necessary to repeat this survey except when the ISU is removed from the table and then "rebolted" in another orientation.

T^{BI} Determination

Given. a set of resolver readings ϕ_1^0, ϕ_2^0, ϕ_3^0, and ϕ_4^0 from position zero and the transformation from body to earth axes via autocollimator readings ($T^{BS0}\ T^{SE0}$)

Find: the matrix T^{BI} which transforms from the body axes to the axes fixed to the inner gimbal of the test table.

1. From the laboratory geometry definitions described in Section 3 we have:

$$T^{BI} = \left(T^{BS0}{}_T{}^{SE0}\right)\left(T^{IO0}{}_T{}^{OR0}{}_T{}^{RT0}{}_T{}^{TF0}{}_T{}^{FE}\right)^{-1}$$

where $T^{BS0}{}_T{}^{SE0}$ is given by the autocollimators and

$$T^{IO0} = \begin{bmatrix} 0 & 1 & 0 \\ \cos\phi_4^0 & 0 & -\sin\phi_4^0 \\ -\sin\phi_4^0 & 0 & -\cos\phi_4^0 \end{bmatrix}$$

$$T^{OR0} = \begin{bmatrix} 0 & 1 & 0 \\ \cos\phi_3^0 & 0 & -\sin\phi_3^0 \\ -\sin\phi_3^0 & 0 & -\cos\phi_3^0 \end{bmatrix}$$

$$T^{RT0} = \begin{bmatrix} 0 & 1 & 0 \\ \cos\phi_2^0 & 0 & -\sin\phi_2^0 \\ -\sin\phi_2^0 & 0 & -\cos\phi_2^0 \end{bmatrix}$$

$$T^{TF0} = \begin{bmatrix} 0 & 1 & 0 \\ \cos\phi_1^0 & 0 & -\sin\phi_1^0 \\ -\sin\phi_1^0 & 0 & -\cos\phi_1^0 \end{bmatrix}$$

$$T^{FE} = \begin{bmatrix} 1 & 0 & 0 \\ 0 & 1 & 0 \\ 0 & 0 & 1 \end{bmatrix}$$

4.4.2 Test Table Resolver Settings

The calibration selections in Section 4.2 were accomplished by dictating values for ϕ_1, ϕ_2 and the first column of the T^{BR} matrix. In implementing those selections it is necessary to equate the T^{BR} choices to the controllable ϕ_3 and ϕ_4 gimbal angles. In Chart 4-33 we see the functional relationship between the first column of T^{BR} and ϕ_3 and ϕ_4 (and T^{BI} which is known from the procedures developed in Section 4.4.1).

In Chart 4-34 we present the ϕ_1, ϕ_2, ϕ_3, and ϕ_4 settings for all fifteen calibration positions. Included in that chart are the equations for the determination of ϕ_3 and ϕ_4 from the choices of the first column of T^{BR}. Those equations are special cases of the arithmetic contained in Chart 4-33 for Positions 1, 3, 5, 13, 14, and 15. A duplicate of Chart 4-34 is presented in the Laboratory Procedures Manual. The numerical solutions for ϕ_3 and ϕ_4 must be accomplished and placed in the chart before calibration can be accomplished.

4.4.3 T^{BRm} Determination

The gyro bias and compliance computations presented in Section 4.3 are functions of (among other things) the second column of the T^{BR} matrix for Positions 1, 3, 5, 13, 14, and 15. The T^{BR} matrix is a function of ϕ_3 and ϕ_4 (see Section 3.2). The gimbal angles ϕ_3 and ϕ_4 are known by the use of the computations presented in Chart 4-33. In Chart 4-35 we present the computations which develop the required second column of T^{BR} from the known ϕ_3 and ϕ_4 angles (and T^{BI} as given by the computations presented in Chart 4-32).

Although not required for calibration purposes, the computations of the third column of the T^{BR} matrix are presented for information purposes in Chart 4-35 The first column of T^{BR} is known because it was utilized as the environment selection control parameter.

4.4.4 Bubble Level Corrections

Throughout the development of the calibration techniques it was assumed that the test table base frame is aligned with the earth axes, that is:

$$T^{FE} = I \text{ (the identity matrix).}$$

In practice this matrix will deviate from identity, due to such things as solar heating of the building and settling of the building. The resultant low frequency motion of the base relative to the earth can be corrected (immediately before calibration data collection) by the use of buble levels. There are three ways in which the corrections can be implemented.

ϕ_3^m ϕ_4^m Equations

Given. T^{BI}, T_{11}^{BRm}, T_{21}^{BRm}, T_{31}^{BRm}

Find: ϕ_3^m and ϕ_4^m

1. We know that

$$T^{BRm} = T^{BI}\, T^{IOm}\, T^{ORm}$$

$$\text{or } (T^{BI})^T T^{BRm} = T^{IOm}\, T^{ORm}$$

where T^{BI} is given from a prior survey and

$$T^{IOm}{}_T{}^{ORm} = \begin{bmatrix} \cos\phi_3^m & 0 & -\sin\phi_3^m \\ \sin\phi_3^m \sin\phi_4^m & \cos\phi_4^m & \cos\phi_3^m \sin\phi_4^m \\ \sin\phi_3^m \cos\phi_4^m & -\sin\phi_4^m & \cos\phi_3^m \cos\phi_4^m \end{bmatrix}$$

2. Solving for the first column of $T^{IOm}{}_T{}^{ORm}$ we have

$$\cos\phi_3^m = T_{11}^{BI}\, T_{11}^{BRm} + T_{21}^{BI}\, T_{21}^{BRm} + T_{31}^{BI}\, T_{31}^{BRm}$$

$$\sin\phi_3^m \sin\phi_4^m = T_{12}^{BI}\, T_{11}^{BRm} + T_{22}^{BI}\, T_{21}^{BRm} + T_{32}^{BI}\, T_{31}^{BRm}$$

$$\sin\phi_3^m \cos\phi_4^m = T_{13}^{BI}\, T_{11}^{BRm} + T_{23}^{BI}\, T_{21}^{BRm} + T_{33}^{BI}\, T_{31}^{BRm}$$

which gives the desired functional relationships.

TEST TABLE RESOLVER SETTINGS

	Position 1	Position 2	Position 3	Position 4	Position 5	Position 6
ϕ_1	90°	90°	90°	90°	90°	90°
ϕ_2	Rotating	Rotating	Rotating	Rotating	Rotating	Rotating
ϕ_3	From $\cos\phi_3^1 = T_{11}^{BI}$ $\sin\phi_3^1 \sin\phi_4^1 = T_{12}^{BI}$ $\sin\phi_3^1 \cos\phi_4^1 = T_{13}^{BI}$	$\phi_3^1 + 180°$	From $\cos\phi_3^3 = T_{21}^{BI}$ $\sin\phi_3^3 \sin\phi_4^3 = T_{22}^{BI}$ $\sin\phi_3^3 \cos\phi_4^3 = T_{23}^{BI}$	$\phi_3^3 + 180°$	From $\cos\phi_3^5 = T_{31}^{BI}$ $\sin\phi_3^5 \sin\phi_4^5 = T_{32}^{BI}$ $\sin\phi_3^5 \cos\phi_4^5 = T_{33}^{BI}$	$\phi_3^5 + 180°$
ϕ_4		ϕ_4^1		ϕ_4^3		ϕ_4^5

	Position 7	Position 8	Position 9	Position 10	Position 11	Position 12
ϕ_1	0°	0°	0°	0°	0°	0°
ϕ_2	90°	90°	90°	90°	90°	90°
ϕ_3	ϕ_3^1	ϕ_3^2	ϕ_3^3	ϕ_3^4	ϕ_3^5	ϕ_3^6
ϕ_4	ϕ_4^1	ϕ_4^2	ϕ_4^3	ϕ_4^4	ϕ_4^5	ϕ_4^6

	Position 13	Position 14	Position 15
ϕ_1	0°	0°	0°
ϕ_2	90°	90°	90°
ϕ_3	From $\cos\phi_3^{13} = \sqrt{1/2}\left[T_{11}^{BI} + T_{21}^{BI}\right]$ $\sin\phi_3^{13} \sin\phi_4^{13} = \sqrt{1/2}\left[T_{12}^{BI} + T_{22}^{BI}\right]$ $\sin\phi_3^{13} \cos\phi_4^{13} = \sqrt{1/2}\left[T_{13}^{BI} + T_{23}^{BI}\right]$	From $\cos\phi_3^{14} = \sqrt{1/2}\left[T_{11}^{BI} + T_{31}^{BI}\right]$ $\sin\phi_3^{14} \sin\phi_4^{14} = \sqrt{1/2}\left[T_{12}^{BI} + T_{32}^{BI}\right]$ $\sin\phi_3^{14} \cos\phi_4^{14} = \sqrt{1/2}\left[T_{13}^{BI} + T_{33}^{BI}\right]$	From $\cos\phi_3^{15} = \sqrt{1/2}\left[T_{21}^{BI} + T_{31}^{BI}\right]$ $\sin\phi_3^{15} \sin\phi_4^{15} = \sqrt{1/2}\left[T_{22}^{BI} + T_{32}^{BI}\right]$ $\sin\phi_3^{15} \cos\phi_4^{15} = \sqrt{1/2}\left[T_{23}^{BI} + T_{33}^{BI}\right]$
ϕ_4			

T^{BRm} Determination

Given: ϕ_3^m, ϕ_4^m, and T^{BI}

Find: T^{BRm}

1. We know that

$$T^{BRm} = T^{BI}{}_T{}^{IOm}{}_T{}^{ORm}$$

where T^{BI} is given from a prior survey and

$$T^{IOm}{}_T{}^{ORm} = \begin{bmatrix} \cos\phi_3^m & 0 & -\sin\phi_3^m \\ \sin\phi_3^m \sin\phi_4^m & \cos\phi_4^m & \cos\phi_3^m \sin\phi_4^m \\ \sin\phi_3^m \cos\phi_4^m & -\sin\phi_4^m & \cos\phi_3^m \cos\phi_4^m \end{bmatrix}$$

2. The first column of T^{BRm} is the calibration control parameter. The values of this column have already been included in the calibration equations.

3. The second column of T^{BRm} which is the only column required for inclusion into the calibration equations, is:

$$T_{12}^{BRm} = T_{12}^{BI} \cos\phi_4^m - T_{13}^{BI} \sin\phi_4^m$$

$$T_{22}^{BRm} = T_{22}^{BI} \cos\phi_4^m - T_{23}^{BI} \sin\phi_4^m$$

$$T_{32}^{BRm} = T_{32}^{BI} \cos\phi_4^m - T_{33}^{BI} \sin\phi_4^m$$

These equations need only be solved for m = 1, 3, 5, 13, 14, and 15.

4. The third column of T^{BRm}, which is <u>not</u> required in the calibration equations, is given for information:

$$T_{13}^{BRm} = -T_{11}^{BI} \sin\phi_3^m + T_{12}^{BI} \cos\phi_3^m \sin\phi_4^m + T_{13}^{BI} \cos\phi_3^m \cos\phi_4^m$$

$$T_{23}^{BRm} = -T_{21}^{BI} \sin\phi_3^m + T_{22}^{BI} \cos\phi_3^m \sin\phi_4^m + T_{23}^{BI} \cos\phi_3^m \cos\phi_4^m$$

$$T_{33}^{BRm} = -T_{31}^{BI} \sin\phi_3^m + T_{32}^{BI} \cos\phi_3^m \sin\phi_4^m + T_{33}^{BI} \cos\phi_3^m \cos\phi_4^m$$

- The first and most obvious way is to incorporate "leveling screws" on the base of the table.
- Another technique is to store the T^{BI} matrix in the computer as other than an identity matrix, and to input the bubble level readings taken before data collection.
- The third technique is to place two of the table gimbal angles in the direction of the two bubble level degrees of freedom, and correct for the lean of the table by small corrections to the gimbals.

We choose the third technique because it is the easiest to implement.

The bubble level corrections for the rotating ISU in Positions 1 through 6 need only be imposed on the trunnion axis (i.e. ϕ_1). As a matter of fact, if the motion of the table base is less than, say, 20 seconds no correction is required. This is because the principal input to the gyros in Positions 1 through 6 is the table speed, which is unaffected by the motion of the base. In Positions 7 through 15, however, the principal input to the instruments is $\underline{g}$; therefore the level corrections are essential. This is why, in every position after the sixth, we placed the outer axis in the north-south direction. Assuming that the two bubble levels are in the east-west and north-south directions, level corrections can be imposed on the ϕ_1 and ϕ_3 gimbals.

4.5 IMPLEMENTATION OF CALIBRATION TECHNIQUES

In this subsection we begin the formulation of all of the aforementioned topics into a formalized laboratory calibration procedure. In formulating these procedures we will introduce several housekeeping operations which have not been previously mentioned.

The discussions in this subsection are directed toward a presentation of the chronology of events which occur during the calibration. We will not go into great detail, the detailed presentation being left as the task of the Laboratory Procedures Manual. This subsection should be considered as the interface between this Development Document and the Laboratory Procedures Manual.

The calibration procedures are divided into four separate activities.

- Turn-on
- Precalibration
- Calibration
- Computation.

Whether accomplishing a complete or partial calibration, the above four activities occur in the order presented. In the following paragraphs we will briefly describe each activity:

Turn-On

These activities include all of the various housekeeping tasks which include such things as:

- Power-on to equipment
- Monitor equipment operation.

The detailed specifications of these activities cannot be tabulated until the laboratory facility is completely defined. In the Laboratory Procedures Manual a space has been allocated in Part I for inclusion of the details of turn-on to be specified at the time when the laboratory is configured.

Precalibration

At some time, between the placement of the ISU on the test table and the initiation of calibration , the following system survey activities must be accomplished:

- Determine T^{BI}
- Find ϕ_3 and ϕ_4 for all calibration positions
- Find the second column of the T^{BR} matrix for all calibration positions
- Store g, ω^E, λ, S^T, and $S.^{\phi}$

The first activity locates the ISU relative to the test table. The second activity determines the inner and outer test table gimbal angles settings for all calibration positions. These settings were shown in Section 4.4.2 to be a function of the T^{BI} matrix. The third precalibration activity computes the second column of the T^{BR} matrix, which was shown in Section 4.3.2 to be necessary for computing the gyro bias and compliance terms. The fourth activity records system numbers required in the calibration equations. All of these activities are described in detail in Part I of the Laboratory Procedures Manual.

Calibration

At any time subsequent to the completion of the Turn-on and Precalibration activities, the ISU can be calibrated. We formally define the calibration activities as the completion of the following list of activities for any or all positions:

- Connect instruments to frequency counters
- Set frequency counters
- Set test table resolvers with bubble level corrections
- Set table speed
- Collect data
- Transfer data to computer.

A complete calibration would accomplish the above activities for all positions The order of positions is completely arbitrary; but the packages of six (1 to 6 and 7 to 12) will probably be accomplished in numerical order. A partial calibration need only accomplish these tasks for positions required for the determination of the required constants. The details of the above activities are found in Part II of the Laboratory Procedures Manual.

Computation

Computation is very simply the solution of any or all of the equations in Section 4.3.2. A complete calibration requires all computations and a partial calibration would require the solution of only a few of the equations in Section 4.3.2. The details of the computation procedures are described in Section II-4 of the Laboratory Procedures Manual.

SECTION 5
DEVELOPMENT OF ALIGNMENT TECHNIQUES

In Section 2 alignment was defined as the initialization of the matrix which transforms from an ISU-fixed set of axes to a navigational set of axes. The ISU axes were defined by use of two mirror normals and the navigation axes were defined as an earth-fixed, local-level frame. Transformation of this alignment problem to any other alignment problem using different ISU and navigational frames is then a simple problem of coordinate transformation. The discussion in Section 2 revealed that alignment could be accomplished by measurement, in body and/or earth-frame, of the components of two system vectors. Three different choices of these vectors lead to the three alignment techniques: Mirror Alignment, Level Alignment, and Gyrocompass.

Further analyses in Sections 2 and 3 lead to the functional description of the three alignment techniques shown in Chart 5-1. In this description each technique is further broken down into four basic types of computational routines. These are:

- Preprocessing Computations
- Estimation Routine
- Estimation Matrix Computations
- Alignment Matrix Computations.

These routines have as inputs certain a priori information, calibration constants, instrument outputs, and/or outputs from other routines as indicated in Chart 5-1.

Before beginning the detailed development of alignment it is important to note several points which dictate the viewpoint adopted in the remainder of this section. First note that there are basically three types of routines indicated in Chart 5-1. They are Preprocessing, Estimation (including both Estimation Routine and Estimation Matrix Computations), and Alignment Matrix routines. The mathematics of the Preprocessing Routine was developed in subsection 2.2.5 and will be considered only briefly here (in Section 5.1). The Alignment Matrix routine uses estimated values of $\underline{g}\cdot\underline{B}_k$ and mirror azimuth (Level Alignment) or $\underline{g}\cdot\underline{B}_k$ and $\underline{\omega}^E\cdot\underline{B}_k$ (Gyrocompass) to initialize the alignment matrix T. This relatively straightforward mathematical problem has been discussed in Section 2 and is considered again rather briefly in Section 5.5. The remaining routine, Estimation, is the major subject of discussion in this section. Before developing various estimation techniques, the

CHART 5-1

ALIGNMENT FUNCTIONAL DIAGRAMS

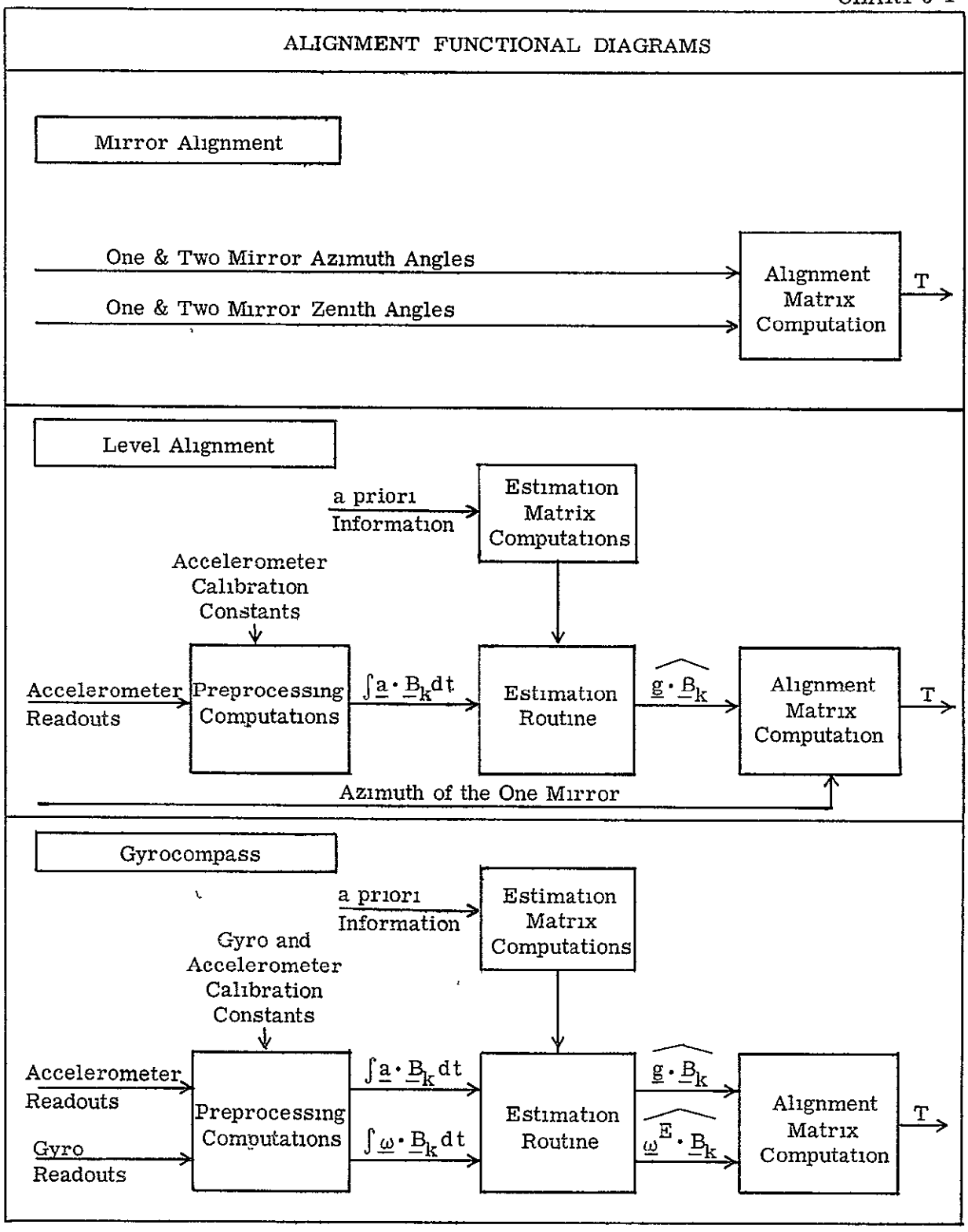

environment and sensor noises are modelled in Section 5.2. Then in Section 5.3 and 5.4 specific estimation techniques are developed under different assumptions. The explicit equations for the recommended alignment techniques are summarized in Section 5.6.

Second, it should be noted that there is no detailed discussion of Mirror Alignment since this section emphasizes estimation which is not relevant to the mirror alignment problem. The Alignment Matrix Calculation discussion of Section 5.5 is, of course, applicable to the mirror approach when mirror azimuth and zenith angles are given.

Third, the reader should be forewarned of the emphasis on Level Alignment over Gyrocompass in this section. It was found, not unexpectedly, that the alignment errors in Gyrocompass may easily be two orders of magnitude larger than those expected in Level Alignment. This is, of course, mainly due to the low signal-to-noise ratio of the earth-rate signal in gyro quantization noise. Further details of this comparison of Level Alignment versus Gyrocompass are given in Section 5 of the trade-off document (Volume 2) where a Monte Carlo simulation of an alignment problem is used to obtain quantitative results.

Finally note that Section 5 of the trade-off document justifies many of the comments included below. Section 5 of Volume 2 includes further discussion of the assumptions required and the results of a simulation of the proposed estimation techniques. It is important to note that in several places important assumptions have been made with little justification when the data was not available to include completely realistic values. The collection of accurate data about the noise environment is a very difficult and expensive problem. However, all results of this study have been presented in such a manner that when more accurate data is available, modifications can easily be made.

5.1 PREPROCESSING COMPUTATIONS

The Preprocessing Computations yield integrals of angular velocity and acceleration in the body frame.

$$\int_t^{t+\Delta t} \underline{\omega}\cdot\underline{B}_j\,dt \qquad \int_t^{t+\Delta t} \underline{a}\cdot\underline{B}_j\,dt\,, \qquad j = 1, 2, 3.$$

The inputs to the computations are the counter outputs $(\Sigma\gamma)_{k2}$, $(\Sigma\gamma)_{k1}$, $(\Sigma\delta)_k$, and (Σn_2^T), $k = 1,2,3$. The calibration constants for each sensor are required, along with the transformations from the sensor axes to body axes Q^A, Q^G. The notation is defined in Section 2. The preprocessing equations are developed in subsection 2.2.5. They are reproduced in Chart 5-2. In this chart, dots at the left hand margin indicate the alternative computations used for Level Alignment or for Gyrocompass. Note that Δt was assumed to be small in the development of the equations in Section 2.2.5. This restriction is not required in the Preprocessing Computations used in alignment since the ISU is relatively stationary.

5.2 ENVIRONMENT AND SENSOR NOISE MODELS

Before developing processing techniques, we must describe the effect on sensor outputs of various random inputs: environment translational acceleration and rotation, accelerometer noise, and gyro noise. This section is a continuation of Section 3.2.2 which describes the general characteristics of the environment noise. In the development of estimation techniques, quantization errors are not included. Several of the resulting techniques are tested with a Monte Carlo simulation to determine the effect of quantization, computer word length, and anomalous noise inputs. The results are presented in Section 5 of the trade-off document. In the following paragraphs, we first describe the environmental components of the sensor inputs (5.2.1) and subsequently describe their effects on the observed sensor outputs (5.2.2).

5.2.1 Sensor Input Acceleration and Angular Velocity

It is convenient to define a "level frame" that moves with the ISU and whose average orientation is collinear with the earth axes, as indicated in Figure 5-1. The body axes are fixed relative to the level axes. If there were no environment disturbance, the level frame would coincide with the earth frame.

Let a_{Lk} be the acceleration of the level frame along $\underline{L}_k$. Then

$$\underline{a}_L = \begin{bmatrix} a_{L1} \\ a_{L2} \\ a_{L3} \end{bmatrix} = \begin{bmatrix} g\underline{U}\cdot\underline{L}_1 + \alpha_1 \\ g\underline{U}\cdot\underline{L}_2 + \alpha_2 \\ g\underline{U}\cdot\underline{L}_3 + \alpha_3 \end{bmatrix}$$

PREPROCESSING COMPUTATIONS

Inputs $(\Sigma\gamma)_{k2}, (\Sigma\gamma)_{k1}, (\Sigma\delta)_k$, and $\left(\Sigma n_2^T\right)$ for k = 1, 2, 3

The outputs $\int_t^{t+\Delta t} (\underline{\omega}\cdot\underline{B}_k)dt$ and $\int_t^{t+\Delta t} (\underline{a}\cdot\underline{B}_k)dt$ (k = 1, 2, 3) are given by the following computations

Level GC

- $P_k^A \equiv [(\Sigma\gamma)_{k2} - (\Sigma\gamma)_{k1}]$
- $P_k^G \equiv (\Sigma\delta)_k$
- $\Delta t \equiv S_2^T\left(\Sigma n_2^T\right)$
- $\overline{(\underline{\omega}\cdot\underline{G}_k)\Delta t} \equiv P_k^G(\Delta\Phi)_k - (R)_k\Delta t$
- $\overline{(\underline{a}\cdot\underline{A}_k)\Delta t} \equiv P_k^A/(D_1)_k - (D_O)_k\Delta t$
- $\overline{(\underline{\omega}\cdot\underline{G}_k)} \equiv \overline{(\underline{\omega}\cdot\underline{G}_k)\Delta t}/\Delta t$
- $\overline{(\underline{a}\cdot\underline{A}_k)} \equiv \overline{(\underline{a}\cdot\underline{A}_k)\Delta t}/\Delta t$
- $\overline{(\underline{a}\cdot\underline{G}_k)} \equiv \overline{(\underline{a}\cdot\underline{A}_k)}$
- $\overline{(\underline{a}\cdot\underline{O}_k)} = \begin{bmatrix}0&0&1\\1&0&0\\1&0&0\end{bmatrix}\begin{bmatrix}\overline{(\underline{a}\cdot\underline{A}_1)}\\\overline{(\underline{a}\cdot\underline{A}_2)}\\\overline{(\underline{a}\cdot\underline{A}_3)}\end{bmatrix}$
- $\overline{(\underline{a}\cdot\underline{S}_k)} = \begin{bmatrix}0&-1&0\\0&0&-1\\0&1&0\end{bmatrix}\begin{bmatrix}\overline{(\underline{a}\cdot\underline{A}_1)}\\\overline{(\underline{a}\cdot\underline{A}_2)}\\\overline{(\underline{a}\cdot\underline{A}_3)}\end{bmatrix}$
- $\int_t^{t+\Delta t}(\underline{\omega}\cdot\underline{G}_k)dt = [\overline{(\underline{\omega}\cdot\underline{G}_k)\Delta t} - [(B_I)_k\overline{(\underline{a}\cdot\underline{G}_k)} + (B_O)_k\overline{(\underline{a}\cdot\underline{O}_k)} + (B_S)_k\overline{(\underline{a}\cdot\underline{S}_k)}]\Delta t$
  $- [(C_{II})_k\overline{(\underline{a}\cdot\underline{G}_k)}^2 + (C_{SS})_k\overline{(\underline{a}\cdot\underline{S}_k)}^2]\Delta t$
  $- [(C_{IS})_k\overline{(\underline{a}\cdot\underline{G}_k)}\overline{(\underline{a}\cdot\underline{S}_k)} + (C_{OS})_k\overline{(\underline{a}\cdot\underline{O}_k)}\overline{(\underline{a}\cdot\underline{S}_k)} + (C_{IO})_k\overline{(\underline{a}\cdot\underline{G}_k)}\overline{(\underline{a}\cdot\underline{O}_k)}]\Delta t$
  $- [(Q_{II})_k\overline{(\underline{\omega}\cdot\underline{G}_k)}^2 + (Q_{IS})_k\overline{(\underline{\omega}\cdot\underline{G}_k)}\overline{(\underline{\omega}\cdot\underline{S}_k)}]\Delta t$
- $\int_t^{t+\Delta t}(\underline{a}\cdot\underline{A}_k)dt = [\overline{(\underline{a}\cdot\underline{A}_k)\Delta t} - (D_2)_k\overline{(\underline{a}\cdot\underline{A}_k)}^2\Delta t - (D_3)_k\overline{(\underline{a}\cdot\underline{A}_k)}^3\Delta t$
- $\int_t^{t+\Delta t}(\underline{\omega}\cdot\underline{B}_k)dt = \sum_\ell Q^G_{k\ell}\int_t^{t+\Delta t}(\underline{\omega}\cdot\underline{G}_\ell)dt$
- $\int_t^{t+\Delta t}(\underline{a}\cdot\underline{B}_k)dt = \sum_\ell Q^A_{k\ell}\int_t^{t+\Delta t}(\underline{a}\cdot\underline{A}_\ell)dt$

where

- $Q^G = \begin{bmatrix}1 & -(\underline{G}_1\cdot\underline{B}_2) & -(\underline{G}_1\cdot\underline{B}_3)\\ -(\underline{G}_2\cdot\underline{B}_1) & 1 & -(\underline{G}_2\cdot\underline{B}_3)\\ -(\underline{G}_3\cdot\underline{B}_1) & -(\underline{G}_3\cdot\underline{B}_2) & 1\end{bmatrix}$
- $Q^A = \begin{bmatrix}1 & -(\underline{A}_1\cdot\underline{B}_2) & -(\underline{A}_1\cdot\underline{B}_3)\\ -(\underline{A}_2\cdot\underline{B}_1) & 1 & -(\underline{A}_2\cdot\underline{B}_3)\\ -(\underline{A}_3\cdot\underline{B}_1) & -(\underline{A}_3\cdot\underline{B}_2) & 1\end{bmatrix}$

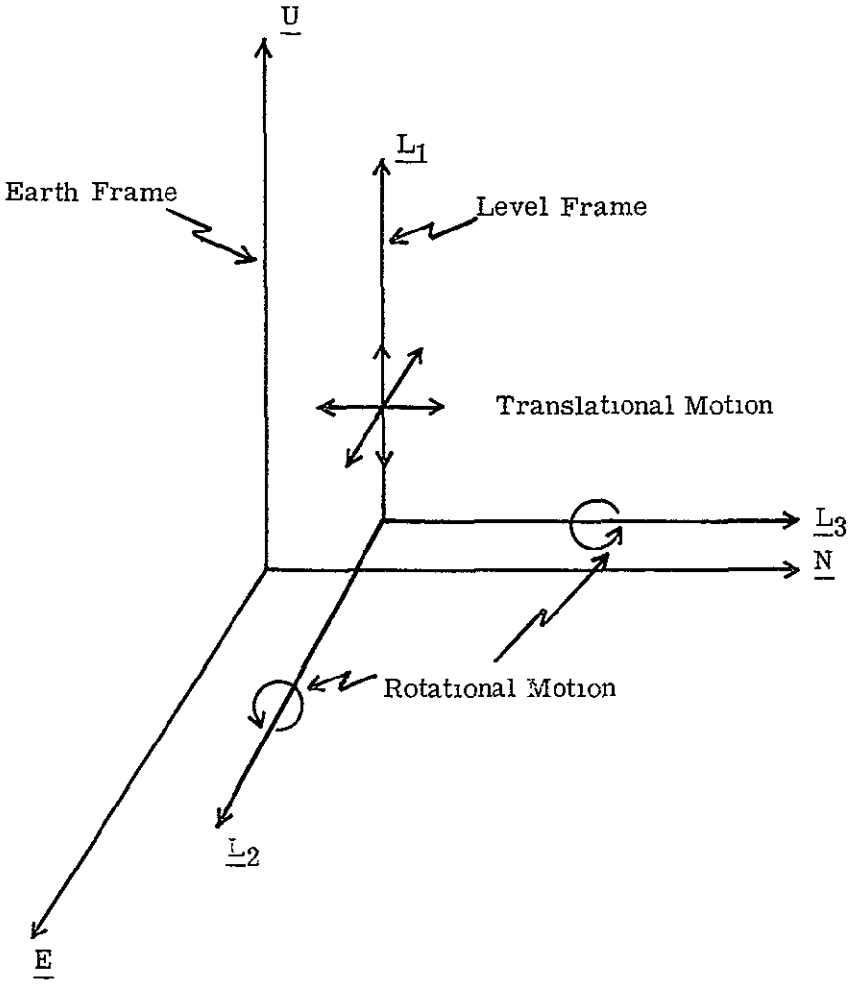

Figure 5-1. Level Frame

where α_1, α_2, α_3 are the environment-induced accelerations along $\underline{L}_1$, $\underline{L}_2$, $\underline{L}_3$. The expected value of α_j is zero. To first order, $\underline{L}_1 \cdot \underline{U} = 1$ since the rotation from vertical is the order of one minute of arc or less. Further, $\underline{U} \cdot \underline{L}_2$ and $\underline{U} \cdot \underline{L}_3$ can be represented as small rotations about $\underline{L}_3$ and $\underline{L}_2$, respectively. Let $\theta_3 = -\underline{U} \cdot \underline{L}_2$ and $\theta_2 = \underline{U} \cdot \underline{L}_3$. Then, to first order,

$$\underline{a}_L = \begin{bmatrix} g & + \alpha_1 \\ -g\theta_3 & + \alpha_2 \\ g\theta_2 & + \alpha_3 \end{bmatrix}$$

Further, the angles θ_2 and θ_3 have zero expectations. Let T_1 be the orthogonal transformation from the level frame to the body frame. Then the acceleration in the body frame $\underline{a}_B$ is

$$\underline{a}_B = T_1 \underline{a}_L = T_1 \begin{bmatrix} g \\ 0 \\ 0 \end{bmatrix} + T_1 \begin{bmatrix} 0 \\ -g\theta_3 \\ g\theta_2 \end{bmatrix} + T_1 \begin{bmatrix} \alpha_1 \\ \alpha_2 \\ \alpha_3 \end{bmatrix}$$

The first term is the average gravitational acceleration in the body frame. The second term is the variation of the acceleration due to level frame rotation. The last term is the environmental acceleration disturbance. The power spectra of α_1, α_2, α_3, θ_2, θ_3 can be obtained from environmental test measurements.

Next, consider the angular velocity. Let ω_{Lk} be the angular velocity of the level frame about $\underline{L}_k$. Then

$$\underline{\omega}_L = \begin{bmatrix} \omega_{L1} \\ \omega_{L2} \\ \omega_{L3} \end{bmatrix} = \begin{bmatrix} \omega_U^E \underline{U} \cdot \underline{L}_1 + \omega_N^E \underline{N} \cdot \underline{L}_1 + \beta_1 \\ \omega_U^E \underline{U} \cdot \underline{L}_2 + \omega_N^E \underline{N} \cdot \underline{L}_2 + \beta_2 \\ \omega_U^E \underline{U} \cdot \underline{L}_3 + \omega_N^E \underline{N} \cdot \underline{L}_3 + \beta_3 \end{bmatrix}$$

where $\omega_U^E \underline{U} + \omega_N^E \underline{N}$ is the angular velocity of the earth and β_k is the environment-induced angular velocity about $\underline{L}_k$. To first order, $\underline{U} \cdot \underline{L}_1 = \underline{N} \cdot \underline{L}_3 = 1$. Further assume that there is no rotation about $\underline{U}$ and hence $\beta_1 = 0$ and $\underline{N} \cdot \underline{L}_2 = 0$. Also, $\beta_2 = \dot{\theta}_2$, $\beta_3 = \dot{\theta}_3$, and $\underline{N} \cdot \underline{L}_1 = \theta_2$. Hence,

$$\underline{\omega}_L = \begin{bmatrix} \omega_U^E & - & \omega_N^E\theta_2 \\ -\omega_U^E\theta_3 & & + \dot{\theta}_2 \\ \omega_U^E\theta_2 & + & \omega_N^E + \dot{\theta}_3 \end{bmatrix}$$

$$\underline{\omega}_B = T_1 \begin{bmatrix} \omega_U^E \\ 0 \\ \omega_N^E \end{bmatrix} + T_1 \begin{bmatrix} -\omega_N^E\theta_2 \\ -\omega_U^E\theta_3 \\ \omega_U^E\theta_2 \end{bmatrix} + T_1 \begin{bmatrix} 0 \\ \dot{\theta}_2 \\ \dot{\theta}_3 \end{bmatrix}$$

where $\underline{\omega}_B$ is the angular velocity in the body frame. These three terms have interpretations analogous to the corresponding terms in $\underline{a}_B$.

Since the system has been calibrated, the transformation from body axes to sensor input axes is known. Let T_2 transform $\underline{a}_B$ to the accelerometer input axes; let T_3 transform $\underline{\omega}_B$ to the gyro input axes. Let

$$\underline{a}_A = T_2\underline{a}_B$$

and

$$\underline{\omega}_G = T_3\underline{\omega}_B$$

These vectors represent the sensor inputs.

There are two alternatives in estimating gravity and angular velocity. First, we can estimate the average components in the body frame:

$$T_1 \begin{bmatrix} g \\ 0 \\ 0 \end{bmatrix} \quad \text{and} \quad T_1 \begin{bmatrix} \omega_U^E \\ 0 \\ \omega_N^E \end{bmatrix} \tag{5-1}$$

Second, we can estimate the components at some time t^* in the future, $t^* > K\Delta t$:

$$T_1 \begin{bmatrix} g \\ 0 \\ 0 \end{bmatrix} + T_1 \begin{bmatrix} 0 \\ -g\theta_3(t^*) \\ g\theta_2(t^*) \end{bmatrix} \tag{5-2}$$

$$T_1\begin{bmatrix}\omega_U^E\\0\\\omega_N^E\end{bmatrix} + T_1\begin{bmatrix}-\omega_N^E\theta_2(t^*)\\-\omega_U^E\theta_3(t^*)\\\omega_U^E\theta_2(t^*)\end{bmatrix} \tag{5-3}$$

Where the strapdown system is initiated $t^* - K\Delta t$ seconds after the last measurement. Let $t^* - K\Delta t = \epsilon_t$, the prediction interval.

5.2.2 Observed Sensor Output

In the development of a processing method, we will assume that the gyros and accelerometers are linear with unit scale factors and zero bias. Actual values will be used in the application to a real alignment problem. Further, we assume that the gyros and accelerometers have relatively large band widths, i.e., we will neglect the sensor dynamics. The preprocessed sensor outputs are integrals of acceleration and angular velocity. Namely, the outputs are:

$$\underline{P}^A(t) = \int_{t-\Delta t}^{t} \underline{a}_A(\tau)\,d\tau + \int_{t-\Delta t}^{t} \underline{n}_A(\tau)\,d\tau$$

$$\underline{P}^G(t) = \int_{t-\Delta t}^{t} \underline{\omega}_G(\tau)d\tau + \int_{t-\Delta t}^{t} \underline{n}_G(\tau)\,d\tau$$

where $\underline{n}_A(\tau)$ and $\underline{n}_G(\tau)$ represent noises introduced by the sensors. Further the outputs are observed at discrete times Δt, $2\Delta t$, ---, $K\Delta t$. Denote these outputs by $\underline{P}^A(j)$ and $\underline{P}^G(j)$. It is convenient to transform the outputs $\underline{P}^A(j)$ and $\underline{P}^G(j)$ to the body frame: namely

$$\underline{P}_B^A(j) = T_2^{-1}\underline{P}^A(j) = \int_{(j-1)\Delta t}^{j\Delta t}\left\{T_1\begin{bmatrix}g\\0\\0\end{bmatrix} + T_1\begin{bmatrix}0\\g\theta_3(\tau)\\g\theta_2(\tau)\end{bmatrix}\right\}d\tau$$

$$+ \int_{(j-1)\Delta t}^{j\Delta t}\left\{T_1\begin{bmatrix}\alpha_1(\tau)\\\alpha_2(\tau)\\\alpha_3(\tau)\end{bmatrix} + T_2^{-1}\begin{bmatrix}n_{A1}(\tau)\\n_{A2}(\tau)\\n_{A3}(\tau)\end{bmatrix}\right\}d\tau \tag{5-4}$$

$$\underline{P}_B^G(j) = T_3^{-1}\underline{P}^G(j) = \int_{(j-1)\Delta t}^{j\Delta t} \left\{ T_1 \begin{bmatrix} \omega_U^E \\ 0 \\ \omega_N^E \end{bmatrix} + T_1 \begin{bmatrix} -\omega_N^E & \theta_2(\tau) \\ -\omega_U^E & \theta_3(\tau) \\ \omega_U^E & \theta_2(\tau) \end{bmatrix} \right\} d\tau$$

$$+ T_1 \int_{(j-1)\Delta t}^{j\Delta t} \begin{bmatrix} 0 \\ \dot{\theta}_2(\tau) \\ \dot{\theta}_3(\tau) \end{bmatrix} d\tau + \int_{(j-1)\Delta t}^{j\Delta t} T_3^{-1} \begin{bmatrix} n_{G1}(\tau) \\ n_{G2}(\tau) \\ n_{G3}(\tau) \end{bmatrix} d\tau \qquad (5\text{-}5)$$

Since T_1 is orthogonal, and since T_2 and T_3 are nearly orthogonal, $T_1\underline{\alpha}(\tau) + T_2^{-1}\underline{n}_A(\tau)$ and $T_3^{-1}\underline{n}_G(\tau)$ have the same power spectrum as $\underline{\alpha}(\tau) + \underline{n}_A(\tau)$ and $\underline{n}_G(\tau)$, respectively. This simplification will be used in equations (5-4) and (5-5) since only second order statistics are used in the following discussion.

Note that the components of $\underline{\alpha}(\tau)$, $\underline{n}_A(\tau)$, and $\underline{n}_G(\tau)$ have been assumed statistically independent and identically distributed.

In the following sections, estimation techniques are developed based on the above models.

5.3 ESTIMATION OF GRAVITY IN LEVEL ALIGNMENT

Estimations of the components of gravitational acceleration in the body frame are based on the observation equation

$$\underline{P}_B^A(j) = \int_{(j-1)\Delta t}^{j\Delta t} \left\{ T_1 \begin{bmatrix} g \\ 0 \\ 0 \end{bmatrix} + T_1 \begin{bmatrix} 0 \\ -g\,\theta_3(\tau) \\ g\,\theta_2(\tau) \end{bmatrix} + \underline{\alpha}(\tau) + \underline{n}_A(\tau) \right\} d\tau \qquad (5\text{-}6)$$

with $j=1,\ldots,K$. Using the observed accelerometer outputs in the body frame, $\underline{P}_B^A(j)$ $(j=1,\ldots,K)$, our goal is to estimate the average components (5-1) or instantaneous components (5-2) in the presence of the disturbances $\underline{\alpha}(t)$ and $\underline{n}_A(t)$ given in (5-6). The former problem is described in the following Section (5.3.1); the latter problem is discussed in (5.3.2). Note that the basic operation is differentiation; we obtain acceleration from velocity measurements.

In the following subsections several estimation methods are developed from mathematical statistics. A general discussion of Level Alignment techniques appears in 5.3.3; and the recommended technique is presented in 5.6. The characteristics of several techniques are described in Section 5 of the trade-off document. These techniques are simple average, posterior-mean estimate of average components, posterior-mean estimate of instantaneous components, and iterative estimate of instantaneous components.

5.3.1 Estimation of Average Components

The objective here is to estimate the average gravitational acceleration components in the body frame namely:

$$\bar{\underline{g}}_B = T_1 \begin{bmatrix} g \\ 0 \\ 0 \end{bmatrix}$$

Let $\underline{g}_B(t^*)$ denote the true gravitational components at time t^*. Then the rms deviation of the estimated average components (say $\hat{\underline{g}}_B$) from the true components can be bounded, namely:

$$E[(\underline{g}_B(t^*)-\hat{\underline{g}}_B)^T(\underline{g}_B(t^*)-\hat{\underline{g}}_B)] = E[(\underline{g}_B(t^*)-\bar{\underline{g}}_B)^T(\underline{g}_B(t^*)-\bar{\underline{g}}_B)] + E[(\bar{\underline{g}}_B-\hat{\underline{g}}_B)^T(\bar{\underline{g}}_B-\hat{\underline{g}}_B)]$$

$$+ 2E[(\underline{g}_B(t^*)-\bar{\underline{g}}_B)^T(\bar{\underline{g}}_B - \hat{\underline{g}}_B)] \leq \left\{\left[E[(\underline{g}_B(t^*)-\bar{\underline{g}}_B)^T(\underline{g}_B(t^*)-\bar{\underline{g}}_B)]\right]^{1/2}\right.$$

$$\left. + \left[E[(\bar{\underline{g}}_B-\hat{\underline{g}}_B)^T(\bar{\underline{g}}_B-\hat{\underline{g}}_B)]\right]^{1/2}\right\}^2$$

The first term corresponds to the rotational motion of the level frame about the average. The second term corresponds to the error in $\hat{\underline{g}}_B$ as an estimate of $\bar{\underline{g}}_B$. The objective is to minimize the second term, accepting the first term (the error from the motion about its mean).

In the following subsections three approaches to estimation are considered: simple average, least squares, posterior mean. The first approach does not use any a priori information about the noise spectra, alignment, gravity or earth rate magnitudes. The second approach uses prior measurements of the noise spectra. On the other hand, it does not include the prior geophysical measurements of gravity and earth angular velocity. The third approach uses a priori information about alignment, gravity magnitude, and earth rate magnitude plus measurements of the noise spectra, but the noises are assumed to be gaussian processes. This third approach has several advantages: (i) prior geophysical measurements are included and are weighted with their accuracy; (ii) the estimation techniques are comparable to those obtained from a least squares approach in complexity; (iii) the resulting techniques can be used recursively to continuously update the alignment matrix; (iv) the posterior-mean estimate is optimum with respect to a large class of loss functions, not

just quadratic. From noise simulation, we find that the posterior-mean techniques are not sensitive to the gaussian assumption. (See Section 5 of the trade-off document.)

5.3.1.1 Simple Average

This approach is based on the assumption that we do not have any prior information about the noise, gravity, earth rate, or alignment. In this case

$$\hat{\underline{g}}_B = \frac{1}{K\Delta t} \sum_{j=1}^{K} \underline{P}_B^A(j)$$

Note that the same estimate is obtained if K=1, and Δt is replaced by $K\Delta t$.

5.3.1.2 Least Squares

Before developing a least-squares technique, it is convenient to define certain notations. Let $\underline{X}$ be the 3K vector whose components are

$$X_j = P_{B1}^A(j); \qquad X_{j+K} = P_{B2}^A(j), \qquad X_{j+2K} = P_{B3}^A(j)$$

with $j = 1, \ldots, K$. Let H_1 be the 3Kx3 matrix

$$H_1 = \begin{bmatrix} \Delta t & 0 & 0 \\ \vdots & \vdots & \vdots \\ \Delta t & 0 & 0 \\ 0 & \Delta t & 0 \\ \vdots & \vdots & \vdots \\ 0 & \Delta t & 0 \\ 0 & 0 & \Delta t \\ \vdots & \vdots & \vdots \\ 0 & 0 & \Delta t \end{bmatrix} \begin{matrix} \left.\vphantom{\begin{matrix}a\\b\\c\end{matrix}}\right\} \text{K-rows} \\ \left.\vphantom{\begin{matrix}a\\b\\c\end{matrix}}\right\} \text{K-rows} \\ \left.\vphantom{\begin{matrix}a\\b\\c\end{matrix}}\right\} \text{K-rows} \end{matrix}$$

Let $\phi_{r(j)} = \int_{(j-1)\Delta t}^{j\Delta t} \theta_r(\tau)\, d\tau$, with $r = 2,3$.

Let Φ be a 3K vector with components

$$\Phi_J = + g(T_1)_{13}\, \phi_2(J) - g(T_1)_{12}\, \phi_3(J)$$

$$\Phi_{J+K} = + g(T_1)_{23}\, \phi_2(J) - g(T_1)_{22}\, \phi_3(J) \qquad (5\text{-}7)$$

$$\Phi_{J+2K} = + g(T_1)_{33}\, \phi_2(J) - g(T_1)_{32}\, \phi_3(J) \qquad J = 1,2,\ldots,K.$$

Let $\underline{\phi}_2^T = (\phi_2(1),\ldots,\phi_2(K))$ and $\underline{\phi}_3^T = (\phi_3(1),\ldots,\phi_3(K))$. Then $\Phi = H_2 \begin{bmatrix} \underline{\phi}_2 \\ \underline{\phi}_3 \end{bmatrix}$

where H_2 is the 3Kx2K matrix defined by equation 5-7. Let $\underline{N}$ be a 3K vector with components

$$N_J = \int_{(J-1)\Delta t}^{J\Delta t} [\alpha_1(\tau) + n_{A1}(\tau)]\, d\tau$$

$$N_{J+K} = \int_{(J-1)\Delta t}^{J\Delta t} [\alpha_2(\tau) + n_{A2}(\tau)]\, d\tau$$

$$N_{J+2K} = \int_{(J-1)\Delta t}^{J\Delta t} [\alpha_3(\tau) + n_{A3}(\tau)]\, d\tau$$

with $J = 1, \ldots, K$. Then the basic observation equation 5-6 can be rewritten as

$$\underline{X} = H_1\, \underline{\bar{g}}_B + \underline{\Phi} + \underline{N} \qquad (5\text{-}8)$$

The objective is to estimate $\underline{\bar{g}}_B$ in the presence of noise $\underline{\Phi} + \underline{N}$, given the observations X. The covariance of this composite noise is the sum of the covariances of $\underline{\Phi}$ and $\underline{N}$ since they are independent:

$$\Sigma_{\Phi + N} = \Sigma_\Phi + \Sigma_N$$

Further

$$\Sigma_{\Phi} = H_2 \begin{pmatrix} \Sigma_{\phi\phi} & 0 \\ 0 & \Sigma_{\phi\phi} \end{pmatrix} H_2^T$$

where $\Sigma_{\phi\phi}$ is a K x K matrix with elements

$$(\Sigma_{\phi\phi})_{ij} = E[\phi_2(i)\, \phi_2(j)], \qquad i, j = 1, \ldots, K.$$

Note that θ_2 and θ_3 are assumed to be independent and identically distributed. Further,

$$\Sigma_N = \begin{bmatrix} \Sigma_{\alpha+n} & 0 & 0 \\ 0 & \Sigma_{\alpha+n} & 0 \\ 0 & 0 & \Sigma_{\alpha+n} \end{bmatrix}$$

where $\Sigma_{\alpha+n}$ is a K x K matrix with elements

$$(\Sigma_{\alpha+n})_{ij} = E[N_i N_j], \qquad i, j = 1, \ldots, K.$$

These covariance matrices can be expressed in terms of the correlation functions, namely

$$E[\phi_2(i)\, \phi_2(j)] = \int_0^{\Delta t} [\Delta t - \mu]\, \phi_\theta(\mu + (j-i)\Delta t)\, d\mu + \int_{-\Delta t}^{0} [\Delta t + \mu]\, \phi_\theta(\mu + (j-1)\Delta t)\, d\mu$$

$$E[N_i N_j] = \int_0^{\Delta t} [\Delta t - \mu]\, \phi_\alpha(\mu + (j-i)\Delta t)\, d\mu + \int_{-\Delta t}^{0} [\Delta t + \mu]\, \phi_\alpha(\mu + (j-1)\Delta t)\, d\mu$$

$$+ \int_0^{\Delta t} [\Delta t - \mu]\, \phi_n(\mu + (j-i)\Delta t)\, d\mu + \int_{-\Delta t}^{0} [\Delta t - \mu]\, \phi_n(\mu + (j-i)\Delta t)\, d\mu$$

where ϕ_θ, ϕ_α, and ϕ_n are the correlation functions of $\theta(\tau)$, $\alpha(\tau)$, $n(\tau)$, e.g., $\phi_\theta = E(\theta(0)\theta(\tau))$. From prior experiments we estimate the noise power spectra and correlation functions.* The above integrals may be evaluated numerically or mathematically when the correlation function is approximated by a mathematical formula. For example, assume

$$\phi_\theta(\tau) = c_1 e^{-c_2|\tau|}$$

Then

$$(\Sigma_{\phi\phi})_{ij} = \frac{2c_1 e^{-c_2 |j-i| \Delta t}}{c_2} [\cosh (c_2 \Delta t) - 1], \quad i \neq j$$

$$(\Sigma_{\phi\phi})_{ii} = \frac{2c_1}{(c_2)^2} [e^{-c_2 \Delta t} - 1 + c_2 \Delta t]$$

The same methods can be applied to the other covariance matrices.

Note that H_2 is evaluated by using prior estimates for the value of T_1 and g, denoted by $\tilde{T}_1$ and $\tilde{g}$. Precise values are not needed since H_2 is used in the noise model. Corrections to H_2 would be of second order.

Based on the composite measurement equation (5-8), the objective is to find the unbiased linear estimate of $\underline{\bar{g}}_B$, say $\underline{\hat{g}}_B(\underline{X})$, which minimizes $E|\underline{\bar{g}}_B - \underline{g}(\underline{X})|^2$ as a function of $\underline{g}(\underline{X})$. It follows from the Gauss-Markoff theorem that $\underline{\hat{g}}_B(\underline{X})$ is the value of g that minimizes $|M\underline{X} - M H_1 \underline{g}|^2$, where M is the nonsingular matrix such that $M\Sigma_{\Phi+N}M^T = I$.**

---

*Spectra data is given by H. Weinstock in "Limitations on Inertial Sensor Testing Produced by Test Platform Vibrations", NASA Electronics Research Center, Cambridge, NASA TN D-3683, 1966.

**See H. Scheffe', Analysis of Variance, John Wieley, 1959, p. 14.

In fact $\hat{\underline{g}}_B(\underline{X})$ is a minimum variance estimate for each component of $\bar{\underline{g}}_B$. One can show that

$$\hat{\underline{g}}_B(\underline{X}) = (H_1^T \Sigma_{\Phi+N}^{-1} H_1)^{-1} H_1^T \Sigma_{\Phi+N}^{-1} \underline{X} \tag{5-9}$$

Further the expected value of $\hat{\underline{g}}_B(\underline{X})$ is $\bar{\underline{g}}_B$, even if we have used an incorrect covariance matrix $\Sigma_{\Phi+N}$. The covariance matrix of $\hat{\underline{g}}_B$ is

$$E[(\hat{\underline{g}}_B - \bar{\underline{g}}_B)(\hat{\underline{g}}_B - \bar{\underline{g}}_B)^T] = (H_1^T \Sigma_{\Phi+N}^{-1} H_1)^{-1} \tag{5-10}$$

5.3.1.3 Posterior Mean

In the following discussion we assume that $\theta_j(\tau)$, $\underline{\alpha}(\tau)$, $\underline{n}_A(\tau)$ are gaussian processes. Hence the "optimum" estimate of $\bar{\underline{g}}_B$ is the posterior mean. This estimate is optimum with respect to any loss function $L(\epsilon)$ on each component where*

(i) $L(0) = 0$

(ii) $L(\epsilon_2) \geq L(\epsilon_1) \geq 0$ when $\epsilon_2 \geq \epsilon_1 \geq 0$

(iii) $L(\epsilon) = L(-\epsilon)$.

For example, let $\hat{\underline{g}}_B$ be an estimate of $\bar{\underline{g}}_B$. Then

$$E\left|\bar{g}_{B1} - \hat{g}_{B1}\right|^2$$

and

$$E\left|\bar{g}_{B2} - \hat{g}_{B2}\right|^2$$

and

$$E\left|\bar{g}_{B3} - \hat{g}_{B3}\right|^2$$

*See S. Sherman "Nonmean -Square Error Criteria" IRE TRANS. ON INFORMATION THEORY, Vol. IT-4, No. 3, p. 125.

are all minimized when $\hat{\underline{g}}_B$ is the posterior mean. As a second example, let ϵ_1, ϵ_2, ϵ_3 represent the maximum admissible errors in components of gravity. Let

$$L_j(\epsilon) = \begin{cases} 0, & |\epsilon| \leq \epsilon_j \\ 1, & |\epsilon| > \epsilon_j \end{cases}$$

Then

$$E[L_1(\bar{g}_{B1}-\hat{g}_{B1})] = P_r\left\{\left|\bar{g}_{B1}-\hat{g}_{B1}\right| > \epsilon_1\right\}$$

and

$$E[L_2(\bar{g}_{B2}-\hat{g}_{B2})] = P_r\left\{\left|\bar{g}_{B2}-\hat{g}_{B2}\right| > \epsilon_2\right\}$$

and

$$E[L_3(\bar{g}_{B3}-\hat{g}_{B3})] = P_r\left\{\left|\bar{g}_{B3}-\hat{g}_{B3}\right| > \epsilon_3\right\}$$

are all minimized when $\hat{\underline{g}}_B$ is the posterior mean. (The expression "Pr {-}" denotes "probability that {-}".)

To evaluate the posterior mean, we first determine the conditional distribution of X, given $\bar{\underline{g}}_B$. In this subsection the notation is the same as that in 5.3.1.2. From equation (5-8), it follows that $\underline{X}$ is normally distributed with mean $H_1\bar{\underline{g}}_B$ and covariance $\Sigma_{\Phi+N}$.

From prior observations we have an estimate of orientation of the ISU; and hence we have an estimate of T_1, say $\tilde{T}_1$. Also we have an estimate of the magnitude of $\bar{\underline{g}}_B$, say $\tilde{g}$. With these estimates, a prior distribution can be defined for $\bar{\underline{g}}_B$, namely, gaussian with mean

$$\tilde{\underline{g}}_B = \tilde{T}_1 \begin{bmatrix} \tilde{g} \\ 0 \\ 0 \end{bmatrix}$$

and covariance

$$\Sigma_{\tilde{g}} = \tilde{T}_1 \begin{bmatrix} \sigma_g^2 & 0 & 0 \\ 0 & \tilde{g}^2\sigma_\theta^2 & 0 \\ 0 & 0 & \tilde{g}^2\sigma_\theta^2 \end{bmatrix} \tilde{T}_1^T$$

where σ_g is the rms error in the estimate of $\left|\bar{\underline{g}}_B\right|$; and σ_θ is the rms error in the estimate of vertical (expressed in radians).

This prior distribution implies that the distribution of $\underline{\bar{g}}_B$ is isotropic in a horizontal plane.

Applying Bayes formula we find that the posterior distribution of $\underline{\bar{g}}_B$, given $\underline{X}$, is gaussian with mean

$$\underline{\hat{g}}_B(\underline{X}) = (H_1^T \Sigma_{\Phi+N}^{-1} H_1 + \Sigma_{\tilde{g}}^{-1})^{-1} (H_1^T \Sigma_{\Phi+N}^{-1} \underline{X} + \Sigma_{\tilde{g}}^{-1} \underline{\tilde{g}}_B) \tag{5-11}$$

and covariance matrix

$$\Sigma_{\hat{g}} = (H_1^T \Sigma_{\Phi+N}^{-1} H_1 + \Sigma_{\tilde{g}}^{-1})^{-1} \tag{5-12}$$

The estimate $\hat{g}_B(\underline{X})$ represents the optimum combination of the measurements $\underline{X}$ and prior data weighted by their respective errors. Note that the covariance is

$$E[(\underline{\bar{g}}_B - \underline{\hat{g}}_B(\underline{X}))(\underline{\bar{g}}_B - \underline{\hat{g}}_B(\underline{X}))^T] = (H_1^T \Sigma_{\Phi+N}^{-1} H_1 + \Sigma_{\tilde{g}}^{-1})^{-1}$$

If our prior alignment information is poor, the posterior-mean estimate reduces to the least-square estimate. Specifically, as $\sigma_g \to \infty$ and $\sigma_\theta \to \infty$, then $\Sigma_{\tilde{g}}^{-1} \to 0$ and expression (5-11) approaches expression (5-9). Also the covariance (5-12) approaches (5-10).

The estimate (5-11) and covariance (5-12) are the basis for an iterative alignment technique. Specifically, the initial $\underline{\hat{g}}_B^{(1)}$, $\Sigma_{\hat{g}}^{(1)}$ are obtained from K measurements based on $\underline{\tilde{g}}_B$ and $\Sigma_{\tilde{g}}$. The second estimate $\underline{g}_B^{(2)}$ and covariance $\Sigma_{\hat{g}}^{(2)}$ are obtained from a second set of K measurements based on $\underline{\hat{g}}_B^{(1)}$ and $\Sigma_{\hat{g}}^{(1)}$; etc. This iterative technique is sub-optimal since we are summarizing all of the prior measurements in terms of $\underline{\hat{g}}_B^{(j)}$ and $\Sigma_{\hat{g}}^{(j)}$. A true recursive "least-squares" technique involves significantly more computation since successive measurements are correlated.* Also, all back measurements are used in the current computation. The intermeasurement correlation can be eliminated by augmenting the measurement variable.** This approach also results in a very complex estimation procedure. From a practical viewpoint, the sub-optimal technique described above is a reasonable compromise.

---

*P. Gainer, "A Method For Computing the Effect of an Additional Observation on a Previous Least-Squares Estimate", NASA Langley Research Center, NASA TN D-1599, 1963.

**See M. Aoki, "Optimization of Stochastic Systems", Academic Press, 1967, p. 38ff.

5.3.2 Estimation of Instantaneous Components

In the previous subsection we developed several techniques of estimating the average components of acceleration

$$T_1 \begin{bmatrix} g \\ 0 \\ 0 \end{bmatrix}$$

In this subsection the objective is to estimate the instantaneous components at time $t^* > K\Delta t$; i.e.,

$$T_1 \begin{bmatrix} g \\ 0 \\ 0 \end{bmatrix} + T_1 \begin{bmatrix} 0 \\ -g\theta_3(t^*) \\ g\theta_2(t^*) \end{bmatrix}$$

In the following discussion we assume that the stochastic inputs $\theta_j(\tau)$, $\underline{\alpha}(\tau)$, $\underline{n}_A(\tau)$ are gaussian processes. The discussion in Section 5.3.1.3 applies here; the posterior mean will be used to estimate instantaneous components. If our prior alignment data is poor, the posterior-mean estimate reduces to the least-squares estimate.

The vectors $\underline{X}$, $\underline{N}$, $\underline{\phi}_1$ $\underline{\phi}_2$, and $\underline{\bar{g}}_B$, are defined in Section 5.3.1. Let $\underline{S}^*$ denote the instantaneous components i.e.,

$$\underline{S}^* = T_1 \begin{bmatrix} g \\ 0 \\ 0 \end{bmatrix} + T_1 \begin{bmatrix} 0 \\ -g\theta_3(t^*) \\ g\theta_2(t^*) \end{bmatrix}$$

To obtain the conditional distribution of $\underline{S}^*$ given $\underline{X}$, we first obtain the joint distribution of $(\underline{S}^*, \underline{X})$. The components of $(\underline{S}^*, \underline{X})$ can be expressed in terms of fundamental random variables as follows:

$$\begin{aligned}
S_j^* &= \bar{g}_{Bj} + (T_1)_{j3} g\theta_2^* - (T_1)_{j2} g\theta_3^* \quad , \quad j = 1, 2, 3 \\
X_1 &= \bar{g}_{B1}\Delta t + (T_1)_{13} g\phi_2(i) - (T_1)_{12} g\phi_3(i) + N_i \\
X_{1+K} &= \bar{g}_{B2}\Delta t + (T_1)_{23} g\phi_2(i) - (T_1)_{22} g\phi_3(i) + N_{i+K} \\
X_{i+2K} &= \bar{g}_{B3}\Delta t + (T_1)_{33} g\phi_2(i) - (T_1)_{32} g\phi_3(i) + N_{i+2K} \quad , \quad i = 1, 2, 3, \cdots K
\end{aligned}$$

or in matrix form as follows:

$$\begin{pmatrix} \underline{S}^* \\ \underline{X} \end{pmatrix} = V\underline{Z}$$

where $\underline{Z}^T$ is the vector

$$\underline{Z}^T = [\bar{g}_{B1}, \bar{g}_{B2}, \bar{g}_{B3}, N_1, \cdots, N_{3K}, \theta_2^*, \phi_2(1), \cdots, \phi_2(K), \theta_3^*, \phi_3(1), \cdots, \phi_3(K)]$$

and where V is the corresponding matrix. Note that V can be evaluated using prior estimates $\tilde{g}$ and $\tilde{T}_1$, since they only enter as multipliers of $\underline{\phi}_2$ and $\underline{\phi}_3$. A prior distribution of $\underline{\bar{g}}_B$ is based on prior alignment data – namely, gaussian with mean

$$\underline{\tilde{g}}_B = \tilde{T}_1 \begin{bmatrix} \tilde{g} \\ 0 \\ 0 \end{bmatrix}$$

and covariance

$$\Sigma_{\tilde{g}} = \tilde{T}_1 \begin{bmatrix} \sigma_g^2 & 0 & 0 \\ 0 & \tilde{g}^2\sigma_\theta^2 & 0 \\ 0 & 0 & \tilde{g}^2\sigma_\theta^2 \end{bmatrix} \tilde{T}_1^T$$

a similar prior distribution was used in Section 5.3.1.3. The variate $\underline{Z}$ is gaussian with mean

$$\underline{\tilde{Z}}^T = [\tilde{g}_{B1}, \tilde{g}_{B2}, \tilde{g}_{B3}, 0, \cdots, 0]$$

and covariance

$$\Sigma_Z = \begin{array}{c|c|c|c|c|c|c} \Sigma_{\tilde{g}} & & & & & & 3 \\ \hline & \Sigma_N & & & & & 3K \\ \hline & & c_0 & c_1 \cdots c_K & & & 1 \\ \hline & & \begin{matrix} c_1 \\ \vdots \\ c_K \end{matrix} & \Sigma_{\phi\phi} & & & K \\ \hline & & & & c_0 & c_1 \cdots c_K & 1 \\ \hline & & & & \begin{matrix} c_1 \\ \vdots \\ c_K \end{matrix} & \Sigma_{\phi\phi} & K \\ \hline 3 & 3K & 1 & K & 1 & K & \end{array}$$

where

$$c_0 = E[(\theta_2^*)^2]$$

$$c_j = E[\theta_2^* \phi_2(j)] = \int_0^{\Delta t} \varphi_\theta(\tau - (K+1-j)\Delta t - \epsilon_t)\, d\tau$$

with $t^* = K\Delta t + \epsilon_t$.

If ϕ_θ is approximated by $b_1 e^{-b_2|\tau|}$, then

$$c_0 = b_1$$

$$c_j = \frac{b_1}{b_2} e^{b_2[(j-1)\Delta t - t^*]}[e^{b_2\Delta t} - 1]$$

Hence, $\begin{pmatrix} \underline{S}^* \\ \underline{X} \end{pmatrix}$ is a gaussian variate with mean $V\underline{\bar{Z}}$ and covariance $V\Sigma_Z V^T$. The conditional distribution of $\underline{S}^*$ given $\underline{X}$ is gaussian.† To evaluate the conditional mean and covariance, we must partition the mean and covariance matrix as follows:

---

† See T.W. Anderson, "An Introduction to Multivariate Statistical Analysis", John Wiley, 1958, p. 27ff.

$$V\underline{\bar{Z}} = \begin{bmatrix} a_1 \\ a_2 \end{bmatrix} \quad \text{and} \quad (V\Sigma_Z V^T)^{-1} = \begin{bmatrix} A & B \\ B^T & C \end{bmatrix}$$

where a_1 is 3x1 and A is 3x3. The conditional mean is

$$\hat{\underline{g}}_B^* = -A^{-1}B\underline{X} + \underline{a}_1 + A^{-1}B\underline{a}_2 \tag{5-13}$$

The conditional covariance is A^{-1}. Note that

$$E[(\underline{S}^* - \hat{\underline{g}}_B)(\underline{S}^* - \hat{\underline{g}}_B)^T] = A^{-1}$$

The discussion of iterative techniques in subsection 5.3.1.3 applies here. The estimate (5-13) can be used in such an iterative technique.

5.3.3 Discussion

Several level alignment estimation techniques were suggested in this section. A Monte Carlo simulation was performed to select the best estimation technique. The simulation is discussed in Section 5 of the trade-off report. Three techniques were considered: simple average (5.3.1.1), posterior mean (5.3.1.3), and instantaneous estimation (5.3.2.1). Several values of K, Δt, and T^{EB} were tried. The effect of nongaussian noise was also investigated. The instantaneous estimate is superior to the other estimates, in some cases the rms alignment error being one-half the alignment error obtained with the simple average. The instantaneous estimate is selected as the recommended technique. The simple average is selected as an alternate technique, since it is computationally less complex.

The simulation was also used to investigate the characteristics of the recommended estimation techniques. The results of the simulation suggest the following conclusions for level alignment:

- The instantaneous estimate is probably not sensitive to the noise distribution (gaussian or nongaussian).
- Rotational motion from the environment is most probably the dominant source of error for long integration intervals ($\Delta t > 15$ sec).
- The instantaneous estimate is more accurate than the simple average for $\Delta t \geq 30$ sec.

- Instantaneous estimation and simple average appear to have comparable accuracy for $\Delta t < 15$ sec.
- If Δt is held fixed at about 30 seconds and the quantization increased, the instantaneous estimate becomes less accurate than the simple average.
- Low frequency environment noise is not the dominant source of error for short integration intervals ($\Delta t < 15$ sec).

The above points are a summary of the detailed analysis of the simulation results included in Section 5 of the trade-off document (Volume 2).

5.4 ESTIMATION OF GRAVITY AND EARTH RATE IN GYROCOMPASS

Estimation of the components of gravity and earth rate is based on the observational equations (5-4) and (5-5). Using the observed sensor outputs $\underline{P}_B^A(j)$ and $\underline{P}_B^G(j)$, $j = 1, \cdots, K$, we estimate the average components (5-1) or the instantaneous components (5-2) and (5-3). The average estimate is investigated in the following section, 5.4.1; the instantaneous estimate is discussed in 5.4.2. The basic estimation problem in Gyrocompass Alignment is very similar to estimation in Level Alignment. Note that the basic operation is differentiation. We obtain acceleration from velocity measurements and angular velocity from angle measurements.

In the following subsections several estimation methods are developed from a mathematical statistics viewpoint. A general discussion of Gyrocompass Alignment techniques appears in 5.4.3, and the recommended technique is presented in 5.6. The characteristics of two techniques are described in Section 5 of the trade-off document. These techniques are simple average and posterior-mean estimate of average components.

5.4.1 Estimation of Average Components

The objective here is to estimate the average gravity and earth-rate components in the body frame – namely,

$$\bar{\underline{g}}_B = T_1 \begin{bmatrix} g \\ 0 \\ 0 \end{bmatrix} \quad \text{and} \quad \bar{\underline{\omega}}_B^E = T_1 \begin{bmatrix} \omega_U^E \\ 0 \\ \omega_N^E \end{bmatrix}$$

In using an estimate of the average components, we are neglecting the motion about the average. The error bound derived in subsection 5.3.1 applies to $\underline{\omega}^E$ as well as $\underline{g}$.

In the following subsections three approaches to estimation are considered: simple average, least squares, and posterior mean. The first approach does not use any a priori information about the noise spectra, alignment, gravity, or earth rate. The second approach uses prior measurements of the noise spectra. On the other hand, it does not include the prior geophysical measurements of gravity and earth angular velocity. The third approach uses a priori information about alignment, magnitude of gravity and magnitude of earth angular velocity plus prior measurements of the noise spectra. However, the noises must be assumed to be gaussian processes. This third approach has several advantages: i) prior geophysical measurements are included and are weighted with estimates of their accuracy; ii) the estimation techniques are comparable to those obtained from a least squares approach in complexity; iii) the resulting techniques can be used recursively to continuously update the alignment matrix; iv) the posterior-mean estimate is optimum with respect to a large class of loss functions, not just quadratic. From noise simulation, we find that the posterior-mean techniques are probably not sensitive to the gaussian assumption (see Section 5 of the trade-off document).

5.4.1.1 Simple Average

This approach is based on the assumption that we do not have any prior information about the noise, magnitude of gravity, magnitude of earth rate, or alignment. In this case,

$$\hat{\underline{g}}_B = \frac{1}{K\Delta t} \sum_{j=1}^{K} \underline{P}_B^A(j) \qquad \hat{\underline{\omega}}_B^E = \frac{1}{K\Delta t} \sum_{j=1}^{K} \underline{P}_B^G(j)$$

Note that the same estimate is obtained if $K = 1$ and Δt is replaced by $K\Delta t$.

5.4.1.2 Least Squares

Before developing a least-squares technique, it is convenient to define certain notation. Let $\underline{X}$ be the 6K vector whose components are

$$X_j = P_{B1}^A(j), \quad X_{j+K} = P_{B2}^A(j), \quad X_{j+2K} = P_{B3}^A(j)$$

$$X_{j+3K} = P_{B1}^G(j), \quad X_{j+4K} = P_{B2}^G(j), \quad X_{j+5K} = P_{B3}^G(j)$$

with $j = 1, 2, \cdots, K$. Let H_3 be the $6K \times 6$ matrix

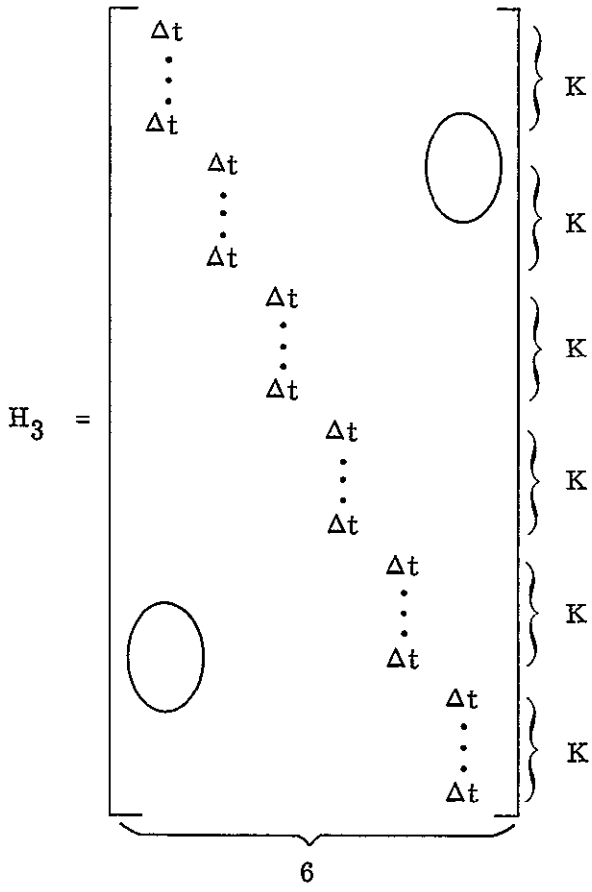

Let

$$\phi_{r(j)} = \int_{(j-1)\Delta t}^{j\Delta t} \theta_r(\tau)\, d\tau$$

$$\phi^{+}_{r(j)} = \int_{(j-1)\Delta t}^{j\Delta t} \dot{\theta}_r(\tau)\, d\tau$$

with $r = 2, 3$.

Let $\underline{\Phi}$ be a 6K vector with components

$$\underline{\Phi}^T = (\Phi_1, \Phi_2, \cdots, \Phi_{6K})$$

where

$$
\begin{aligned}
\Phi_j &= g(T_1)_{13}\,\phi_2(j) - g(T_1)_{12}\,\phi_3(j) \\
\Phi_{j+K} &= g(T_1)_{23}\,\phi_2(j) - g(T_1)_{22}\,\phi_3(j) \\
\Phi_{j+2K} &= g(T_1)_{33}\,\phi_2(j) - g(T_1)_{32}\,\phi_3(j) \\
\Phi_{j+3K} &= [-(T_1)_{11}\omega_N^E + (T_1)_{13}\omega_U^E]\phi_2(j) - (T_1)_{12}\,\omega_U^E\phi_3(j) + (T_1)_{12}\,\phi_2^+(j) \\
&\quad + (T_1)_{13}\,\phi_3^+(j) \\
\Phi_{j+4K} &= [-(T_1)_{21}\omega_N^E + (T_1)_{23}\omega_U^E]\,\phi_2(j) - (T_1)_{22}\,\omega_U^E\phi_3(j) + (T_1)_{22}\,\phi_2^+(j) \\
&\quad + (T_1)_{23}\,\phi_3^+(j) \\
\Phi_{j+5K} &= [-(T_1)_{31}\omega_N^E + (T_1)_{33}\omega_U^E]\,\phi_2(j) - (T_1)_{32}\,\omega_U^E\phi_3(j) + (T_1)_{32}\,\phi_2^+(j) \\
&\quad + (T_1)_{33}\,\phi_3^+(j)
\end{aligned}
\qquad \Bigg\} \quad (5\text{-}14)
$$

with $j = 1, 2, \cdots, K$.

Let $\underline{\phi}_2^T = [\phi_2(1), \phi_2(2), \cdots, \phi_2(K)]$

and $(\underline{\varphi}_2^+)^T = [\varphi_2^+(1), \phi_2^+(2), \cdots, \phi_2^+(K)]$

and $\underline{\phi}_3^T = [\phi_3(1), \phi_3(2), \cdots, \varphi_3(K)]$

and $(\underline{\varphi}_3^+)^T = [\phi_3^+(1), \phi_3^+(2), \cdots, \varphi_3^+(K)]$

Then equation (5-14) can be rewritten as follows.

$$
\underline{\Phi} = H_4 \begin{bmatrix} \underline{\phi}_2 \\ \underline{\phi}_2^+ \\ \underline{\phi}_3 \\ \underline{\varphi}_3^+ \end{bmatrix}
$$

where H_4 is the 6Kx4K matrix defined by equation (5-14) and is introduced for mathematical convenience. Let $\underline{N}$ be a 6K vector with components

$$N_j = \int_{(j-1)\Delta t}^{j\Delta t} [\alpha_1(\tau) + n_{A1}(\tau)]\, d\tau$$

$$N_{j+K} = \int_{(j-1)\Delta t}^{j\Delta t} [\alpha_2(\tau) + n_{A2}(\tau)]\, d\tau$$

$$N_{j+2K} = \int_{(j-1)\Delta t}^{j\Delta t} [\alpha_3(\tau) + n_{A3}(\tau)]\, d\tau$$

$$N_{j+3K} = \int_{(j-1)\Delta t}^{j\Delta t} n_{G1}(\tau)\, d\tau$$

$$N_{j+4K} = \int_{(j-1)\Delta t}^{j\Delta t} n_{G2}(\tau)\, d\tau$$

$$N_{j+5K} = \int_{(j-1)\Delta t}^{j\Delta t} n_{G3}(\tau)\, d\tau$$

with $j = 1, 2, \cdots, K$. The vector $\underline{N}$ represents the environment and sensor noises. The basic observation equations (5-4) and (5-5) can be rewritten as:

$$\underline{X} = H_3 \begin{bmatrix} \underline{\bar{g}}_B \\ \underline{\bar{\omega}}_B^E \end{bmatrix} + \underline{\Phi} + \underline{N} \qquad (5\text{-}15)$$

The objective is to estimate $\underline{\bar{g}}_B$ and $\underline{\bar{\omega}}_B^E$ in the presence of noise $\underline{\Phi} + \underline{N}$.

The covariance matrix of $\underline{\Phi} + \underline{N}$ is the sum of the covariance matrices, since the noises are independent; i.e.,

$$\Sigma_{\Phi+N} = \Sigma_{\Phi} + \Sigma_N$$

Further,

$$\Sigma_{\Phi} = H_4 \left[\begin{array}{c|c|c|c} \Sigma_{\phi\phi} & \Sigma_{\phi\phi+} & 0 & 0 \\ \hline \Sigma_{\phi\phi+}^T & \Sigma_{\phi+\phi+} & 0 & 0 \\ \hline 0 & 0 & \Sigma_{\phi\phi} & \Sigma_{\phi\phi+} \\ \hline 0 & 0 & \Sigma_{\phi\phi+}^T & \Sigma_{\phi+\phi+} \end{array}\right] H_4^T$$

where

$$(\Sigma_{\phi\phi})_{ij} = E[\phi_2(i)\phi_2(j)]$$

$$(\Sigma_{\phi+\phi+})_{ij} = E[\phi_2^+(i)\phi_2^+(j)]$$

$$(\Sigma_{\phi\phi+})_{ij} = E[\phi_2(i)\phi_2^+(j)]$$

with $i, j = 1, 2, \cdots, K$. Note that θ_2 and θ_3 are assumed to be independent and identically distributed. Further,

$$\Sigma_N = \begin{bmatrix} \Sigma_{\alpha+n} & & & & & & \\ & \Sigma_{\alpha+n} & & & & & \\ & & \Sigma_{\alpha+n} & & & & \\ & & & \Sigma_G & & & \\ & & & & \Sigma_G & & \\ & & & & & \Sigma_G & \end{bmatrix}$$

where

$$(\Sigma_{\alpha+n})_{ij} = E[N_i N_j], \quad i, j = 1, \cdots, K$$

$$(\Sigma_G)_{ij} = E[N_i N_j], \quad i, j = 3K+1, \cdots, 4K$$

These covariance matrices can be expressed in terms of the correlation functions (see subsection 5.4.1.2). The following identities* are useful in simplifying $\Sigma_{\phi+\phi+}$ and $\Sigma_{\phi\phi+}$:

$$E[\theta'(0)\theta'(\tau)] = -\frac{d^2}{d\tau^2} E[\theta(0)\,\theta(\tau)]$$

$$E[\theta(0)\,\theta'(\tau)] = \frac{d}{d\tau} E[\theta(0)\,\theta(\tau)]$$

where we have assumed that $\theta_2(\tau)$ and $\theta_3(\tau)$ are stationary processes.

*E. Parzen, "Stochastic Processes", Holden-Day, 1952, p. 83.

Note that H_4 is evaluated using prior estimates for the value of T_1 and g, denoted by $\tilde{T}_1$ and $\tilde{g}$. Precise values are not needed since H_4 is used in the noise model. Corrections to H_4 would be of second order.

Based on the composite measurement equation (5-15), the objective is to find the unbiased linear estimate of $(\bar{g}_B, \bar{\omega}_B^E)$, say $(\hat{g}_B(\underline{X}), \hat{\omega}_B^E(\underline{X}))$, which minimizes $E\left|\bar{g}_B - g(\underline{X})\right|^2$ as a function of $g(\underline{X})$ and minimizes $E\left|\bar{\omega}_B^E - \underline{\omega}(\underline{X})\right|^2$ as a function of $\underline{\omega}(\underline{X})$. It follows from the Gauss-Markoff theorem that $(\hat{g}_B(\underline{X}), \hat{\underline{\omega}}_B^E(\underline{X}))$ is the value of $(g, \underline{\omega})$ that minimizes

$$\left|M\underline{X} - MH_3\begin{pmatrix} g \\ \underline{\omega} \end{pmatrix}\right|^2$$

where M is the nonsingular matrix such that $M\Sigma_{\Phi+N}M^T = I$. In fact $\hat{g}_B(\underline{X})$ and $\hat{\underline{\omega}}_B^E(\underline{X})$ are minimum variance estimates for each component of $\bar{g}_B$ and $\bar{\underline{\omega}}_B^E$. One can show that

$$\begin{bmatrix} \hat{g}_B(\underline{X}) \\ \hat{\underline{\omega}}_B^E(\underline{X}) \end{bmatrix} = (H_3^T\Sigma_{\Phi+N}^{-1}H_3)^{-1}\, H_3^T\Sigma_{\Phi+N}^{-1}\underline{X} \qquad (5\text{-}16)$$

Further the expected value of $\hat{g}_B(\underline{X})$ is $\bar{g}_B$, and expected value of $\hat{\underline{\omega}}_B^E(\underline{X})$ is $\bar{\underline{\omega}}_B^E$, even if we have used an incorrect covariance matrix $\Sigma_{\Phi+N}$. The covariance matrix of $(\hat{g}_B, \hat{\underline{\omega}}_B^E)$ is

$$(H_3^T\Sigma_{\Phi+N}^{-1}H_3)^{-1} \qquad (5\text{-}17)$$

5.4.1.3 Posterior Mean

In the following discussion we assume that the stochastic inputs are gaussian processes. The "optimum" estimate of $\bar{g}_B$ and $\bar{\underline{\omega}}_B^E$ is then the posterior mean as shown in Section 5.3.1.3.

To evaluate the posterior mean, we first determine the conditional distribution of $\underline{X}$ given $(\bar{g}_B, \bar{\underline{\omega}}_B^E)$. In this subsection the notation is the same as that in 5.4.1.2. From equation (5-15) it follows that $\underline{X}$ is normally distributed with mean

$H_3\begin{bmatrix} \bar{g}_B \\ \bar{\underline{\omega}}_B^E \end{bmatrix}$ and covariance $\Sigma_{\Phi+N}$.

From prior observations we have an estimate of the orientation of the ISU, and hence we have an estimate of T_1, say $\tilde{T}_1$. Also we have an estimate of the magnitude of $\underline{\bar{g}}_B$ (say $\tilde{g}$), the magnitude of $\underline{\bar{\omega}}_B^E$, (say $\tilde{\omega}^E$) and latitude (say $\tilde{\lambda}$) from geophysical and astronomical measurements. With these estimates a prior distribution can be defined for $\underline{\bar{g}}_B$ – namely, gaussian with mean

$$\underline{\tilde{g}}_B = \tilde{T}_1 \begin{bmatrix} \tilde{g} \\ 0 \\ 0 \end{bmatrix}$$

and covariance

$$\Sigma_{\tilde{g}} = \tilde{T}_1 \begin{bmatrix} \sigma_g^2 & & \\ & \tilde{g}^2\sigma_\theta^2 & \\ & & \tilde{g}^2\sigma_\theta^2 \end{bmatrix} \tilde{T}_1^T$$

where σ_g is the rms error in the estimate of $\left|\underline{\bar{g}}_B\right|$ and σ_θ is the rms error in the estimate of vertical (expressed in radians). Similarly, we can define a prior distribution for $\underline{\bar{\omega}}_B^E$ – namely, gaussian with mean

$$\underline{\tilde{\omega}}_B^E = \tilde{T}_1 \begin{bmatrix} \sin\tilde{\lambda} & 0 & -\cos\tilde{\lambda} \\ 0 & 1 & 0 \\ \cos\tilde{\lambda} & 0 & \sin\tilde{\lambda} \end{bmatrix} \begin{bmatrix} \tilde{\omega}^E \\ 0 \\ 0 \end{bmatrix}$$

and covariance

$$\Sigma_{\tilde{\omega}} = \tilde{T}_1 \begin{bmatrix} \sin\tilde{\lambda} & 0 & -\cos\tilde{\lambda} \\ 0 & 1 & 0 \\ \cos\tilde{\lambda} & 0 & \sin\tilde{\lambda} \end{bmatrix} \begin{bmatrix} \sigma_\omega^2 & 0 & 0 \\ 0 & (\tilde{\omega}^E)^2\sigma_{\theta\omega}^2 & 0 \\ 0 & 0 & (\tilde{\omega}^E)^2\sigma_{\theta\omega}^2 \end{bmatrix} \begin{bmatrix} \sin\tilde{\lambda} & 0 & \cos\tilde{\lambda} \\ 0 & 1 & 0 \\ -\cos\tilde{\lambda} & 0 & \sin\tilde{\lambda} \end{bmatrix} \tilde{T}_1^T$$

where σ_ω is the rms error in the estimate of $\left|\underline{\bar{\omega}}_B^E\right|$ and $\sigma_{\theta\omega}$ is the rms error in the estimated direction of $\underline{\bar{\omega}}_B^E$ (expressed in radians). Let

$$\Sigma_T = \begin{bmatrix} \Sigma_{\tilde{g}} & \\ & \Sigma_{\tilde{\omega}} \end{bmatrix}$$

Applying Bayes' formula, we find that the posterior distribution of $(\underline{\bar{g}}_B, \underline{\bar{\omega}}_B)$ given $\underline{X}$ is gaussian with mean

$$\begin{bmatrix} \underline{\hat{g}}_B(\underline{X}) \\ \underline{\hat{\omega}}_B^E(\underline{X}) \end{bmatrix} = \left(H_3^T \Sigma_{\Phi+N}^{-1} H_3 + \Sigma_T^{-1} \right)^{-1} \left(H_3^T \Sigma_{\Phi+N}^{-1} \underline{X} + \Sigma_T^{-1} \begin{bmatrix} \underline{\tilde{g}}_B \\ \underline{\tilde{\omega}}_B^E \end{bmatrix} \right) \tag{5-18}$$

and covariance

$$\Sigma_{\hat{g}\hat{\omega}} = (H_3^T \Sigma_{\Phi+N}^{-1} H_3 + \Sigma_T^{-1})^{-1} \tag{5-19}$$

The estimates $\underline{\hat{g}}(\underline{X})$ and $\underline{\hat{\omega}}_B^E(\underline{X})$ represent the optimum combination of the measurements $\underline{X}$ and prior data weighted by their respective errors.

The alignment procedure described by (5-18) and (5-19) reduces to a least squares procedure when the prior measurements are very inaccurate. Also, this procedure can be used recursively to update the alignment matrix (see Section 5.3.1.3).

5.4.2 Estimation of Instantaneous Components

The earth's angular velocity is small compared with gyro quantization, in contrast to gravity and accelerometer quantization. Hence, it is reasonable to estimate the average angular velocity and instantaneous gravity. In Section 5.3.3 we concluded that the posterior-mean estimate of the instantaneous gravity components is best, based on a Monte Carlo simulation. On the other hand, based on the same simulation, there is no advantage in using a posterior-mean estimate of earth rate as opposed to a simple average (see Section 5.4.3).

5.4.3 Discussion

Several alignment estimation techniques are suggested. A Monte Carlo simulation was performed to select the best estimation technique. The simulation is discussed in Section 5 of the trade-off document. Two techniques were considered – simple average (5.4.1.1) and posterior mean (5.4.1.3). Several values of K, Δt, and T^{EB} were tried. The effect of nongaussian noise was also investigated. The simple average was superior to the posterior mean. An alternate technique is to use an instantaneous estimate of $\underline{g}$ (5.3.2) and an average estimate of $\underline{\omega}^E$. The accuracy will be improved but at the price of a significant increase in the computation requirements. Therefore, the recommended technique is simple average of both accelerometer and gyro data.

The simulation is also used to investigate the characteristics of the recommended techniques. The accuracy of gyrocompass alignment is strongly dependent on quantization errors of the gyro. The alignment error is of the order of 100 seconds of arc.

5.5 CALCULATION OF ALIGNMENT MATRICES FROM ESTIMATES OF GRAVITY, EARTH RATE AND OPTICAL ANGLES

The final operation in alignment is the calculation of the alignment matrix (see Chart 5-1). The basic equations are developed in Section 2.3.3 and are repeated here for completeness. The Mirror-Alignment matrix is presented in Chart 5-3, the Level-Alignment matrix in Chart 5-4, and the Gyrocompass matrix in Chart 5-5.

5.6 RECOMMENDED ALIGNMENT TECHNIQUES

Referring back to Chart 5-1, we find that there are four basic types of equations: alignment matrix, preprocessing, estimation, and estimation matrix equations. The alignment matrix equations are presented in Charts 5-3, 5-4, and 5-5 for Mirror Alignment, Level Alignment, and Gyrocompass. The alignment matrix computations are the only computations needed for Mirror Alignment. The preprocessing equations for level alignment and gyrocompass are presented in Chart 5-2 of Section 5.1. Note that the dots on the left indicate which equations are used for Level Alignment and Gyrocompass.

The estimation equations for Level Alignment are presented in Chart 5-6. The estimation matrix equations are presented in Charts 5-7 and 5-8. The estimation equations and matrix equations for Gyrocompass Alignment are presented in Chart 5-9.

The procedures required to implement the preceding alignment techniques are presented in the Procedures Manual, Part 3. The estimation equations were programmed for the Monte Carlo simulation, which is described in Section 5 of the trade-off document.

MIRROR ALIGNMENT MATRIX

Inputs $\theta_1, \alpha_1, \theta_2$ and α_2

From these quantities the alignment matrix is given by.

$$\begin{bmatrix} \\ T \\ \\ \end{bmatrix} = \begin{bmatrix} (\underline{U}\cdot\underline{M}_1) & \dfrac{(\underline{M}_1 \times \underline{U})\cdot(\underline{M}_1 \times \underline{M}_2)}{|\underline{M}_1 \times \underline{M}_2|} & \dfrac{(\underline{E} \times \underline{N})\cdot(\underline{M}_1 \times \underline{M}_2)}{|\underline{M}_1 \times \underline{M}_2|} \\ (\underline{E}\cdot\underline{M}_1) & \dfrac{(\underline{M}_1 \times \underline{E})\cdot(\underline{M}_1 \times \underline{M}_2)}{|\underline{M}_1 \times \underline{M}_2|} & \dfrac{(\underline{N} \times \underline{U})\cdot(\underline{M}_1 \times \underline{M}_2)}{|\underline{M}_1 \times \underline{M}_2|} \\ (\underline{N}\cdot\underline{M}_1) & \dfrac{(\underline{M}_1 \times \underline{N})\cdot(\underline{M}_1 \times \underline{M}_2)}{|\underline{M}_1 \times \underline{M}_2|} & \dfrac{(\underline{U} \times \underline{E})\cdot(\underline{M}_1 \times \underline{M}_2)}{|\underline{M}_1 \times \underline{M}_2|} \end{bmatrix}$$

where

$$|\underline{M}_1 \times \underline{M}_2| = [1 - (\underline{M}_1 \cdot \underline{M}_2)^2]^{1/2}$$

$$(\underline{M}_1 \cdot \underline{M}_2) = (\underline{M}_1 \cdot \underline{U})(\underline{M}_2 \cdot \underline{U}) + (\underline{M}_1 \cdot \underline{E})(\underline{M}_2 \cdot \underline{E}) + (\underline{M}_1 \cdot \underline{N})(\underline{M}_2 \cdot \underline{N})$$

$$\begin{bmatrix} (\underline{U}\cdot\underline{M}_1) \\ (\underline{E}\cdot\underline{M}_1) \\ (\underline{N}\cdot\underline{M}_1) \end{bmatrix} = \begin{bmatrix} \cos\theta_1 \\ \cos\alpha_1 \sin\theta_1 \\ \sin\alpha_1 \sin\theta_1 \end{bmatrix}, \quad \begin{bmatrix} (\underline{U}\cdot\underline{M}_2) \\ (\underline{E}\cdot\underline{M}_2) \\ (\underline{N}\cdot\underline{M}_2) \end{bmatrix} = \begin{bmatrix} \cos\theta_2 \\ \cos\alpha_2 \sin\theta_2 \\ \sin\alpha_2 \sin\theta_2 \end{bmatrix}$$

An optional technique might utilize the value of $|\underline{M}_1 \times \underline{M}_2|$ from a previous alignment thus eliminating the aforementioned dot product and square root operations.

LEVEL ALIGNMENT MATRIX

Inputs $(\underline{g}\cdot \underline{B}_1)$, $(\underline{g}\cdot \underline{B}_2)$, $(\underline{g}\cdot \underline{B}_3)$ and α_1

From these quantities the alignment matrix is given by:

$$\begin{bmatrix} \\ T \\ \\ \end{bmatrix} = \begin{bmatrix} 1 & 0 & 0 \\ 0 & \sin\alpha_1 & \cos\alpha_1 \\ 0 & -\cos\alpha_1 & \sin\alpha_1 \end{bmatrix} \begin{bmatrix} 0 & 1 & 0 \\ 0 & 0 & \dfrac{1}{|\underline{M}_1 \times \underline{U}|} \\ \dfrac{1}{|\underline{M}_1 \times \underline{U}|} & \dfrac{(\underline{M}_1\cdot \underline{U})}{|\underline{M}_1 \times \underline{U}|} & 0 \end{bmatrix} \begin{bmatrix} 1 & 0 & 0 \\ (\underline{U}\cdot\underline{B}_1) & (\underline{U}\cdot \underline{B}_2) & (\underline{U}\cdot\underline{B}_3) \\ 0 & -(\underline{U}\cdot\underline{B}_3) & (\underline{U}\cdot\underline{B}_2) \end{bmatrix}$$

where

- $(\underline{M}_1\cdot \underline{U}) = (\underline{U}\cdot \underline{B}_1)$
- $|\underline{M}_1 \times \underline{U}| = [1 - (\underline{M}_1\cdot \underline{U}^2]^{1/2}$
- $(\underline{U}\cdot \underline{B}_k) = (\underline{g}\cdot \underline{B}_k)/g$
- $g = [(\underline{g}\cdot \underline{B}_1)^2 + (\underline{g}\cdot \underline{B}_2)^2 + (\underline{g}\cdot \underline{B}_3)^2]^{1/2}$

An optional technique might utilize any of the following additional inputs:

- The zenith angle (θ_1) of mirror one might be utilized to find $(\underline{M}_1\cdot \underline{U})$ from

$$(\underline{M}_1\cdot \underline{U}) = \cos\theta_1$$

- The magnitude of gravity (g) might be supplied from a local survey. This piece of information can be utilized to reduce the number of required accelerometers to two.

GYROCOMPASS MATRIX

Inputs $(\underline{g} \circ \underline{B}_1)$, $(\underline{g} \cdot \underline{B}_2)$, $(\underline{g} \cdot \underline{B}_3)$, $(\underline{\omega}^E \cdot \underline{B}_1)$, $(\underline{\omega}^E \cdot \underline{B}_2)$, and $(\underline{\omega}^E \circ \underline{B}_3)$

From these quantities the alignment matrix is given by:

$$\left[\begin{array}{c} \\ T \\ \\ \end{array}\right] = \left[\begin{array}{ccc} 0 & 1 & 0 \\ 0 & 0 & \dfrac{1}{|\underline{W} \times \underline{U}|} \\ \dfrac{1}{|\underline{W} \times \underline{U}|} & -\dfrac{(\underline{W} \cdot \underline{U})}{|\underline{W} \times \underline{U}|} & 0 \end{array}\right] \left[\begin{array}{ccc} (\underline{W} \cdot \underline{B}_1) & (\underline{W} \cdot \underline{B}_2) & (\underline{W} \cdot \underline{B}_3) \\ (\underline{U} \cdot \underline{B}_1) & (\underline{U} \cdot \underline{B}_2) & (\underline{U} \cdot \underline{B}_3) \\ (\underline{W} \times \underline{U}) \cdot (\underline{B}_2 \times \underline{B}_3) & (\underline{W} \times \underline{U}) \cdot (\underline{B}_3 \times \underline{B}_1) & (\underline{W} \times \underline{U}) \cdot (\underline{B}_1 \times \underline{B}_2) \end{array}\right]$$

where

- $(\underline{W} \circ \underline{U}) = (\underline{W} \cdot \underline{B}_1)(\underline{U} \cdot \underline{B}_1) + (\underline{W} \cdot \underline{B}_2)(\underline{U} \cdot \underline{B}_2) + (\underline{W} \circ \underline{B}_3)(\underline{U} \cdot \underline{B}_3)$
- $|\underline{W} \times \underline{U}| = [1 - (\underline{W} \cdot \underline{U})^2]^{1/2}$
- $(\underline{W} \cdot \underline{B}_k) = (\underline{\omega}^E \cdot \underline{B}_k)/\omega^E$
- $(\underline{U} \circ \underline{B}_k) = (\underline{g} \cdot \underline{B}_k)/g$
- $\omega^E = [(\underline{\omega}^E \circ \underline{B}_1)^2 + (\underline{\omega}^E \cdot \underline{B}_2)^2 + (\underline{\omega}^E \cdot \underline{B}_3)^2]^{1/2}$
- $g = [(\underline{g} \cdot \underline{B}_1)^2 + (\underline{g} \cdot \underline{B}_2)^2 + (\underline{g} \cdot \underline{B}_3)^2]^{1/2}$

An optional technique might utilize any of the following additional inputs:

- The local latitude (λ) might be utilized to find $(\underline{W} \cdot \underline{U})$ from
$$(\underline{W} \cdot \underline{U}) = \cos \lambda$$
- The magnitude of gravity (g) might be supplied from a local survey.
- The magnitude of earth rate (ω^E) might be supplied from a local survey.

A use of all additional inputs could reduce the number of necessary instruments to three (either two accelerometers and one gyro, or one accelerometer and two gyros).

ESTIMATION ROUTINE COMPUTATIONS – LEVEL

Inputs: Preprocessed accelerometer measurements, $\underline{X}$, estimation matrix, M, and vector, $\underline{b}$

Output Estimate of acceleration components in body frame, $\underline{\hat{g}} \cdot \underline{B}_i$, $i = 1, 2, 3$ at time t*

The basic estimation computation is

$$\begin{bmatrix} \underline{\hat{g}} \cdot \underline{B}_1 (t^*) \\ \underline{\hat{g}} \cdot \underline{B}_2 (t^*) \\ \underline{\hat{g}} \cdot \underline{B}_3 (t^*) \end{bmatrix} = M\underline{X} + \underline{b}$$

where

$$\underline{X}^T = \left[\int_0^{\Delta t} \underline{a} \cdot \underline{B}_1 \, dt, \int_{\Delta t}^{2\Delta t} \underline{a} \cdot \underline{B}_1 \, dt, \cdots \int_{(K-1)\Delta t}^{K\Delta t} \underline{a} \cdot \underline{B}_1 \, dt, \int_0^{\Delta t} \underline{a} \cdot \underline{B}_2 \, dt, \cdots, \int_{(K-1)\Delta t}^{K\Delta t} \underline{a} \cdot \underline{B}_2 \, dt, \cdots \int_{(K-1)\Delta t}^{K\Delta t} \underline{a} \cdot \underline{B}_3 \, dt \right]$$

Δt = Intersample time

K = Number of samples

- Posterior Mean Technique (Instantaneous): Computations of $\underline{b}$ and M from the Estimation Matrix Computation Chart
- Simple Average Technique·

$$\underline{b} = \underline{0}$$

$$M = \begin{bmatrix} \underbrace{(K\Delta t)^{-1} \cdots (K\Delta t)^{-1}}_{K} & \underbrace{0}_{K} & \underbrace{0}_{K} \\ \underbrace{0}_{K} & \underbrace{(K\Delta t)^{-1} \cdots (K\Delta t)^{-1}}_{K} & \underbrace{0}_{K} \\ \underbrace{0}_{K} & \underbrace{0}_{K} & \underbrace{(K\Delta t)^{-1} \cdots (K\Delta t)^{-1}}_{K} \end{bmatrix}$$

ESTIMATION MATRIX COMPUTATIONS – LEVEL

Inputs: intersample time, Δt (sec)

number of samples, K

estimate of gravity, $\tilde{g}$ (ft/sec^2)

rms error in gravity estimate σ_g (ft/sec^2)

estimate of T^{EB}, $\tilde{T}_1$

rms angular error in prior estimate of vertical, σ_θ (radians)

noise covariance functions (tabular)

- accelerometer noise $\phi_n(t)$ (ft^2/sec^4)
- translational acceleration noise $\phi_\alpha(t)$ (ft^2/sec^4)
- rotational noise $\phi_\theta(t)$ (radian^2)

prediction time ϵ_t (sec)

Outputs alignment parameters M and $\underline{b}$

The intermediate quantities Σ_α, Σ_n, $\Sigma_{\phi\phi}$, c_0, c_j and $\Sigma_{\tilde{g}}$ are computed from the inputs.

- Σ_α is K x K matrix with components

$$(\Sigma_\alpha)_{ij} = \int_0^{\Delta t} [\Delta t - u]\,\phi_\alpha(u + (j-i)\Delta t)\,du$$

$$+ \int_{-\Delta t}^{0} [\Delta t + u]\,\phi_\alpha(u + (j-i)\Delta t)\,du$$

- Σ_n is K x K matrix with components

$$(\Sigma_n)_{ij} = \int_0^{\Delta t} [\Delta t - u]\,\phi_n(u + (j-i)\Delta t)\,du$$

$$+ \int_{-\Delta t}^{0} [\Delta t + u]\,\phi_n(u + (j-i)\Delta t)\,du$$

CONTINUATION OF CHART 5-7

- $\Sigma_{\phi\phi}$ is a K x K matrix with components

$$(\Sigma_{\phi\phi})_{ij} = \int_0^{\Delta t} [\Delta t - u]\, \phi_\theta (u + (j-1)\Delta t)\, du$$

$$+ \int_{-\Delta t}^{0} [\Delta t + u]\, \phi_\theta (u + (j-i)\Delta t)\, du$$

- $c_0 = \phi_0(0)$

- $c_j = \int_0^{\Delta t} \phi_\theta (u + (j-1)\Delta t - K\Delta t - \epsilon_t)\, du \qquad j = 1, 2, \cdots, K$

  where the integrals are evaluated by a convenient integration technique such as trapezoidal rule or Simpson's rule.

- $\Sigma_{\tilde{g}}$ is a 3 x 3 matrix

$$\Sigma_{\tilde{g}} = \tilde{T}_1 \begin{bmatrix} \sigma_g^2 & & 0 \\ & \tilde{g}^2 \sigma_\theta^2 & \\ 0 & & \tilde{g}^2 \sigma_\theta^2 \end{bmatrix} \tilde{T}_1^T$$

From these intermediate quantities, Σ_N, Σ_Z, V, A, B, $\underline{a}_1$, and $\underline{a}_2$ are computed.

- Σ_N is a 3K x 3K matrix

$$\Sigma_N = \begin{bmatrix} \Sigma_n + \Sigma_\alpha & & 0 \\ & \Sigma_n + \Sigma_\alpha & \\ 0 & & \Sigma_n + \Sigma_\alpha \end{bmatrix}$$

CONTINUATION OF CHART 5-7

- Σ_Z is a $(5K + 5) \times (5K + 5)$ matrix

$$\Sigma_Z = \begin{bmatrix} \Sigma_{\tilde{g}} & & & 0 & & \\ & \Sigma_N & & & & \\ & & c_0\ c_1 \cdots c_K & & & \\ & & c_1 & & & \\ & & \vdots & \Sigma_{\phi\phi} & & \\ & & c_K & & & \\ & & & & c_0\ c_1 \cdots c_K & \\ & & & & c_1 & \\ 0 & & & & \vdots & \Sigma_{\phi\phi} \\ & & & & c_K & \end{bmatrix} \begin{matrix} 3 \\ 3K \\ 1 \\ K \\ 1 \\ K \end{matrix}$$

$3 \quad 3K \quad 1 \quad K \quad 1 \quad K$

Numbers at edges of matrices denote dimension of submatrices.

- Matrices A (3 x 3) and B (3 x 3K) are submatrices

$$\begin{bmatrix} A & B \\ B^T & D \end{bmatrix} = (V \Sigma_Z V^T)^{-1}$$

where matrix V is the $(3K + 3) \times (5K + 5)$ matrix given on the following chart.

- $$\underline{a}_1 = \begin{bmatrix} \tilde{g}(\tilde{T}_1)_{11} \\ \tilde{g}(\tilde{T}_1)_{21} \\ \tilde{g}(\tilde{T}_1)_{31} \end{bmatrix} \qquad \underline{a}_2 = \begin{bmatrix} \Delta t\, \tilde{g}(\tilde{T}_1)_{11} \\ \vdots \\ \Delta t\, \tilde{g}(\tilde{T}_1)_{11} \\ \Delta t\, \tilde{g}(\tilde{T}_1)_{21} \\ \vdots \\ \Delta t\, \tilde{g}(\tilde{T}_1)_{21} \\ \Delta t\, \tilde{g}(\tilde{T}_1)_{31} \\ \vdots \\ \Delta t\, \tilde{g}(\tilde{T}_1)_{31} \end{bmatrix} \begin{matrix} \\ \\ \\ \\ \\ \\ \\ \\ \end{matrix} \begin{matrix} \\ \\ K \\ \\ \\ K \\ \\ \\ K \end{matrix}$$

CONTINUATION OF CHART 5-7

Then, the outputs are given by:

- $M = -A^{-1}B$

  Note that A^{-1} is the covariance matrix of the estimate.

- $\underline{b} = \underline{a}_1 + A^{-1}B\underline{a}_2$

V MATRIX

$$
V = \begin{bmatrix}
1 & & & \tilde{g}(\tilde{T}_1)_{13} & & & -\tilde{g}(\tilde{T}_1)_{12} & & & 3 \\
& 1 & 0 & \tilde{g}(\tilde{T}_1)_{23} & 0 & 0 & -\tilde{g}(\tilde{T}_1)_{22} & 0 & & \\
& & 1 & \tilde{g}(\tilde{T}_1)_{33} & & & -\tilde{g}(\tilde{T}_1)_{32} & & & \\
\hline
\Delta t & & & 1 & & & -\tilde{g}(\tilde{T}_1)_{12} & & & \\
\vdots & & & & \ddots & & & \ddots & & K \\
\Delta t & & & & & \tilde{g}(\tilde{T}_1)_{13} & & & -\tilde{g}(\tilde{T}_1)_{12} & \\
\hline
& \Delta t & & & \tilde{g}(\tilde{T}_1)_{23} & & & -\tilde{g}(\tilde{T}_1)_{22} & & \\
& \vdots & & & & \ddots & & & \ddots & K \\
& \Delta t & & & 0 & & 0 & & -\tilde{g}(\tilde{T}_1)_{22} & \\
\hline
& & \Delta t & & & \tilde{g}(\tilde{T}_1)_{33} & & -\tilde{g}(\tilde{T}_1)_{32} & & \\
& & \vdots & & & & \ddots & & \ddots & K \\
& & \Delta t & & & \tilde{g}(\tilde{T}_1)_{33} & & & -\tilde{g}(\tilde{T}_1)_{32} &
\end{bmatrix}
$$

3 | 3K (diagonal) | 1 | K (diagonal) | 1 | K (diagonal)

All missing entries are zero.

$(\tilde{T}_1)_{ij}$ denotes the (i, j) component of $\tilde{T}_1$.

Numbers at the edge of the V matrix denote the dimension of the submatrices.

CHART 5-8

ESTIMATION ROUTINE COMPUTATIONS – GYROCOMPASS

Inputs: Preprocessed accelerometer measurements, $\underline{X}$, estimation matrix, M, and vector, $\underline{b}$

Outputs. Estimates of gravity and earth rate components in body frame, $\widehat{\underline{g} \cdot \underline{B}_i}$ and $\widehat{\underline{\omega}^E \cdot \underline{B}_1}$, $i = 1, 2, 3$

The basic estimation computation is

$$\begin{bmatrix} \widehat{\underline{g} \cdot \underline{B}_1} \\ \widehat{\underline{g} \cdot \underline{B}_2} \\ \widehat{\underline{g} \cdot \underline{B}_3} \\ \widehat{\underline{\omega}^E \cdot \underline{B}_1} \\ \widehat{\underline{\omega}^E \cdot \underline{B}_2} \\ \widehat{\underline{\omega}^E \cdot \underline{B}_3} \end{bmatrix} = M\underline{X} + \underline{b}$$

where

$$\underline{X}^T = \left[\int_0^{\Delta t} \underline{a} \cdot \underline{B}_1 \, dt, \cdots, \int_{(K-1)\Delta t}^{K\Delta t} \underline{a} \cdot \underline{B}_1 \, dt, \int_0^{\Delta t} \underline{a} \cdot \underline{B}_2 \, dt, \cdots, \int_{(K-1)\Delta t}^{K\Delta t} \underline{a} \cdot \underline{B}_3 \, dt, \right.$$

$$\left. \int_0^{\Delta t} \underline{\omega} \cdot \underline{B}_1 \, dt, \cdots, \int_{(K-1)\Delta t}^{K\Delta t} \underline{\omega} \cdot \underline{B}_1 \, dt, \cdots, \int_{(K-1)\Delta t}^{K\Delta t} \underline{\omega} \cdot \underline{B}_3 \, dt \right]$$

Δt = Intersample time

K = Number of samples

CONTINUATION OF CHART 5-9

- Simple Average Technique:

$\underline{b} = \underline{0}$

$$M = \begin{bmatrix} (K\Delta t)^{-1} \cdots (K\Delta t)^{-1} & & & & & 0 \\ & (K\Delta t)^{-1} \cdots (K\Delta t)^{-1} & & & & \\ & & (K\Delta t)^{-1} \cdots (K\Delta t)^{-1} & & & \\ & & & (K\Delta t)^{-1} \cdots (K\Delta t)^{-1} & & \\ & & & & (K\Delta t)^{-1} \cdots (K\Delta t)^{-1} & \\ 0 & & & & & (K\Delta t)^{-1} \cdots (K\Delta t)^{-1} \end{bmatrix}$$

K K K K K K

Diagonal 6 x 6K

- Hybrid Technique: Use posterior-mean estimate of gravity as given for Level Alignment and simple average for earth rate.

APPENDIX A
THE MATHEMATICAL MODEL OF THE VIBRATING STRING ACCELEROMETER

A-1.0 INTRODUCTION

This appendix describes the operation of the Vibrating String Accelerometer (VSA) that has been selected for the ERC Strapdown Inertial Guidance System and develops a mathematical model to be used to relate the output of this type instrument to an estimate of applied acceleration.

A-2.0 DESCRIPTION OF THE ACCELEROMETER'S OPERATION

A functional block diagram of the Vibrating String Accelerometer (VSA) is shown in Figure A-1. The accelerometer consists of a seismic mass (mass 1 and mass 2 separated by a spring) which is supported by. 1) two taut strings that function as oscillator "tank" circuits, and 2) ligaments as shown in Figure A-1 and normal to the plane of Figure A-1.

When the VSA is at rest or moving with constant velocity, the sum of forces acting on its seismic mass is zero. When the VSA is accelerated, the resultant force acting on the seismic mass changes so that it accelerates with the case. The displacement of the seismic mass, relative to the case, that is produced by this resultant force is negligible except along the sensitive axis, A, as shown in Figure A-1. The tension in the strings as a result will not be affected by any motion other than that along the sensitive axis. This change in tension (from the at rest tension) of each string is, therefore, a function of the acceleration acting along the A axis of the instrument.

Since the natural frequency of a vibrating string is a function of its tension, the vibrating frequencies of the strings in the accelerometer are directly related to the applied acceleration along A.

Each of the strings of the VSA passes through a magnetic field supplied by the two permanent magnets of Figure A-1. When set to vibrating in its field, an electric signal is generated by the string. This signal is amplified and fed back to the string in such a manner that a sustained vibration occurs. The electric signals so generated are nominally sinusoidal with frequency equal to the resonant frequency of the individual string. The vibrating string

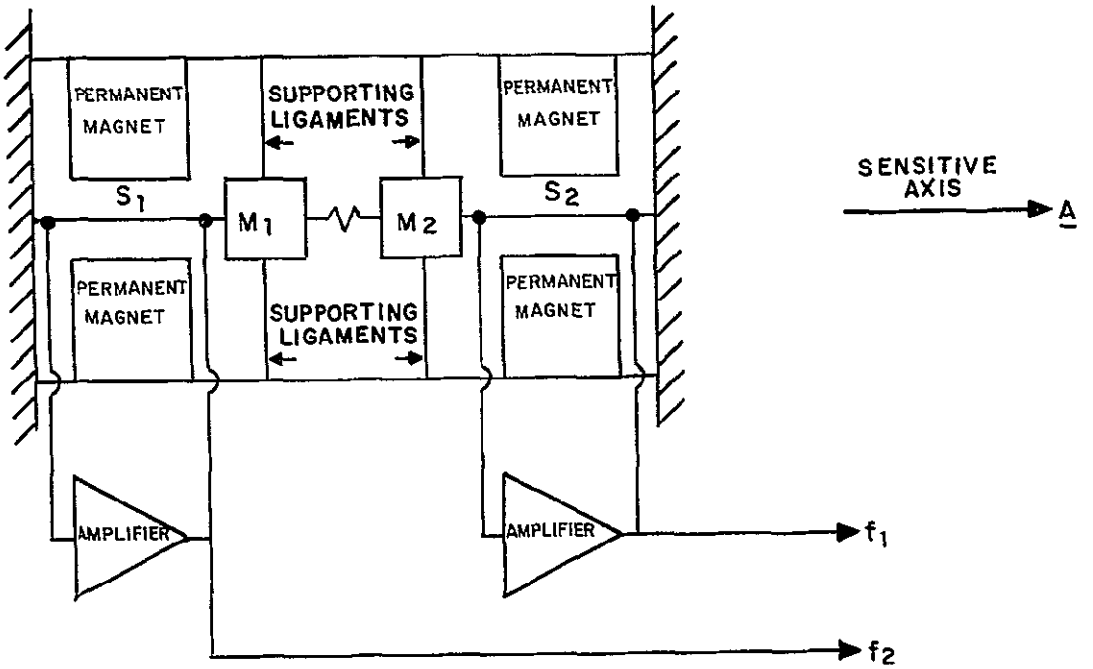

Model: ARMA D4E Vibrating String Accelerometer

Axis: $\underline{A}$ is a unit vector directed along strings S_1 and S_2 (the sensitive axis)

Figure A-1. A Schematic Diagram of the Accelerometer

acts as a high Q tank circuit for the oscillator within the associated feedback amplifier electronics. The vibrating frequency of each string is read by using Schmidt triggers to generate pulses corresponding to zero crossings of the respective sine waves. The frequency of the zero crossing pulse train is proportional to the frequency of the vibrating string.

A-3.0 KINETICS OF VSA

A-3.1 COORDINATE AXES

The accelerometer coordinate axes ($\underline{A}$, $\underline{O}$, $\underline{P}$) used in the derivation of the fundamental mathematical model are illustrated in Figure A-2. The unit vector $\underline{A}$ is along the nominal position of the string, while $\underline{O}$ and $\underline{P}$ are unit vectors arbitrarily defined to make $\underline{A}$, $\underline{O}$, and $\underline{P}$ a right handed, orthogonal system.

A-3.2 THE TENSION IN THE STRING

The forces acting on M_1 and M_2 along $\underline{A}$ are shown in Figure A-3. The lateral supporting forces along $\underline{P}$ (normal to the page) are not shown in this figure.

The equations of motion for the two masses can be written

$$\underline{F}_1 = \sum_i \underline{F}_{1i} = M_1\underline{a}; \quad \underline{F}_2 = \sum_j \underline{F}_{2j} = M_2\underline{a} \tag{A-1}$$

As we are interested in the tension of the strings, only the $\underline{A}$ component of equation A-1 will be considered.

$$\begin{aligned} (\underline{F}_1 \cdot \underline{A}) &= M_1(\underline{a} \cdot \underline{A}) \\ (\underline{F}_2 \cdot \underline{A}) &= M_2(\underline{a} \cdot \underline{A}) \end{aligned} \tag{A-2}$$

Because the supporting force from the ligaments acts orthogonally to the string, we have

$$\begin{aligned} (\underline{F}_1 \cdot \underline{A}) &= T_3 - T_1 \\ (\underline{F}_2 \cdot \underline{A}) &= T_2 - T_3 \end{aligned} \tag{A-3}$$

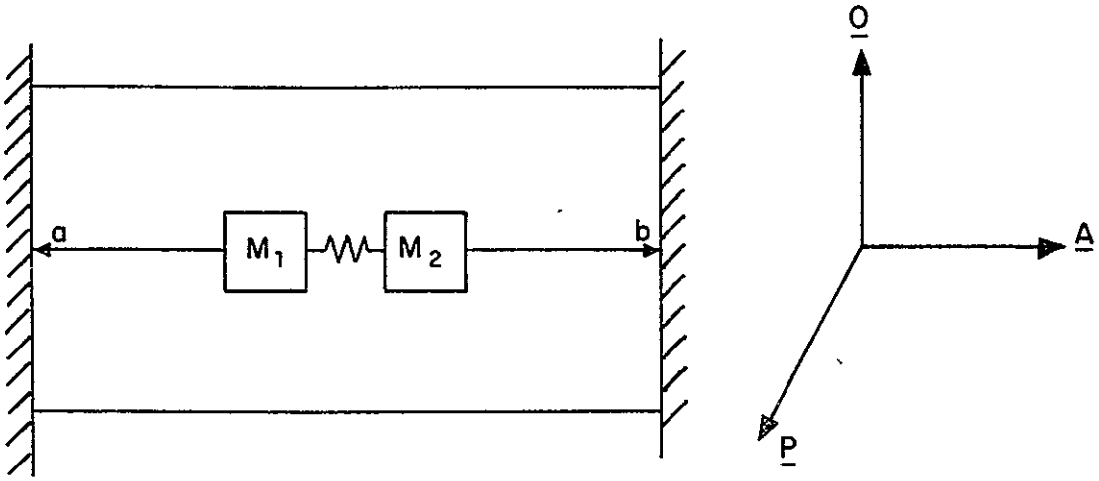

Figure A-2. Coordinate Axes

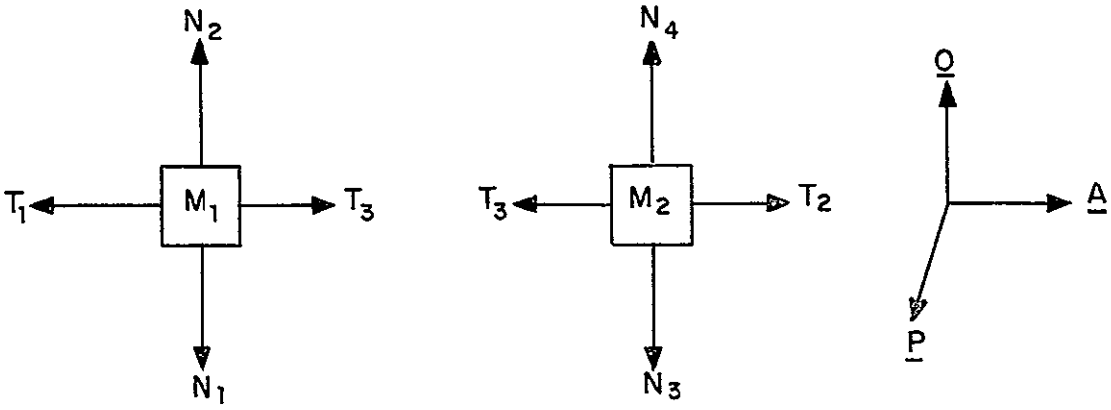

Figure A-3. Forces Acting on the Masses

Therefore from equations A-2 and A-3, we have

$$T_3 - T_1 = M_1(\underline{a} \cdot \underline{A})$$

$$T_2 - T_3 = M_2(\underline{a} \cdot \underline{A})$$

which can be combined as

$$T_2 - T_1 = (T_2 - T_3) + (T_3 - T_1) = (M_1 + M_2)(\underline{a} \cdot \underline{A}) \qquad \text{(A-4)}$$

When the accelerometer is stationary $\underline{a} = 0$ and equation A-4 gives $T_2 = T_1$. Let this tension in the strings be defined as T_o. When the VSA experiences an acceleration $\underline{a}$, T_1 and T_2 will be changed to cause the seismic masses to accelerate with the case. If $(\underline{a} \cdot \underline{A})$ is positive $(T_2 - T_1)$ will also be positive. The tension in each of the strings can be written as

$$T_2 = T_o + \Delta T_2$$

$$T_1 = T_o + \Delta T_1 \qquad \text{(A-5)}$$

and

$$\Delta T_1 + \Delta T_2 = (M_1 + M_2)(\underline{a} \cdot \underline{A})$$

The amount of change in the tension of both strings will be the same if the strings are identical. In practice, however, the strings cannot be made to be identical.

For the range of accelerations that is within the proportional limit of the strings, we can write

$$\Delta T_1 = K_1(\underline{a} \cdot \underline{A})$$

$$\Delta T_2 = K_2(\underline{a} \cdot \underline{A}) \qquad \text{(A-6)}$$

where $K_1 + K_2 = M_1 + M_2$

Beyond that range of applied acceleration, the strings creep and the mathematical model derived in the following pages will not apply.

A-4.0 MODEL DEVELOPMENT

A-4.1 THE RESONANT FREQUENCY OF A VIBRATING STRING

The resonant frequency of a uniform string under tension is directly proportional to the square root of the tension.

For the vibrating strings S_1 and S_2, their pulse train frequencies f_1 and f_2 (which are proportional to the respective resonant frequencies) can be written as

$$f_1 = C_1\sqrt{T_1}$$
$$f_2 = C_2\sqrt{T_2} \qquad \text{(A-7)}$$

C_1 and C_2 are proportionality constants determined by the dimensions, density and other physical properties of the strings. Combining equations A-5, A-6 and A-7, we have

$$f_1 = C_1\sqrt{T_o - K_1(\underline{a}\cdot\underline{A})}$$
$$f_2 = C_2\sqrt{T_o + K_2(\underline{a}\cdot\underline{A})}$$

By Taylor's expansion, this becomes

$$f_1 = C_1\left[\sqrt{T_o} - \frac{1}{2\sqrt{T_o}}K_1(\underline{a}\cdot\underline{A}) - \frac{1}{8T_o\sqrt{T_o}}K_1^2(\underline{a}\cdot\underline{A})^2 - \frac{1}{16T_o^2\sqrt{T_o}}K_1^3(\underline{a}\cdot\underline{A})^3 - \frac{5}{128T_o^3\sqrt{T_o}}K_1^4(\underline{a}\cdot\underline{A})^4 \ldots\right]$$

$$f_2 = C_2\left[\sqrt{T_o} + \frac{1}{2\sqrt{T_o}}K_2(\underline{a}\cdot\underline{A}) - \frac{1}{8T_o\sqrt{T_o}}K_2^2(\underline{a}\cdot\underline{A})^2\right.$$

$$\left. + \frac{1}{16T_o^2\sqrt{T_o}}K_2^3(\underline{a}\cdot\underline{A})^3 - \frac{5}{128T_o^3\sqrt{T_o}}K_2^4(\underline{a}\cdot\underline{A})^4\cdots\right]$$

The above expansions will converge rapidly since the instrument is constructed so that T_o is much greater than either $K_1(\underline{a}\cdot\underline{A})$ and $K_2(\underline{a}\cdot\underline{A})$. The frequency difference of the two strings is

$$f_2 - f_1 = (C_2 - C_1)\sqrt{T_o} + \frac{1}{2\sqrt{T_o}}(C_2K_2 + C_1K_1)(\underline{a}\cdot\underline{A}) - \frac{1}{8T_o\sqrt{T_o}}(C_2K_2^2 - C_1K_1^2)(\underline{a}\cdot\underline{A})^2$$

$$+ \frac{1}{16T_o^2\sqrt{T_o}}(C_2K_2^3 + C_1K_1^3)(\underline{a}\cdot\underline{A})^3 - \frac{5}{128T_o^3\sqrt{T_o}}(C_2K_2^4 - C_1K_1^4)(\underline{a}\cdot\underline{A})^4\cdots \quad \text{(A-8)}$$

The series given in equation A-8 converges rapidly because T_o is made large. However, C_1, C_2, K_1 and K_2 are constants determined by the dimension and material of the vibrating strings S_1 and S_2. The accelerometer is manufactured so that $(C_1\text{-}C_2)$ and $(K_1\text{-}K_2)$ are kept as small as possible (a highly symmetric instrument). For this reason, the even order terms are very small and the linear term is the most significant. The approximated frequency difference obtained by truncating equation A-8 after the third degree terms may be written:

$$f_2\text{-}f_1 = D_1D_0 + D_1(\underline{a}\cdot\underline{A}) + D_1D_2(\underline{a}\cdot\underline{A})^2 + D_1D_3(\underline{a}\cdot\underline{A})^3 \quad \text{(A-9)}$$

where, by definition,

$$D_1D_0 = (C_2 - C_1)\sqrt{T_o}$$

$$D_1 = \frac{1}{2\sqrt{T_o}}(C_2K_2 + C_1K_1)$$

$$D_1D_2 = \frac{-1}{8T_o\sqrt{T_o}}(C_2K_2^2 - C_1K_1^2)$$

$$D_1D_3 = \frac{1}{16T_o^2\sqrt{T_o}} \quad (C_2K_2^3 + C_1K_1^3)$$

A-4.2 THE ACCELEROMETER READOUT

Let the signal generated by the string S be

$$e_1(t) = \sin\left[\theta_1 + \int_{t_o}^{t} \pi f_1 dt\right]$$

where f is the frequency of the pulse train from string S (in pulses per second) and θ is a constant. The number of zero crossings in the interval (t_a, t_b) is

$$N_1 = \int_{t_a + \Delta t_1}^{t_b - \Delta t_2} f_1 dt = Eq_1 + \int_{t_a}^{t_b} f_1 dt$$

where $(t_a + \Delta t_1)$ and $(t_b - \Delta t_2)$ are the times of the first and last zero crossings in the interval (t_a, t_b) and Eq_1 is the quantization error given by

$$Eq_1 = \int_{t_a}^{t_a + \Delta t_1} f_1 dt - \int_{t_b - \Delta t_2}^{t_b} f_1 dt$$

The time increments Δt_1 and Δt_2 are defined by illustration in Figure A-4. In the same way, for string S_2, we have

$$N_2 = Eq_2 + \int_{t_a}^{t_b} f_2 dt$$

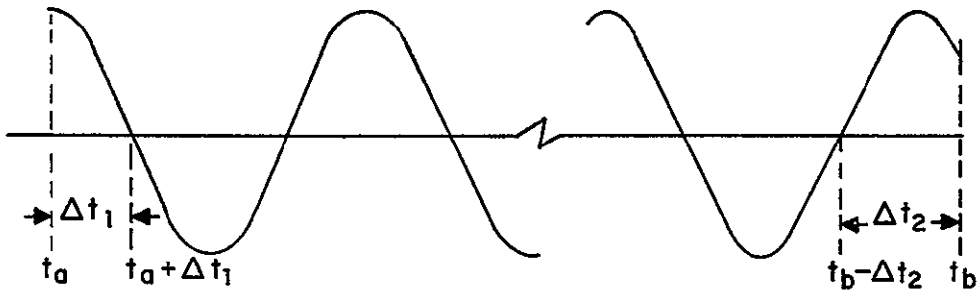

Figure A-4. Δt_1 and Δt_2

The difference in the number of zero crossings of the two strings can be written, using equation A-9, as

$$N_2 - N_1 = (Eq_1 - Eq_2) + \int_{t_a}^{t_b} (f_2 - f_1)\, dt$$

$$= Eq + \int_{t_a}^{t_b} D_1 D_0\, dt + \int_{t_a}^{t_b} D_1 (\underline{a} \cdot \underline{A})\, dt$$

$$+ \int_{t_a}^{t_b} D_1 D_2 (\underline{a} \cdot \underline{A})^2\, dt + \int_{t_a}^{t_b} D_1 D_3 (\underline{a} \cdot \underline{A})^3\, dt$$

A-4.3 THE VSA FUNDAMENTAL MATHEMATICAL MODEL

In summary, the readout of the VSA is two pulse trains corresponding to the zero crossings of the sinusoidal signals from the two vibrating strings. The input to the VSA is the acceleration of the case along its sensitive axis. The accelerometer readout is related to its input by the mathematical model given in Chart A-1.

THE FUNDAMENTAL ACCELEROMETER MODEL

THE ACCELEROMETER MODEL IS:

$$\int_{t_a}^{t_b} f_2\,dt - \int_{t_a}^{t_b} f_1\,dt = (N_2 - N_1) + Eq = D_1 \int_{t_a}^{t_b} (\underline{a}\cdot\underline{A})dt + D_1 \left\{ \int_{t_a}^{t_b} [D_0 + D_2(\underline{a}\cdot\underline{A})^2 + D_3(\underline{a}\cdot\underline{A})^3]dt \right\}$$

WHERE:

- $\underline{a}$ is the acceleration applied to the accelerometer
- $t_a \leq t \leq t_b$ is the time interval over which $\underline{a}$ is measured
- $\underline{A}$ is a unit vector directed along the input axis of the accelerometer
- N_1 and N_2 are the number of zero crossings detected in $t_a \leq t \leq t_b$ from both strings of the accelerometer
- Eq is the instrument quantization error due to the fact that t_a and t_b do not correspond to zero crossings
- D_1 is the accelerometer scale factor
- D_0 is the accelerometer bias
- D_2 is the second order coefficient
- D_3 is the third order coefficient
- f_2 and f_1 are string frequencies in pulses/second

APPENDIX B
THE MATHEMATICAL MODEL OF THE GYROSCOPE

B-1.0 INTRODUCTION

The purpose of this appendix is to find the mathematical expression that relates the outputs of the Honeywell GG 334A gyroscope to the environmental input to which this gyro is subjected.

Section B-2.0 is devoted to the general description of the 334A gyro and its principle of operation. The mathematical model is then developed in Section B-3.0.

B-2.0 DESCRIPTION OF THE GYRO OPERATION

The Honeywell GG 334A gyro contains a gimballed rotor spinning at a very high angular rate (see Figure B-1). A hydrodynamic gas bearing is used to support the rotor. The gimbal is restricted by the gimbal bearing to rotate only about the output axis relative to the case. The signal generator of Figure B-1 consists of a moving coil attached to the gimbal and a stationary wound stator attached to the gyro case. It generates an a-c voltage with an amplitude that is directly proportional to the angular displacement of the moving coil from its null position. In this way the gimbal deflection relative to the case is measured. At each sampling cycle (3.6 KHz rate), the gimbal deflection is detected, sampled and compared to two thresholds (positive and negative of equal level) to determine if a positive, zero or negative rebalance torque is to be generated. A current switch and associated electronics provide the torque generator with correct torquing current pulses of constant strength. The timing information (3.6 KHz) used to derive the cycle periods is furnished.

Any angular motion of the gyro case about the input axis, $\underline{G}$, will generate a gyroscopic torque that tends to rotate the gimbal about the output axis, $\underline{O}$. The signal generator senses the resulting gimbal deflection and produces the signal to the gyro electronics necessary to generate the correct torquing current pulses to the torque generator. In this way, the gyroscopic torque developed initially about the gimbal axis is rebalanced by the pulsive torque produced by the torque generator. The average rebalance torque is proportional to the average gyroscopic torque which is in turn proportional to the gyro angular rate about $\underline{G}$. A readout of the pulse train of the rebalance current is used as the instrument's output.

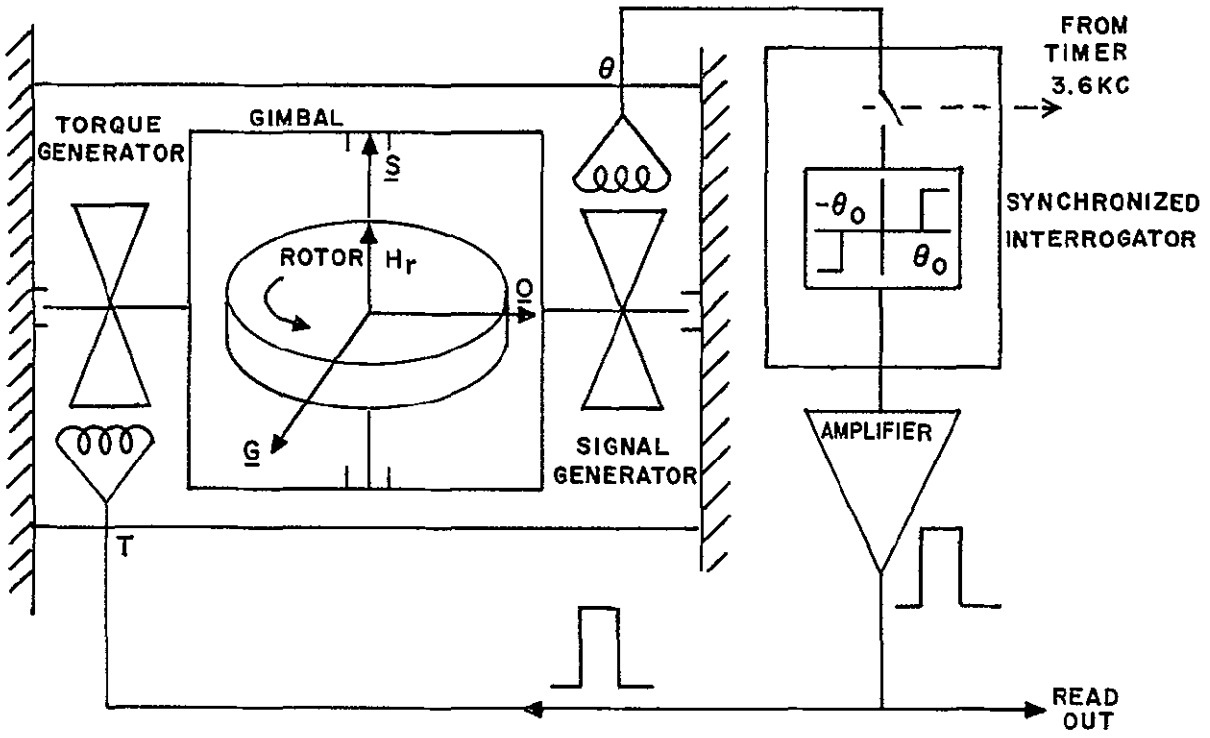

Model. Honeywell GG 334A single-degree-of-freedom, pulse rebalance gyroscope.

Axes: $\underline{S}$ is a unit vector along the spin axis of the rotor.
$\underline{O}$ is a unit vector along the output axis as defined by the gimbal.
$\underline{G} = \underline{O} \times \underline{S}$ is the sensitive axis of the gyro.

Figure B-1. A Schematic Diagram of the Gyro

B-3.0 MATH MODEL DEVELOPMENT

B-3.1 COORDINATE AXES

The coordinate system used in the following derivations is illustrated in Figure B-2. The gimbal axes ($\underline{G}$, $\underline{O}$, $\underline{S}$) are defined as fixed to the gyro gimbal with $\underline{O}$ (the output axis) directed along the gimbal rotary axis, $\underline{S}$ (the spin axis) directed along the gyro rotor spin axis and $\underline{G}$ (the input axis) directed along the direction of $\underline{O} \times \underline{S}$.

The set ($\underline{G}$, $\underline{O}$, $\underline{S}$) is right handed, orthogonal and is assumed to be coincident with the gimbal principal axes.

B-3.2 THE GIMBAL DYNAMICS

The gimbal angular momentum can be expressed in the gimbal coordinate axes as

$$\underline{H} = [I_{GG}(\underline{\omega}^g \cdot \underline{G})]\underline{G} + [I_{OO}(\underline{\omega}^g \cdot \underline{O})]\underline{O} + [I_{SS}(\underline{\omega}^g \cdot \underline{S}) + H_r]\,\underline{S} \qquad (B\text{-}1)$$

where I_{GG} is the moment of inertia of the gimbal and the rotor about $\underline{G}$, I_{OO} is the moment of inertia of the gimbal and the rotor about $\underline{O}$, I_{SS} is the moment of inertia of the gimbal about $\underline{S}$, and H_r is the constant rotor spinning angular momentum. $(\underline{\omega}^g \cdot \underline{G})$, $(\underline{\omega}^g \cdot \underline{O})$, and $(\underline{\omega}^g \cdot \underline{S})$ are the components of the gimbal angular velocity about $\underline{G}$, $\underline{O}$, and $\underline{S}$, respectively.

Since $\underline{G}$, $\underline{O}$, $\underline{S}$ are assumed to be the principal axes of the gimbal, all the products of inertias I_{GO}, I_{OS}, I_{GS}, etc. are assumed to be zero. The second law of rotational motion states that the torque applied to the gimbal is equal to the derivative of the gimbal angular momentum.

$$\underline{T} = \frac{d\underline{H}}{dt} \qquad (B\text{-}2)$$

Using equation B-1 and writing equation B-2 in component form, we have

$$(\underline{T} \cdot \underline{G}) = I_{GG}(\dot{\underline{\omega}}^g \cdot \underline{G}) + (\underline{\omega}^g \cdot \underline{O})(\underline{\omega}^g \cdot \underline{S})(I_{SS} - I_{OO}) + H_r(\underline{\omega}^g \cdot \underline{O}) \qquad (B\text{-}3)$$

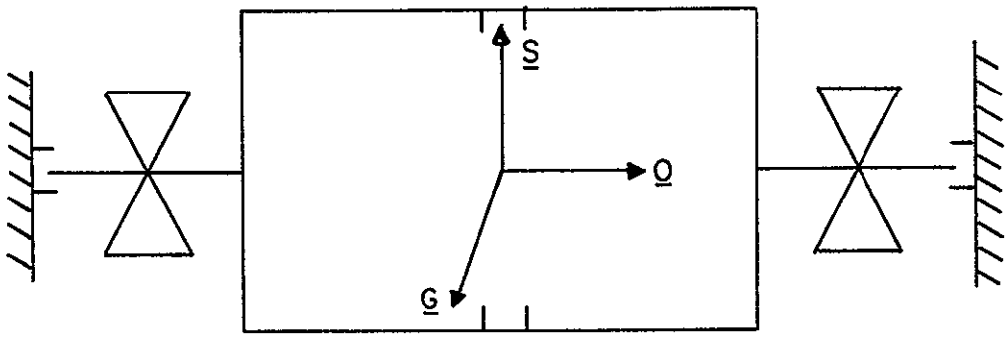

Figure B-2. Coordinate Axes

$$(\underline{T}\cdot\underline{O}) = I_{OO}(\dot{\underline{\omega}}^{g}\cdot\underline{O}) + (\underline{\omega}^{g}\cdot\underline{S})(\underline{\omega}^{g}\cdot\underline{G})(I_{GG}-I_{SS}) - H_r(\underline{\omega}^{g}\cdot\underline{G})$$

$$(\underline{T}\cdot\underline{S}) = I_{SS}(\dot{\underline{\omega}}^{g}\cdot\underline{S}) + (\underline{\omega}^{g}\cdot\underline{G})(\underline{\omega}^{g}\cdot\underline{O})(I_{OO}-I_{GG}) \qquad \text{(B-3)}$$

$(\underline{T}\cdot\underline{G})$ and $(\underline{T}\cdot\underline{S})$ are reaction torques from the gimbal bearing. Since we are concerned only with the torque about the output axis, $\underline{O}$, we may write

$$T_o = (\underline{T}\cdot\underline{O}) = I_{OO}(\dot{\underline{\omega}}^{g}\cdot\underline{O}) - H_r(\underline{\omega}^{g}\cdot\underline{G}) + (\underline{\omega}^{g}\cdot\underline{S})(\underline{\omega}^{g}\cdot\underline{G})(I_{GG}-I_{SS})$$

For a single-degree-of-freedom gyro, the gimbal can only move relative to the case about the gimbal axis $\underline{O}$. Thus the gimbal angular velocity can be expressed in terms of the case angular velocity and the relative angular velocity between the gimbal and the case.

$$\underline{\omega}^{g} = \underline{\omega} + (\underline{\omega}^{g}-\underline{\omega}) = \underline{\omega} + \dot{\theta}\,\underline{O}$$

where $\underline{\omega}$ is the gyro case angular velocity and θ is the gimbal deflection with respect to the case (see Figure B-3). Therefore,

$$T_o = (\underline{T}\cdot\underline{O}) = I_{OO}\ddot{\theta} + I_{OO}(\dot{\underline{\omega}}\cdot\underline{O}) - H_r(\underline{\omega}\cdot\underline{G}) + (\underline{\omega}\cdot\underline{S})(\underline{\omega}\cdot\underline{G})(I_{GG}-I_{SS}) \qquad \text{(B-4)}$$

B-3.3 THE GIMBAL TORQUE

The gimbal torque, T_o, is the sum of all torques applied to the gimbal about the output axis, $\underline{O}$. T_o includes a dampening torque, T_d; a rebalance torque, T_r, provided by the torque generator; and error torques.

The dampening torque is proportional to the rate of change of gimbal deflection angle, $\dot{\theta}$.

$$T_d = -C\dot{\theta}$$

The rebalance torque is

$$T_r = -L\delta_k$$

where δ_k is the logic value of the pulse at the instant t_k. $\delta_k = +1$, -1, or 0 for positive, negative or zero pulses, respectively.

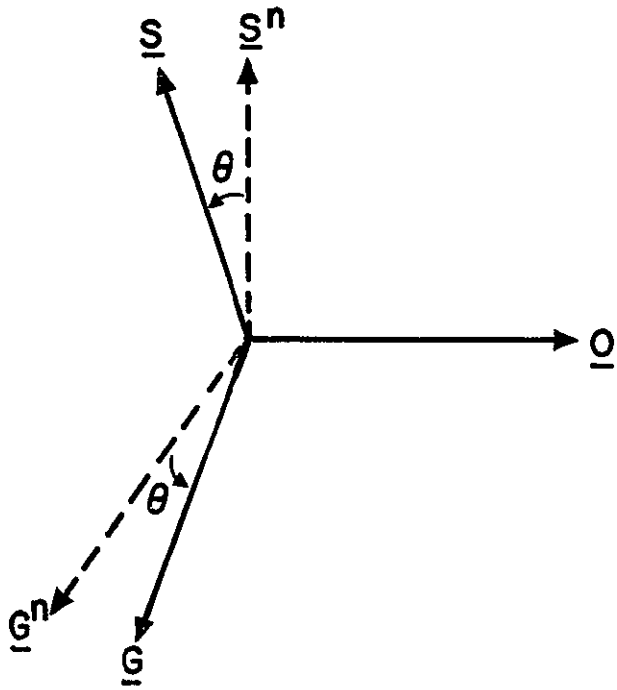

Figure B-3. The Gimbal Deflection

$$L = L_o [U(t - t_k) - U(t - t_k - h)]$$

where L_o is the amplitude of the pulse

h is the pulse width

U(t) is the unit step function

t_k is the k^{th} sampling period.

$L_o h = \int_{t_k}^{t_{k+1}} L\,dt$ is the strength of the pulse and would be constant for a linear rebalance loop. However, the torque rebalance loop will not be linear in reality, and $L_o h$ will be a function of $\underline{\omega}$. To take into account the effect of nonlinearity, let us assume

$$L_o h = \overline{L_o h}(1 + \alpha(\underline{\omega} \cdot \underline{G}_t))$$

where $\overline{L_o h}$ is constant and α very small.

The error torques include a constant torque, an $\underline{a}$-sensitive torque, an $\underline{a}^2$-sensitive torque, and other torques considered as noise (for example, reaction torque from the signal generator).

The constant torque is denoted by R'.

The $\underline{a}$-sensitive torques are mainly due to the fact that the center of support of the gimbal is not coincident with its center of mass. If the gyro acceleration is $\underline{a}$, the $\underline{a}$-sensitive error torque is

$$T_1 = B'_I(\underline{a} \cdot \underline{G}) + B'_O(\underline{a} \cdot \underline{O}) + B'_S(\underline{a} \cdot \underline{S})$$

where B'_I, B'_O and B'_S are gyro unbalance coefficients.

The $\underline{a}^2$-sensitive error torque is due to the fact that the gyro gimbal is not a rigid body. To make the gimbal follow the motion of the gyro case, there are forces acting on the gimbal through the gimbal bearing. The gimbal deforms when subjected to these forces. Because of this deformation, the center of mass of the gimbal will be displaced from the center of support and therefore produce an $\underline{a}^2$-sensitive torque about the output axis. It is assumed that the deformations also occur in the lateral direction as well as along the direction of the acceleration.

If the acceleration is $\underline{a}$, the $\underline{a}^2$-sensitive error torque is

$$T_2 = C'_{II}(\underline{a}\cdot\underline{G})^2 + C'_{SS}(\underline{a}\cdot\underline{S})^2 + C'_{IS}(\underline{a}\cdot\underline{G})(\underline{a}\cdot\underline{S}) + C'_{OS}(\underline{a}\cdot\underline{O})(\underline{a}\cdot\underline{S}) + C'_{IO}(\underline{a}\cdot\underline{G})(\underline{a}\cdot\underline{O})$$

where C'_{II}, C'_{SS}, C'_{IS}, C'_{OS}, and C'_{IO} are so-called compliance coefficients.

The total gimbal torque is then

$$T_o = -C\dot{\theta} - L\delta_k + R' + B'_I(\underline{a}\cdot\underline{G}) + B'_O(\underline{a}\cdot\underline{O}) + B'_S(\underline{a}\cdot\underline{S}) + C'_{II}(\underline{a}\cdot\underline{G})^2 + C'_{SS}(\underline{a}\cdot\underline{S})^2 + C'_{IS}(\underline{a}\cdot\underline{G})(\underline{a}\cdot\underline{S})$$

$$+ C'_{OS}(\underline{a}\cdot\underline{O})(\underline{a}\cdot\underline{S}) + C'_{IO}(\underline{a}\cdot\underline{G})(\underline{a}\cdot\underline{O}) + T_n \qquad \text{(B-5)}$$

where T_n is the torque due to other effects and is considered as a noise component.

B-3.4 CONCLUSION

Combining equation B-4 and equation B-5 we have

$$-C\dot{\theta} - L\delta_k + R' + B'_I(\underline{a}\cdot\underline{G}) + B'_O(\underline{a}\cdot\underline{O}) + B'_S(\underline{a}\cdot\underline{S}) + C'_{II}(\underline{a}\cdot\underline{G})^2 + C'_{SS}(\underline{a}\cdot\underline{S})^2 + C'_{IS}(\underline{a}\cdot\underline{G})(\underline{a}\cdot\underline{S})$$

$$+ C'_{OS}(\underline{a}\cdot\underline{O})(\underline{a}\cdot\underline{S}) + C'_{IO}(\underline{a}\cdot\underline{G})(\underline{a}\cdot\underline{O}) + T_n = I_{OO}(\dot{\underline{\omega}}\cdot\underline{O}) - H_r(\underline{\omega}\cdot\underline{G}) + (\underline{\omega}\cdot\underline{S})(\underline{\omega}\cdot\underline{G})(I_{GG} - I_{SS})$$

where $\dot{\theta}$ is the gyro case angular velocity, and the component of the reaction torque, $I_{OO}\ddot{\theta}$, has been neglected since it is small compared with the damping torque, $C\dot{\theta}$.

A rearrangement of equation B-6 gives

$$\frac{L}{H_r}\delta_k = (\underline{\omega}\cdot\underline{G}) + \frac{1}{H_r}\Big[R' + B'_I(\underline{a}\cdot\underline{G}) + B'_O(\underline{a}\cdot\underline{O}) + B'_S(\underline{a}\cdot\underline{S}) + C'_{II}(\underline{a}\cdot\underline{G})^2$$

$$+ C'_{SS}(\underline{a}\cdot\underline{S})^2 + C'_{IS}(\underline{a}\cdot\underline{G})(\underline{a}\cdot\underline{S}) + C'_{OS}(\underline{a}\cdot\underline{O})(\underline{a}\cdot\underline{S}) + C'_{IO}(\underline{a}\cdot\underline{G})(\underline{a}\cdot\underline{O})$$

$$- (I_{GG} - I_{SS})(\underline{\omega}\cdot\underline{S})(\underline{\omega}\cdot\underline{G}) - I_{OO}(\dot{\underline{\omega}}\cdot\underline{O})\Big] + \frac{T_n}{H_r} - \frac{C\dot{\theta}}{H_r} \qquad \text{(B-7)}$$

Let us now integrate equation B-7 over the N sampling periods starting at time t_o and ending at time t_n. We have

$$\frac{L_o h}{H_r}\left(\sum_{k=1}^{n}\delta_k\right) = \int_{t_o}^{t_n}(\underline{\omega}\cdot\underline{G})\,dt + \int_{t_o}^{t_n}\Big[R + B_I(\underline{a}\cdot\underline{G}) + B_O(\underline{a}\cdot\underline{O}) + B_S(\underline{a}\cdot\underline{S})$$

$$+ C_{II}(\underline{a}\cdot\underline{G})^2 + C_{SS}(\underline{a}\cdot\underline{S})^2 + C_{IS}(\underline{a}\cdot\underline{G})(\underline{a}\cdot\underline{S}) + C_{OS}(\underline{a}\cdot\underline{O})(\underline{a}\cdot\underline{S})$$

$$+ C_{IO}(\underline{a}\cdot\underline{G})(\underline{a}\cdot\underline{O}) + Q_{IS}(\underline{\omega}\cdot\underline{G})(\underline{\omega}\cdot\underline{S}) + J(\dot{\underline{\omega}}\cdot\underline{O})\Big]dt + \Delta n + Eq \qquad (B\text{-}8)$$

where $\underline{\omega}$ is the gyro case angular velocity

$\delta_k = 1, 0, -1$ is the k^{th} rebalance pulse

R, B_I, B_O, B_S, C_{II}, C_{SS}, C_{IS}, C_{OS}, and C_{IO} equal $\frac{R'}{H_r}$, $\frac{B_I'}{H_r}$, $\frac{B_O'}{H_r}$, $\frac{B_S'}{H_r}$, $\frac{C_{II}'}{H_r}$, $\frac{C_{SS}'}{H_r}$, $\frac{C_{IS}'}{H_r}$, $\frac{C_{OS}'}{H_r}$, and $\frac{C_{IO}'}{H_r}$, respectively

$$Q_{IS} = \frac{-(I_{GG} - I_{SS})}{H_r}$$

$$J = \frac{I_{OO}}{H_r}$$

$\Delta n = \int_{t_o}^{t_n}\frac{T_n}{H_r}\,dt$ is the effect of noise torques

$Eq = \int_{t_o}^{t_n}\frac{C}{H_r}\dot{\theta}\,dt$ is a quantization error.

However,

$$L_0 h = \overline{L_0 h}[1 + \alpha(\underline{\omega} \cdot \underline{G})]$$

With α very small, we can write

$$\overline{L_0 h} = \frac{1}{1 + \alpha(\underline{\omega} \cdot \underline{G})} L_0 h \approx (1 - \alpha(\underline{\omega} \cdot \underline{G})) L_0 h$$

Multiplying both sides of equation B-8 by $(1 - \alpha(\underline{\omega} \cdot \underline{G}))$ produces the gyro model as given on Chart B-1.

In the model, $\Delta\Phi = \frac{\overline{L_0 h}}{H_r}$ is the instrument scale factor. $Q_{II} = -\alpha \frac{\overline{L_0 h}}{H_r}$ is the coefficient of the term of the scale factor nonlinearity. α is very small, and the higher order effects of it have been ignored.

THE FUNDAMENTAL GYRO MODEL

THE GYRO MODEL IS

$$\Delta\Phi \left[\sum_{k=1}^{N} \delta_k\right] = \int_{t_0}^{t_N} (\underline{\omega}\cdot\underline{G})\, dt + \int_{t_0}^{t_N} \Big[R + B_I(\underline{a}\cdot\underline{G}) + B_O(\underline{a}\cdot\underline{O}) + B_S(\underline{a}\cdot\underline{S}) + C_{II}(\underline{a}\cdot\underline{G})^2 + C_{SS}(\underline{a}\cdot\underline{S})^2 + C_{IS}(\underline{a}\cdot\underline{G})(\underline{a}\cdot\underline{S}) + C_{OS}(\underline{a}\cdot\underline{O})(\underline{a}\cdot\underline{S}) + C_{IO}(\underline{a}\cdot\underline{G})(\underline{a}\cdot\underline{O}) + Q_{II}(\underline{\omega}\cdot\underline{G})^2 + Q_{IS}(\underline{\omega}\cdot\underline{G})(\underline{\omega}\cdot\underline{S}) + J\frac{d}{dt}(\underline{\omega}\cdot\underline{O})\Big] dt + \Delta n + Eq$$

WHERE

- $\underline{\omega}$ is the angular velocity applied to the gyro
- $\underline{a}$ is the acceleration applied to the gyro
- $t_0 \le t \le t_N$ is the time interval over which $\underline{a}$ and $\underline{\omega}$ are measured
- $t_N - t_0 = N\tau$, where N is an integer, and τ is the gyro sampling period
- $\underline{S}$ is a unit vector along the spin axis of the rotor
- $\underline{O}$ is a unit vector directed along the output axis as defined by the gimbal
- $\underline{G}$ is a unit vector along $\underline{O} \times \underline{S}$ (that is, the sensitive axis of the gyro)
- δ_k is the kth gyro pulse, equal to +1, -1, or 0 for positive, negative, or no pulse
- $\Delta\Phi$ is the gyro scale factor
- R is the gyro bias
- B_I B_O and B_S are the gyro unbalance coefficients
- C_{II} C_{SS} C_{IS} C_{OS} and C_{IO} are the gyro compliance coefficients
- Q_{IS} and Q_{II} are dynamic coupling coefficients due to gimbal deflection and scale factor nonlinearity, respectively
- J is the angular rate coefficient
- Δn is the effect of gyro noise over the $[t_0, t_N]$ interval
- Eq is the gyro quantization error

APPENDIX C
ALTERNATE FORM OF Q MATRICES

In Section 2.2.4 the Q^G and Q^A matrices were expressed in terms of $(Q^A)^{-1}$ and $(Q^G)^{-1}$, which are the matrices calibrated in the ERC laboratory. The calibrated elements were seen in Section 2.2.4 to have either the form $\underline{A}_k \cdot \underline{B}_\ell$ or $\underline{G}_k \cdot \underline{B}_\ell$. Because the body axes ($\underline{B}_k$) are defined, the elements do not equate directly to physical ISU angles – angles like the angle between, say, two gyro axes. It is possible, however, to express the Q matrices as a function of physical angles only. Those expressions are found in Chart C-1 and C-2. In Chart C-1 we see the general expression, and in Chart C-2 we see the first order approximation of the matrices. (Recall that the nominal Q^G and Q^A matrices are identity matrices.)

The form of the two matrices (Q^A and Q^G) in Chart C-1 and C-2 are, naturally, the same. In Chart C-1 the Q matrices have been separated into sums and products of submatrices, where each submatrix is a function of only one type of ISU angle. For example, the first submatrix is a function of only the angle between the mirrors, the second submatrix is a function of only the angles between the mirrors and instruments, the third submatrix is a function of only the angles between the accelerometers or gyros, and so forth.

The calibrated Q^A and Q^G elements can be equated to the elements found in Chart C-2, allowing for the solution of the physical ISU angles. Such solutions could be useful for the determination of the satisfaction of design requirements.

Q MATRICES

$$
\left[Q^A\right] = \begin{bmatrix} 1 & 0 & 0 \\ \dfrac{-(\underline{M}_1\,\underline{M}_2)}{|\underline{M}_1 \times \underline{M}_2|} & \dfrac{1}{|\underline{M}_1 \times \underline{M}_2|} & 0 \\ 0 & 0 & \dfrac{1}{|\underline{M}_1 \times \underline{M}_2|} \end{bmatrix} \left\{ \begin{bmatrix} (\underline{M}_1\,\underline{A}_1) & (\underline{M}_1\,\underline{A}_2) & (\underline{M}_1\,\underline{A}_3) \\ (\underline{M}_2\,\underline{A}_1) & (\underline{M}_2\,\underline{A}_2) & (\underline{M}_2\,\underline{A}_3) \\ 0 & 0 & 0 \end{bmatrix} \begin{bmatrix} \dfrac{(\underline{A}_2 \times \underline{A}_3)\,(\underline{A}_2 \times \underline{A}_3)}{(\underline{A}_1\,\underline{A}_2 \times \underline{A}_3)^2} & \dfrac{(\underline{A}_2 \times \underline{A}_3)\,(\underline{A}_3 \times \underline{A}_1)}{(\underline{A}_1\,\underline{A}_2 \times \underline{A}_3)^2} & \dfrac{(\underline{A}_2 \times \underline{A}_3)\,(\underline{A}_1 \times \underline{A}_2)}{(\underline{A}_1\,\underline{A}_2 \times \underline{A}_3)^2} \\ \dfrac{(\underline{A}_3 \times \underline{A}_1)\,(\underline{A}_2 \times \underline{A}_3)}{(\underline{A}_1\,\underline{A}_2 \times \underline{A}_3)^2} & \dfrac{(\underline{A}_3 \times \underline{A}_1)\,(\underline{A}_3 \times \underline{A}_1)}{(\underline{A}_1\,\underline{A}_2 \times \underline{A}_3)^2} & \dfrac{(\underline{A}_3 \times \underline{A}_1)\,(\underline{A}_1 \times \underline{A}_2)}{(\underline{A}_1\,\underline{A}_2 \times \underline{A}_3)^2} \\ \dfrac{(\underline{A}_1 \times \underline{A}_2)\,(\underline{A}_2 \times \underline{A}_3)}{(\underline{A}_1 \cdot \underline{A}_2 \times \underline{A}_3)^2} & \dfrac{(\underline{A}_1 \times \underline{A}_2)\,(\underline{A}_3 \times \underline{A}_1)}{(\underline{A}_1 \cdot \underline{A}_2 \times \underline{A}_3)^2} & \dfrac{(\underline{A}_1 \times \underline{A}_2)\,(\underline{A}_1 \times \underline{A}_2)}{(\underline{A}_1\,\underline{A}_2 \times \underline{A}_3)^2} \end{bmatrix} \right.
$$

$$
\left. + \begin{bmatrix} 0 & 0 & 0 \\ 0 & 0 & 0 \\ (\underline{M}_1 \times \underline{M}_2)\,(\underline{A}_2 \times \underline{A}_3) & (\underline{M}_1 \times \underline{M}_2)\,(\underline{A}_3 \times \underline{A}_1) & (\underline{M}_1 \times \underline{M}_2)\,(\underline{A}_1 \times \underline{A}_2) \end{bmatrix} \begin{bmatrix} \dfrac{1}{(\underline{A}_1\,\underline{A}_2 \times \underline{A}_3)} & 0 & 0 \\ 0 & \dfrac{1}{(\underline{A}_1 \cdot \underline{A}_2 \times \underline{A}_3)} & 0 \\ 0 & 0 & \dfrac{1}{(\underline{A}_1\,\underline{A}_2 \times \underline{A}_3)} \end{bmatrix} \right\}
$$

$$
\left[Q^G\right] = \begin{bmatrix} 1 & 0 & 0 \\ \dfrac{-(\underline{M}_1\,\underline{M}_2)}{|\underline{M}_1 \times \underline{M}_2|} & \dfrac{1}{|\underline{M}_1 \times \underline{M}_2|} & 0 \\ 0 & 0 & \dfrac{1}{|\underline{M}_1 \times \underline{M}_2|} \end{bmatrix} \left\{ \begin{bmatrix} (\underline{M}_1\,\underline{G}_1) & (\underline{M}_1\,\underline{G}_2) & (\underline{M}_1\,\underline{G}_3) \\ (\underline{M}_2\,\underline{G}_1) & (\underline{M}_2\,\underline{G}_2) & (\underline{M}_2\,\underline{G}_3) \\ 0 & 0 & 0 \end{bmatrix} \begin{bmatrix} \dfrac{(\underline{G}_2 \times \underline{G}_3)\,(\underline{G}_2 \times \underline{G}_3)}{(\underline{G}_1\,\underline{G}_2 \times \underline{G}_3)^2} & \dfrac{(\underline{G}_2 \times \underline{G}_3) \cdot (\underline{G}_3 \times \underline{G}_1)}{(\underline{G}_1\,\underline{G}_2 \times \underline{G}_3)^2} & \dfrac{(\underline{G}_2 \times \underline{G}_3) \cdot (\underline{G}_1 \times \underline{G}_2)}{(\underline{G}_1 \cdot \underline{G}_2 \times \underline{G}_3)^2} \\ \dfrac{(\underline{G}_3 \times \underline{G}_1)\,(\underline{G}_2 \times \underline{G}_3)}{(\underline{G}_1\,\underline{G}_2 \times \underline{G}_3)^2} & \dfrac{(\underline{G}_3 \times \underline{G}_1)\,(\underline{G}_3 \times \underline{G}_1)}{(\underline{G}_1\,\underline{G}_2 \times \underline{G}_3)^2} & \dfrac{(\underline{G}_3 \times \underline{G}_1)\,(\underline{G}_1 \times \underline{G}_2)}{(\underline{G}_1\,\underline{G}_2 \times \underline{G}_3)^2} \\ \dfrac{(\underline{G}_1 \times \underline{G}_2)\,(\underline{G}_2 \times \underline{G}_3)}{(\underline{G}_1\,\underline{G}_2 \times \underline{G}_3)^2} & \dfrac{(\underline{G}_1 \times \underline{G}_2)\,(\underline{G}_3 \times \underline{G}_1)}{(\underline{G}_1\,\underline{G}_2 \times \underline{G}_3)^2} & \dfrac{(\underline{G}_1 \times \underline{G}_2)\,(\underline{G}_1 \times \underline{G}_2)}{(\underline{G}_1\,\underline{G}_2 \times \underline{G}_3)^2} \end{bmatrix} \right.
$$

$$
\left. + \begin{bmatrix} 0 & 0 & 0 \\ 0 & 0 & 0 \\ (\underline{M}_1 \times \underline{M}_2)\,(\underline{G}_2 \times \underline{G}_3) & (\underline{M}_1 \times \underline{M}_2)\,(\underline{G}_3 \times \underline{G}_1) & (\underline{M}_1 \times \underline{M}_2)\,(\underline{G}_1 \times \underline{G}_2) \end{bmatrix} \begin{bmatrix} \dfrac{1}{(\underline{G}_1\,\underline{G}_2 \times \underline{G}_3)} & 0 & 0 \\ 0 & \dfrac{1}{(\underline{G}_1 \cdot \underline{G}_2 \times \underline{G}_3)} & 0 \\ 0 & 0 & \dfrac{1}{(\underline{G}_1\,\underline{G}_2 \times \underline{G}_3)} \end{bmatrix} \right\}
$$

Q MATRICES (OPERATIONAL)

LET

$$\underline{A}_1^N = \underline{M}_1^N = \underline{G}_1^N$$
$$\underline{A}_2^N = \underline{M}_2^N = \underline{G}_2^N$$
$$\underline{M}_1^N \text{ be perpendicular to } \underline{M}_2^N$$

where the superscript N denotes the nominal vector

IGNORING SECOND ORDER TERMS, WE HAVE:

$$\left[Q^A\right] = \begin{bmatrix} 1 & (\underline{M}_1\cdot\underline{A}_2 - \underline{A}_1\cdot\underline{A}_2) & (\underline{M}_1\cdot\underline{A}_3 - \underline{A}_3\cdot\underline{A}_1) \\ (\underline{M}_2\cdot\underline{A}_1 - \underline{M}_1\cdot\underline{M}_2 - \underline{A}_1\cdot\underline{A}_2) & 1 & (\underline{M}_2\cdot\underline{A}_3 - \underline{A}_2\cdot\underline{A}_3) \\ -(\underline{M}_1\cdot\underline{A}_3) & -(\underline{M}_2\cdot\underline{A}_3) & 1 \end{bmatrix}$$

Or, letting $\underline{A}_2\cdot(\underline{M}_1 - \underline{A}_1) = \underline{M}_2\cdot(\underline{M}_1 - \underline{A}_1)$

and $\underline{A}_1\cdot(\underline{M}_2 - \underline{A}_2) = \underline{M}_1\cdot(\underline{M}_2 - \underline{A}_2)$

$$= \begin{bmatrix} 1 & (\underline{M}_1\cdot\underline{M}_2 - \underline{M}_2\cdot\underline{A}_1) & (\underline{M}_1\cdot\underline{A}_3 - \underline{A}_3\cdot\underline{A}_1) \\ -(\underline{M}_1\cdot\underline{A}_2) & 1 & (\underline{M}_2\cdot\underline{A}_3 - \underline{A}_2\cdot\underline{A}_3) \\ -(\underline{M}_1\cdot\underline{A}_3) & -(\underline{M}_2\cdot\underline{A}_3) & 1 \end{bmatrix}$$

$$\left[Q^G\right] = \begin{bmatrix} 1 & (\underline{M}_1\cdot\underline{G}_2 - \underline{G}_1\cdot\underline{G}_2) & (\underline{M}_1\cdot\underline{G}_3 - \underline{G}_3\cdot\underline{G}_1) \\ (\underline{M}_2\cdot\underline{G}_1 - \underline{M}_1\cdot\underline{M}_2 - \underline{G}_1\cdot\underline{G}_2) & 1 & (\underline{M}_2\cdot\underline{G}_3 - \underline{G}_2\cdot\underline{G}_3) \\ -(\underline{M}_1\cdot\underline{G}_3) & -(\underline{M}_2\cdot\underline{G}_3) & 1 \end{bmatrix}$$

Or, letting $\underline{G}_2\cdot(\underline{M}_1 - \underline{G}_1) = \underline{M}_2\cdot(\underline{M}_1 - \underline{G}_1)$

and $\underline{G}_1\cdot(\underline{M}_2 - \underline{G}_2) = \underline{M}_1\cdot(\underline{M}_2 - \underline{G}_2)$

$$= \begin{bmatrix} 1 & (\underline{M}_1\cdot\underline{M}_2 - \underline{M}_2\cdot\underline{G}_1) & (\underline{M}_1\cdot\underline{G}_3 - \underline{G}_3\cdot\underline{G}_1) \\ -(\underline{M}_1\cdot\underline{G}_2) & 1 & (\underline{M}_2\cdot\underline{G}_3 - \underline{G}_2\cdot\underline{G}_3) \\ -(\underline{M}_1\cdot\underline{G}_3) & -(\underline{M}_2\cdot\underline{G}_3) & 1 \end{bmatrix}$$

APPENDIX D
COMPUTER SYSTEM DESCRIPTION

This appendix contains a description of the laboratory computer and its associated equipment. Section 1 describes the laboratory computer. Section 2 describes the Interface Electronics Unit (IEU), the device that interfaces the computer to the ISU. Section 3 describes briefly the devices used for the computer manual interface.

D-1.0 COMPUTER

The Honeywell DDP-124 computer is a small scale scientific/control digital computer with a 1.75 microsecond memory access time. The memory is an 8,192 word, 24-bit/word core memory. Arithmetic is performed on 24-bit sign-magnitude (not complement) data with the left-most bit of the data word containing the sign and the other 23 bits containing a binary representation of the magnitude. The basic arithmetic register is a 24-bit A Register which is extended by a 24-bit B Register for multiplication, division and shifting.

The instruction repertoire contains 47 instructions allowing fairly flexible fixed point processing. Unique instructions include a step multiple precision, store address portion of A, output and input to A (may be ANDs) as well as input/output to memory, direct control pulse outputs and sense line skips. Because of the sign magnitude number representation, the computer has both arithmetic shifts (sign bit(s) do not shift) and logical shifts.

Indirect addressing may be performed by use of one bit in the instruction Three index registers are available.

A Fortran IV Compiler is available and is considered preferable by NASA for calibration programming. The 124 is not equipped with floating point hardware so use of the Fortran Compiler will necessitate use of time consuming floating point software routines Because of real-time considerations, Fortran shall not be used for alignment

The computer interfaces with the Interface Electronics Unit, the displays and magnetic tape unit via a direct memory access (DMA) subunit. This allows direct transfer of data from and to memory under buffer control in one of two modes. These modes are the time sharing mode and the hog mode. In the hog mode, the input/output will hold the memory until the

entire transfer is completed. In the time sharing mode the input/output and the processor share memory with either locked out for one memory cycle while the other completes one transfer.

Execution times of instructions are as given in the DPP-124 Programmers Reference Manual, and execution times and memory sizing for standard arithmetic subroutines are as given in the DDP-124 Users Guide. One magnetic tape handler is available for program storage and/or other uses.

D-2.0 INTERFACE ELECTRONIC UNIT (IEU)

The IEU provides the computer an interface to the system equipment. A block diagram of the IEU is shown in Figure D-1.

The IEU counts information in its counters from the gyros, the accelerometer strings and the timer. Each counter is compared to a manually selected interrupt condition. This condition is selected as any number for the time counters or any power of two for gyro and accelerometer inputs. When an interrupt condition is met, a signal is sent to interrupt logic 3 if time counter 2 has satisfied it condition, interrupt logic 2 if time counter 1 has satisfied its condition or interrupt logic 1 if a gyro or accelerometer register has satisfied its condition. The interrupt logic generates an interrupt to the computer on its own interrupt channel and sends a reset signal to the counters Interrupt logic 1 and 2 send reset signals to all of the counters other than time counter 2 and interrupt logic 3 sends a reset signal only to time counter 2. When a counter receives a reset signal, it will hold the contents of the main register, clear an auxiliary register and begin to accumulate data in the auxiliary register.

When the computer has received an interrupt, it will initiate a direct memory access (DMA) controlled input from the IEU of the counters and ISU status registers. The main registers of the counters are read. After the reading process has been completed, a resume signal will be sent to all the counters from the DMA input control. This signal will cause any counter that is counting in an auxiliary register to clear the main register, add the auxiliary register to the main register, and continue accumulating in the main register

While the IEU has the capability of using any of the inputs to determine sampling rate as described above, it is not expected that any criterion other than time counter 1 is needed for the main calibration and alignment routines. The IEU interface program should verify that the time criterion has been met (Interrupt 1).

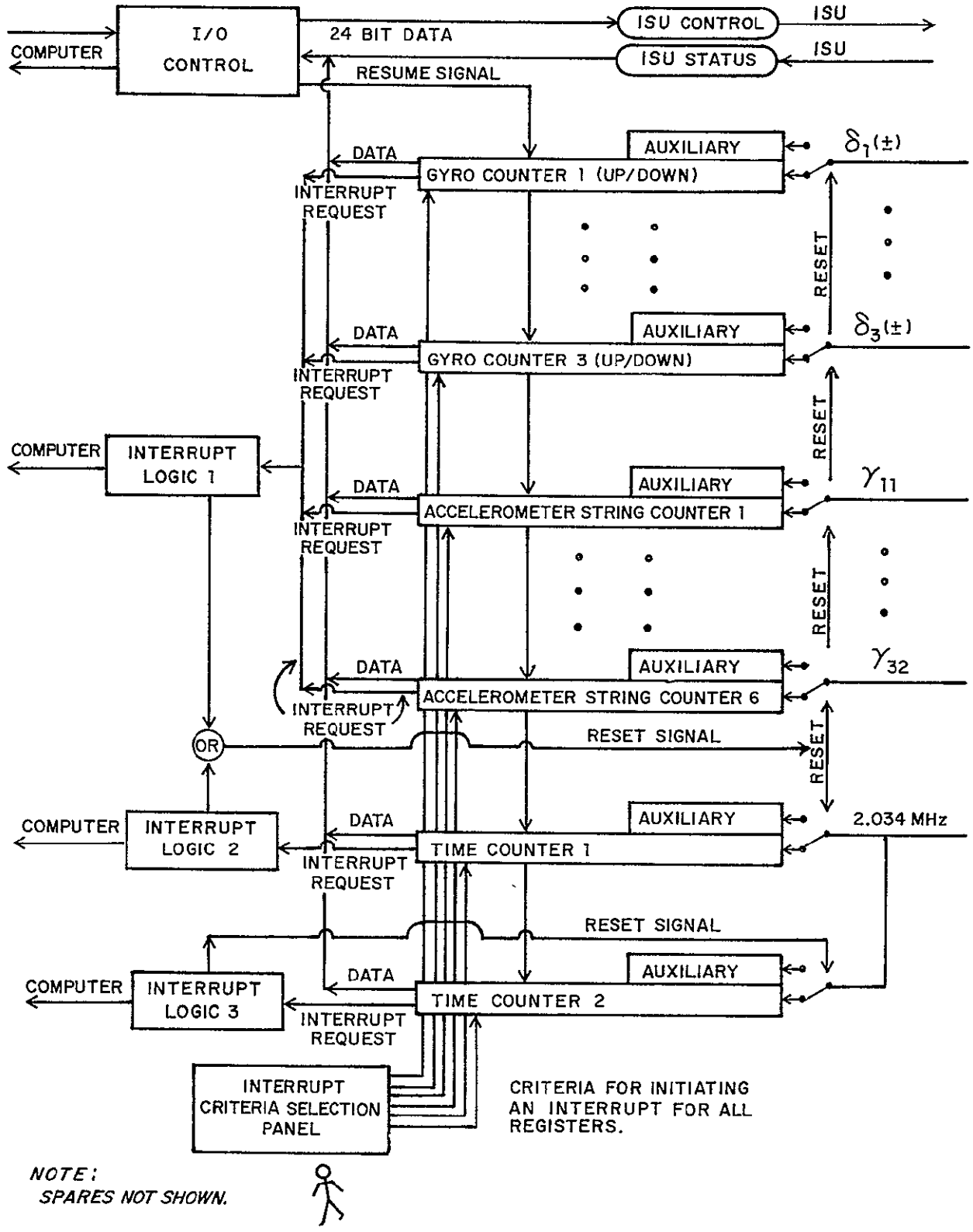

Figure D-1. IEU Block Diagram

Since the IEU sampling determines the time to sample ISU data on the basis of a time criterion, use of the IEU results in the maximum worst-case quantization error.

The IEU will transfer up to four 24-bit parallel data words from (and to) the ISU to (and from) the computer. Output from the computer is via DMA transfer.

D-3.0 COMPUTER MANUAL INTERFACE DEVICES

The operator interfaces with the computer via the display panel, a keyboard and typewriter and a paper tape reader and punch.

The display panel can display nine numbers. Each number has a signed one decimal digit mantissa and a signed five decimal digit characteristic. This capability will be used to display results or intermediate results or request and to display normalized data output from the ISU during real-time data collection by the computer

The display panel has three rows of eight buttons each to be used to select parameters to be displayed and 24 buttons to select program options.

The keyboard and typewriter may be used to enter data into the computer in small amounts and to furnish the operator with information such as desired settings of test table axes. Maximum transfer rate is 15.5 characters per second.

The paper tape reader and punch will be used to enter large amounts of data into the computer and for output of the results of the procedure Maximum transfer rates are 110 6-bit characters per second for the reader and 300 6-bit characters per second for the punch.

END

DATE FILMED
DEC. 31, 1970